สารออกฤทธิ์ทางชีวภาพจากราเอนโดไฟต์จากหญ้าน้ำดับไฟ *Lindenbergia philippensis* Benth. และ กะตังใบ *Leea rubra* Blume ex Spreng.

นายพรเทพ ชมชื่น

วิทยานิพนธ์นี้เป็นส่วนหนึ่งของการศึกษาตามหลักสูตรปริญญาวิทยาศาสตรดุษฎีบัณฑิต
สาขาวิชาเทคโนโลยีชีวภาพ
คณะวิทยาศาสตร์ จุฬาลงกรณ์มหาวิทยาลัย
ปีการศึกษา 2552

BIOACTIVE COMPOUNDS OF ENDOPHYTIC FUNGI FROM *Lindenbergia philippensis*
Benth. AND *Leea rubra* Blume ex Spreng.

Mr. Porntep Chomcheon

A Thesis Submitted in Partial Fulfillment of the Requirements

for the Degree of Doctor of Philosophy Program in Biotechnology

Faculty of Science

Chulalongkorn University

Academic Year 2009

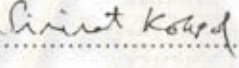520591
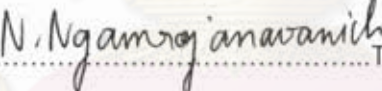
Thesis Title            BIOACTIVE COMPOUNDS OF ENDOPHYTIC FUNGI FROM

                        *Lindenbergia philippensis* Benth. AND *Leea rubra* Blume ex Spreng.

By                      Mr. Porntep Chomcheon

Field of study          Biotechnology

Thesis Advisor          Associate Professor Nattaya  Ngamrojanavanich, Ph.D.

Thesis Co-advisor       Assistant Professor Suthep  Wiyakrutta, Ph.D.

Thesis Co-advisor       Prasat  Kittakoop, Ph.D.

---

        Accepted by the Faculty of Science, Chulalongkorn University in Partial Fulfillment of
the Requirements for the Doctoral Degree

...................................................Dean of the Faculty of Science

(Professor Supot  Hannongbua, Dr.rer.nat)

THESIS COMMITTEE

...................................................Chairman

(Associate Professor Sirirat  Kokpol, Ph.D.)

...................................................Thesis advisor

(Associate Professor Nattaya  Ngamrojanavanich, Ph.D.)

...................................................Thesis Co-advisor

(Assistant Professor Suthep  Wiyakrutta, Ph.D.)

...................................................Thesis Co-advisor

(Prasat  Kittakoop, Ph.D.)

...................................................Examiner

(Associate Professor Nongluksna  Sriubolmas, Ph.D.)

...................................................Examiner

(Associate Professor Amorn  Petsom, Ph.D.)

...................................................External Examiner

(Maneekarn  Chinworrungsee, Ph.D.)

พรเทพ      ชมชื่น:     สารออกฤทธิ์ทางชีวภาพจากราเอนโดไฟต์จากหญ้าน้ำดับไฟ
*Lindenbergia philippensis* Benth. และ กะตังใบ *Leea rubra* Blume ex Spreng.
(BIOACTIVE COMPOUNDS OF ENDOPHYTIC FUNGI FROM *Lindenbergia*
*philippensis* Benth. AND *Leea rubra* Blume ex Spreng.) อ.ที่ปรึกษาวิทยานิพนธ์
หลัก: รศ. ดร. นาตยา งามโรจนวณิชย์, อ.ที่ปรึกษาวิทยานิพนธ์ร่วม: ผศ. ดร. สุเทพ
ไวครุฑธา, ดร. ประสาท  กิตตะคุปต์, 235 หน้า.

งานวิจัยนี้ทำการแยกสารออกฤทธิ์ทางชีวภาพจากราเอนโดไฟต์ไอโซเลต  LRUB20  ที่แยกได้จากกิ่ง
กะตังใบ และไอโซเลต LPHIL36 ที่แยกได้จากใบหญ้าน้ำดับไฟ โดยนำสารสกัดหยาบจากราเอนโดไฟต์ไอโซเลต
LRUB20 มาทำการแยกสารบริสุทธิ์โดยเทคนิคโครมาโทกราฟีได้สารใหม่ 4 ชนิด คือ สาร dothideopyrones A–
D (1, 3, 4, และ 5) และผลิตสารที่มีรายงานแล้วได้แก่ สาร *cis,trans*-muconic acid (9), สาร questin (10),
สาร asterric  acid  (11), สาร methyl asterrate (12), สาร sulochrin (13) สาร eugenitin (14), และ สาร 6-
hydroxymethyleugenitin (15)    ในส่วนน้ำหมักเชื้อจากราเอนโดไฟต์ไอโซเลต LPHIL36 พบสารใหม่ 3 ชนิด
คือ สาร corynesidones A-B (16 และ 18), และสาร corynether A (20), และผลิตสารที่มีรายงานแล้วคือ สาร
diaryl ether (22)       การพิสูจน์โครงสร้างทางเคมีของสารเหล่านี้ใช้วิธีการวิเคราะห์ข้อมูลทางสเปคโตรสโคปี
เมื่อนำสารบริสุทธิ์ที่แยกได้จากราไอโซเลต LRUB20 ไปทดสอบฤทธิ์ทางชีวภาพพบว่า สาร (5) และสารอนุพันธ์
(6) ซึ่งได้ถูกสังเคราะห์จากสาร 5 แสดงฤทธิ์ในการยับยั้งการเจริญของเซลล์มะเร็งชนิดต่างๆ อย่างอ่อน ส่วนสาร
(16, 18, 20, และ 22) แสดงฤทธิ์ต้านเซลล์มะเร็งชนิดต่างๆ อย่างอ่อนและไม่มีฤทธิ์ในการยับยั้งการเจริญของ
เซลล์ปรกติ โดยเฉพาะสาร 16 มีฤทธิ์ในการยับยั้งการทำงานของเอนไซม์ aromatase มีค่า $IC_{50}$ เท่ากับ 5.3 µM
การศึกษาทางสัณฐานวิทยาและการวิเคราะห์ลำดับนิวคลีโอไทด์ในบริเวณ    ITS1-5.8S-ITS2    ของ    rDNA
สามารถจำแนกประเภทราเอนโดไฟต์ไอโซเลต LPHIL36 คือ *Corynespora cassiicola* ขณะที่การศึกษาทาง
สัณฐานวิทยาพบว่าราเอนโดไฟต์ไอโซเลต  LRUB20  สร้างสปอร์ที่มีลักษณะเฉพาะ  นอกจากนี้การวิเคราะห์
ลำดับนิวคลีโอไทด์ในบริเวณ 18S และ ITS1-5.8S-ITS2 ของ rDNA พบว่ามีความแตกต่างจากเชื้อชนิดอื่นๆ ใน
ฐานข้อมูล GenBank จากข้อมูลเหล่านี้สามารถจำแนกประเภทราเอนโดไฟต์ไอโซเลต LRUB20 คือ mitosporic
Dothideomycete LRUB20 ซึ่งเป็นเชื้อราสายพันธุ์ใหม่

สาขาวิชา.......เทคโนโลยีชีวภาพ.... ลายมือชื่อนิสิต.........พรเทพ  ชมชื่น........................
ปีการศึกษา....2552..................... ลายมือชื่ออ.ที่ปรึกษาวิทยานิพนธ์หลัก..นาตยา  งามโรจนวณิชย์...
                                             ลายมือชื่ออ.ที่ปรึกษาวิทยานิพนธ์ร่วม......................
                                             ลายมือชื่ออ.ที่ปรึกษาวิทยานิพนธ์ร่วม......................

## 4873830423: BIOTECHNOLOGY

KEYWORD:     Endophytic fungi / Bioactive compounds / *Corynespora cassiicola* / Dothideomycete sp. / Cytotoxic activity / Aromatase inhibitor

PORNTEP CHOMCHEON: BIOACTIVE COMPOUNDS OF ENDOPHYTIC FUNGI FROM *Lindenbergia philippensis* Benth. AND *Leea rubra* Blume ex Spreng. THESIS ADVISOR: ASSOC. PROF. NATTAYA NGAMROJANAVANICH, Ph.D., THESIS CO-ADVISOR: ASST. PROF. SUTHEP WIYAKRUTTA, Ph.D., PRASAT KITTAKOOP, Ph.D., 235 pp.

The purpose of this research was to characterize bioactive compounds from endophytic fungi isolate LRUB20 from *Leea rubra* and isolate LPHIL36 from *Lindenbergia philippensis*. An organic extract from cultures of the isolate LRUB20 was purified by chromatographic techniques to afford four new pyrone derivatives, dothideopyrones A–D (1, 3, 4, and 5), along with seven known compounds, including *cis,trans*-muconic acid (9), questin (10), asterric acid (11), methyl asterrate (12), sulochrin (13), eugenitin (14), and 6-hydroxymethyleugenitin (15). The fermentation broth of the strain LPHIL36 afforded three new metabolites, corynesidones A (16) and B (18), and corynether A (20), together with a known diaryl ether (22). Their structures were elucidated by analysis of spectroscopic data. Dothideopyrone D (5) and its acetate derivative 6 exhibited moderate cytotoxic activity, while compounds 16, 18, 20, and 22 were relatively non-toxic against cancer cells, and inactive toward normal cell line. In addition, compound 16 inhibited aromatase activity with an $IC_{50}$ value of 5.30 µM. On the basis of morphology and nucleotide sequences of ITS1-5.8S-ITS2 regions of rDNA, the fungus LPHIL36 was identified as *Corynespora cassiicola*. The LRUB20 isolate produced characteristic conidia. DNA sequences of its 18S, and ITS1-5.8S-ITS2 ribosomal RNA gene regions were found to be unique having no similar sequences in the GenBank. Based on both microscopic morphology and molecular data, this fungus was classified as mitosporic Dothideomycete LRUB20, a potentially new species.

Field of study......Biotechnology...... Student's signature.........*Porntep Chomcheon*

Academic year ...2009................... Advisor's signature.....*N. Ngamrojanavanich*

Co-advisor's signature.........*Suthep Wiyakrutta*

Co-advisor's signature...........

# ACKNOWLEDGEMENTS

I would like to express my deepest grateful appreciation to my thesis advisor, Associate Professor Dr. Nattaya Ngamrojanavanich for her valuable advice, guidance, and encouragement throughout the research study.

I would like to express my greatest appreciation to Associate Professor Dr. Nongluksna Sriubolmas for her guidance, suggestion, encouragement, and great kindness throughout the research study.

I would like to thank Assistant Professor Dr. Suthep Wiyakrutta for his helpful suggestion, guidance, and also his kindness throughout the research, that enable me to pass through this course successfully.

I would like to express my sincere gratitude to my thesis co-advisor, Dr. Prasat Kittakoop for his guidance, consultation, constructive criticism, and great kindness throughout the research study.

I would like to express my deepest and sincere gratitude to Professor Dr. Somsak Ruchirawat for his helpful suggestion, and kindness throughout the research study.

I would like to thank Associate Professor Dr. Pintip Pongpetch for her kindly provided on methicillin-resistant MRSA 384.

I am particularly grateful to chairman of thesis committee, Associate Professor Sirirat Kokpol, Associate Professor Amorn Petsom and Dr Maneekarn Chinworrungsee as committee and for their editorial assistance and comments.

I would like to thank my friends and all members of the Program of Biotechnology, Faculty of Sciences, Chulalongkorn University, the Department of Microbiology (B600 and B601), Faculty of Sciences, Mahidol University, and Chulabhorn Research Institute (CRI) for their friendship, help and encouragement.

Finally, I am thankful to my family and especially my parents who have shown their great patience, moral support, and encouragement in every way possible to enable me to succeed in my education.

# CONTENTS

ศูนย์วิทยทรัพยากร
จุฬาลงกรณ์มหาวิทยาลัย

# LIST OF TABLES

ศูนย์วิทยทรัพยากร
จุฬาลงกรณ์มหาวิทยาลัย

# LIST OF FIGURES

| Figure | | page |
|---|---|---|

# LIST OF SCHEMES

# LIST OF ABBREVIATIONS

| | | |
|---|---|---|
| acetone-$d_6$ | = | deuterated acetone |
| bp | = | Base pairs |
| $^{\circ}$C | = | degree Celsius |
| $^{13}$C NMR | = | carbon-13 nuclear magnetic resonance |
| $CDCl_3$ | = | deuterated chloroform |
| $CHCl_3$ | = | chloroform |
| $CH_2Cl_2$ | = | methylene chloride |
| CMA | = | Corn Meal Agar |
| $\delta$ | = | chemical shift |
| $d$ | = | doublet (for NMR spectral data) |
| $dd$ | = | doublet of doublets (for NMR spectral data) |
| DNA | = | Deoxyribonucleic acid |
| DEPT | = | distortionless enhancement by polarization transfer |
| $\varepsilon$ | = | molar absorptivity |
| e.g. | = | for example |
| et al. | = | and other |
| EtOAc | = | ethyl acetate |
| ESI-TOF MS | = | Electrospray Ionization Time of Flight Mass |
| g | = | gram |
| µg | = | microgram |
| h | = | hour |
| $^1$H-$^1$H COSY | = | Homonuclear (proton-proton) correlation spectroscopy |
| $^1$H NMR | = | proton nuclear magnetic resonance |
| HMBC | = | $^1$H-detected heteronuclear multiple bond correlation |
| HMQC | = | $^1$H-detected heteronuclear multiple quantum coherence |
| Hz | = | Hertz |

| | | |
|---|---|---|
| $IC_{50}$ | = | inhibitory concentration required for 50% inhibition of growth |
| IR | = | infrared |
| ITS | = | internally transcribed spacers |
| $J$ | = | coupling constant |
| L | = | liter |
| µl | = | microliter |
| $\lambda_{max}$ | = | wavelength at maximum absorption |
| M | = | Molar |
| $[M+Na]^+$ | = | pseudomolecular ion |
| $m$ | = | multiplet (for NMR spectral data) |
| MCzB | = | Malt Czapek Broth |
| MEA | = | Malt Extract Agar |
| MeOH | = | methanol |
| MES | = | Malt Extract Sucrose medium |
| mg | = | milligram |
| MIC | = | minimum inhibitory concentration |
| min | = | minute |
| ml | = | milliliter |
| mm | = | millimeter |
| mM | = | millimolar |
| MHz | = | megahertz |
| MS | = | mass spectroscopy |
| m/z | = | mass to charge ratio |
| $\gamma_{max}$ | = | wave number at maximum absorption |
| nm | = | nanometer |
| NMR | = | nuclear magnetic resonance |
| NTP | = | Nucleotide triphosphate |
| PCR | = | polymerase chain reaction |

| | | |
|---|---|---|
| PDA | = | Potato Dextrose Agar |
| PDB | = | Potato Dextrose Broth |
| ppm | = | part per million |
| $q$ | = | quartet (for NMR spectral data) |
| rDNA | = | Ribosomal deoxyribonucleic acid |
| rpm | = | Round per minute |
| rRNA | = | Ribosomal ribonucleic acid |
| $s$ | = | singlet (for NMR spectral data) |
| SDA | = | Sabouraud's Dextrose Agar |
| SDB | = | Sabouraud's Dextrose Broth |
| sp. | = | species |
| $t$ | = | triplet (for NMR spectral data) |
| TAE | = | Tris-HCl, acetate and EDTA |
| TE | = | Tris-HCl and EDTA |
| $T_m$ | = | Melting temperature |
| TLC | = | thin layer chromatography |
| U | = | Unit |
| UV | = | ultraviolet |
| V | = | Volt |
| v | = | Volume |
| w | = | Weight |
| YCzB | = | Yeast Czapek Broth |
| YEA | = | Yeast Extract Agar |
| YES | = | Yeast Extract Sucrose medium |

# CHAPTER I

## INTRODUCTION

The development of drug resistance in human pathogenic bacteria such as *Staphylococcus* sp., *Mycobacterium tuberculosis*, *Streptococcus* sp. and others has prompted an urgent need to search for more and better antibiotics. Together with this is increasing need for more and better antimycotics, especially as the human population is encountering more fungal infections as a result of the AIDS epidemic and the increased numbers of patients with organ transplants, or other immunocompromised conditions. In addition, there are not many drugs for the treatment of parasitic protozoan infections, e.g. malaria (Strobel, 2003). Increased efforts are therefore needed to search for and develop new drugs from natural bioresources. Of the drug-producing microbes employed for pharmaceutical industry, fungi are probably not only the most important, but also the most poorly studied organisms. Fungi are everywhere, and affect us in many ways. They are one of the most diverse groups of organisms on earth (Hawksworth, 1991). Very importantly, fungi have been known to be a rich source of bioactive compounds which are of pharmaceutical interest. Examples are *Penicillium chrysogenum* (penicillin), *Cephalosporium acremonium* (cephalosporin), *P. griseofulvum* (griseofulvin), *Monascus ruber* and *Aspergillus terreus* (lovastatin). The estimated numbers of fungi are over 1.5 million species worldwide. To date, however, approximately 72,000 fungal species have been recorded and they are associated with various higher organisms as either parasites or saprophytes on dead and dying biological materials. Cumulatively from previous reports, 5,000 – 7,000 taxonomic species have been studied and about 4,000 fungal metabolites are describes (Dreyfuss & Chapela, 1994). Some relatively unexplored fungal groups derived from such ecosystems, e.g., fresh-water fungi, marine fungi and endophytic fungi which are potential sources for the production of a diverse array of bioactive metabolites.

Interestingly, particular fungal endophytes are able to produce bioactive molecules including a useful anticancer drug paclitaxel (Taxol[®]) from a fungal endophyte *Taxomyces andreanae* derived from Pacific yew (*Taxus brevifolia*) (Strobel and Stierle, 1993) and camptothecin, a drug for treatment of ovarian and colon cancers, from an unidentified endophytic fungi derived from *Nothapodytes foetida* (Puri *et al.*, 2005). Thus, living plants are interesting source for screening of new microorganisms that may produce novel functional metabolites.

Endophytic fungi are fungi which spend the whole or part of their life cycles colonizing inter- and/or intra-cellularly inside the healthy tissues of their host plants and typically causing no apparent symptoms of diseases (Chanway, 1996). Some of these fungal endophytes produce bioactive substances that may involve in a host-endophyte relationship. For example, 3-NPA (3-Nitropropionic acid), which have both ecological and biological impacts, is involved in nitrification process in leguminous plants and benefits the hosts to fight against plant parasitic nematodes (Chomcheon *et al.*, 2005). A direct result of the role that these secondary metabolites may play in nature, they may ultimately have application in medicine. A worldwide scientific effort to isolate fungal endophytes and study their natural products is now under way. While there are myriads of epiphytic microorganisms associated with plants, the fungal endophytes now seem to attract more attention. This may be the case, since closer biological associations may have developed between these organisms in their respective hosts than the fungal epiphytes (fungi living on the outside of the plant) or soil-related organisms. Hence, the result of this may be the production of a greater number and diversity of classes of biologically derived molecules, possessing a range of biological activities. In fact, a recent comprehensive study has indicated that 51% of biologically active substances isolated from endophytic fungi were previously unknown. This compares with only 38% of novel substances from soil microflora (Strobel, 2003).

In Thailand, there are a few reports on Thai endophytic fungi. For instances, endophytic fungi were isolated from indigenous dicotyledonous plants at Doi Suthep-Pui area from the northern Thailand (Lumyong *et al.*, 1997). Wiyakrutta *et al.*, (2004) have

isolated endophytic fungi from 81 Thai medicinal plant species collected from forests in four geographical regions of Thailand, and evaluated their crude extracts for biological activities. Chemical investigation of a broth extract of *Phomosis* sp. that was isolated from leaf of *Urobotrya siamensis* led to the isolation of a potent antimycobacterial agent ($IC_{50}$ 3.3 µM), 3-nitropropionic acid (Chomcheon *et al.*, 2005). Kongsaeree and co-workers, in 2003, isolated antimalarial dihydroisocoumarins produced by *Geotrichum* sp. from *Crassocephalum crepidioides*. Mycoepoxydiene derivatives, cytotoxic compounds, produced by *Phomopsis* sp. Hant25, have been isolated from *Hydnocarpus anthelminthicus* (Prachya *et al.*, 2007). In 2008, Chinworrungsee and colleagues reported about "brefeldin A", a cytotoxic compound, produced by *Hypocreales* sp. Klar5 isolated from *Knema laurina (Blume) Warb*. Two antimalarial compounds, monocerin and 11-hydroxymonocerin, were produced by *Exserohilum rostratum* which was isolated from *Stemona* sp. (Sappapan *et al.*, 2008). The great diversity of flora and fauna in Thai forests are well documented, however very little is known about the fungal endophytes. Those background information led us to speculate that Thai medicinal plants might constitute another source of endophytic fungi with biologically active compounds. Examples of secondary metabolites of fungal endophytes from Thai medicinal plants are shown in Figure 1.

In this research, endophytic fungi isolated from *Lindenbergia philippensis* and *Leea rubra* will be screened for their abilities to produce bioactive substances because both plants have been used in Thai traditional medicines for the treatment of many diseases. Until now, there has been no report on fungal endophytes isolated from *L. philippensis* before. In previous study by Chomcheon *et al.*, (2006), two new natural products, 2-hydroxymethyl-3-methyl-cyclopent-2-enone (synthetically known), and *cis* 2-hydroxymethyl-3-methyl-cyclopentanone and a known compound, asterric acid, were isolated from the endophytic fungus, mitosporic Dothideomycete sp. LRUB20, which was isolated from the stem of *L. rubra*. Cyclopentanones are useful intermediates in organic syntheses. The term "white biotechnology" has been recently introduced for microbial production of chemical building blocks. We therefore explored bioactive

compounds and other useful substances from Thai medicinal plants (*Lindenbergia philippensis* and *Leea rubra*).



3-Nitropropionic acid

1, R = OH
2, R = Ac

Mycoepoxydiene and its derivative

Dihydroisocoumarins

Brefeldin

Monocerin          11-Hydroxymonocerin
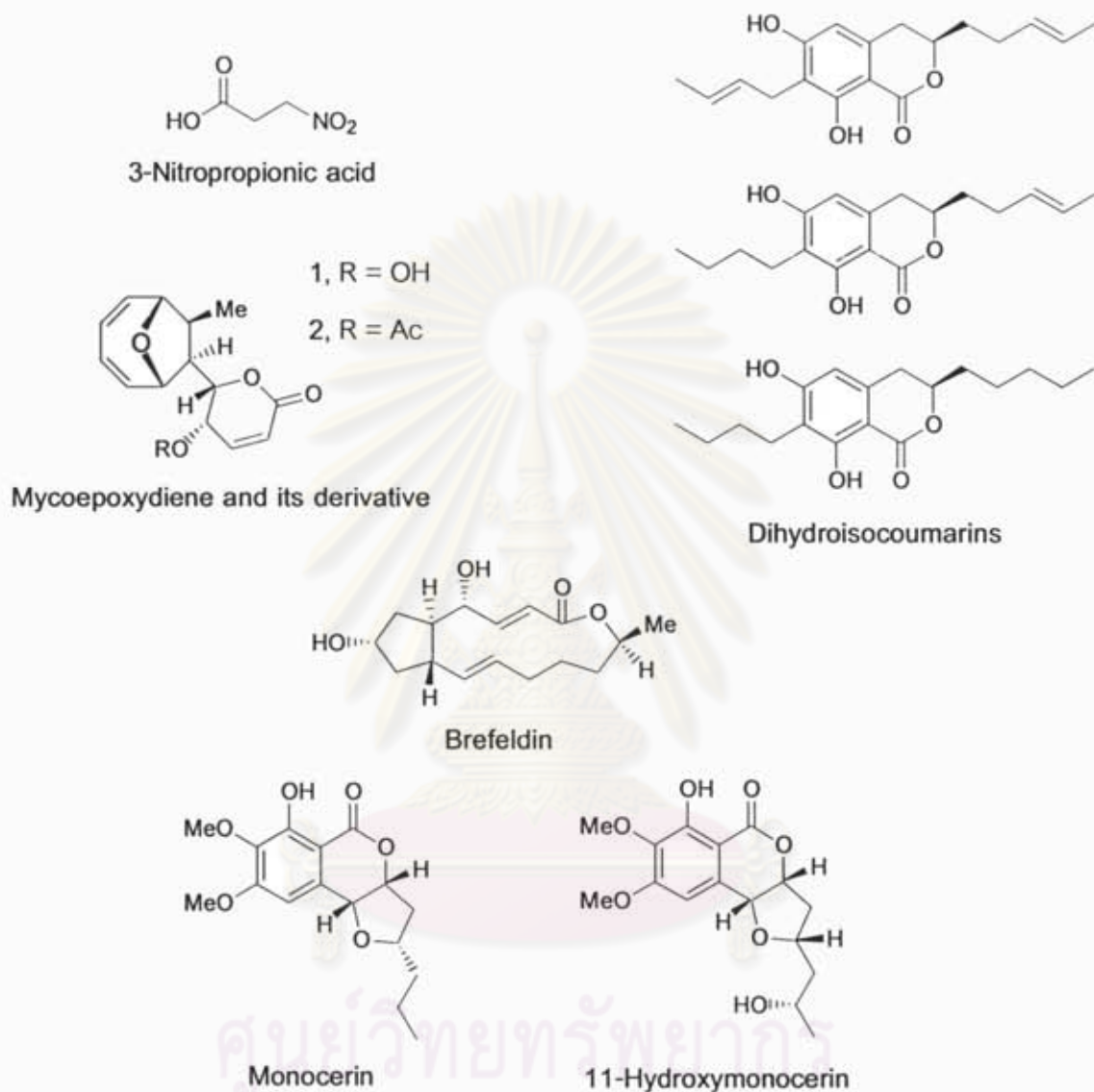
**Figure 1**    Examples of secondary metabolites obtained from fungal endophytes of Thai medicinal plants.

The objectives of this study are as follows:

1. To isolate endophytic fungi from *Lindenbergia philippensis* and *Leea rubra*

2. To isolate and chemically characterize bioactive compounds from selected endophytic fungi

3. To identify endophytic fungi based on morphology and molecular methods

4. To evaluate biological activities of the isolated compounds

# CHAPTER II

# REVIEW OF LITERATURES

Fungal endopytes live internally, either intercellularly or intracellularly, and asymptomatically (i.e. without causing any signs of tissue damage) within plant tissue (Figure 2) (Bills, 1996). Endophytes usually occur in above-ground plant tissues, but also occasionally in roots, and are distinguished from mycorrhizae by lacking external hyphae or mantels. They differ from pathogenic fungi on the basis of asymptomatic growth under most conditions while they, in contrast to epiphytes, are contained entirely within the substrate plant and may be either parasitic or symbiotic. The relationship between the fungal endophytes and its host plant may range from mutualistic symbiosis, or commensalism to borderline parasitism (Isaac, 1992).
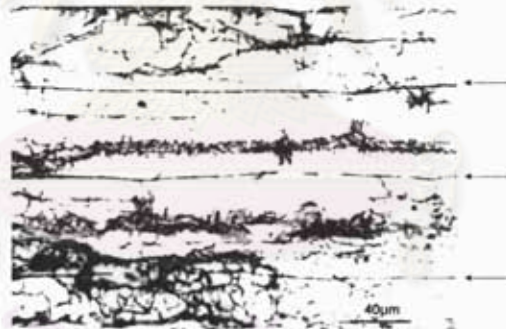


Figure 2    Endophytic fungal hyphae (arrows) in plant tissue (Image from: http://www. forages.oregonstate.edu).

Nowadays, research attention is being focused to the endophytic biodiversity related ecological functions and bioactivities of fungal metabolites.

2.1.    Biological survey of endophytic fungi

### 2.1.1 Distribution and biodiversity

Almost all vascular plant species examined to date were found to harbor endophytic bacteria and/or fungi (Arnold et al., 2000). Moreover, the colonization of endophytes in marine algae, mosses and ferns has also been recorded. As a matter of fact, endophytes are important components of microbial biodiversity. Commonly, several to hundreds of fungal species can be isolated from a single plant, among them, at least one species showing host specificity. The environmental conditions under which the host is growing also affect the endophytic population and the endophyte profile may be more diversified in tropical areas. Tropical endophytes themselves could be hyperdiverse with host preference and spatial heterogeneity. Accordingly, endophytes are presumably ubiquitous in the plant kingdom with the population being dependent on host species and location (Charlie and Watkinson, 2001).

### 2.1.2 Origin and evolution

Some phytopathogens in the environment are of endophyte origins. Many harmless endophytic fungi are quiescent phytopathogens which may cause infectious symptoms when the host plant is aged and/or stressed. On the other hand, during the long co-evolution of the phytopathogen and its host plant, an endophytic mutant may result from balanced antagonism and/or gene mutation. Dual cultures of the host calli and endophytes demonstrated that both the endophytes and the host calli excrete metabolites toxic to each other (Tan and Zou, 2001). Further investigation led to the development of a hypothesis that the endophyte–host interaction could be a balanced pathogen–host antagonism. Some naturally occurring nonpathogenic endophytes developed from the mutation such as some single locus in the genome of the wild-type. This mutant is able to grow systemically inside the host plant without pathogenic symptoms, but retaining wild-type levels of in vitro sporulation, spore adhesion, appressoria formation, infection and host specificity (Freeman and Rodriguez, 1993).

The Acremonium (an anamorph form in the genus Neotyphodium) endophytes, which usually inhabit tall fescue of Lolium perenne L. (perennial ryegrass) and many cool-

season grasses, are considered mutualistic symbionts of the host grasses. The grass and the endophytic fungus are so intimately associated that they act 'as a whole', much like 'a single organism'. And, indeed, some of these endophytic *Neotyphodium* species can only spread by infecting seeds from the mother plants (Figure 3) (Schardl *et al.*, 2004).
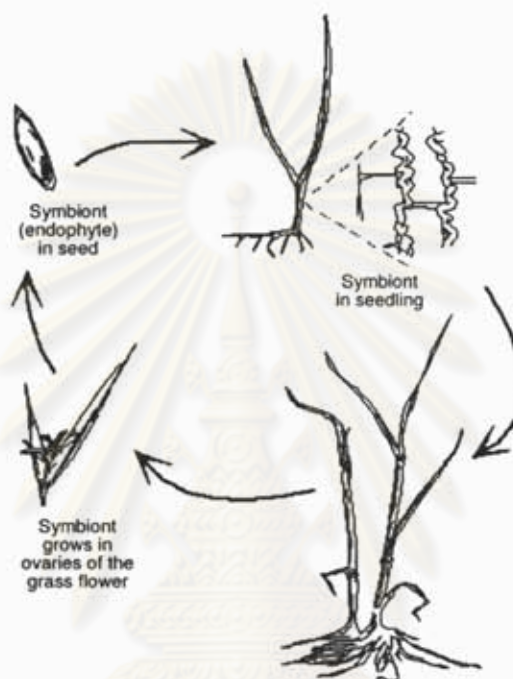


Figure 3      Schematic illustration of endophyte–grass symbiont (Image from University of Kentucky, http://www.ca.uky.edu)

Grass endophytes are generally considered to be mutualists because the fungus subsists entirely on the resources of the host. The host receives benefits through increased resistance to herbivores, pathogens and drought and flooding stress, and enhanced competitive abilities.

2.1.3   Physiological and ecological roles
Endophytes colonizing inside plant tissues usually get nutrition and protection from the host plant. In return, they confer profoundly enhanced fitness to the host plants by producing certain functional metabolites as shown in Table 1.

Table 1    Benefits to the partner

| Benefits | |
|---|---|
| Plant | Fungus |
| Increased : - Growth | - Refuge |
|      - Reproduction | - Nutrition |
|      - Resistance | - Transmission |

[Table adapted from: Saikkonen *et al*. 2004. Trends in Plant Science. 9: 276]

### 2.1.3.1 Growth promotion of the host plant

Plants infected by endophytic fungi often grow faster than non-infected ones. The effect is at least in part due to the phytohormones production of endophytic fungi e.g. cytokines, indole-3-acetic acid (IAA), and other plant growth-promoting substances, and/or partly owing to the fact that endophytes could have enhanced the nutritional elements uptake rate of host such as nitrogen and phosphorus. A culture broth of *Colletotrichum gloeosporioides*, an endophyte fungus of *Artemisia annua* L., has also been found to be able to promote the growth of the host callus (Figure 4) (Tan and Zou, 2001).



Figure 4    An *Artemisia annua* endophyte culture liquid can significantly promote the growth of host callus incubated on MS medium without (A) and with (B) 10% endophyte culture liquid (Tan and Zou, 2001)

### 2.1.3.2 Improvement of the hosts' ecological adaptability

Endophytic fungi are able to improve the ecological adaptability of hosts by enhancing their tolerance to environmental stresses and resistance to phytopathogens and/or herbivores e.g. endophyte-infected grasses usually possess an increased tolerance to drought and aluminium toxicity. Furthermore, some endophytes can provide the protection against some nematodes to their hosts, mammal and insect herbivores as well as bacterial and fungal pathogens (Christensen *et al.*, 1997). Some endophytes are capable of enhancing the allelopathic effects of their hosts on other species co-growing nearby, usually being competitor(s) for the nutrition and the space. This could be the reason why some plants with special fungal endophytes are usually competitive enough to become dominant species in successional fields (Tan and Zou, 2001).

## 2.2 Study of bioactive compounds from the endophytic fungi

In the 1970's, endophytic fungi were initially considered only for identification and classification, not causing benefits nor showing detriment to plants. Until in the past two decades, the interest for endophytic fungi was as potential sources of novel bioactive compounds that exhibited interesting bioactivities such as antibiotic, antiviral, anticancer, antioxidant, insecticidal, antidiabetic, and immunosuppressive activities (Azevedo *et al.*, 2000).

### 2.2.1 Antibiotic activity

Antibiotics are low-molecular-weight organic natural products made by microorganisms that are active at low concentration against other microorganisms (Demain, 1981). Fungal endophytes are a source of these antibiotics which were produced to inhibit or kill a wide variety of harmful disease-causing agents including phytopathogens, as well as bacteria, fungi, viruses, and protozoans that affect humans and animals.

*Cryptosporiopsis quercina* demonstrated its ability to produce a unique peptide antimycotic 'cryptocandin' against some important human fungal pathogens such as

*Candida albicans* and *Trichophyton* spp. (Strobel *et al.*, 1999). This compound contains a number of unusual hydroxylated amino acids and a novel amino acid: 3-hydroxy-4-hydroxy methyl proline (Figure. 5).
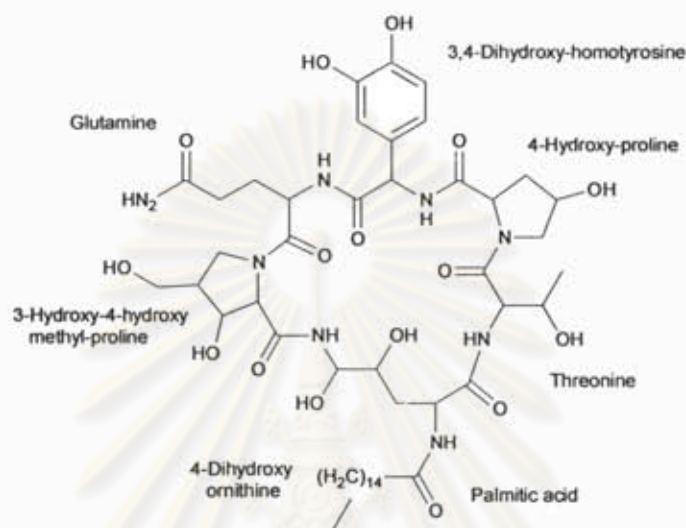


**Figure 5** Cryptocandin A, an antifungal peptide obtained from the endophytic fungus *C. quercina.*

Cryptocandin is also active against some plant-pathogenic fungi, for example, *Botrytis cinerea* and *Sclerotinia sclerotiorum*, and together with its related compounds, they are currently being considered for use against diseases of skin and nails caused by some fungi. *C. quercina* is able to produce cryptocin (a unique tetramic acid), (Figure 6), the unusual compound possesses potent activity against *Pyricularia oryzae* and some of other plant-pathogenic fungi (Li *et al.*, 2000) but, was generally ineffective against a general array of human pathogenic fungi. Nevertheless, with MICs of cryptocin for *P. oryzae* being 0.39 µg/ml, it is being examined as a natural chemical control agent for rice blast and is also being used as a base model to synthesize other antifungal compounds.

A rainforest endophytic fungi *Pestalotiopsis microspora* is able to produce ambuic acid, a secondary metabolite with an antifungal activity. Ambuic acid (Figure 7), a higly

functionalized cyclohexenone, has served as a model to develop new solid-state NMR methods for the structural determination of organic substances (Harper *et al.*, 2003a).
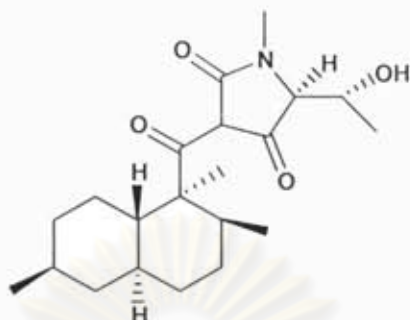
**Figure 6** Cryptocin, a tetramic acid antifungal compound produced by *C. quercina*.
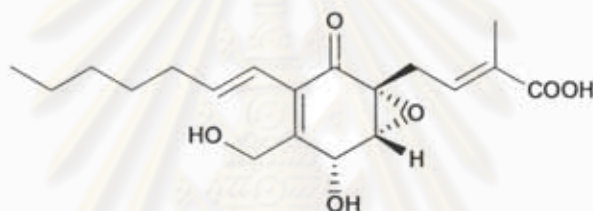
**Figure 7** Ambuic acid, an antifungal compound, produced by *P. microspora*.

*Pestalotiopsis jesteri*, a newly described species of *Pestalotiopsis* from the Sepik River area of Papua New Guinea, produces jesterone (Figure 8) and hydroxy-jesterone which exhibit antioomycete activity against a variety of plant-pathogenic fungi (Li and Strobel, 2001). Subsequently, jesterone has been prepared by organic synthesis with complete retention of biological activity (Hu *et al.*, 2001).
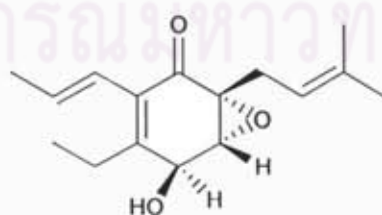
**Figure 8** Jesterone, a cyclohexenone epoxide from *P. jetsteri*, has antioomycete activity.

### 2.2.2 Antiviral activity

The inhibition of viruses is another fascinating use of antibiotic products from endophytic fungi. Two human cytomegalovirus (HCMV) protease inhibitors, cytonic acids A and B (Figure 9), have been isolated from the solid-state fermentation of the endophytic fungus *Cytonaema* sp. Their structures as *p*-tridepside isomers were elucidated by mass spectrometry and NMR methods (Guo *et al.*, 2000a).



Cytonic acid A                                             Cytonic acid B
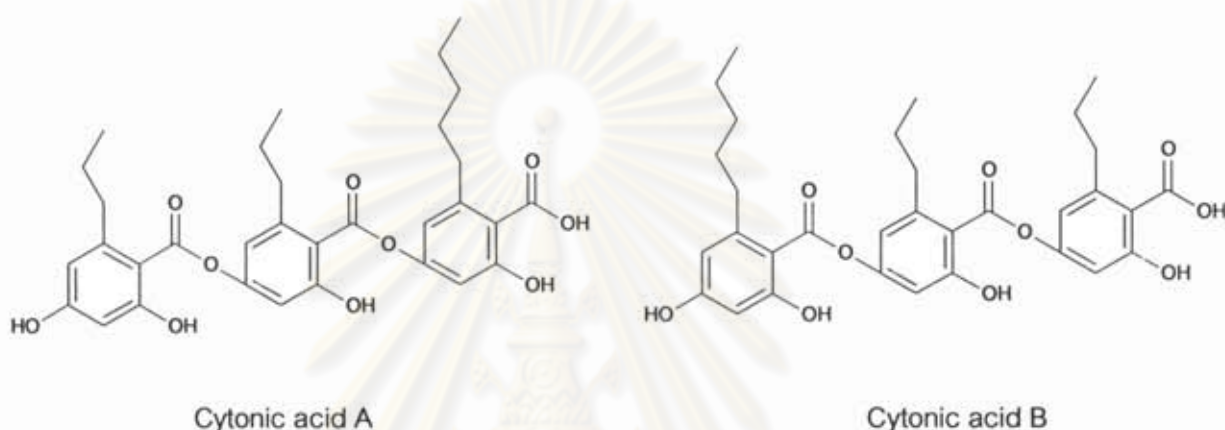
Figure 9        Cytonic acid A and B, a tridepside inhibitors of HCMV protease, derived from *Cytonaema* species.

### 2.2.3 Anticancer activity

The first major group of anticancer agents that is produced by endophytes are Paclitaxel and some of its derivatives (Figure 10). Paclitaxel, a highly functionalized diterpenoid, is found in yew (*Taxus*) species. The action mode of paclitaxel is to preclude tubulin molecules from depolymerizing during the processes of cell division (Suffness, 1995).

Surprisingly, in the year 1993, Strobel *et al.* isolated paclitaxel (Taxol[®], anticancer drug) from the endophytic fungus *Taxomyces andreanae* from its host Pacific yew *Taxus brevifolia*. After that, many reports shows that paclitaxel was also found in other endophytic fungi, for examples, *Pestalotiopsis guepinii* from *Wollemia nobilis* (Strobel *et al.*, 1997), *Periconia* sp. from *Torreya grandifolia* (Li *et al.*, 1998a), *Pestalotiopsis microspora* from *Taxus wallachina* (Li *et al.*, 1998b), *Tubercularia* sp. from *Taxus mairei* (Wang *et al.*, 2000),

*Aspergillus niger* from *Taxus chinensis* (Wang *et al.*, 2001), and *Stegolerium kukenani* from *Stegolepis guianensis* (Strobel *et al.*, 2001).
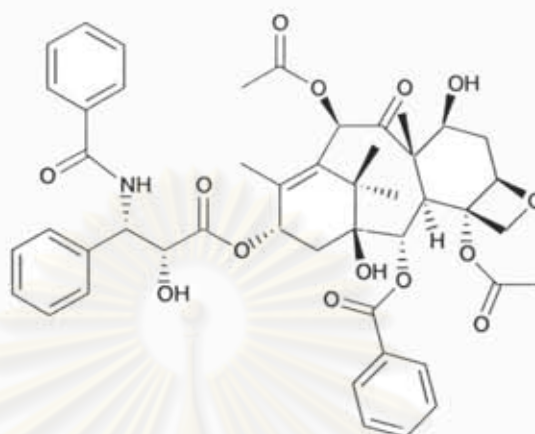


Figure 10    Paclitaxel produced by Pacific yew tree and endophytic fungi.

A pentacyclic quinoline alkaloid, camptothecin (Figure 11), belongs to a group of antineoplastic agents with a unique mechanism of action involving interference with eukaryotic DNA. Camptothecin and its derivatives show strong antineoplastic activity and were used for the treatment of skin diseases. Moreover, one of the primary cellular responses to its exposure is a rapid cessation of RNA synthesis. Camptothecin also displays a unique mechanism of action by inhibiting the intranuclear enzyme topoisomerase I, which is required for the swiveling and relaxation of DNA during molecular events, such as DNA replication and transcription (Puri *et al.*, 2005).

In 1966, 20(*S*)-camptothecin, the naturally occurring enantiomer, was first isolated from the wood of a plant native to mainland China *Camptotheca acuminata* Decne (Nyssaceae). Puri *et al.* (2005) found that camptothecin was produced by a fungus, belongs to the family Phycomycetes which was isolated from the inner bark of the plant *Nothapodytes foetida* (Wight) Sleumer (formerly *Mappia* foetida, Icacinaceae) from the western coast of India.
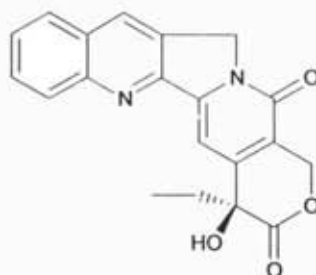
**Figure 11**    Camptothecin, a pentacyclic quinoline alkaloid, is a lead compound for anticancer drug.

Many alkaloids are also commonly found in fungal endophytes. Such fungal genera as *Xylaria, Phoma, Hypoxylon*, and *Chalara* are representative producers of a relatively large group of substances known as the cytochalasins, of which over 20 compounds are now known (Wagenaar *et al.*, 2000). Many of these compounds possess antitumor and antibiotic activities, but because of their cellular toxicity, they have not been developed into pharmaceuticals.

### 2.2.4    Antioxidant antivity

Pestacin and isopestacin have been obtained from culture fluids of *P. microspora*, a fungal endophyte isolated from a combretaceaous plant, *Terminalia morobensis*, growing in the Sepik River drainage of Papua New Guinea. Both pestacin and isopestacin display antimicrobial as well as antioxidant activity. Isopestacin was proposed to posses antioxidant activity based on its structural similarity to flavonoids (Figure 12). Indeed, the antioxidant activity of pestacin is at least 1 order of magnitude greater than that of trolox, a vitamin E derivative (Harper *et al.*, 2003b).
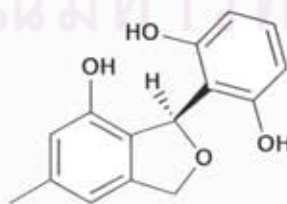


**Figure 12**    Pestacin, a metabolite of a fungal endophyte *P. microspora*, isolated from *T. morobensis*.

### 2.2.5 Insecticidal activity

Many reports showed that several fungal endophytes are known to have anti-insect properties. And even bioinsecticides are only a small part of the insecticide field, but their market is increasing rapidly, for example, nodulisporic acids, novel indole diterpenes that exhibit potent insecticidal properties against the larvae of the blowfly. The mechanism of action of nodulisporic acid (Figure 13) is by activating insect glutamate-gated chloride channels. The first nodulisporic compound was isolated from an endophyte, a *Nodulisporium* sp., from the plant *Bonlia daphnoides.* As all around our world worries about ecological damage done by synthetic insecticides, fungal endophytic research continues for the discovery of powerful, selective, and safe alternatives (Stobel and Daisy 2003).
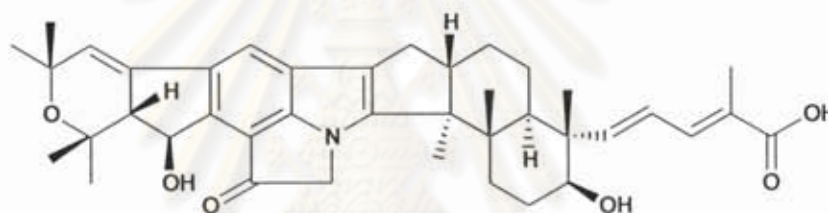


**Figure 13**   Nodulisporic acid, an indole diterpene, exhibited potent insecticidal property.

### 2.2.6 Antidiabetic activity

Zhang *et al.* (1999) reported on compound L-783,281 (Figure 14), a nonpeptidal fungal metabolite, which was isolated from an endophytic fungus (*Pseudomassaria* sp.) collected from an African rainforest near Kinshasa in the Democratic Republic of the Congo. These researchers found that L-783,281 acts as an insulin mimetic and is not destroyed in the digestive tract and may be given orally. Oral administration of this compound to two mouse models of diabetes resulted in significant lowering of blood glucose levels. These results may lead to new therapies for diabetic patients.

### 2.2.7 Immunosuppressive activity

Lee *et al.* (1995) showed that the endophytic fungus *Fusarium subglutinans*, isolated from *Tripterygium wilfordii*, is able to produce the immunosuppressive but noncytotoxic diterpene pyrone subglutinol A (Figure 15). At present, many immunosuppressive drugs are applied to prevent allograft rejection in transplant patients, and in the future they could be used to treat autoimmune diseases such a rheumatoid arthritis and insulin-dependent diabetes.
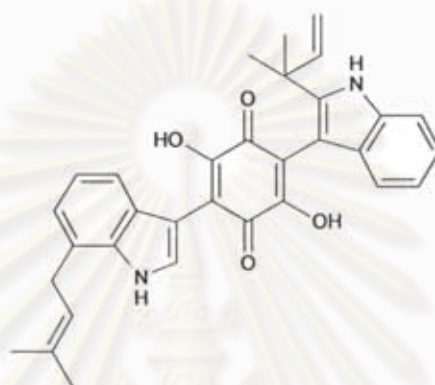
**Figure 14** Structure of L-783,281, a nonpeptidal metabolite, isolated from *Pseudomassaria* sp.
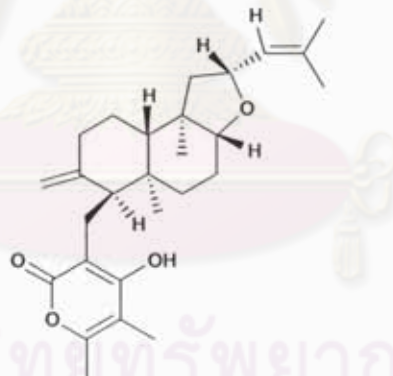
**Figure 15** Subglutinol A, an immunosuppressant, produced by the endophytic fungus *F. subglutinans.*

2.3    Plant sources of endophytic fungi

2.3.1   *Leea rubra*

*Leea rubra*, which is called in Thai as "กระตังใบ", "กระตังแดง", "เขือง", "บังใบ", "กระตังใบ" or "เขืองแขงม้า", (Figure 16), is a plant species in the genus Leea

commonly found throughout Northern and eastern Australia, New Guinea, South and Southeast Asia and parts of Africa. It is the only genus in the family Leeaceae.

The height of *L. rubra* is about 2 to 4 meters. Leaves are alternately imparipinnate type; leaflets have oblong shape with the width about 4 to 6 cm and 12 to 18 cm in length, with its stipules forming a sheath. It is inflorescence in leaf-opposed, corymb with light green corolla. Their fruits have compressed-globose shape and will turn dark red or black when they ripe. Its root can be used as the antipyretic and diaphoretic drug for relief of muscular pain or used as an ingredient in the preparation to treat leucorrhea, intestinal cancer, and uterus cancer (Chuakul *et al.*, 1997).



Figure 16    The picture of *Leea rubra* or "กระตังใบ" in Thai

### 2.3.2  *Lindenbergia philippensis*

*Lindenbergia philippensis* Benth, or in Thai name "หญ้าน้ำดับไฟ" (Figure 17), is a plant in the family Scrophulariaceae. It is widely spread on dry mountain sides, rocky crevices about 1,200-2,600 m above sea level in China (Guangdong, Guangxi, Guizhou, Hubei, Hunan, Yunnan), Cambodia, India, Laos, Myanmar, Philippines, Vietnam, and Thailand.

*Lindenbergia philippensis* Benth is a perennial tree with stout, erect, straight, much branched, glandular hairy. It has about 1 m in height. Their stems are terete in shape. Petiole is about 6-12 mm, and the leaf blades have ovate or ovate-lanceolate shapes. Papery leaves are about 2-8 cm, with cuneate shape; their margin are serrate type with

apex acute to acuminate. Inflorescences have at terminal with densely spicate-racemose shape about 6-20 cm. Its bracts are narrowly lanceolate shorter than calyx. Flowering has with subsessile. Calyx is about 5-6 mm, conspicuously 5-veined; lobes subulate-triangular, as long as tube, apex acute. Corolla are yellow and outside with purple patches, sparsely hairy; tube about 2 times as long as calyx's size; lower lip long, conspicuously plicate; upper lip apically subtruncate, sometimes emarginate. Anthers have long stalked which is style basally and apically hairy. Capsule with narrowly ovoid shape about 5-6 mm, densely brown hirsute apically. And seeds are yellow about 0.5 mm in size.

Fresh whole plant can be crushed with small amount of rice wisky and applied to the forehead for headache or common colds in children, or applied to relieve pain and inflammation from burns or abscesses. This plant can be squeezed to obtain juice which can be applied for vesicular skin infections.



Figure 17     The picture of *Lindenbergia philippensis* Benth or "หญ้าน้ำดับไฟ" in Thai

In the present study, endophytic fungi have been isolated from the surface-sterilized leaves and stems of *L. philippensis* and *L. rubra*, respectively, these plant species are of our interest because they have been used in Thai traditional medicine with various pharmacological activities. Therefore, the present study is involved in the isolation of endophytic fungi from *L. philippensis* and *L. rubra* and the isolation and characterization of bioactive compounds from the isolated fungi.

# CHAPTER III

# MATERIALS AND METHODS

## 3.1 Culture media and chemicals

### 3.1.1 Culture media

Culture media used for cultivation of endophytic fungi were Corn meal agar (CMA) (Difco), Malt extract agar (MEA) (Merck), Potato dextrose agar (PDA) (Merck), Sabouraud's dextrose agar (SDA) (Merck), malt extract powder (Merck), yeast extract powder (Merck), soytone (Merck) and agar base (agar-agar ultrapure granulated, Merck). Other mycological media were tap water agar (TWA), yeast extract sucrose medium (agar and broth) (YES), malt Czapek medium (agar and broth) (MCz), malt extract broth (MEB), malt extract sucrose broth (MES), potato dextrose broth (PDB), Sabouraud's dextrose broth (SDB), yeast Czapek broth (YCz), and M1D medium; the formula are shown in Appendix A.

### 3.1.2 Chemicals

Chemicals used in this study are as follows: boric acid (Merck, GR), ammonium tartrate (Merck, GR), sodium nitrate ($NaNO_3$) (BHD, AR), sodium chloride (NaCl) (Merck, GR), sodium hydrogen carbonate ($NaHCO_3$) (Merck, GR), sodium acetate (NaOAc) (Sigma, AR), disodium hydrogen phosphate ($Na_2HPO_4$) anhydrous (Merck, GR), potassium dihydrogen phosphate ($KH_2PO_4$) anhydrous (Merck, GR), magnesium chloride ($MgCl_2$) (Merck, GR), calcium dinitrate [$Ca(No_3)_2$] (Merck, GR), potassium nitrate ($KNO_3$) (Merck, GR), ferric chloride ($FeCl_3$) (Merck, GR), manganese sulphate ($MnSO_4$) (Merck, GR), potassium iodide (KI) (Merck, GR), magnesium sulphate heptahydrate ($MgSO_4.7H_2O$) (Merck, GR), potassium chloride (KCl) (RiedeldeHaen, AR), dipotassium hydrogen phosphate ($K_2HPO_4$) (Merck, GR), zinc sulphate heptahydrate ($ZnSO_4.7H_2O$) (Merck, GR), copper sulphate pentahydrate ($CuSO_4.5H_2O$) (Merck, GR),

ferrous sulphate heptahydrate ($FeSO_4.7H_2O$) (Merck, GR), absolute ethanol (Merck, AR), 95 % ethanol (industrial grade), liquid paraffin (specific gravity of 0.83-0.89, medicinal grade), dichloromethane ($CH_2Cl_2$) (Labscan, AR), ethyl acetate (EtOAc) (Labscan, AR), phenol ($C_6H_5OH$) (Amersham, AR), Tris-HCl (Sigma), EDTA (Sigma, AR), methylene blue (Sigma), glycerol (Merck, GR), bromophenol blue (Sigma), chloroform-D, 99.9 atom %D (Merck), acetone-$d_6$, 99.9 atom %D (Aldrich), DMSO- $d_6$, 99.9 atom %D (Aldrich), silica gel 60 (70-230 mesh ASTM, Merck), and Sephadex LH-20 (Amersham Pharmacia Biotech Inc.).

Molecular biology grade reagents used were deoxynucleotide triphosphate (dATP, dCTP, dGTP, and dUTP) (FINNZYMES), *Taq* DNA polymerase (FINNZYMES), *Pst*I (FINNZYMES), and LE agarose (Seakerm®, FMC).

## 3.2    Collection of plant samples

Healthy leaves and branches of *Lindenbergia philippensis* and *Leea rubra* were collected from Kanchanaburi and Phitsanulok provinces, Thailand, respectively. The fresh-cut ends of plant samples were wrapped with paraffin film and they were placed in zip-lock plastic bags and stored in a refrigerator prior to isolation of endophytic fungi. The plant samples were used for the fungal isolation within 72 h after collection.

## 3.3    Isolation of fungal endophytes

Samples were washed under running tap water and then air-dried. The surface of leaves and branches was sterilized by immersion in 70% ethanol for 1 min, sodium hypochlorite solution (6% available chlorine) for 5 min, and sterile distilled water for 1 min two times. The surface-sterilized leaves and branches were cut into small pieces and placed on sterile water agar plates for incubation at 30°C. The hyphal tip of endophytic fungus growing out from the plant tissue were cut by a sterile pasture pipette and transferred to sterile potato dextrose agar plate. After incubation at 30°C for 7-14

days, culture purity was determined from colony morphology. The fungal isolates were stored for further study.

## 3.4    Selection of endophytic fungal isolates

Fungal isolates were selected for chemical investigation if they exhibited antimicrobial activities. The endophytic fungal isolates were grown on six mycological media, i.e. Czapek yeast autolysate agar, malt Czapek agar, malt extract agar, potato dextrose agar, Sabouraud's dextrose agar and yeast extract sucrose agar; and screened for antimicrobial activities by dual-culture agar diffusion assay (Sriubolmas *et al*., 2001). Agar plugs taken from grown culture were placed on the test plate previously inoculated with *Staphylococcus aureus* ATCC 25923, *Enterococcus faecalis* ATCC 29212, *Escherichia coli* ATCC 25922, *Pseudomonas aeruginosa* ATCC 27853, and *Candida albicans* ATCC 90028.

## 3.5    Screening of selected endophytic fungal isolates for the production of bioactive compounds

The endophytic fungal isolates were grown in 1-L Erlenmeyer flasks, containing 200 ml of appropriate culture medium. After 3 weeks of still culture at $25^{\circ}$C, the culture broth was filtered through four layers of cheesecloth to remove mycelium. The culture broth was extracted with ethyl acetate, and this crude extract was examined by analysis of its $^{1}$H NMR spectrum. Scheme 1 summarizes the whole extraction process. The fungal isolate LRUB20 was grown on Czapek yeast autolysate medium (CzYA) and M1D medium (supplemented with 0.5 g/L malt extract) and the isolate LPHIL36 was cultured on malt extract broth (MEB). They provided high yield of crude extract, and also showed interesting $^{1}$H NMR spectral profiles, (figures 18, 19 and 20), therefore, these fermentation conditions were selected for further studies.

Fungal isolates

↓ cultured in

1 L Erlenmeyer flask, containing 200 ml of various media (Tables 2 & 3)

static culture

25 $^{0}$C 3 weeks

Culture broth (200 ml)

filtered

Culture broth          Mycelia

partitioned with EtOAc (3 times)

EtOAc layers          Culture broth

concentrated

Crude extract

Analysis by $^{1}$H NMR spectrum
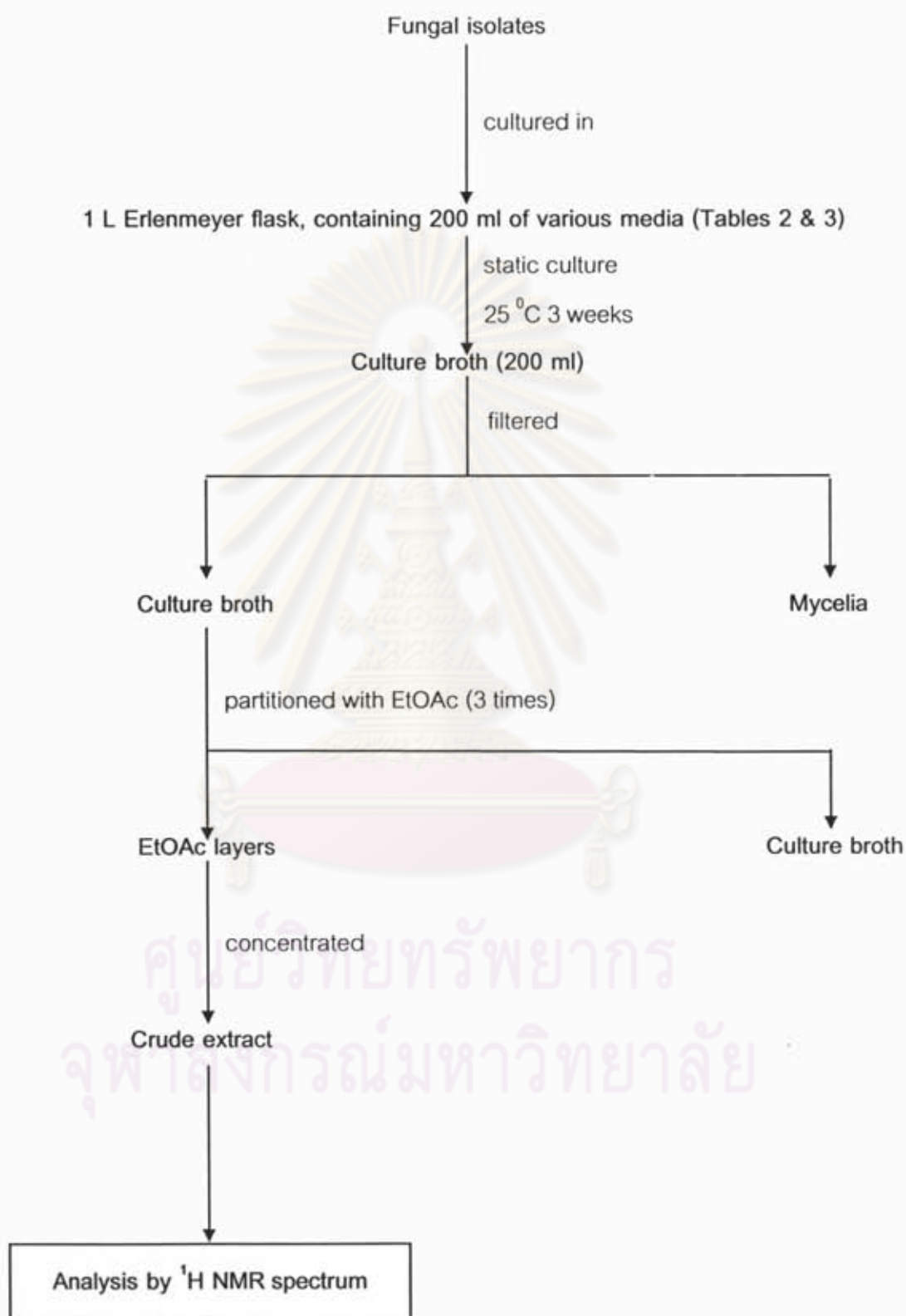
Scheme 1      General procedure for extraction of fungal culture broth
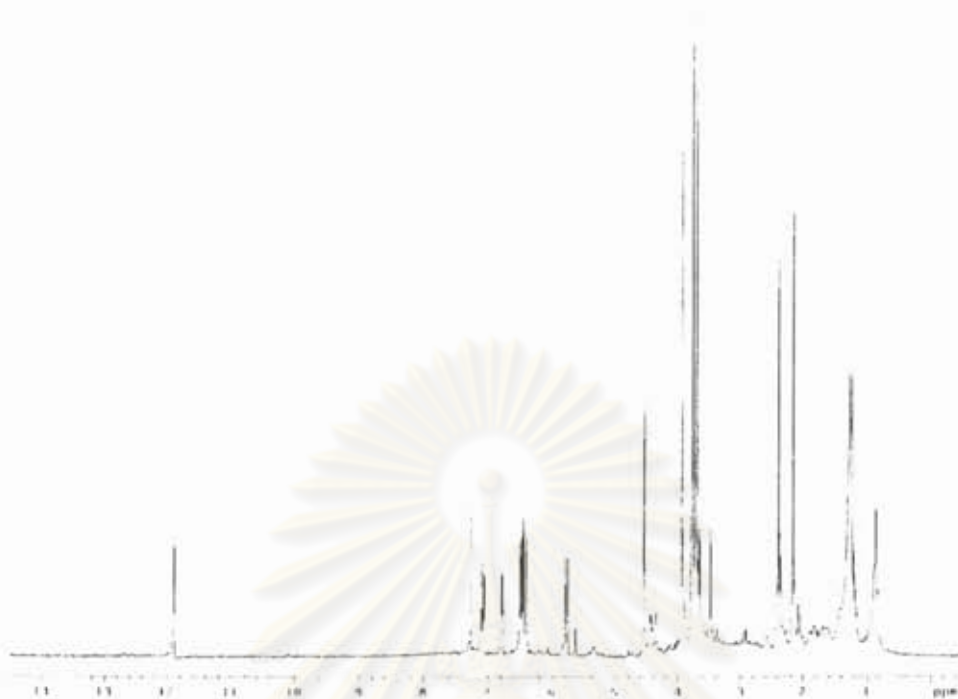
**Figure 18** The 200 MHz $^1$H-NMR (in CDCl$_3$) spectrum of crude extract on CzYA medium of the endophytic fungus isolate LRUB20
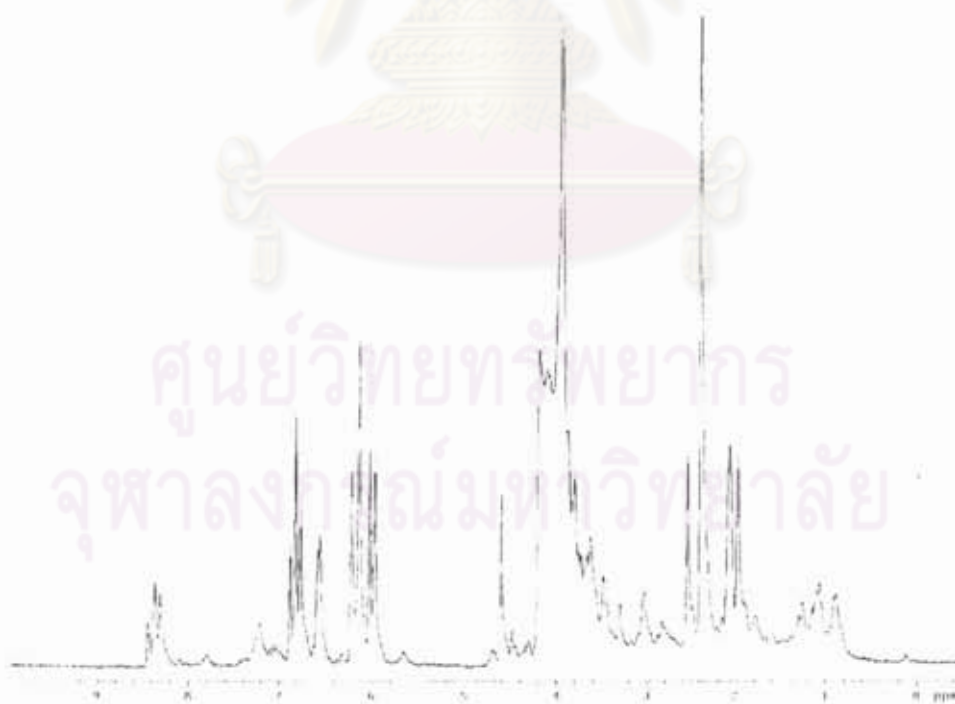


**Figure 19** The 200 MHz $^1$H-NMR (in CDCl$_3$) spectrum of crude extract on M1D medium (supplemented with 0.5 g/L malt extract) of the endophytic fungus isolate LRUB20
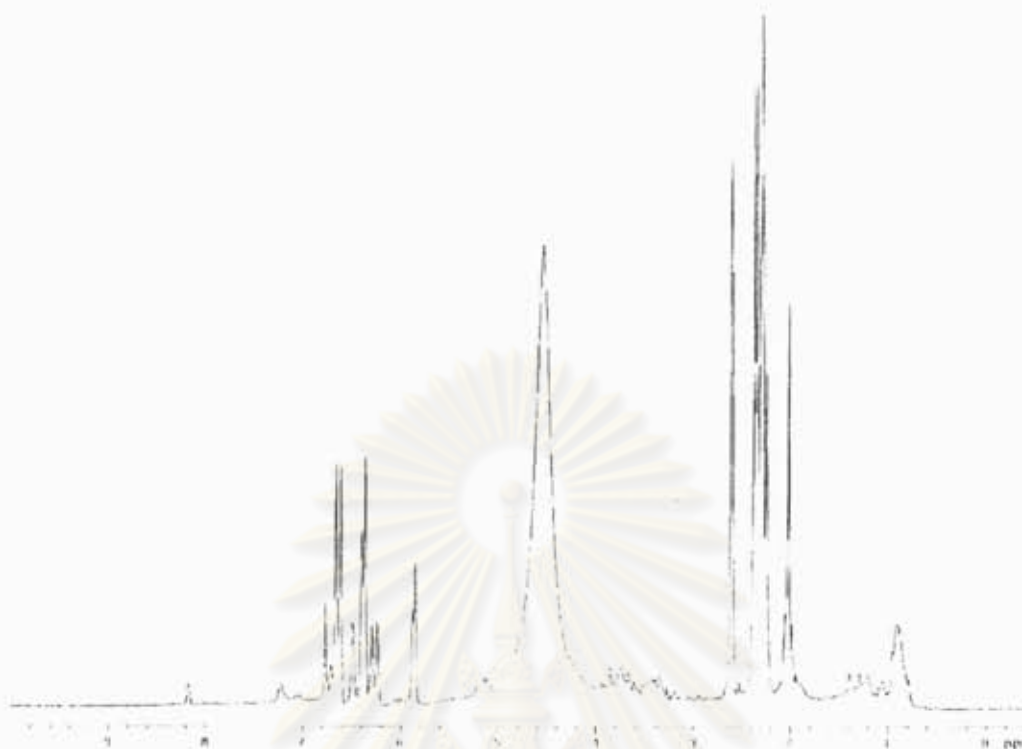
**Figure 20**     The 200 MHz $^1$H-NMR (in CDCl$_3$) spectrum of crude extract on MEB medium of the endophytic fungus isolate LPHIL36

## 3.6     Cultivation, extraction and deposition of fungi

### 3.6.1     Cultivation of fungi

The fungi of interest were grown on PDA plate at 30 $^\circ$C for 7 days. Six pieces (6x6 mm$^2$) of the grown culture cut from the plate were inoculated into 1-L Erlenmeyer flasks containing 200 ml of Czapek yeast autolysate medium (CzYA) or M1D medium (supplemented with 0.5 g/L malt extract) for the isolate LRUB20, and malt extract broth (MEB) for the isolate LPHIL36. Several flasks of culture were prepared to obtain 5 L of CzYA broth, 3.2 L of MID medium, and 5 L of MEB.

### 3.6.2 Extraction of fungi

The culture broth was passed through four layers of cheese cloth which were exhaustively pressed. The filtrate was extracted with an equal volume of ethyl acetate (EtOAc) for 3 times. The organic layers were combined and evaporated at $40\,^\circ C$ to yield a crude extract. The crude extract was dissolved in methanol or methylene chloride ($CH_2Cl_2$), and transferred to a vial. Fungal cells were sequentially macerated in MeOH and $CH_2Cl_2$, respectively, at room temperature, each of 2 days. Both MeOH and $CH_2Cl_2$ extracts were combined and evaporated under reduced pressure and partitioned twice with an equal volume of hexane. Then, the MeOH layer was added with 100 ml of $H_2O$ and partitioned with EtOAc to obtain mycelia crude extract. The extractions of the culture broth and cells of the isolates LRUB20 and LPHIL36 are shown in Scheme 2, Scheme 3 and Scheme 4.

### 3.6.3 Deposition of fungi

Endophytic fungi, isolate LRUB20 and isolate LPHIL36, were deposited at the Bioactive Metabolite Unit (B600), Department of Microbiology, Faculty of Science, Mahidol University. For short-term storage (< 1 year), the fungi were placed in distilled $H_2O$, and for longer term storage they were kept frozen at $-70\,^\circ C$ in 15% glycerol.

```
              ┌─────────────────────────────┐
              │   CzYA broth (5 L) of LRUB20 │
              └─────────────────────────────┘
                            │
                         filtered
                            │
          ┌─────────────────┴─────────────────┐
     ┌──────────┐                        ┌──────────┐
     │ Filtrate │                        │ Mycelia  │
     └──────────┘                        └──────────┘
```

partitioned (EtOAc) 3 times

marcerated
MeOH 2 days
CH₂Cl₂ 2 days

EtOAc layer     Residue

concentrated

**Broth crude extract**
**(1,400 mg)**

**Combine both MeOH and CH₂Cl₂ extracts**

filtered and

concentrated

**Extract with MeOH**

partitioned with

hexane (3 times)

Methanol layer     Hexane layer

concentrated

**MeOH extract**

added H₂O    Hexane fraction (lipids)

100 ml

**Aqueous extract**

partitioned (EtOAc) 3 times

EtOAc layer     Residue

concentrated

**Mycelial crude extract (900 mg)**

Scheme 2     Extraction of culture broth and mycelia of the fungus isolate LRUB20

```
                    ┌─────────────────────────┐
                    │  M1D broth (3.2 L) of LRUB20 │
                    └─────────────────────────┘
                                │ filtered
              ┌─────────────────┴─────────────────┐
        ┌──────────┐                        ┌──────────┐
        │ Filtrate │                        │ Mycelia  │
        └──────────┘                        └──────────┘
```

Filtrate → partitioned (EtOAc) 3 times

EtOAc layer                    Residue

EtOAc layer → concentrated → Broth crude extract (630 mg)

Mycelia → marcerated MeOH 2 days CH$_2$Cl$_2$ 2 days

Combine both MeOH and CH$_2$Cl$_2$ extracts

filtered and concentrated

Extract with MeOH

partitioned with hexane (3 times)

Methanol layer                Hexane layer

Methanol layer → concentrated → MeOH extract

added H$_2$O 100 ml

Hexane layer → Hexane fraction (lipids)

Aqueous extract

partitioned (EtOAc) 3 times

EtOAc layer                   Residue

EtOAc layer → concentrated → Mycelial crude extract (850 mg)

**Scheme 3**    Extraction of culture broth and mycelia of the fungus isolate LRUB20

```
                    ┌─────────────────────────────┐
                    │   MEB broth (5 L) of LPHIL36 │
                    └─────────────────────────────┘
                                   │ filtered
              ┌────────────────────┴────────────────────┐
        ┌───────────┐                             ┌───────────┐
        │  Filtrate │                             │  Mycelia  │
        └───────────┘                             └───────────┘
```

partitioned (EtOAc) 3 times        marcerated

                            MeOH 2 days

EtOAc layer      Residue         $CH_2Cl_2$ 2 days

        concentrated          Combine both MeOH and $CH_2Cl_2$ extracts

                                    filtered and

**Broth crude extract**             concentrated

**(4,500 mg)**                   Extract with MeOH

                                    partitioned with

                                    hexane (3 times)

Methanol layer        Hexane layer

         concentrated

MeOH extract

                added $H_2O$    Hexane fraction (lipids)

                100 ml

Aqueous extract

             partitioned (EtOAc) 3 times

EtOAc layer          Residue

       concentrated

**Mycelial crude extract (1,900 mg)**

**Scheme 4**      Extraction of culture broth and mycelia of the fungus isolate LPHIL36

3.7    Chromatographic techniques

    3.7.1    Thin-layer chromatography (TLC)

        3.7.1.1 Analytical thin-layer chromatography

| | |
|---|---|
| Technique | : one dimension ascending |
| Adsorbent | : silica gel $F_{254}$ coated on aluminium sheet (E. Merck) |
| Layer thickness | : 250 µm |
| Distance | : 4 cm |
| Temperature | : laboratory temperature 25 $^{\circ}$C |
| Detection | : 1. Visual detection under daylight |
| | 2. Visual detection under ultraviolet light at wavelengths of 254 and 356 nm |
| | 3. Visual detection under daylight after spraying with anisaldehyde reagent or 10% $H_2SO_4$ reagent and heat until color developed |

        3.7.1.2 Preparative thin-layer chromatography (PTLC)

| | |
|---|---|
| Technique | : one dimension ascending |
| Adsorbent | : silica gel $F_{254}$ coated on aluminium sheet (E. Merck) |
| Layer thickness | : 2000 µm |
| Distance | : 20 cm |
| Temperature | : laboratory temperature 25 $^{\circ}$C |
| Detection | : 1. Visual detection under daylight |
| | 2. Visual detection under ultraviolet light at wavelengths of 254 and 356 nm |

3.7.2 Column chromatography

3.7.2.1 Gel filtration chromatography

| | |
|---|---|
| Gel filter | : Sephadex LH-20 (Amersham Pharmacia Biotech Inc.) |
| Packing method | : Sephadex gel was suspended in the eluent and left overnight prior to use. It was then poured into the column and allowed to settle. |
| Sample loading | : The sample was dissolved in a small amount of eluent then applied gently on the top of the column. |
| Detection | : Fractions were examined by $^1$H NMR (400 MHz) spectroscopy and thin-layer chromatography. |

3.7.2.2 Silica gel column chromatography

| | |
|---|---|
| Gel filter | : Silica gel 60H (Merck code no. 7734) |
| Packing method | : Silica gel 60H was suspended in the eluent and left about 1-2 h prior to use. It was then poured into the column and allowed to settle. |
| Sample loading | : The sample was dissolved in eluent, added with a small amount of Silica gel 60H, dried and then applied gently on the top of the column. |
| Detection | : Fractions were examined by thin-layer chromatography and $^1$H NMR (400 MHz) spectroscopy. |

### 3.7.2.3 High performance liquid chromatography (HPLC)

Adsorbent : Reversed-phase column (LichroCARTRP $C_{18}$)

Sample loading : The sample was dissolved in a small amount of eluent (a mixture of MeOH and $H_2O$) then injected into the loop of the column.

Flow rate : 4.0 or 8.0 ml/min

Detection : UV-photodiode array detector

### 3.7.2.4 Medium pressure liquid chromatography (MPLC)

Adsorbent : Reversed-phase column (LichroCARTRP $C_{18}$)

Sample loading : The sample was dissolved in a small amount of eluent (a mixture of MeOH and $H_2O$) then injected into the loop of the column.

Flow rate : 20.0 ml/min

Detection : UV-photodiode array detector

## 3.8    Structure elucidation

Structures were elucidated by the interpretation of one and two dimensional NMR spectra. Additional spectroscopic techniques such as MS, UV-vis, FT-IR, and optical rotation properties and by comparison with literature values were also employed for the structural elucidation.

### 3.8.1 Nuclear magnetic resonance spectroscopy (NMR)

$^1$H NMR spectra were recorded on a Varian Gemini 2000 spectrometer operating at 200 MHz spectrometer (with $CDCl_3$, acetone-$d_6$ and DMSO-$d_6$ as solvents). $^1$H NMR spectra of pure compounds and all other NMR measurements were performed on a Bruker AM-400 (400 MHz), a Bruker ADVANCE DRX-500 (500 MHz) or a Bruker AVANCE 600 (600 MHz) spectrometer. NMR spectrometer was operated at 400, 500 or 600 MHz for proton, and 100, 125 or 150 MHz for carbon, respectively. NMR spectra of

pure compounds were processed using Bruker software. NMR spectra were calibrated using solvent signals ($^{13}$C: CDCl$_3$ 77.00 ppm, acetone-$d_6$ (CD$_3$COCD$_3$) 29.8 and 206.0 ppm and DMSO-$d_6$ (CD$_3$SOCD$_3$) 39.5 ppm) or a signal of the portion of the partly or non deuterated solvent ($^1$H: CHCl$_3$ in CDCl$_3$ $\delta$ 7.26 ppm, acetone in acetone-$d_6$ $\delta$ 2.05 ppm, water (H$_2$O) in acetone-$d_6$ $\delta$ 2.8 ppm, DMSO in DMSO-$d_6$ $\delta$ 2.50 ppm, and water (H$_2$O) in DMSO-$d_6$ $\delta$ 3.31 ppm). Structural assignments were based on the interpretation of the following NMR experiments: $^1$H, $^{13}$C, DEPT, $^1$H-$^1$H COSY, NOESY, $^1$H-$^{13}$C direct correlation (HMQC), and $^1$H-$^{13}$C long-range correlation (HMBC).

### 3.8.2 Mass spectrometry (MS)

EI-MS spectra were obtained from a Finnigan Mat GCQ mass spectrometer.

Accurate mass was obtained from the time of flight (TOF) mass spectrometric technique, using a Micro TOF, Bruker daltoincs by APCI ionization mode or ESI mode.

### 3.8.3 Ultraviolet-visible measurements (UV-vis)

UV-vis spectra were recorded on a Shimadzu UV-vis 2001s spectrophotometer.

### 3.8.4 Fourier transform infrared spectroscopy (FT-IR)

FT-IR spectra were recorded on a Perkin Elmer Spectrum One spectrophotometer. Samples for IR were examined using a Universal Attenuted Total Reflectance (UATR), solid or liquid (UATR-solid, UATR-liquid).

### 3.8.5 Optical rotation

Optical rotations were measured with using a sodium D line (589 nm) JASCO DPI-370 digital polarimeter equipped with a 1 mL cell (cell length 1.00 cm).

### 3.8.6 Melting point

Melting points were recorded on a Büchi 535.

3.9    Isolation of bioactive compounds from endophytic fungi isolate LRUB20 and isolate LPHIL36

### 3.9.1   Isolation of secondary metabolites from the endophytic fungus isolate LRUB20

A crude extract (1,400 mg) of the isolate LRUB20 cultured on CzYA medium (5 L) was subjected to Sephadex LH-20 column chromatography (CC) (3 x 85 cm), eluted with MeOH, to yield 14 fractions (A1-A14). Fraction A9 was re-crystallized from MeOH to afford asterric acid (11; 147 mg). Fraction A6 was further purified by Sephadex LH-20 CC (3 x 48 cm), eluted with MeOH, and ten fractions (B1-B10) were obtained. Fraction B6 was again subjected to purification on Sephadex LH-20 CC (2.5 x 52 cm) using MeOH as a mobile phase to provide fourteen fractions ($B_61$-$B_614$). Fraction $B_66$ was subjected to semi-preparative HPLC ($C_{18}$ reversed-phase column, $MeCN:H_2O$ (1:1, v/v) as eluent, a flow rate of 8.0 mL/min), to furnish dothideopyrone C (4; 28.8 mg; $t_R$ 8 min). Fractions B4 and B5 were combined and subjected to further CC over silica gel (2.5 x 40 cm), eluting with a mixture of $EtOAc/CH_2Cl_2$ (2:8, v/v) to yield ten fractions (C1-C9). Fraction C4 contained dothideopyrone A (1) 126 mg, while fraction C6 gave dothideopyrone B (3) 12 mg. Fraction C8 was further purified by preparative TLC using hexane:acetone (2:1, v/v) as eluent to furnish dothideopyrone D (5) 48 mg. Fraction A11 was re-crystallized from MeOH, and subjected to preparative TLC eluted with a hexane: $CH_2Cl_2$:acetone (1:1:1, v/v), yielding sulochrin (13) (10 mg). Fraction A13 was purified by a preparative TLC, using acetone:hexane (1:1, v/v) as eluent, to yield questin (10) (25 mg), as shown in Scheme 5. Crude cell extract (900 mg) was separated by Sephadex LH-20 CC (3 x 85 cm), eluted with MeOH, yielding twelve fractions (D1-D12). Fractions D7 and D8 were combined and subjected to further CC over silica gel (2 x 30 cm), eluting with EtOAc/hexane (2:3, v/v), to yield eight fractions (E1-E8). Fraction E3 gave methyl asterrate (12) 98 mg. Fraction D4 was subjected to Sephadex LH-20 CC (2 x 100.5 cm) to give night fractions (F1-F9). Fraction F7 was separated on a preparative TLC using hexane:acetone (7:3, v/v) as eluent, yielding eugenitin (14) (12 mg), as shown in Scheme 6.

For the culture grown in M1D medium (supplemented with 0.5 g/L malt extract; 3.2L), a crude broth extract (630 mg) was purified by MPLC ($C_{18}$ reversed-phase column, 3.6 x 46 cm), with a stepwise elution starting with a mixture of MeOH/$H_2O$ (1:1, v/v) to MeOH, to afford *cis,trans*-muconic acid (9; 153 mg, $t_R$ 22 min) and 6-hydroxymethyleugenitin (15; 72.3 mg, $t_R$ 66 min) (Scheme 7), while a mycelial crude extract was found to be, as shown by $^1$H NMR spectroscopic analysis, a mixture of triglycerides and fatty acids.

### 3.9.1.1 Acetylation of dothideopyrone A (1) and dothideopyrone D (5)

A solution containing dothideopyrone A (1; 22 mg), pyridine (1mL), and acetic anhydride (3 mL) was stirred at room temperature for 2 h $H_2O$ (6 mL) was added to the reaction mixture, which was subsequently extracted with $CHCl_3$. The organic layer was evaporated to give an oily mixture (33 mg), which was purified by preparative TLC eluted with a mixture of $CH_2Cl_2$:EtOAc (9:1), to afford the acetate 2 (17.8 mg). Acetylation of dothideopyrone D (5; 19.6 mg) was performed in a similar manner, yielding the acetate derivative 6 (9.1 mg).



2
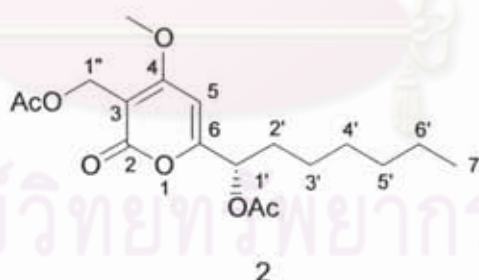
Diacetate derivative (2) was isolated as colorless oil and the APCI-TOF mass spectrum of the diacetate derivative revealed a pseudo molecular ion peak at *m/z* 389.1382 [M + Cl]$^-$(calculated for $C_{18}H_{26}ClO_7$, 389.1367) shown in Figure L49 (Appendix C). A structure of a diacetate derivative was assigned by analyses of the $^1$H NMR, $^{13}$C NMR, HMQC, and HMBC spectral data, as shown in Figures L50 to L54 of Appendix C. On the $^1$H NMR and $^{13}$C NMR spectral data of the diacetate derivative are follows: $^1$H NMR (CDCl$_3$, 400 MHz) δ 6.16 (1H, *s*, H-5), 5.37 (H, *t*, *J* = 6.7, H-1′), 4.90 (2H, *s*, H-1″), 3.88 (3H,*s*, 4-OMe), 2.07 (3H, *s*, 1′-CO$_2$Me), 1.99 (3H, *s*, 1″-CO$_2$Me), 1.83 (2H, *m*, H-2′),

1.21 (8H, *m*, H-3′, H-4′, H-5′ and H-6′), 0.81 (3H, *t*, *J* = 6.7, H-7′); $^{13}$C NMR (CDCl$_3$, 100 MHz) δ 171.0 (C, 1″-CO$_2$Me), 169.9 (C, 1′-CO$_2$Me), 168.4 (C, C-6), 163.8 (C, C-4), 162.7 (C, C-2), 100.5 (C, C-3), 94.4 (CH, C-5), 72.3 (CH, C-10), 56.8 (CH$_3$, 4-OMe), 56.1 (CH$_2$, C-1″), 32.1 (CH$_2$, C-2′), 31.5 (CH$_2$, C-5′), 28.7 (CH$_2$, C-4′), 24.9 (CH$_2$, C-3′), 22.5 (CH$_2$, C-6′), 20.9 (CH$_3$, 1″-CO$_2$Me), 20.8 (CH$_3$, 1″-CO$_2$Me), 13.9 (CH$_3$, C-7′).



6, R = Ac
7, R = (*S*)-MTPA
8, R = (*R*)-MTPA
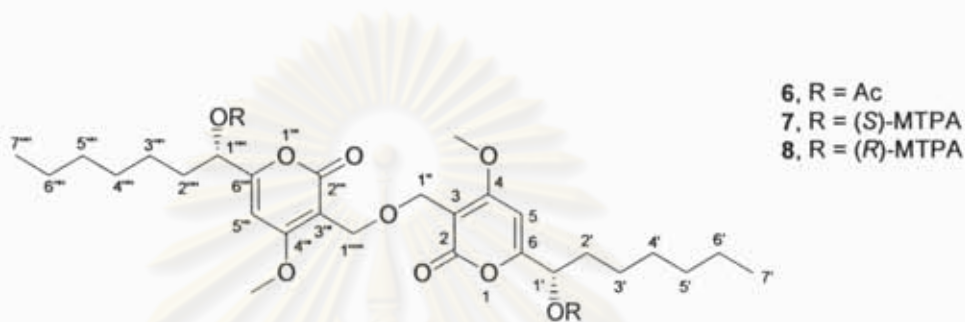
The diacetate derivative (**6**) was obtained as colorless oil, and the ESI-TOF mass spectrum suggested the molecular formular C$_{32}$H$_{46}$O$_{11}$, calculated for C$_{32}$H$_{46}$ClO$_{11}$, 641.2729), exhibited in Figure L55 (Appendix C). The $^1$H and $^{13}$C NMR spectral data of the diacetate derivative **6** (CDCl$_3$, 400 MHz) are as follows: δ 6.20 (2H, *s*, H-5 or H-5″″), 5.42 (2H, *t*, *J* = 6.7, H-1′ or H-1″″), 4.44 (4H, *s*, H-1″ or H-1″″), 3.92 (6H, *s*, 4-OMe or 4″′-OMe), 2.12 (6H, *s*, 1′-CO$_2$Me or 1″″-CO$_2$Me), 1.87 (4H, *m*, H-2′ or H-2″″), 1.28 (16H, *m*, H-3′ or H-3″″, H-4′ or H-4″″, H-5′ or H-5″″, and H-6′ or H-6″″), 0.88 (6H, *t*, *J* = 6.7, H-7′ or H-7″″); $^{13}$C NMR (CDCl$_3$, 100 MHz) δ 169.9 (C, 1′-CO$_2$Me or 1″″-CO$_2$Me), 168.3 (C, C-6 or C-6″′), 163.9 (C, C-4 or C-4″′), 162.8 (C, C-2 or C-2″′), 102.9 (C, C-3 or C-3″″), 94.9 (CH, C-5 or C-5″′), 72.3 (CH, C-1′ or C-1″″), 61.5 (CH$_2$, C-1″ or C-1″″), 56.7 (CH$_3$, 4-OMe or 4″′-OMe), 32.1 (CH$_2$, C-2′ or C-2″″), 31.5 (CH$_2$, C-5′ or C-5″″), 28.8 (CH$_2$, C-4′ or C-4″″), 24.9 (CH$_2$, C-3′ or C-3″″), 22.5 (CH$_2$, C-6′ or C-6″″), 20.8 (CH$_3$, 1′-CO$_2$Me or 1″″-CO$_2$Me), 13.9 (CH$_3$, C-7′ or C-7′). The 1D NMR and 2D NMR spectral data of the diacetate derivative **6** are in Figures 56 to 59 of Appendix B.

### 3.9.1.2 Preparation of (*R*)- and (*S*)- MTPA esters of 5

The reaction mixture containing dothideopyrone D (**5**; 3 mg), (*R*)-(+)-α-methoxy-α-(trifluoromethyl)phenylacetic acid (MTPA; 13.9 mg), *N*-[3-

(dimethyllaminopropyl)-$N'$-ethylcarbodiimide hydrochloride (12.6 mg), and a catalytic amount of $N,N$-(dimethylamino)pyridine was dissolved in 4 mL of methylene chloride ($CH_2Cl_2$), and heated unit reflux began, this being maintained for 4 h. The reaction mixture was added to $H_2O$ (5 mL) and extracted with $CHCl_3$ (5 mL). The mixture was purified by preparative TLC, using EtOAc-$CH_2Cl_2$ (1:4, v/v) as an eluent, to give the ($R$)-MTPA ester (4.5 mg). The ($S$)- MTPA ester was prepared in the same manner; dothideopyrone D (5) was reacted with ($S$)-(-)-$\alpha$-methoxy-$\alpha$-(trifluoromethyl)-phenylacetic acid (MTPA), to give the ($S$)-MTPA ester (4.5 mg).

The ESI-TOF mass spectrum of the ($S$)-MTPA ester (7) revealed a pseudo molecular ion peak at $m/z$ 955.3620 [M + H]$^+$(calculated for $C_{48}H_{57}F_6O_{13}$, 955.3703) (Figure L61 in Appendix C). The $^1$H NMR spectral data of the ($S$)-MTPA ester (7) (CDCl$_3$, 400 MHz) are as follows (Data for half of a molecule): δ 7.53 (2H, $m$, aromatic signals of MTPA), 7.43 (3H, $m$, aromatic signals of MTPA), 6.23 (1H, $s$, H-5), 5.67 (1H, $t$, $J = 6.4$, H-1'), 4.54 (2H, $s$, H-1″), 3.83 (3H, $s$, 4-OMe), 3.52 (3H, $br$ $d$, OMe of MTPA), 1.94 (1H, $m$, H-2'a), 1.60 (1H, $m$, H-2'b), 1.25 (4H, $m$, overlapping signals of H-3' and H-4'), 1.23 (2H, $m$, H-4'), 1.23 (2H, $m$, H-5'), 1.23 (2H, $m$, H-6'), 0.86 (3H, $t$, $J = 6.9$, H-7'). The $^1$H NMR spectrum of the methyl ester (7) is in Figure L60 of Appendix B.

The ESI-TOF mass spectrum of the ($R$)-MTPA ester (8) revealed a pseudo molecular ion peak at $m/z$ 955.3610 [M + H]$^+$(calculated for $C_{48}H_{57}F_6O_{13}$, 955.3703), as shown in Figure L63 (Appendix C). The $^1$H NMR spectral data of the ($R$)-MTPA ester (8) (CDCl$_3$, 400 MHz) are as follows (data for half of a molecule): δ 7.51 (2H, $m$, aromatic signals of MTPA), 7.44 (3H, $m$, aromatic signals of MTPA), 5.95 (1H, $s$, H-5), 5.72 (1H, $t$, $J = 6.1$, H-1'), 4.52 (2H, $s$, H-1″), 3.69 (3H, $s$, 4-OMe), 3.58 (3H, $br$ $d$, OMe of MTPA), 1.95 (1H, $m$, H-2'a), 1.60 (1H, $m$, H-2'b), 1.29 (4H, $m$, overlapping signals of H-3' and H-4'), 1.25 (2H, $m$, H-4'), 1.25 (2H, $m$, H-5'), 1.25 (2H, $m$, H-6'), 0.88 (3H, $t$, $J = 6.7$, H-7'). The $^1$H NMR spectrum of the methyl ester (8) is in Figure L62 of Appendix B.

The structures of the isolated compounds and their derivatives of LRUB20 are shown in Figure 21.

Crude broth extract of LRUB20 grown on CzYA medium (1,400 mg)

Sephadex LH-20
100% MeOH

A6

A9

Sephadex LH-20
100% MeOH

re-crystallized
from MeOH

A11

re-crystallized
from MeOH

PTLC (1:1:1)
Hexane/CH$_2$Cl$_2$/acetone

A13

PTLC (1:1)
hexane/acetone

Asterric acid (11)

147.0 mg

Sulochrin (13)

10.0 mg

Questin (10)

25.0 mg

B4 & B5

Silica gel (2:8)
EtOAc/CH$_2$Cl$_2$

B6

Sephadex LH-20
100% MeOH

B$_6$6

PTLC (2:1)
hexane/acetone

Dothideopyrone A (1)

126.0 mg

Dothideopyrone B (3)

12.0 mg

Dothideopyrone D (5)

48.0 mg

HPLC 1:1
MeCN/H$_2$O

Dothideopyrone C (4)

28.8 mg

Scheme 5    Isolation of a broth extract of LRUB20 cultured on CzYA medium

Crude mycelial extract of LRUB20 grown on CzYA medium (900 mg)

Sephadex LH-20
100% MeOH

D4

Sephadex LH-20
100% MeOH

F7

PTLC (7:3)
hexane/acetone

Eugenitin (14)
12.0 mg

D7 & D8

Silica gel (2:3)
EtOAc/Hexane

Methyl asterrate (12)
98.0 mg
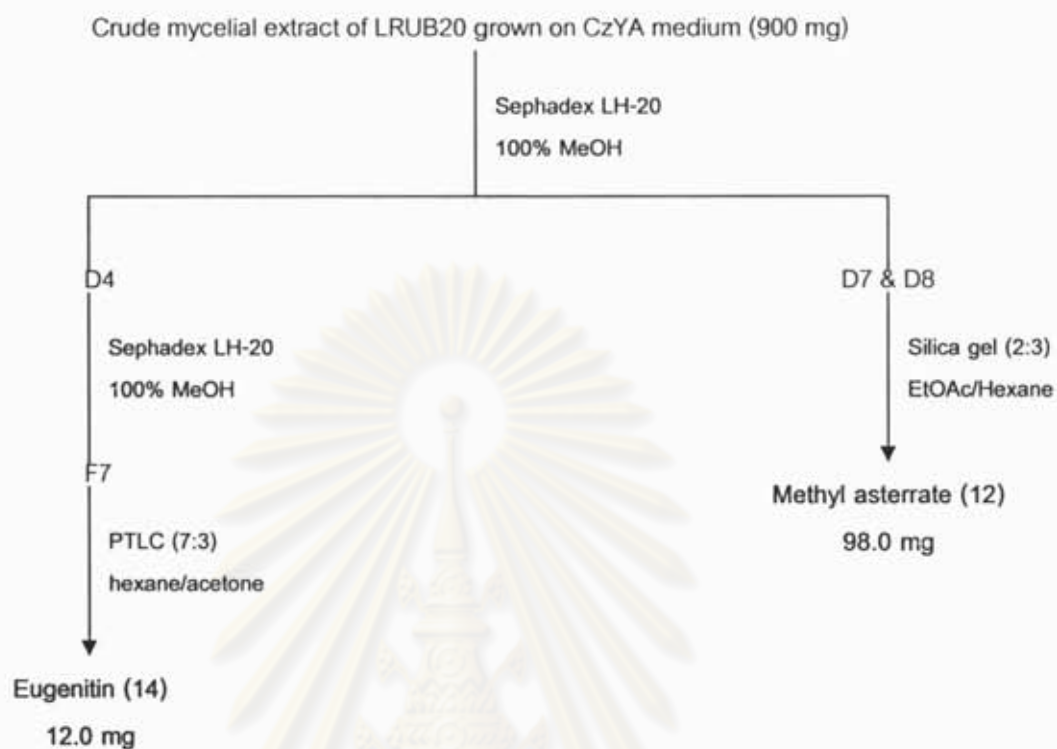
Scheme 6    Isolation of a mycelial extract of LRUB20 grown on CzYA medium

Crude broth extract of LRUB20 cultured on M1D medium (630 mg)

MPLC
MeOH/H$_2$O (1:1) to MeOH

Cis,trans-muconic acid (9)
153.0 mg

6-hydroxymethyleugenitin (15)
72.3 mg
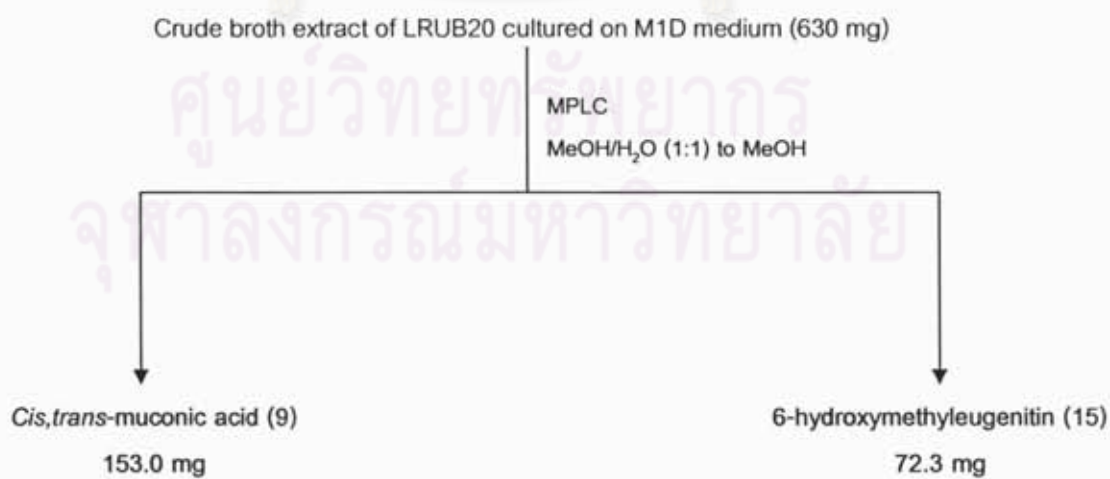
Scheme 7    Isolation of a broth extract of LRUB20 grown on M1D medium

**1**, R₁ = H, R₂ = H
**2**, R₁ = Ac, R₂ = Ac
**3**, R₁ = H, R₂ = Me

**4**

**5**, R = H
**6**, R = Ac
**7**, R = (S)-MTPA
**8**, R = (R)-MTPA

**9**

**10**

**11**, R = H
**12**, R = Me

**13**

**14**, R = Me
**15**, R = CH₂OH
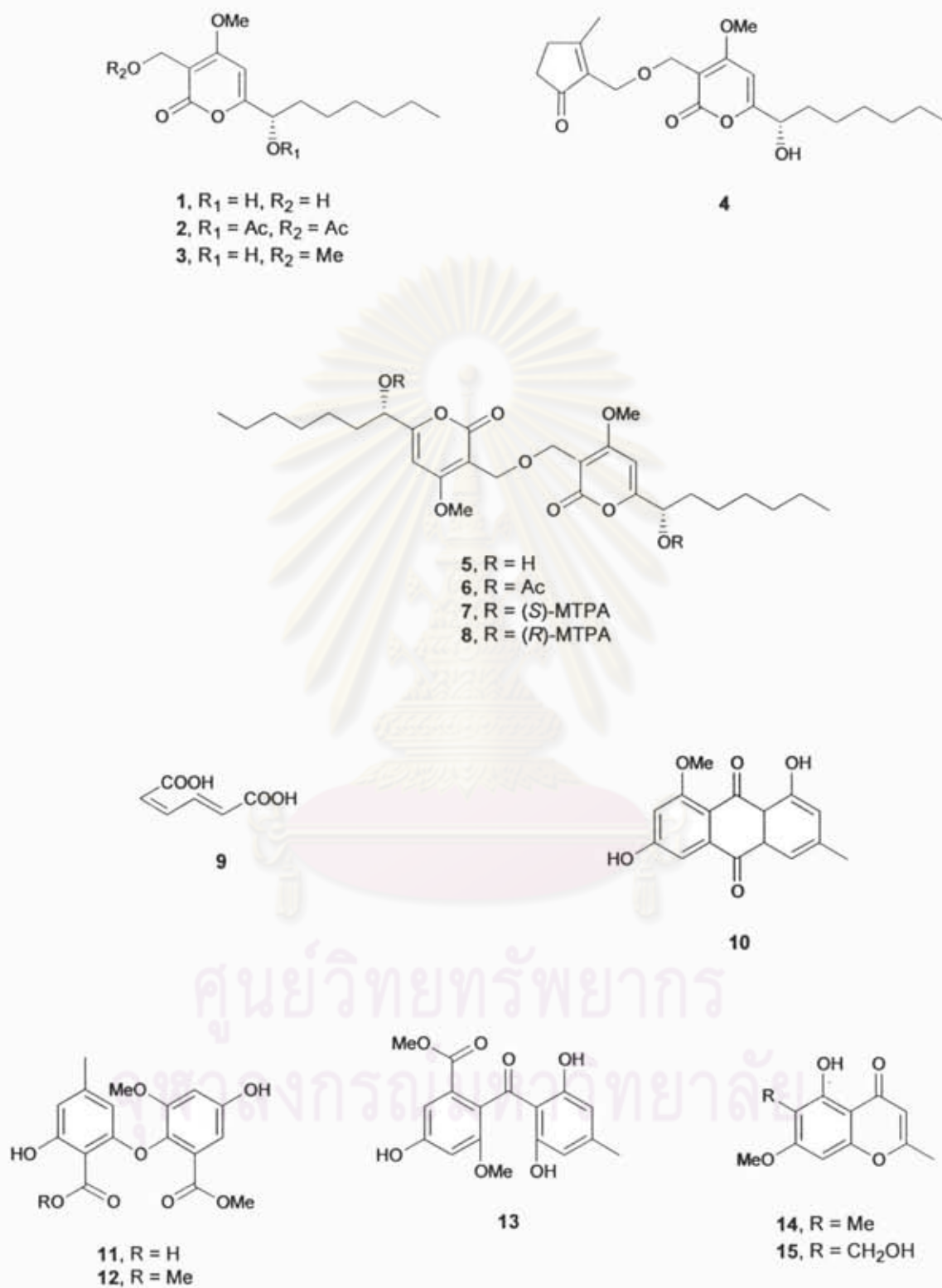
**Figure 21**     Structures of the isolated compounds and their derivatives

### 3.9.2 Isolation of secondary metabolites from the endophytic fungus isolate LPHIL36

A crude broth extract was subjected to Sephadex LH-20 CC (3 x 90 cm), eluted with MeOH, to yield 14 fractions (A1-A14). Fractions A8-A11 were combined and further purified by Sephadex LH-20 CC (3 x 90 cm), eluted with acetone:MeOH (1:1), and twelve fractions (B1-B12) were obtained. Fractions B5 and B6 gave corynether A (20, 460 mg), while fractions B8, B9 and B10 contained corynesidone B (18, 1.2 g). Fractions A5 and A6 were combined and subjected to Sephadex LH-20 CC (3 x 48 cm), eluted with 100% MeOH, yielding eight fractions (C1-C8). Fractions C2 and C3 were combined and purified by Sephadex LH-20 CC (2 x 100.5 cm) using MeOH as a mobile phase to obtain eight fractions (D1-D8). Fraction D3 was further purified on preparative TLC eluded with hexane: $CH_2Cl_2$: acetone (2:2:1), to yield 40 mg of diaryl ether (22). Fraction C5 was subjected to Sephadex LH-20 CC (2 x 100.5 cm), eluted with MeOH, to provide nine fractions (E1-E9). Fractions E5 and E6 were combined and purified on preparative TLC using hexane: $CH_2Cl_2$: acetone (2:2:1) as eluent, yielding 89 mg of corynesidone A (16), as shown in Scheme 8. A crude extract of mycelia was found to be a mixture of fatty acids and triglycerides.

**Methylation of corynesidones A (16) and B (18), corynether A (20), and diaryl ether (22)**

To a solution of corynesidone A (16) (9 mg) in DMF (1 mL) was added $K_2CO_3$ (20 mg) and MeI (0.3 mL), and the mixture was left stirring at room temperature for 20 h. The mixture was dried under vacuum, then dissolved in EtOAc (8 mL) and subsequently washed with $H_2O$ (5 × 8 mL), to afford a methylated derivative 17 (6.9 mg). Methylation of corynesidone B (18) (20 mg), corynether A (20) (10 mg) and diaryl ether (22) (16 mg) were performed in a similar manner as that of 16, yielding methylated derivatives 19 (17.5 mg), 21 (8.2 mg), and 23 (13.5 mg), respectively. The structures of compounds and their derivatives isolated from the isolate LPHIL36 are shown in Figure 22.

Crude broth extract of LPHIL36 grown on MEB medium (4.5 g)

Sephadex LH-20
100% MeOH

A5 & A6

Sephadex LH-20
100% MeOH

A8 – A11

Sephadex LH-20 (1:1)
acetone/MeOH

C2 & C3

Sephadex LH-20
100% MeOH

D3

PTLC (2:2:1)
hexane/CH$_2$Cl$_2$/acetone

Diaryl ether (22)
40 mg

C5

Sephadex LH-20
100% MeOH

E5 & E6

PTLC (2:2:1)
hexane/CH$_2$Cl$_2$/acetone

Corynesidone A (16)
89 mg

Corynether A (20)
460 mg

Corynesidone B (18)
1,200 mg
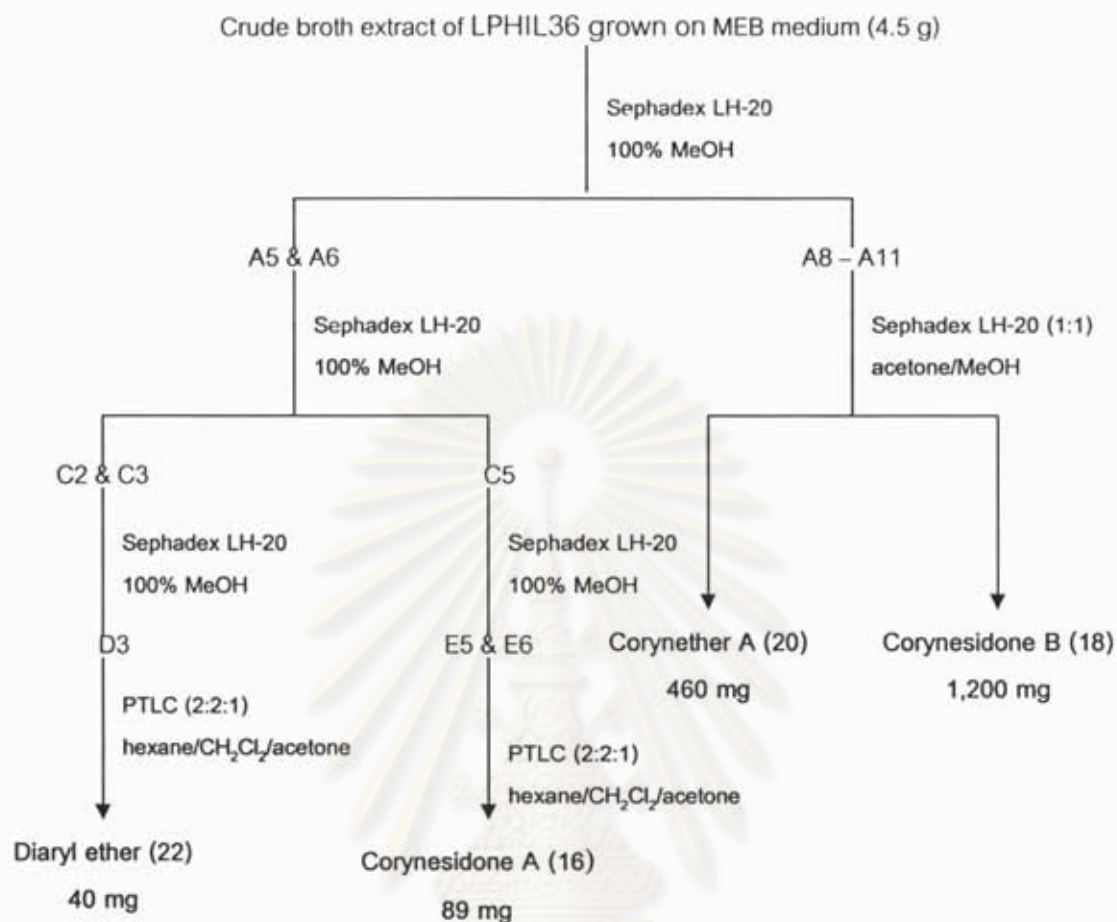
Scheme 8    Isolation of a broth extract of LPHIL36 cultured on MEB medium.
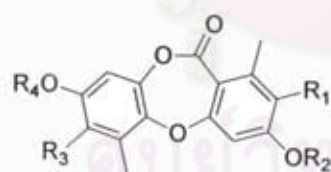


16, R$_1$ = H, R$_2$ = H, R$_3$ = H, R$_4$ = H
17, R$_1$ = H, R$_2$ = Me, R$_3$ = H, R$_4$ = Me
18, R$_1$ = OH, R$_2$ = H, R$_3$ = COOH, R$_4$ = H
19, R$_1$ = OMe, R$_2$ = Me, R$_3$ = COOMe, R$_4$ = Me
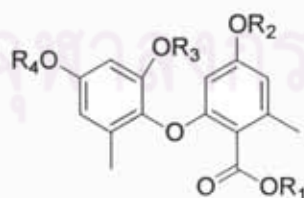
20, R$_1$ = H, R$_2$ = H, R$_3$ = H, R$_4$ = H
21, R$_1$ = Me, R$_2$ = Me, R$_3$ = Me, R$_4$ = Me
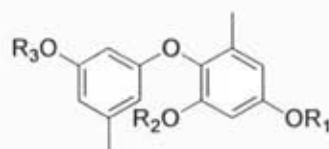
22, R$_1$ = H, R$_2$ = H, R$_3$ = H
23, R$_1$ = Me, R$_2$ = Me, R$_3$ = Me

Figure 22    Structures of compounds and their derivatives isolated from LPHIL36.

3.10    Physical properties of bioactive compounds

### 3.10.1 Dothideopyrones A (1) of the fungus isolate LRUB20

UV                : $\lambda_{max}$ (log $\varepsilon$) in methanol; Figure L1 in Appendix B

248 (3.2), 299 (4.1)

IR                : $\gamma_{max}$ cm$^{-1}$; Figure L2 in Appendix B

3373, 2926, 1682, 1600, 1466, 1392, 1252, 1138, 999,

795

ESI-TOF MS    : $m/z$; Figure L3 in Appendix B

$m/z$ 271.1540 (found)

271.1546 (calculated for $C_{14}H_{23}O_5$)

Optical rotation: $[\alpha]_D^{28}$ -77 (c 0.22, CHCl$_3$)

$^1$H NMR        : $\delta_H$ (ppm), 500 MHz, in CDCl$_3$

see Figure L4 in Appendix B

$^{13}$C NMR       : $\delta_C$ (ppm), 125 MHz, in CDCl$_3$

see Figure L5 in Appendix B

### 3.10.2 Dothideopyrones B (3) of the fungus isolate LRUB20

UV                : $\lambda_{max}$ (log $\varepsilon$) in methanol; Figure L12 in Appendix B

233 (3.0), 299 (3.7)

IR                : $\gamma_{max}$ cm$^{-1}$; Figure L13 in Appendix B

3400, 2925, 1687, 1561, i466, 1395, 1230, 1083, 800

ESI-TOF MS    : $m/z$; Figure L14 in Appendix B

$m/z$ 307.1516 (found)

307.1521 (calculated for $C_{15}H_{24}O_5Na$)

Optical rotation: $[\alpha]_D^{28}$ -45 (c 0.15, CHCl$_3$)

$^1$H NMR        : $\delta_H$ (ppm), 400 MHz, in CDCl$_3$

see Figure L15 in Appendix B

$^{13}$C NMR       : $\delta_C$ (ppm), 100 MHz, in CDCl$_3$

see Figure L17 in Appendix B

### 3.10.3 Dothideopyrones C (4) of the fungus isolate LRUB20

UV : $\lambda_{max}$ (log $\varepsilon$) in methanol; Figure L25 in Appendix B

207 (4.4), 228 (4.0), 299 (3.9)

IR : $\nu_{max}$ cm$^{-1}$; Figure L26 in Appendix B

3403, 2927, 1694, 1643, 1563, 1466, 1390, 1269, 1227,

1049, 823

ESI-TOF MS : $m/z$; Figure L27 in Appendix B

$m/z$ 401.1936 (found)

401.1940 (calculated for $C_{21}H_{30}O_6Na$)

Optical rotation: $[\alpha]_D^{28}$ -64 ($c$ 0.10, CHCl$_3$)

$^1$H NMR : $\delta_H$ (ppm), 500 MHz, in CDCl$_3$

see Figure L28 in Appendix B

$^{13}$C NMR : $\delta_C$ (ppm), 125 MHz, in CDCl$_3$

see Figure L30 in Appendix B

### 3.10.4 Dothideopyrones D (5) of the fungus isolate LRUB20

UV : $\lambda_{max}$ (log $\varepsilon$) in methanol; Figure L38 in Appendix B

248(3.0), 301 (5.0)

IR : $\nu_{max}$ cm$^{-1}$; Figure L39 in Appendix B

3389, 2927, 1687, 1640, 1561, 1466, 1393, 1270, 1229,

1033, 823

ESI-TOF MS : $m/z$; Figure L40 in Appendix B

$m/z$ 545.2715 (found)

545.2727 (calculated for $C_{28}H_{42}O_9Na$)

$^1$H NMR : $\delta_H$ (ppm), 400 MHz, in CDCl$_3$

see Figure L41 in Appendix B

$^{13}$C NMR : $\delta_C$ (ppm), 100 MHz, in CDCl$_3$

see Figure L43 in Appendix B

### 3.10.5 Corynesidones A (16) of the fungus isolate LPHIL36

| | |
|---|---|
| UV | : $\lambda_{max}$ (log $\varepsilon$) in methanol; Figure P1 in Appendix B |
| | 222 (4.12), 267 (3.80) |
| IR | : $\nu_{max}$ cm$^{-1}$; Figure P2 in Appendix B |
| | 3373, 3253, 2924, 2854, 1693, 1615, 1459, 1380, 1354, |
| | 1343, 1294, 1252, 1218, 1146, 1092, 283, 845, 732 |
| ESI-TOF MS | : $m/z$; Figure P3 in Appendix B |
| | $m/z$ 271.0616 (found) |
| | 271.0607 (calculated for $C_{15}H_{11}O_5$) |
| m.p. | : 235-237 $^\circ$C |
| $^1$H NMR | : $\delta_H$ (ppm), 400 MHz, in acetone-$d_6$ |
| | see Figure P4 in Appendix B |
| $^{13}$C NMR | : $\delta_C$ (ppm), 100 MHz, in acetone-$d_6$ |
| | see Figure P6 in Appendix B |

### 3.10.6 Corynesidones B (18) of the fungus isolate LPHIL36

| | |
|---|---|
| UV | : $\lambda_{max}$ (log $\varepsilon$) in methanol; Figure P24 in Appendix B |
| | 223 (4.38), 304 (3.80) |
| IR | : $\nu_{max}$ cm$^{-1}$; Figure L25 in Appendix B |
| | 3241, 2924, 2853, 1703, 1687, 1616, 1460, 1370, 1306, |
| | 1243, 1214, 1154, 1067, 846 |
| ESI-TOF MS | : $m/z$; Figure L26 in Appendix B |
| | $m/z$ 331.0458 (found) |
| | 331.0454 (calculated for $C_{16}H_{11}O_8$) |
| m.p. | : 212-214 $^\circ$C |
| $^1$H NMR | : $\delta_H$ (ppm), 400 MHz, in acetone-$d_6$ |
| | see Figure P27 in Appendix B |
| $^{13}$C NMR | : $\delta_C$ (ppm), 100 MHz, in acetone-$d_6$ |
| | see Figure P28 in Appendix B |

3.10.7  Corynether A (20) of the fungus isolate LPHIL36

    UV            : $\lambda_{max}$ (log $\varepsilon$) in methanol; Figure P42 in Appendix B

                  221 (3.87), 282 (3.18)

    IR            : $\nu_{max}$ cm$^{-1}$; Figure P43 in Appendix B

                  3275, 2926, 2860, 1691, 1606, 1460, 1380, 1318, 1267,

                  1206, 1153, 1051, 979, 840

    ESI-TOF MS    : $m/z$; Figure P44 in Appendix B

                  $m/z$ 289.0720 (found)

                        289.0712 (calculated for $C_{15}H_{13}O_6$)

    m.p.         : 145-147 $^\circ$C

    $^1$H NMR    : $\delta_H$ (ppm), 400 MHz, in DMSO-$d_6$

                  see Figure P45 in Appendix B

    $^{13}$C NMR    : $\delta_C$ (ppm), 100 MHz, in DMSO-$d_6$

                  see Figure P46 in Appendix B

3.10.8  Diaryl ether (22) of the fungus isolate LPHIL36

    UV             : $\lambda_{max}$ (log $\varepsilon$) in methanol; Figure P62 in Appendix B

                  223 (4.14), 282 (3.51)

    IR             : $\nu_{max}$ cm$^{-1}$; Figure P63 in Appendix B

                  3336, 2923, 1692, 1596, 1469, 1319, 1264, 1206, 1147,

                  1122, 1051, 1027, 967, 834, 800, 737, 682

    ESI-TOF MS    : $m/z$; Figure P64 in Appendix B

                  $m/z$ 281.0590 (found)

                        281.0581 (calculated for $C_{14}H_{14}O_4Cl$)

    $^1$H NMR    : $\delta_H$ (ppm), 400 MHz, in acetone-$d_6$

                  see Figure P65 in Appendix B

    $^{13}$C NMR    : $\delta_C$ (ppm), 100 MHz, in acetone-$d_6$

                  see Figure P67 in Appendix B

3.11    Determination of biological activities

### 3.11.1 Antimicrobial assays

Antimicrobial activity of isolated compounds against particular microorganisms was determined by a broth microdilution test as described in the Clinical and Laboratory Standards Institute (CLSI, formerly NCCLS) M7-A4 and M27-A2 methods.

#### 3.11.1.1 Test microorganisms

The in vitro antimicrobial activity tests were performed by using standard test microorganisms as follows: three Gram-positive bacteria (*Staphylococcus aureus* ATCC 25923, methicillin-resistant *Staphylococcus aureus* (MRSA 384) and *Enterococcus faecalis* ATCC 29212), two Gram-negative bacteria (*Escherichia coli* ATCC 25922 and *Pseudomonas aeruginosa* ATCC 27853) and a yeast fungus (*Candida albicans* ATCC 90028).

#### 3.11.1.2 Preparation of bacterial and yeast inocula

Bacteria were grown on Mueller Hinton agar (MHA) for 24 h at 37 °C. Selected fresh single colonies were inoculated into 5 ml of tryptic soy broth and incubated in shaking incubator for 2-3 h at 37°C. The turbidity of the bacterial suspension was adjusted with sterile normal saline solution to match the turbidity of 0.5 McFarland standard (OD 0.1 at 625 nm). Then the suspension was diluted 1:100 with Mueller Hinton broth (MHB) to contain $1 \times 10^6$ CFU/ml.

Yeast were grown on SDA slant at 25 °C for 24 h. The turbidity of the yeast suspension was adjusted with sterile normal saline solution to match the turbidity of 0.5 McFarland standard. The final inoculum suspension was diluted 1:1000 with RPMI 1640 medium to contain $1 \times 10^3 - 5 \times 10^3$ CFU/ml.

### 3.11.1.3 Determination of minimum inhibitory concentration (MIC)

Solution of a test compound in DMSO (25.6 mg/ml) was diluted with MHB or RPMI 1640 for assays of antibacterial or antifungal activity, respectively. The test compound was prepared at the concentration ranges of 0.5 to 256 µg/mL. Ampicillin and nystatin were used as positive controls for bacteria and yeast, respectively. MIC is defined as the lowest concentration that inhibits growth of test microorganisms.

A 50-µl volume of MHB and a 100-µl volume of RPMI 1640 containing the test compound were dispensed into each well of sterile microtiter plates (96-flat-bottom wells) for the evaluation of antibacterial and antifungal activities, respectively. Sterile compound-free medium containing the corresponding amount of DMSO was dispensed in the growth control well. The final adjusted bacterial and yeast suspensions were inoculated into each well with volumes of 50 µl and 100 µl, respectively. Compound-free MHB and compound-free RPMI 1640 in volumes of 100 µl and 200 µl were used as the sterility control. The experiments were done in duplicate. After incubation at 37 °C for 24 h, a 20-µl of $p$-iodonitrotetrazolium (INT) solution (1mg/ml) was added into each well. The antibacterial and antifungal assay plates were further incubated for 1 h and 24 h, respectively. Growth in each well was indicated by a color change from colorless to violet. Compounds that inhibit microbial growth would prevent the development of a violet color. The well that shows no change in color indicates antimicrobial activity of the test compound.

Antimalarial activity, anticancer activity and cancer chemoprevention were evaluated at the Chulabhorn Research Institute (CRI), Bangkok, Thailand. Details of each bioassay are described below.

### 3.11.2 Antimalarial activity

#### 3.11.2.1 Parasite culture

Human erythrocytes (type O) infected with *Plasmodium falciparum* strain 94, (Chloroquine resistant) was maintained in continuous culture, according to the method described by Trager and Jensen (1976). RPMI 1640 culture

medium (Gibco, USA) supplemented with 25 mM of HEPES (Sigma, USA), 40 mg/L gentamicin sulfate (Government Pharmaceutical Organization, Thailand) and 10 mL of human serum was used in continuous culture.

Before starting the experiment, *P. falciparum* culture was synchronized by using sorbitol induced hemolysis according to the method of Lambros and Vanderberg (1979) to obtain only ring-infected cells and then incubated for 48 h prior to the drug testing to avoid effect of sorbitol.

The experiments were started with synchronized suspension of 0.5% - 1% infected red blood cell during ring stage. Parasites were suspended with culture medium supplemented with 15% human serum to obtain 10% cell suspension. The parasite suspension was put into 96-well microculture plate; 50 µL in each well and then added 50 µL of various test drug concentrations. These parasite suspensions were incubated for 48 h in the atmosphere of 5% $CO_2$ at 37 °C.

After 48 h incubation, parasite culture was fixed by adding 0.25% (v/v) glutaraldehyde (Sigma) in phosphate buffer saline (PBS) and these were kept for DNA staining.

### 3.11.2.2 Parasite DNA staining and flow cytometric analysis

Before parasite DNA staining, $5 \times 10^6$ red blood cells from each glutaraldehyde-fixed sample were washed once with PBS and resuspended in PBS containing propidium iodide (PI) (Molecular Probe) at a final concentration of 10 µg/mL, and held for at least 1 h in the dark. The PI stained cells were excited with 488 nm. Red fluorescence was detected at 585 nm. Red blood cells were gated on the basis of their forward scatter and side scatter. For each sample, 30,000 cells were required, stored and analyzed. Percent parasitemia, fluorescence intensity, and any abnormal fluorescence pattern were obtained from an integrated fluorescence histogram between the test and the control sample (chloroquine hydrochloride, $IC_{50} = 2.98 \times 10^{-7}$ M).

### 3.11.3 Anticancer activity

The MTT assay (Carmichael *et al.*, 1987; Doyle and Griffiths, 1997; Mosmann, 1983; Tominaga et al., 1999) was applied for the evaluation of cytotoxicity

against HeLa (human cervical carcinoma), HuCCA-1 (human cholangiocarcinoma), HepG2 (human hepatoblastoma carcinoma), T47D (hormone-dependent breast cancer), MDA–MB231 (hormone-independent breast cancer), S102 (human hepatocellular carcinoma), A549 (human lung adenocarcinoma), and MRC-5 (normal embryonic lung cell) cancer cell lines. Cells were plated in a 96-well microplate (Costar No. 3599, USA, 100 μL/well at a density of $5 \times 10^3 - 2 \times 10^4$ cells/well), and incubated for 24 h at 37 °C under 5% $CO_2$ and 95% humidity. The tested compounds at various concentrations were added to the cell lines, which were incubated further for 48 h. Cell viability was determined by staining with MTT [3-(4,5-dimethylthiazol-2-yl)-2,5-diphenyltetrazolium bromide]. The MTT stock solution (5 mg/mL) was prepared in phosphate buffered saline (PBS), which was diluted (1:10) with a culture medium prior to use. After removing the culture medium, the diluted MTT solution (50 μL) was added to the adhesive cells, and plates were incubated at 37 °C under 5% $CO_2$ and 95% humidity for 2–4 h. Subsequently, DMSO (100 μL) was added to dissolve the resulting formazan by sonication. The plates were read on a microplate reader (Molecular Devices, CA, USA), using a test wavelength of 550 nm and a reference wavelength of 650 nm.

The cytotoxic activity against non-adhesive cells, HL-60 (human promyelocytic leukemia cell) and MOLT-3 (acute lymphoblastic leukemia cell line) cancer cell lines, was evaluated using the XTT assay (Doyle and Griffiths, 1997). Cells were plated in a 96-well microplate as mentioned above, and the tested compounds at various concentrations were added to cell lines, which were incubated further for 48 h. A dye solution was prepared by mixing 5 mL of XTT (2,3-bis-(2-methoxy-4-nitro-5-sulfophenyl)-2H-tetrazolium-5-carboxanilide) solution (1 mg/mL) with 100 μL of phenazine methosulfate solution (0.383 mg/mL). The dye solution (50 μL) was added to cells, which were further incubated for 4 h. The plates were read on a microplate reader (Molecular Devices, CA, USA) at the wavelengths of 492 and 690 nm. Etoposide and doxorubicin were used as the reference drugs.

### 3.11.4 Cancer chemoprevention

Activity of cancer chemoprevention was evaluated based upon 6 independent models, including DPPH (scavenging of diphenyl picrylhydrazyl radicals), XXO (scavenging of $O_2^-$ generating by xanthine/xanthine oxidase), IXO (inhibition of xanthine oxidase), HL-60 antioxidation (inhibition of TPA-induced $O_2^-$ generation in differentiated HL-60 cell), ORAC (oxygen radical absorbance capacity-against $ROO^-$), and inhibition of aromatase (CYP19).

#### 3.11.4.1 Diphenyl-picryl-hydrazyl (DPPH) assay

The DPPH assay was performed according to Gerhauser et al. (2003) with some modifications. Samples were reacted with 1, 1-diphenyl-2-picrylhydrazyl (DPPH) stable free radical generating formazan form which was measured photometrically. For the reaction, 195 µL of 100 µM DPPH solution was pipetted in 96-well plate. 5 µL of sample or DMSO as blank or 10 mM Vitamin C as positive control was mixed. After 37 °C incubation for 30 min, the optical density (OD) at 515 nm wavelength was measured by a microplate reader. Percentage of scavenging of DPPH radical (% scavenging) was calculated using the equation shown below. The samples which contain scavenging activity higher than 50% were further analyzed the value of 50% inhibitory concentration ($IC_{50}$) which was calculated using Microsoft Excel. Ascorbic acid was used as the reference compound, exhibiting an $IC_{50}$ value of 21.2 µM.

$$\% \, \text{Scavenging} = 100 - \frac{(\text{ODsample})}{(\text{ODcontrol})} \times 100$$

#### 3.11.4.2 HL-60 antioxidant by reduction of cytochrome C differentiation of HL-60

The differentiation of human promyelocytic leukemic cells (HL-60) to granulocyte was performed following the method established by Takeuchi et al. (1994) with minor modifications. $2.5 \times 10^5$ cells/mL of HL-60 were differentiated with

culture medium containing 1.3% DMSO and incubated in $CO_2$ incubator at 37 °C for 4 days. The differentiated cells were harvested by centrifugation and washed twice with Hank's balanced salt solution, containing 30 mM Hepes (pH 7.8) and resuspended at concentration $1 \times 10^6$ cells/mL.

### HL-60 antioxidant assay

Inhibition of TPA-induced superoxide radical formation in differentiated HL60 was performed by determination of cytochrome c reduction (Pick and Mizel, 1981). For this assay, 25 µL of a 10-fold diluted sample in $H_2O$ or 10% DMSO as negative control was mixed with 100 µL of $1 \times 10^6$ cells/mL cell suspension in 96-well plate. After incubation at 37 °C for 5 min, 25 µL of HBSS was added to sample and negative control while added 25 µL of 600 U/mL of SOD for positive control and then 75 µL of 4.17 mg/mL cytochrome c was added. To start the reaction, 25 µL of 0.55 mg/mL 12-O-tetradecanoylphorbol-13-acetate (TPA) was added. The mixture was incubated at 37 °C for 30 min. The reaction was stopped by keeping on ice for 15 min. After centrifugation at 2000 rpm for 10 min, 200 µL of the supernatant was aspirated and the optical density (OD) was measured at 550 nm with a microplate reader. Percentage of inhibition of TPA-induced superoxide radical formation (% inhibition) was calculated using the equation shown below. The samples which provide inhibition of TPA-induced superoxide radical formation activity more than 50% were further investigated, and $IC_{50}$ value was computed using Microsoft Excel.

$$\% \text{ Inhibition} = 100 - \frac{(\text{OD sample})}{(\text{OD}_{DMSO})} \times 100$$

### Cell viability assay

Since some samples exert high toxicity, cell viability was examined in parallel to avoid false positive results. Cell viability was measured fluorimetrically by enzymatic hydrolysis of the fluorogenic esterase substrate calcein AM. For this assay, the cell pellet after HL-60 antioxidant assay was collected by centrifugation, washed twice with PBS and then added 50 µL of warm 0.25 µM calcein

AM. The fluorescence was continuously measured every 1 min for 10 min using an excitation wavelength of 485 nm and an emission wavelength of 520 nm with cutoff 515 nm using a microplate fluorescence reader. Percentage of cell viability (% cell viability) was calculated from $V_{max}$ by the following equation.

$$\% \text{ Cell viability} = 100 - \frac{(V_{max} \text{of sample})}{(V_{max} \text{of DMSO})} \times 100$$

### 3.11.4.3 Scavenging of superoxide anion by reduction of XTT

Superoxide anion radical was generated by the xanthine/xanthine oxidase system. Superoxide anion could reduce XTT to form a water soluble formazan. The amount of superoxide anion can be determined indirectly by measuring the formazan product of XTT.

### Measurement of the XTT-reduction for XXO model

The ability to scavenge superoxide anion was performed by following the formazan product of XTT. The procedure was done as described by Ukeda et al. (1997) with some modifications. The premix containing 110 µL of 50 mM NaHCO$_3$ buffer, pH 9.4, 20 µL of 0.5 mM hypoxanthine, 20 µL of EDTA, 20 µL of 0.25 mM XTT and 10 µL of sample or 10 µL of pure DMSO as negative control or 2 mM allopurinol as positive control was pipetted in a 96-well plate. The reaction was initiated with 20 µL of 150 mU/mL xanthine oxidase or buffer as background. The kinetic measurement was immediately performed by microplate reader at 480 nm for 5 min, every 20 seconds. Percentage of scavenging of superoxide anion (% scavenging) was calculated from the following equation.

$$\% \text{ Scavenging} = 100 - \frac{(V_{max} \text{of sample})}{(V_{max} \text{of DMSO})} \times 100$$

### Measurement of uric acid formation for IXO model

Xanthine oxidase activity was determined by quantifying the amount of uric acid produced from xanthine. This method was previously described by Nagao *et al.* (1999) with some modifications. The premix containing 130 µL of 50 mM NaHCO$_3$ buffer, pH 9.4, 20 µL of 0.5 mM xanthine, 20 µL of EDTA and 10 µL of sample or 10 µL of pure DMSO as negative control or 2 mM allopurinol as positive control was pipetted in 96-well plate. The reaction was initiated with 20 µL of 150 mU/mL xanthine oxidase and then immediately measured a kinetic at 295 nm for 5 min, every 30 seconds. Percentage of inhibition of uric acid formation (% inhibition) was quantitated and calculated from the following equation.

$$\% \text{ Inhibition} = 100 - \frac{(V_{max} \text{ of sample})}{(V_{max} \text{ of DMSO})} \times 100$$

#### 3.11.4.4 Microplate-oxygen radical absorbance capacity assay (ORAC)

The oxygen radical absorbance capacity assay (ORAC) was developed by Cao and Prior (1999). The mixture containing 175 µL of 75 mM phosphate buffer, pH 7.0, 10 µL of $7 \times 10^{-5}$ mM fluorescein and 10 µL of 1/80 dilution sample or DMSO as negative control or 20 µM Trolox as positive control was preincubated at 37 °C for 10 min. The reaction was initiated by addition of 15 µL of 255 mM AAPH as ROO$^{-}$ generator. The plate was subjected immediately to the fluorescence microplate reader at 37 °C measuring at excitation 485 nm and emission 530 nm with cutoff 530 nm. The signal was read every 2 min for 45 min, and the area under curve (AUC) was calculated automatically.

The final results were expressed as ORAC units, where 1 ORAC unit equals the net protection of fluorescein produced by 1 µM trolox, a water soluble vitamin E analog. Scavenging capacities >1 ORAC unit were considered as positive. The ORAC values were calculated using the equation shown below.

$$ORAC = \frac{(AUCsample - AUCblank)}{(AUCtrolox - AUCblank)}$$

### 3.11.4.5 Aromatase (CYA19) inhibition assay

Aromatase inhibitory assay was performed according to the method reported by Stresser *et al.* (2000), using CYA19/methoxy-4-trifluoromethyl-coumarin (MFC) high throughput inhibition screening kit (BD Biosciences, Woburn MA, USA). The reference compound, ketoconazole, typically exhibits the $IC_{50}$ value of 2.4 µM.

## 3.12 Classification of the endophytic fungal isolates LRUB20 and LPHIL36

### 3.12.1 Conventional method

#### 3.12.1.1 Macroscopic morphology

Both LRUB20 and LPHIL36 isolates were grown on six and five different media, respectively, including corn meal agar (CMA), malt extract agar (MEA), potato dextrose agar (PDA), Sabouraud's dextrose agar (SDA), yeast Czapek agar (YCzA) and yeast extract sucrose agar (YEA). After cultivation for 14 days at room temperature they were photographed. Colony morphology of specimens such as shape, size, color, margin, pigment, and others were examined.

#### 3.12.1.2 Microscopic morphology

Both LRUB20 and LPHIL36 isolates were grown on water agar and small pieces of sterilized banana leaves at room temperature for 2 months. Fungal spores and fruiting bodies appearing on the banana leaves were examined by light microscopy.

### 3.12.2 Molecular method

#### 3.12.2.1 DNA extraction

Both LRUB20 and LPHIL36 isolates were grown on potato dextrose broth at 25 °C for 7 days. The mycelia were harvested by centrifugation and washed 3 times with sterile distilled water. The pellets were lyophilized and then ground into fine powder using a mortar and pestle. The ground powder was further subjected to DNA extraction.

The ground mycelium was filled up to one third of a 1.5 ml microcentrifuge tube and subjected to DNA extraction according to Lee and Taylor (1990). A 400-µl volume of lysis buffer (Appendix A) was added and the mixture was mixed with vortex until being homogeneous. The tube was then incubated at 65 °C for 1 h. A 400-µl volume of chloroform: phenol (Appendix A) was added to the mixture and the tube was inverted several times. The mixture was centrifuged at 10,000 rpm (Sigma 202MC) for 15 min at room temperature. The aqueous (top) phase containing the DNA was transferred to a new tube. Then, 10 µl of 3 M sodium acetate was added to the aqueous phase followed by 0.54 volume of cold isopropanol. The tube was inverted gently and DNA precipitate was spun down at room temperature as previously for 2 min. The pellet was washed once with cold 70% ethanol before leaving at room temperature to dryness. The DNA pellet was resuspended in 100 µl TE (10mM Tris HCl pH 8.0, 0.1 mM EDTA) buffer.

#### 3.12.2.2 Polymerase chain reaction (PCR) amplification

ITS1-5.8-ITS2 regions of ribosomal DNA (rDNA) (Figure 23) were amplified by PCR using the forward primer ITS5 and the reverse primer ITS4, while primers NS1 and NS8 were used to amplify 18S region of rRNA gene according to White *et al.* (1990). The primer sequences are shown in Table 2. Oligonucleotide primers were synthesized using ABI PRISM™, DNA/RNA synthesizer model 392, Perkin Elmer, by the Bioservice Unit (BSU) at the National Center for Genetic Engineering and Biotechnology (BIOTEC). The reaction mixture was prepared on ice. The amplification reaction was performed in the total volume of 50 µl: 2 ng/µl of template DNA , 0.5 mM of each primer,

0.2 mM of individual dNTP, 3 mM of MgCl$_2$, 50 mM KCl, 10 mM of Tris-HCl at pH 8.8 and 1.0 U of *Taq* DNA polymerase (Appendix A). For each test, a primer negative control was included without template DNA. Ice-cold PCR reaction tubes were transferred to an Eppendrof Mastercycler Gradient PCR machine.

The thermal cycling program was as follow: 3 min initial denaturation at 95 °C, followed by 30 cycles of 50 s denaturation at 95 °C, 40 s primer annealing at 48 °C, 50 s extension at 72 °C, and a final 10 min extension at 72 °C.

Four microlitres of PCR products from each PCR reaction were examined by electrophoresis at 80V (8 V cm$^{-1}$) for 45 min in a 1% (w/v) agarose gel in Tris-acetate-EDTA (TEA) buffer (Appendix A) and visualized with UV light after staining with ethidium bromide (0.5 µg/ml).

### 3.12.2.3    DNA sequencing

PCR products were purified using minicolumns (Wizard® PCR Preps DNA Purification System, Promega) according to the manufacture's protocol (Guo *et al.*, 2003). Primers NS1, NS2, NS3, NS4, NS5, NS6, NS7, and NS8 and ITS4, and ITS5 were directly subjected to sequencing reactions for the 18S rRNA and the ITS1-5.8S-ITS2 regions, respectively. All DNA strands were sequenced. Purified PCR products were sequenced using dye terminator cycle sequencing, and reactions were resolved on the ABI Prism 3100 Genetic Analyzer (AME Bioscience). This was done at the Bioservice Unit (BSU), the National Center for Genetic Engineering and Biotechnology (BIOTEC).

### 3.12.3 Phylogenetic Analysis

18S and ITS1-5.8S-ITS2 DNA sequence were used as query sequence to search for similar sequence from GenBank using BLASTN 2.2.10 (Altschul *et al.*, 1997). Sequences similar to the query sequences were obtained and used for subsequent phylogenetic analyses. DNA sequence alignment and identity were performed and determined, respectively, using ClustalW (1.82) multiple sequence

alignment program (Thompson *et al.*, 1994). The alignment results were adjusted manually where necessary to maximize alignment using BioEdit. The alignment data were subsequently used for maximum-parsimony analysis in which searches for most parsimonious trees were conducted with the heuristic search algorithms with tree-bisection-reconnection (TBR) branch swapping in PAUP® (v 4.0b10) (Swofford, 2003). For each search, 10 replicates of random stepwise sequence addition were performed and 100 trees were saved per replicate. Gaps were treated as missing data. Character states were treated as unordered. Statistical support for the internal branches was estimated by bootstrap analysis with 1000 replications.



[Diagram adapted from: White et al. 1990 PCR protocols: 316]

Figure 23    Location on nuclear rDNAs of ITS5, ITS4, NS1, ands NS8 primers. The arrow heads represent the 3' end of each primer.

Table 2    Primers for amplification of ribosomal RNA genes of fungal isolates

LRUB20 and LPHIL36

| rRNA | GenePrimer[a] | Product Size (bp)[b] | Tm (°C)[c] |
|---|---|---|---|
| Nuclear, ITS | | | |
| ITS5 | GGAAGTAAAAGTCGTAACAAGG | ~ 620 | 65 |
| ITS4 | TCCTCCGCTTATTGATATGC | | 58 |
| Mitochondrial, 18S | | | |
| NS1 | GTAGTCATATGCTTGTCTC | ~ 2280 | 68 |
| NS8 | TCCGCAGGTTCACCTACGGA | | 57 |

[a] Primers ITS5 and NS1 is forward primer; ITS4 and NS8 and reverse primer.

[b] Product sizes are approximated based on the rRNA genes of *Saccharomyces cerevisiae*; the size of the region amplified is the product size minus the primers.

[c] Tm's were calculated by the method of Meinkoth and Wahl (1988).

# CHAPTER IV

# RESULTS AND DISCUSSION

## 4.1 Isolation of fungal endophytes

Endophytic fungus LPHIL36 was isolated from apparently healthy leaves of a Thai medicinal plant, *Lindenbergia philippensis* (Cham.) Benth. [H]. (family Scrophulariaceae) collected from Kanchanaburi Province, Thailand. This fungal isolate was grown on five different culture media, including Czapek yeast autolysate agar (CzYA), malt Czapek agar (MCzA), potato dextrose agar (PDA), Sabouraud's dextrose agar (SDA), and yeast extract sucrose agar (YEA), for 14 days at room temperature, as shown in Figure 24, while the other isolate LRUB20 was obtained from the healthy twig of the plant *Leea rubra* Blume Ex Spreng. (family Leeaceae) collected from the forest areas of Pitsanulok Province, Thailand. Culture purity was determined from colony morphology, as demonstrated on previous study by Chomcheon, 2004 (in Master's thesis).
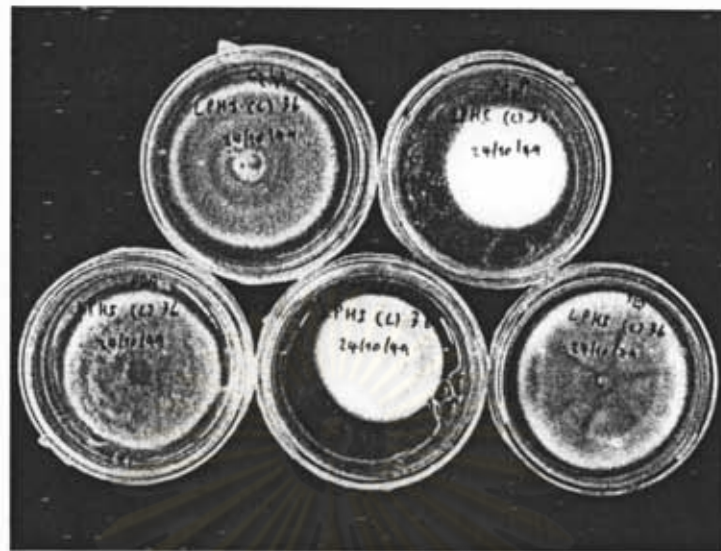
Obverse
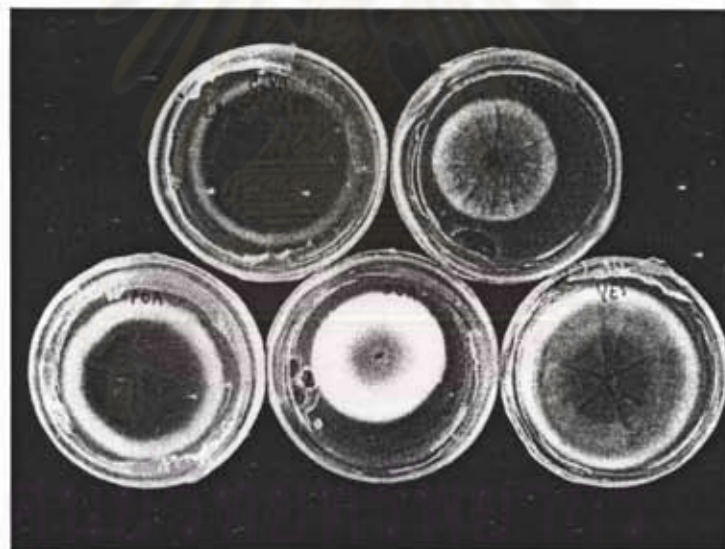


Reverse

**Figure 24** Colony morphology of endophytic fungus isolate LPHIL36 on five mycological media. Culture: top left, Czapek yeast autolysate agar (CzYA); top right, malt Czapek agar (MCzA); bottom left, potato dextrose agar (PDA); bottom middle, Sabouraud's dextrose agar (SDA) and bottom right, Yeast extract agar (YEA).

4.2   Structure elucidation of the isolated compounds from endophytic fungal isolate LRUB20

   We recently isolated the endophytic fungus LRUB20 from a Thai medicinal plant, Leea rubra Blume ex Spreng (family Leeaceae). Based upon analysis of the DNA sequences of the 18S and ITS region of the ribosomal RNA gene, the fungus LRUB20 is potentially a new species (see Section 4.5). Interestingly, we have found that this fungus can produce a large amount (gram scale) of 2-hydroxymethyl-3-methyl-cyclopent-2-enone, a useful scaffold for organic synthesis and its minor derivative, 2-hydroxymethyl-3-methyl-cyclopentanone shown in Figure 25 (Chomcheon *et al.*, 2006).



   **A**                                                        **B**

**Figure 25**     Structure of 2-hydroxymethyl-3-methyl-cyclopent-2-enone (A) and 2-hydroxymethyl-3-methyl-cyclopentanone (B), a secondary metabolite from the fermentation of fungal isolate LRUB20

   Because, the LRUB20 fungus is potentially a new species, we have extended our study on secondary metabolites by varying the culture media. It was found that a crude extract of the endophytic mitosporic Dothideomycete LRUB20 cultured in Czapek yeast autolysate medium was separated by Sephadex LH-20 and silica gel column chromatography, preparative TLC, and semi-preparative C18 reversed-phase HPLC, furnishing four novel pyrone derivatives, dothideopyrones A–D (**1**, **3**, **4**, and **5**), together with known fungal metabolites questin (**10**), asterric acid (**11**), methyl asterrate (**12**), sulochrin (**13**), and eugenitin (**14**). However, the LRUB20 fungus cultured in the M1D medium (Strobel *et al.*, 1996) supplemented with malt extract produced two known

compounds, 6-hydroxymethyleugenitin (**15**) and *cis,trans*-muconic acid (**9**). The chemical structures of the isolated compounds were elucidated by spectroscopic methods and comparison with literature values.

### 4.2.1 Structure elucidation of dothideopyrone A (1)



**1**
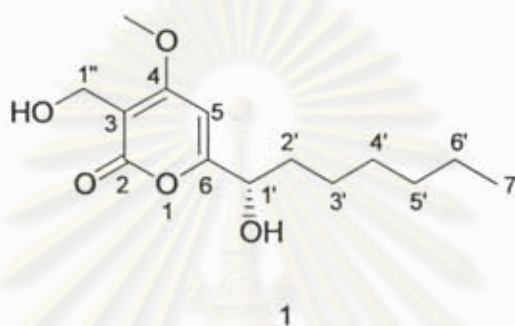
Dothideopyrone A (**1**) was isolated as colorless oil and the APCI–TOF mass spectrum (Figure L3 in Appendix B) revealed a pseudo molecular ion peak at *m/z* 271.1540 [M + H]$^+$ (calculated for $C_{14}H_{23}O_5$, 271.1546). The IR spectrum (Figure L2 in Appendix B) of dothideopyrone A showed absorption bands for hydroxyl group at 3373 cm$^{-1}$ and a conjugated carbonyl at 1682 cm$^{-1}$. The UV spectrum (Figure L1 in Appendix B) exhibited a maximum absorption at 299 nm, characteristic of a pyrone.

The 500 MHz $^1$H NMR spectrum (Figure L4 in Appendix B) of dothideopyrone A (**1**) in CDCl$_3$ demonstrated signals for an isolated sp$^2$ methine ($\delta_H$ 6.44), an oxygenated sp$^3$ methine ($\delta_H$ 4.40), a methoxy group ($\delta_H$ 3.92), an oxygenated methylene ($\delta_H$ 4.48), and a hexyl moiety ($\delta_H$ 0.86–1.82).

The 125 MHz $^{13}$C NMR spectrum of dothideopyrone A (**1**) in CDCl$_3$ (Figure L5 in Appendix B) gave fourteen carbon signals, which were classified by DEPT 135 (Figure L5 in Appendix B) and HMQC spectral data (Figure L6 in Appendix B) as two methyl carbon signal at $\delta$ 13.9 (C-7′), and 56.7 ppm (4-OMe); six methylene carbon signals at $\delta$ 22.5 (C-6′), 24.9 (C-3′), 28.9 (C-4′), 31.6 (C-5′), 35.3 (C-2′) and 54.3 ppm (C-1″); two methine carbon signals at $\delta$ 70.5 (C-1′), and 92.8 ppm (C-5); four non-protonated carbon signals at $\delta$ 103.6 (C-3), 165.2 (C-2), 167.7 (C-4) and 169.1 ppm (C-6).

The $^1$H-$^1$H COSY analytical spectrum of dothideopyrone A (1) in CDCl$_3$ (Figures L10 in Appendix B) assisted the assembling of a partial structure from C-1' to C-7'. The complete $^{13}$C assignments were established from the HMBC spectrum (Figures L7 in Appendix B) showing the following long-range correlations; H-7' ($\delta$ 0.86, $t$, $J = 6.7$ Hz) to C-6' ($\delta$ 22.5) and C-5' ($\delta$ 31.6); overlapping signals of H-4', H-5', and H-6' ($\delta$ 1.25, $m$) to C-7' ($\delta$ 13.9), C-6' ($\delta$ 22.5), C-3' ($\delta$ 24.9), C-5' ($\delta$ 31.6), and C-2' ($\delta$ 35.3); H-3' ($\delta$ 1.40, $m$) to C-4' ($\delta$ 28.9), C-5' ($\delta$ 31.6), C-2' ($\delta$ 35.2), and C-1' ($\delta$ 70.5); H-2' ($\delta$ 1.64, and 1.82, $m$) to C-3' ($\delta$ 24.9), C-4' ($\delta$ 28.9), and C-1' ($\delta$ 70.5); H-1' ($\delta$ 4.40, $dd$, $J = 4.0$ and 7.9) to C-3' ($\delta$ 24.9), and C-2' ($\delta$ 35.3). This spectral data established a partial structure of dothideopyrone A (1), as shown in Figure 26.



— Bold lines are from $^1$H-$^1$H COSY correlations
→ HMBC correlations
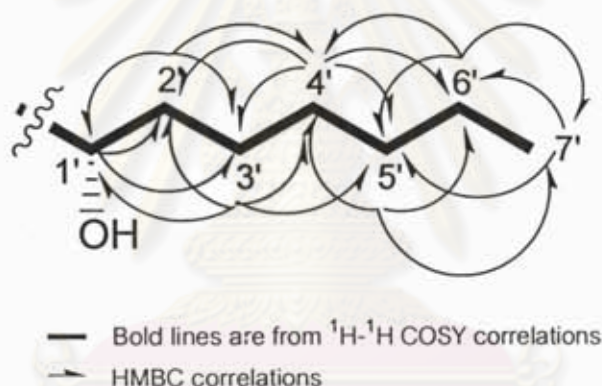
Figure 26    The partial structure of dothideopyrone A (1) from C-1' to C-7'

Analysis of HMBC spectrum showed correlations from H-5 ($\delta$ 6.44, $s$) to C-1' ($\delta$ 70.5), C-4 ($\delta$ 167.7), and C-6 ($\delta$ 169.1); from the 4-OMe protons ($\delta$ 3.92, $s$) to C-4 ($\delta$ 167.7); from H-1' ($\delta$ 4.40, $dd$, $J = 4.0$ and 7.9) to C-5 ($\delta$ 92.8) and C-6 ($\delta$ 169.1); and from H$_2$-1''($\delta$ 4.48, $s$) to C-2 ($\delta$ 165.2), C-3 ($\delta$ 103.6) and C-4 ($\delta$ 167.7). These correlations established the positions of the substituents on the pyrone ring, as summarized in Figure 27.
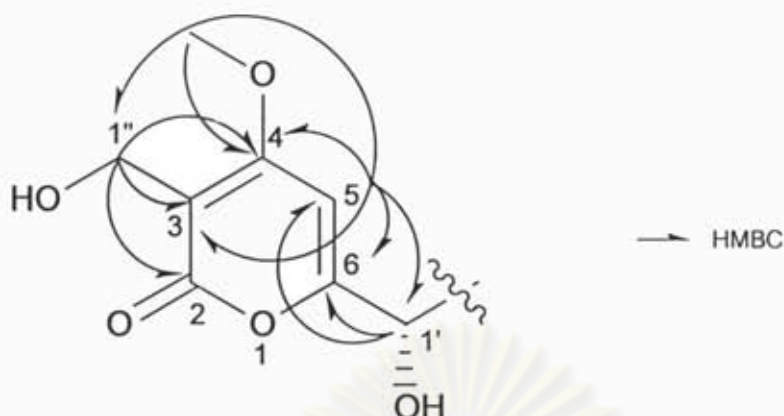
**Figure 27**       HMBC correlations of pyrone ring of dothideopyrone A (1)

The side chain in dothideopyrone A (1), 1-heptanol, was linked to the pyrone unit at C-6 as evident from the HMBC correlations of H-1′ and $H_2$-2′ to C-6 (Figure 28).
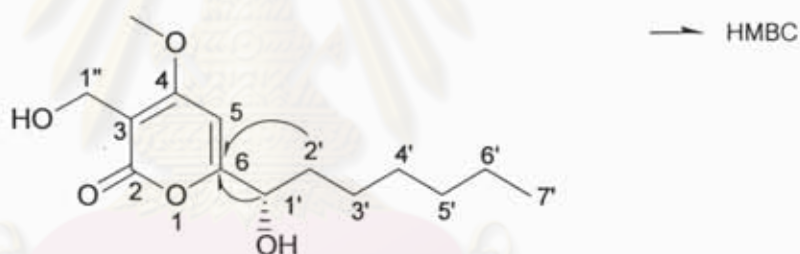


**Figure 28**       HMBC correlations between the 1-heptanol segment and pyrone unit in 1

Acetylation of dothideopyrone A yielded a diacetate derivative 2, both the hydroxyl groups at C-1′ and C-1″ (Figure 29), confirming the presence of two hydroxyl groups in dothideopyrone A (1).
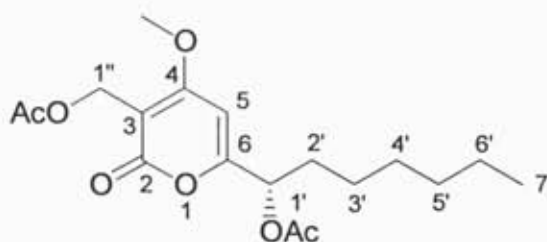


**Figure 29**       The diacetate derivative (2) of dothideopyrone A (1)

Upon the basis of these data, the gross structure of dothideopyrone A (1) was established. Assignments of all $^1$H and $^{13}$C NMR spectroscopic signals for dothideopyrone A were made by analysis of $^1$H–$^1$H COSY and HMBC spectra summarized in Table 3.
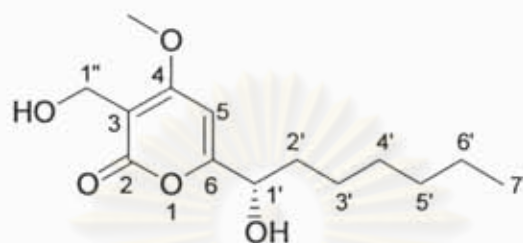


A gross structure of the dothideopyrone A (1)

Table 3    The $^1$H, $^{13}$C, $^1$H–$^1$H COSY and HMBC spectral data of dothideopyrone A (1) in CDCl$_3$

| Position | $\delta_C$ | $\delta_H$, multiplicity, $J_{H,H}$ (Hz) | COSY (H to H) | HMBC (H to C) |
|---|---|---|---|---|
| 2 | 165.2 | - | - | - |
| 3 | 103.6 | - | - | - |
| 4 | 167.7 | - | - | - |
| 5 | 92.8 | 6.44, s | - | 2', 1'', 1', 3, 4, 6 |
| 6 | 169.1 | - | - | - |
| 1' | 70.5 | 4.40, dd, 4.0 and 7.9 | 2' | 3', 2', 5, 6 |
| 2' | 35.3 | 1.64, m (H-2'α) | 1', 3', H-2'α | 3', 4', 1', 6 |
| | | 1.82, m (H-2'β) | 1', 3', H-2'β | |
| 3' | 24.9 | 1.40, m | 2', 4' | 4', 5', 2', 1' |
| 4' | 28.9 | 1.25, m | 3' | 6', 3', 5', 2' |
| 5' | 31.6 | 1.25, m | - | 7', 6', 3', 4' |
| 6' | 22.5 | 1.25, m | 7' | 7', 4', 5' |
| 7' | 13.9 | 0.86, t, 6.7 | 6' | 6', 5' |
| 1'' | 54.3 | 4.48, s | - | 3, 2, 4 |
| 4-OMe | 56.7 | 3.92, s | - | 4 |

4.2.2　Structure elucidation of dothideopyrone B (3)



3
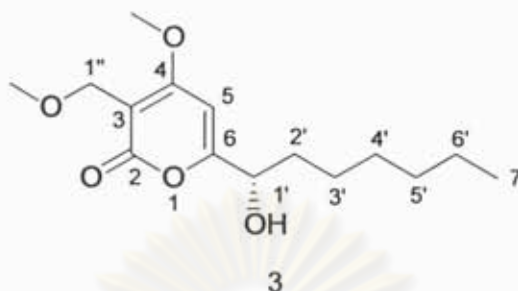
Dothideopyrone B (3) was obtained as colorless oil, and this metabolite possessed the molecular formula $C_{15}H_{24}O_5$, as deduced from APCI–TOF mass spectrum (Figure L14 in Appendix B), showing a pseudo-molecular ion peak at $m/z$ 307.1561 [M + Na]$^+$.

The $^1H$ NMR spectrum of the dothideopyrone B (3) revealed signals for an isolated $sp^2$ methine ($\delta_H$ 6.34), an oxygenated $sp^3$ methine ($\delta_H$ 4.36), two methoxy group ($\delta_H$ 3.33, and $\delta_H$ 3.87), an oxygenated methylene ($\delta_H$ 4.25), and a hexyl moiety ($\delta_H$ 0.81–1.79), as shown in Figure L15 in Appendix B. The $^{13}C$ NMR spectrum of the dothideopyrone B (3) contained 15 lines (Figure L17 in Appendix B), and the DEPT data established the presence of three methyls, six methylenes, two methines, and four non-protonated carbons (Figure L18 in Appendix B). The $^1H$–$^1H$ COSY spectrum of dothideopyrone B (3) exhibited the assembling of a partial structure from C-1′ to C-7′ (Figure L24 in Appendix B). The HMBC spectrum showed the correlations from H-5 to C-1′, C-4, and C-6; from the 4-OMe protons and the1″-OMe to C-4 and C-1″, respectively; from H-1′ to C-5 and C-6; and from H$_2$-1″ to C-2, C-3 and C-4. These correlations established the positions of the substituents on the pyrone ring. The side chain in 3, 1-heptanol, was also linked to the pyrone unit at C-6 as evident from the HMBC correlations of H-1′ and H$_2$-2′ to C-6 (Figure L20 in Appendix B). These spectroscopic data of dothideopyrone B (3) were similar to those of dothideopyrone A (1), except for the presence of additional methoxy signals in dothideopyrone B (3). In

the HMBC spectrum, 1″-OMe protons ($\delta_H$ 3.33) correlated to C-1″, indicating that dothideopyrone B (3) was a 1″-O-methyl derivative of dothideopyrone A (1).

Protons and carbons in dothideopyrone B (3) were assigned by analysis of $^1$H–$^1$H COSY and HMBC spectra, as summarized in Figure 30 and Table 4.



— Bold lines are from $^1$H-$^1$H COSY correlations
→ HMBC correlations
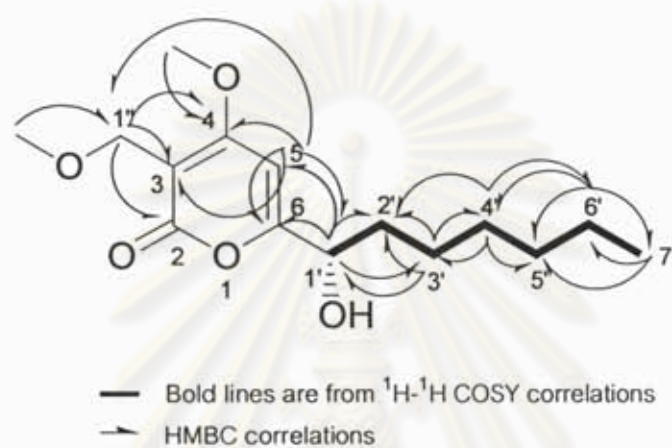
Figure 30    HMBC and $^1$H-$^1$H COSY correlations of dothideopyrone B (3)

Table 4    The $^1$H, $^{13}$C, $^1$H–$^1$H COSY and HMBC spectral data of dothideopyrone B (3) in CDCl$_3$



3

| Position | $\delta_C$ | $\delta_H$, multiplicity, $J_{H,H}$ (Hz) | COSY (H to H) | HMBC (H to C) |
|---|---|---|---|---|
| 2 | 164.6 | - | - | - |
| 3 | 101.3 | - | - | - |
| 4 | 169.1 | - | - | - |
| 5 | 92.4 | 6.34, s | - | 2′, 1″, 1′, 3, 4, 6 |
| 6 | 169.2 | - | - | - |
| 1′ | 70.8 | 4.36, dd, 4.1 and 8.1 | 2′ | 3′, 2′, 5, 6 |
| 2′ | 35.5 | 1.58, m (H-2′α) | 1′, 3′, H-2′β | 3′, 4′, 1′, 6 |
|  |  | 1.79, m (H-2′β) | 1′, 3′, H-2′α |  |
| 3′ | 25.0 | 1.35, m | 2′, 4′ | 4′, 5′, 2′, 1′ |
| 4′ | 28.9 | 1.21, m | 3′ | 6′, 3′, 5′, 2′ |
| 5′ | 31.6 | 1.21, m | - | 7′, 6′, 3′, 4′ |
| 6′ | 22.5 | 1.21, m | 7′ | 7′, 4′, 5′ |
| 7′ | 14.0 | 0.81, t, 6.7 | 6′ | 6′, 5′ |
| 1″ | 63.2 | 4.25, s | - | 3, 2, 4 |
| 4-OMe | 56.8 | 3.87, s | - | 4 |
| 1″-OMe | 58.4 | 3.33, s | - | 1″ |

### 4.2.3 Structure elucidation of dothideopyrone C (4)



4
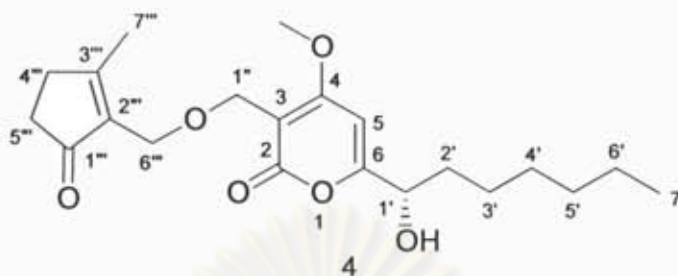
Dothideopyrone C (4) was isolated as colorless oil, and the APCI–TOF mass spectrum suggested the molecular formula $C_{21}H_{30}O_6$.

The $^1H$ NMR spectrum of dothideopyrone C (4) in $CDCl_3$ consisted of $sp^2$ methine ($\delta_H$ 6.40), an oxygenated $sp^3$ methine ($\delta_H$ 4.41), a methoxy group ($\delta_H$ 3.92), two oxygenated methylene ($\delta_H$ 4.20 and $\delta_H$ 4.37), six $sp^3$ methylene (overlapping signals of three protons at $\delta_H$ 1.28, $\delta_H$ 1.40, $\delta_H$ 1.64, $\delta_H$ 1.85, $\delta_H$ 2.38 to 2.40 and $\delta_H$ 2.53 to 2.55), and two $sp^3$ methyl ($\delta_H$ 2.20 and $\delta_H$ 0.88), as demonstrated in Figure L28 (Appendix B). The $^{13}C$ NMR spectrum of the dothideopyrone C (4) contained 21 lines (Figure L30 in Appendix B), and the DEPT data established the presence of three methyls, nine methylenes, two methines, and seven non-protonated carbons shown in Figure L31 in Appendix B.

Based upon the $^1H$ and $^{13}C$ NMR spectral data, dothideopyrone C (4) was a derivative of dothideopyrone A (1). The 1H-1H COSY and HMBC spectra of compound (4) established the structure of a segment A, as shown in Figure 31.
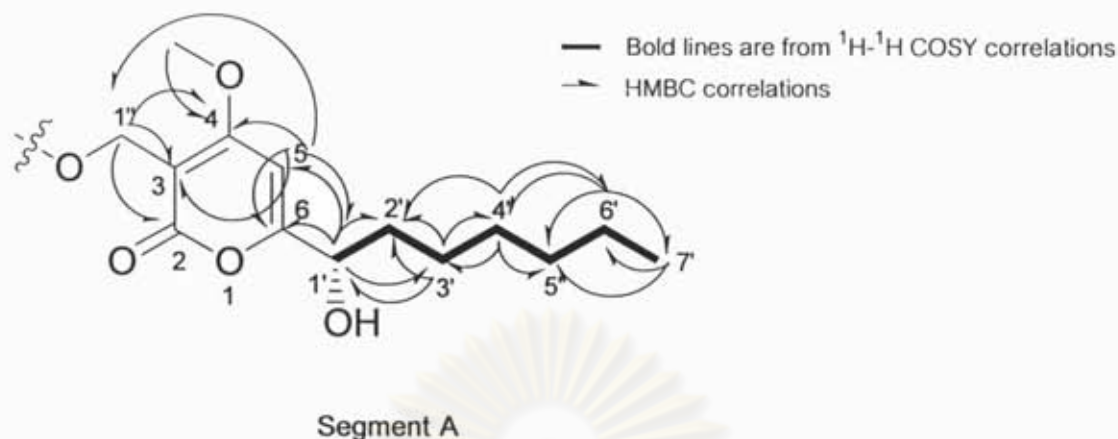
Segment A

Figure 31    Correlations of the $^1$H-$^1$H COSY and the HMBC spectra of segment A

Furthermore, analysis of $^1$H and $^{13}$C NMR spectra of dothideopyrone C (**4**) indicated additional signal characteristic of a 2-hydroxymethyl-3-methylcyclopent-2-enone unit. The $^1$H-$^1$H COSY spectra of a segment B established the correlation between H-4''' and H-5'''. The complete $^{13}$C assignments of this segment were established from the HMBC spectrum showing the following long-range correlations; H-4''' ($\delta$ 2.53 to 255) to C-5''' ($\delta$ 34.5), C-2''' ($\delta$ 136.9), C-3''' ($\delta$ 177.5), and C-1''' ($\delta$ 208.6); H-5''' ($\delta$ 2.38 to 2.40) to C-4''' ($\delta$ 31.7), C-3''' ($\delta$ 177.5), and C-1''' ($\delta$ 208.6); H-6''' ($\delta$ 4.20) to C-2''' ($\delta$ 136.9), C-3''' ($\delta$ 177.5), and C-1''' ($\delta$ 208.6); and H-7''' ($\delta$ 2.20) to C-4''' ($\delta$ 31.7), C-2''' ($\delta$ 136.9), C-3''' ($\delta$ 177.5), and C-1''' ($\delta$ 208.6). It should be noted that $\delta_c$ (177.5) of the C-3''' double bond in the segment B was significantly shifted downfield, similar to the carbonyl resonances for carboxylic acids or esters. However, X-ray single-crystal analysis of the 2-hydroxymethyl-3-methylcyclopent-2-enone in a form of 2,4-dinitrophenylhydrazone derivative confirmed the structure of the 2-hydroxymethyl-3-methylcyclopent-2-enone (see reference information, Chomcheon *et al.*, 2006). The segment B was therefore proposed on the basis of the above NMR data as depicted in Figure 32.
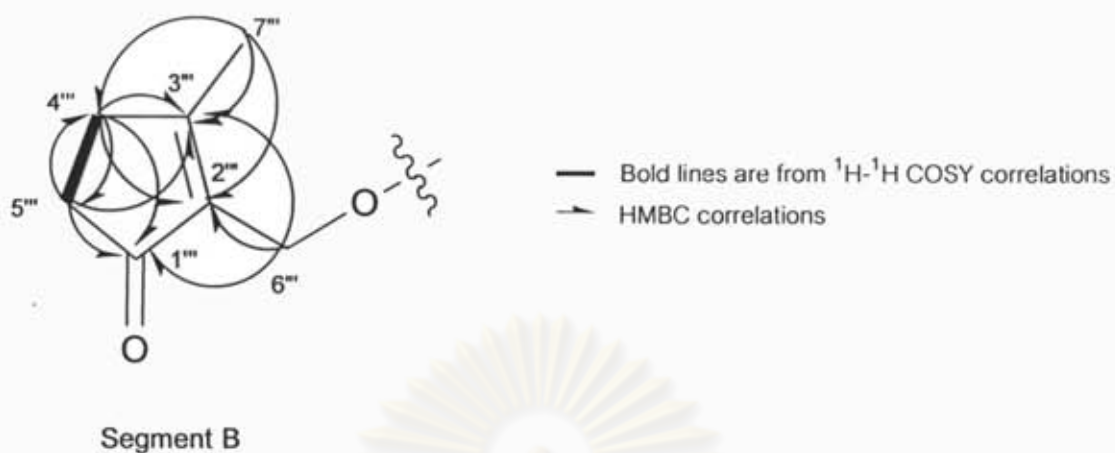
Segment B

Figure 32    Assignment of the $^1$H-$^1$H COSY and the HMBC correlations of segment B

The HMBC spectrum of dothideopyrone C (4) revealed correlations of H$_2$-1″ to C-6‴, and H$_2$-6‴ to C-1″, indicating the presence of C-1″/C-6‴ ether linkage between the 2-hydroxymethyl-3-methyl-cyclopent-2-enone unit and a dothideopyrone A (1) unit (Figure 33). The gross structure of dothideopyrone C (4) was demonstrated in Figure 33. The $^1$H–$^1$H COSY and HMBC spectra assisted the assignment of all proton and carbon signals for dothideopyrone C (4) summarized in Table 5.
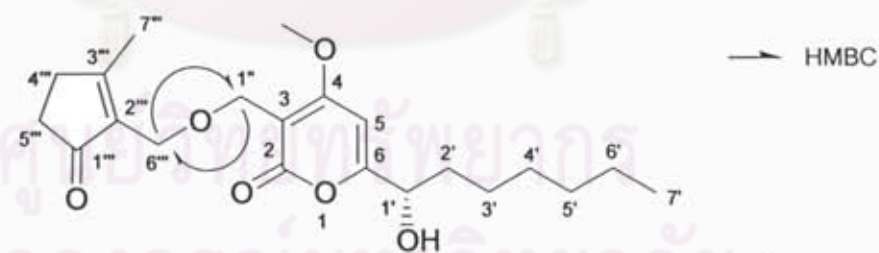


Figure 33    A gross structure of dothideopyrone C (4)

Table 5    The $^1$H, $^{13}$C, $^1$H–$^1$H COSY and HMBC spectral data of dothideopyrone C

(4) in CDCl$_3$

| Position | $\delta_C$ | $\delta_H$, multiplicity, $J_{H,H}$ (Hz) | COSY (H to H) | HMBC (H to C) |
|---|---|---|---|---|
| 2 | 164.6 | - | - | - |
| 3 | 101.3 | - | - | - |
| 4 | 169.2 | - | - | - |
| 5 | 92.6 | 6.40, s | - | 1″, 1′, 3, 4, 6 |
| 6 | 169.2 | - | - | - |
| 1′ | 70.8 | 4.41, dd, 4.0 and 8.1 | 2′ | 3′, 2′, 6 |
| 2′ | 35.5 | 1.64, m (H-2′α) | 1′, 3′, H-2′β | 3′, 4′, 1′, 6 |
|  |  | 1.85, m (H-2′β) | 1′, 3 H-2′α |  |
| 3′ | 25.1 | 1.40, m | 2′, 4′ | 4′, 5′, 2′, 1′ |
| 4′ | 29.0 | 1.28, m | 3′ | 6′, 3′, 5′, 2′ |
| 5′ | 32.0 | 1.28, m | - | 7′, 6′, 3′, 4′ |
| 6′ | 22.6 | 1.28, m | 7′ | 7′, 4′, 5′ |
| 7′ | 14.1 | 0.88, t, 6.6 | 6′ | 6′, 5′ |
| 1″ | 61.2 | 4.37, s | - | 3, 2, 4, 6‴ |
| 4-OMe | 56.8 | 3.92, s | - | 4 |
| 1‴ | 208.6 | - | - | - |
| 2‴ | 136.9 | - | - | - |
| 3‴ | 177.5 | - | - | - |
| 4‴ | 31.7 | 2.53-2.55, m | 5‴ | 5‴, 2‴, 3‴, 1‴ |
| 5‴ | 34.5 | 2.38-2.40, m | 4‴ | 4‴, 3‴, 1‴ |
| 6‴ | 60.9 | 4.20, s | - | 1″, 2‴, 3‴, 1‴ |
| 7‴ | 17.7 | 2.20, s | - | 4‴, 2‴, 3‴, 1‴ |

### 4.2.4 Structure elucidation of dothideopyrone D (5)



5
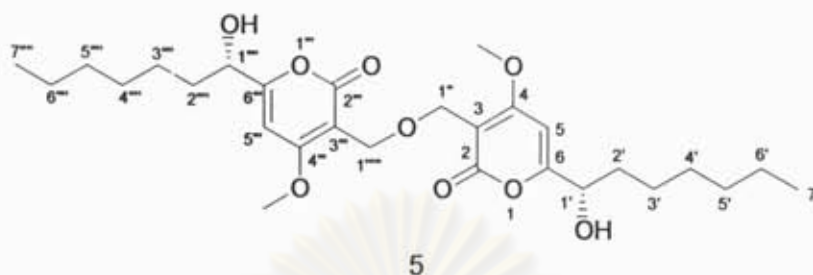
The $^1$H NMR spectrum in CDCl$_3$ of dothideopyrone D (5) demonstrated signals of a sp$^2$ methine ($\delta_H$ 6.35), an oxygenated sp$^3$ methine ($\delta_H$ 4.32), a methoxy group ($\delta_H$ 3.85), an oxygenated methylene ($\delta_H$ 4.32), and a hexyl moiety ($\delta_H$ 0.80 to 1.74) (Figure L41 in Appendix B). The $^{13}$C NMR spectrum of the dothideopyrone D (5) showed 14 lines (Figure L43 in Appendix B), and the DEPT data established the presence of two methyls, six methylenes, two methines, and four non-protonated carbons (Figure L44 in Appendix B). Based on these spectral information, dothideopyrone D (5) was a derivative of dothideopyrone A (1). However, dothideopyrone D (5) has a molecular formula of C$_{28}$H$_{42}$O$_9$, as established by APCI-TOF mass spectral data, while 14 carbon signals were observed in the $^{13}$C NMR spectrum, therefore 5 possessed a homodimer structure.

The HMBC spectrum of dothideopyrone D (5) readily established the ether linkage of the two identical units at the hydroxyl methylene, showing correlations from H$_2$-1″ to C-1″″″ and from H$_2$-1″″″ to C-1″ as shown in Figure 34.
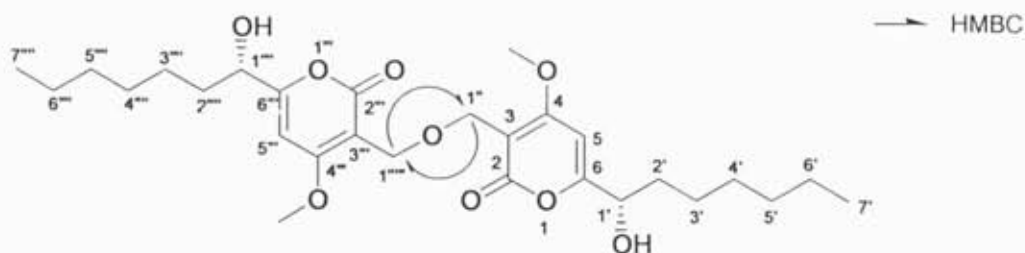
**Figure 34** HMBC correlations between the two subunits of dothideopyrone D (5)
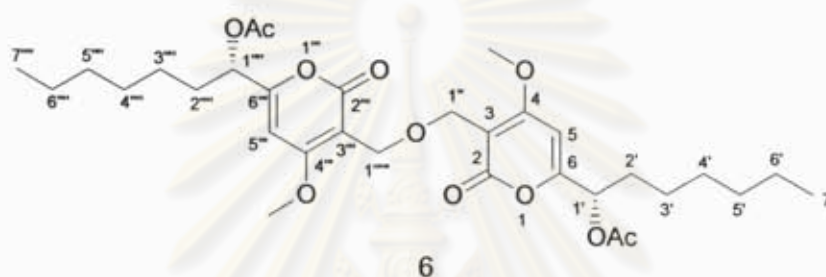


Upon acetylation of dothideopyrone D (5), a diacetate derivative **6** was obtained; only the hydroxyl groups at C-1′ and C-1″″ were acetylated, which further confirmed the structure of dothideopyrone D (5). Interestingly, pyrone dimers are very rare in nature. To our knowledge, multiforisin D is the only natural bis-pyrone dimer, previously isolated from the fungus *Gelasinospora multiforis* (Fujimoto *et al.*, 1995) (Figure 35).
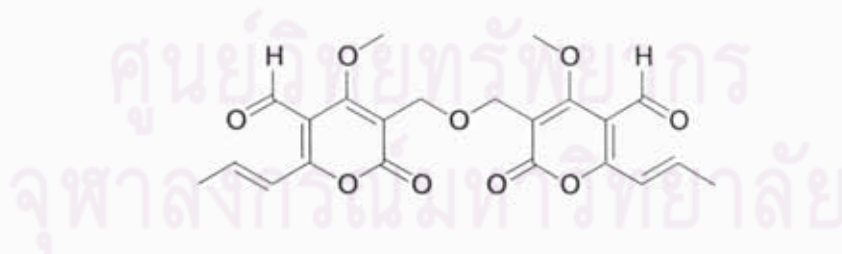


**Figure 35** The chemical structure of multiforisin D

Proton and carbon signals for dothideopyrone D (5) were assigned by analysis of ¹H–¹H COSY and HMBC spectra (Figure 36 and Table 6).

Figure 36    The HMBC and $^1$H-$^1$H COSY correlations of dothideopyrone D (5)

Table 6    The $^1$H, $^{13}$C, $^1$H–$^1$H COSY and HMBC spectral data of dothideopyrone D (5) in CDCl$_3$

| Position | $\delta_C$ | $\delta_H$, multiplicity, $J_{H,H}$ (Hz) | COSY (H to H) | HMBC (H to C) |
|---|---|---|---|---|
| 2 | 164.9 | - | - | - |
| 3 | 101.3 | - | - | - |
| 4 | 169.4 | - | - | - |
| 5 | 92.9 | 6.35, s | - | 2', 1'', 1', 3, 4, 6 |
| 6 | 169.4 | - | - | - |
| 1' | 70.6 | 4.32, dd, 4.0 and 8.1 | 2' | 3', 2', 6 |
| 2' | 35.3 | 1.57, m (H-2'α) | 1', 3', H-2'β | 3', 4', 1', 6 |
|  |  | 1.74, m (H-2'β) | 1', 3', H-2' α |  |
| 3' | 25.1 | 1.33, m | 2', 4' | 4', 5', 2', 1' |
| 4' | 29.0 | 1.20, m | 3' | 6', 3', 5', 2' |
| 5' | 31.7 | 1.20, m | - | 7', 6', 3', 4' |
| 6' | 22.5 | 1.20, m | 7' | 7', 4', 5' |
| 7' | 14.0 | 0.80, t, 6.7 | 6' | 6', 5' |
| 1'' | 61.3 | 4.32, s | - | 3, 2, 4, 1''''''' |
| 4-OMe | 56.9 | 3.85, s | - | 4 |

Compound 5 has C2 symmetry, so NMR data for the two halves are identical.

### 4.2.5 The absolute configuration of dothideopyrones A-D
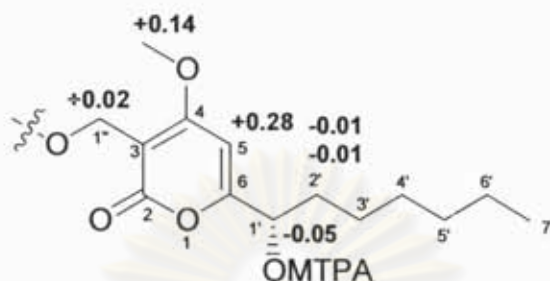


**Figure 37** Δδ Valures [δ ₍S₎ − δ ₍R₎] for the MTPA esters 7 and 8

Dothideopyrones A–D (1, 3, 4, and 5) all process a chiral secondary alcohol unit, and all exhibited similar negative specific rotations. The absolute configuration of dothideopyrones A–D was assigned by application of the modified Mosher's method (Dale and Mosher, 1973), and dothideopyrone D (5) was selected as a model compound. (S)-MTPA (7) and (R)-MTPA (8) esters (Figure 38) of dothideopyrone D (5) were prepared. The Δδ values [δ ₍S₎ − δ ₍R₎] of the MTPA esters indicated the S-configuration at C-1′ (or C-1″″) in dothideopyrone D (5) (Figure 37). Based on the similar negative specific rotations, the absolute configuration of C-1′ in dothideopyrones A–D (1, 3, 4, and 5) was also assumed to be S.



7, R = (S)-MTPA        8, R = (R)-MTPA
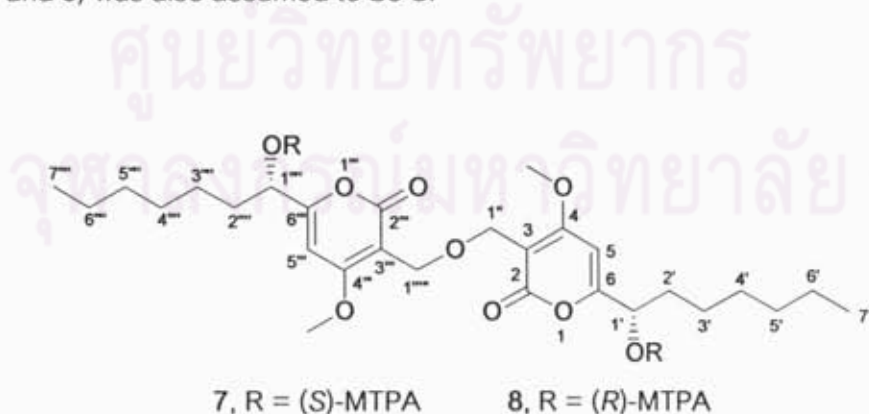
**Figure 38** The (S)-MTPA (7) and the (R)-MTPA (8) esters of dothideopyrone D (5)

### 4.2.6 Structure elucidation of *cis,trans*-muconic acid (9)
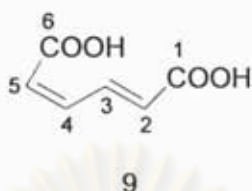


Compound 9 was obtained as white solid. The ESI-TOF mass spectrum of this compound displayed the molecular formula $C_6H_6O_4$ (m/z 141.0187 [M+H]⁻, calculated for 141.0193) (Figure L67 in Appendix B). The IR absorption band at 1693 cm⁻¹ suggested the presence of a carbonyl group (Figure L65 of Appendix B).

The ¹H NMR spectrum of compound (9) showed four $sp^2$ methine protons including H-5: δ 6.05 ppm, *ddd*, J = 11.4, 0.9, 0.9 Hz); H-2: δ 6.23 ppm, *ddd*, J = 15.5, 0.8, 0.8 Hz); H-4: δ 6.88 ppm, *ddd*, J = 11.5, 11.5, 0.8 Hz), and H-3: δ 8.46 ppm, *ddd*, J = 15.5, 11.5, 1.1 Hz). The ¹³C NMR spectrum showed six signals at δ, 124.5 (CH, C-5), 128.9 (CH, C-2), 138.8 (CH, C-3), 140.8 (CH, C-4), 165.7 (C, C-6), and 166.3 (C, C-1) ppm. The ¹H NMR and ¹³C NMR spectra of compound (9) are in Figure L67 and Figure L69 of Appendix B, respectively.

The ¹H-¹H COSY spectrum of compound (9) indicated that H-5 to H-4, H-4 to H-5 and H-3, H-3 to H-2 and H-4 as shown in Figure L73 (Appendix B).

Analysis of HMBC experiment (Figure L72 in Appendix B) assisted in assignments of a metabolite 9 from which the following correlations were observed: H-5 (δ 6.05) to C-3 (δ 138.8), C-4 (δ 140.8), and C-6 (δ 165.7); H-2 (δ 6.23) to C-3 (δ 138.8), C-4 (δ 140.8), and C-1 (δ 166.3); H-4 (δ 6.88) to C-5 (δ 124.5), C-2 (δ 128.9), C-3 (δ 138.8), and C-1 (δ 166.3); H-3 (δ 8.46) to C-5 (δ 124.5), C-2 (δ 128.9), C-4 (δ 140.8), and C-1 (δ 166.3).

In addition, compound 9 was methylated to yield a dimethyl derivative (Figure L74 in Appendix B) which demonstrated the molecular formula $C_8H_{10}O_4$, calculated by APCI-TOF mass spectral data, as shown in Figure L75 (Appendix B). Accordingly, this

metabolite possibly presents two carboxylic groups in the structure. On the basis of these spectral data, compound (9) was identified as *cis,trans*-muconic acid. It is to be noted that to date, only a monomethyl ester of *cis,cis*-muconic acid isolated from a marine sponge *Plakortis simplex* has been reported as a natural product (Shen *et al.*, 2001). To our knowledge, the present work is the first report on naturally occurring muconic acid.

Complete assignments of protons and carbons of *cis,trans*-muconic acid (9) are summarized in Figure 39 and Table 7.



**Figure 39**  The correlations from $^1$H-$^1$H COSY and HMBC spectra of *cis,trans*-muconic acid (9)

**Table 7**  The $^1$H, $^{13}$C, $^1$H–$^1$H COSY and HMBC spectral data of *cis,trans*-muconic acid (9) in acetone-$d_6$

| Position | $\delta_C$ | $\delta_H$, multiplicity, $J_{H,H}$ (Hz) | COSY (H to H) | HMBC (H to C) |
|---|---|---|---|---|
| 1 | 166.3 | - | - | - |
| 2 | 128.9 | 6.23, *ddd*, $J$ = 15.5, 0.8, 0.8 | 3 | 3, 4, 1 |
| 3 | 138.8 | 8.46, *ddd*, $J$ = 15.5, 11.5, 1.1 | 2, 4 | 5, 2, 4, 1 |
| 4 | 140.8 | 6.88, *ddd*, $J$ = 11.5, 11.5, 0.8 | 3, 5 | 5, 2, 3, 6 |
| 5 | 124.5 | 6.05, *ddd*, $J$ = 11.4, 0.9, 0.9 | 4 | 3, 4, 6 |
| 6 | 165.7 | - | - | - |

### 4.2.7    Structure elucidation of known metabolites

Chemical structures of known compounds, questin (**10**), asterric acid (**11**), methyl asterrate (**12**), subchrin (**13**), eugenitin (**14**), and 6-hydroxymethyleugenin (**15**) were elucidated by comparison of their NMR data with literature values. $^1$H, and $^{13}$C NMR spectra and other spectroscopic data of known metabolites are shown in Figure L76 to Figure L105 of Appendix B.

Questin (**10**) was isolated as orange yellow needles, and APCI-TOF MS suggested the molecular formula $C_{16}H_{12}O_5$. The $^1$H NMR spectral data (DMSO-$d_6$, 400 MHz) are as follows: δ 13.23 (1H, $s$, OH), 7.41 (1H, $s$), 7.18 (1H, $d$, $J$ = 2.2), 7.11 (1H, $s$,), 6.82 (1H, $d$, $J$ = 2.2), 3.89 (3H, $s$), 2.37 (3H, $s$). These $^1$H NMR data were consistent with literature values (Kimura $et$ $al.$, 1983).

Asterric acid (**11**) was isolated as white solid, and APCI-TOF MS suggested the molecular formula $C_{17}H_{16}O_8$. The $^1$H NMR spectral data (acetone-$d_6$, 400 MHz) are as follows: δ 7.06 (1H, $d$, $J$ = 2.8), 6.91 (1H, $d$, $J$ = 2.8), 6.47 (1H, $s$), 5.91 (1H, $s$), 3.81 (3H, $s$), 3.74 (3H, $s$), 2.10 (3H, $s$). The $^1$H NMR data of **11** were consistent with literature values (Jaih $et$ $al.$, 2002).

Methyl asterrate (**12**) was isolated as white solid, and APCI-TOF MS suggested the molecular formula $C_{18}H_{18}O_8$. The $^1$H NMR spectral data  (acetone-$d_6$, 400 MHz) are as follows: δ 11.32 (1H, $s$, OH), 8.89 (1H, $s$, OH), 6.91 (1H, $d$, $J$ = 2.8), 6.83 (1H, $d$, $J$ = 2.8), 6.38 (1H, $s$), 5.85 (1H, $s$), 3.90 (3H, $s$), 3.75 (3H, $s$), 3.64 (3H, $s$), 2.10 (3H, $s$). The $^1$H NMR data of **12** were consistent with literature values (Jaih $et$ $al.$, 2002).

Subchrin (**13**) was isolated as yellow amorphous solid, and APCI-TOF MS suggested the molecular formula $C_{17}H_{16}O_7$. The $^1$H NMR spectral data (DMSO-$d_6$, 400 MHz) are as follows: δ 11.43 (2H, $s$, OH), 9.89 (1H, $s$, OH), 6.81 (1H, $d$, $J$ = 2.1), 6.67

(1H, *d*, *J* = 2.1), 6.27 (2H, *s*), 3.63 (3H, *s*), 3.62 (3H, *s*), 2.14 (3H, *s*). These $^1$H NMR data were consistent with literature values (Shimada *et al.*, 2003).

Eugenitin (**14**) was isolated as white crystalline solid, and APCI-TOF MS suggested the molecular formula $C_{12}H_{12}O_4$. The $^1$H NMR spectral data (acetone-$d_6$, 400 MHz) are as follows: δ 13.0 (1H, *s*, OH), 7.41 (1H, *s*), 6.55 (1H, *s*), 6.10 (1H, *s*), 3.94 (3H, *s*), 2.38 (3H, *s*), 2.01 (3H, *s*). The $^1$H NMR data of **14** were consistent with literature values (Fox, 1969).

6-Hydroxymethyleugenin (**15**) was isolated as white solid, and APCI-TOF MS suggested the molecular formula $C_{12}H_{12}O_5$. The $^1$H NMR spectral data (CDCl$_3$, 400 MHz) are as follows: δ 13.03 (1H, *s*, OH), 6.39 (1H, *s*), 6.07 (1H, *s*), 4.79 (1H, *s*), 3.92 (3H, *s*), 2.37 (3H, *s*). These $^1$H NMR data were consistent with literature values (Feng *et al.*, 2002).

The chemical structures of the known metabolites are depicted in Figure 40.



10

11, R = H

12, R = Me

13

14, R = Me

15, R = CH$_2$OH
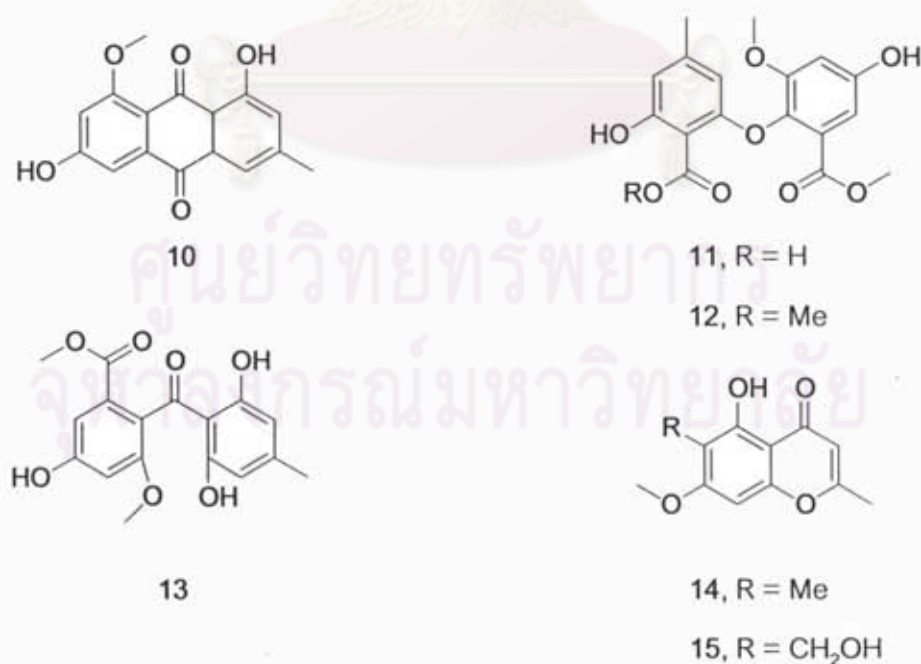
**Figure 40**    The chemical structures of known metabolites separated from the fungal LRUB20.

4.3 Structure elucidation of the isolated compounds from endophytic fungal isolate LPHIL36

A crude broth extract of the endophytic fungus *Corynespora cassiicola* (LPHIL36) was separated by Sephadex LH-20 and preparative TLC to yield new depsidones **16** and **18** named corynesidones A (**16**) and B (**18**), respectively and diaryl ether **20** named corynether A (**20**), together with a new natural product, diaryl ether **22** from the endophytic fungus *C. cassiicola* (LPHIL36). The chemical structures of the isolated compounds were elucidated by analyses of the NMR spectral data and physical properties.

### 4.3.1 Structure elucidation of corynesidones A (16)



16
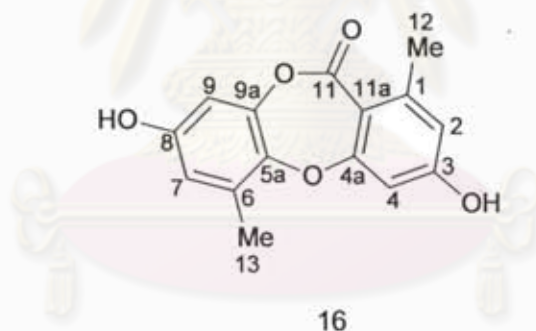
Corynesidone A (**16**) was obtained as white solid and the ESI-TOF mass spectrum (Figure P3 in Appendix B) established a pseudo-molecular ion peak at *m/z* 271.0616 [M - H]⁻ (calculated for $C_{15}H_{11}O_5$, 271.0607). The IR spectrum (Figure P2 in Appendix B) of corynesidone A (**16**) revealed absorption band for a conjugated carbonyl at 1693 cm⁻¹ and the ¹³C resonance at $\delta_C$ 163.3 suggested the presence of a carbonyl of an aromatic ester, as shown in Table 8.

The 400 MHz ¹H NMR spectrum (Figure P4 in Appendix B) of corynesidone A (**16**) in acetone-$d_6$ showed signal attributable to: $\delta_H$ 2.37 ppm (3H, *s*, ArCH₃), $\delta_H$ 2.39 ppm (3H, *s*, ArCH₃), $\delta_H$ 6.52 ppm (1H, *d* = 2.8, ArH), $\delta_H$ 6.53 ppm (1H, *d* = 2.8, 0.7, ArH),

and $\delta_H$ 6.60 ppm (2H, br $s$, ArH). These spectral data revealed that corynesidone A (16) had two pairs of meta-coupling aromatic protons.

The 100 MHz $^{13}$C NMR spectrum of corynesidone A (16) in acetone-$d_6$ (Figure P6 of Appendix B) revealed fifteen lines, which corynesidone A (16) were classified by DEPT 135 (Figure P7 of Appendix B) and HMQC spectral data (Figure P8 in Appendix B) as two sp$^3$ methyl carbon signals at $\delta$ 15.1 (C-13), and 20.2 ppm (C-12), four sp$^2$ methine carbon signals at $\delta$ 104.7 (C-4), 104.9 (C-9), 113.5 (C-7), and 115.5 (C-2), nine non-protonated carbon signals at $\delta$ 112.8 (C-11a), 131.3 (C-6), 142.1 (C-5a), 144.9 (C-9a), 145.1 (C-1), 154.5 (C-8), 161.5 (C-4a), 162.4 (C-3), and 163.3 ppm (C-11).

The NOESY spectrum of corynesidone A (16) in acetone-$d_6$ (Figure P16 of Appendix B) established the correlation from H-4 to H-13, and H-2 to H-12 (Figure 41).
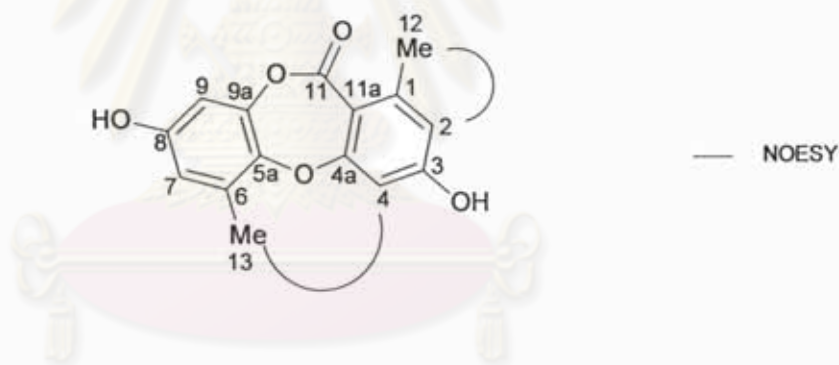


Figure 41    The NOESY correlations of corynesidone A (16)

Analysis of HMBC correlations (Figure P11 in Appendix B) well assembled the structure of corynesidone A (16) showing the following long-range correlations; H-2 ($\delta$ 6.66) to C-3 ($\delta$ 162.4), C-4 ($\delta$ 104.7), C-11a ($\delta$ 112.8),  and C-12 ($\delta$ 20.2); H-4 ($\delta$ 6.66) to C-2 ($\delta$ 115.5), C-3 ($\delta$ 162.4), C-4a ($\delta$ 161.5), and C-11 ($\delta$ 163.3); H-7 ($\delta$ 6.53) to C-5a ($\delta$ 142.1), C-8 ($\delta$ 154.5), C-9 ($\delta$ 104.9), and C-13 ($\delta$ 15.1); H-9 ($\delta$ 6.52) to C-5a ($\delta$ 142.1), C-8 ($\delta$ 154.5), and C-9a ($\delta$ 144.9); H$_3$-12 ($\delta$ 2.39) to C-1 ($\delta$ 145.1), C-2 ($\delta$ 115.5), and C-11a ($\delta$ 112.8);  and H$_3$-13 ($\delta$ 2.37) to C-5a ($\delta$ 142.1), C-6 ($\delta$ 131.3),  and C-7 ($\delta$ 113.5), as shown in Figure 42.
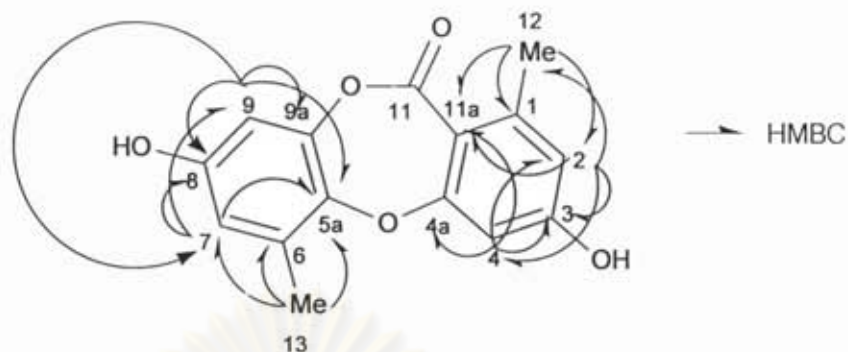
**Figure 42**    Long-range correlations from HMBC spectrum of corynesidone A (16)

Assignments of all $^1$H and $^{13}$C NMR spectroscopic signals for corynesidone A (16) were made by analysis of NOESY and HMBC spectra as summarized in Table 8.

However, these HMBC data could not place position of the C-11 ester carbonyl on the structure of corynesidone A (16). This compound was methylated to give a di-O-methyl derivative (17), confirming the presence of two hydroxyl groups in the chemical structure of corynesidone A (16).

Di-O-methyl derivative (17) was isolated as pale brown viscous oil and the ESI-TOF mass spectrum of the methylated derivative revealed a pseudo molecular ion peak at $m/z$ 301.1064 [M + H]$^+$ (calculated for $C_{17}H_{17}O_5$, 301.1076) shown in Figure P18 (Appendix B). Interestingly, the HMBC spectrum of di-O-methyl derivative (17) showed a four-bond correlation ($^4J_{CH}$ coupling) from $H_3$-12 to C-11 (Figure 43), which confirmed the position of the C-11 ester carbonyl in di-O-methyl derivative 17. It is known that H–H couplings substantially reduce intensities of the C–H correlation, therefore, $^nJ_{CH}$ correlations for $n > 3$ are very weak or non-observable (Griesinger et al., 1994). The observation of longer range $^nJ_{CH}$ couplings could be possible for compounds with either few or no H–H couplings, for example, the observation of $^5J_{CH}$ and $^7J_{CH}$ couplings in excelsione, a depsidone from an unidentified endophytic fungus (Lang et al., 2007).

Table 8 The $^1$H, $^{13}$C, NOESY and HMBC spectral data of corynesidone A (16) in acetone-$d_6$
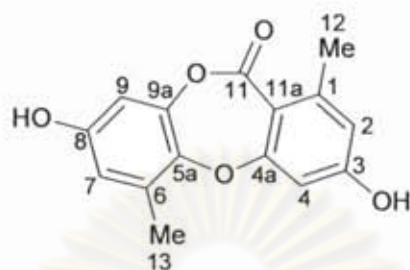


Corynesidone A 16

| Position | $\delta_C$ | $\delta_H$, multiplicity, $J_{H,H}$ (Hz) | NOESY | HMBC (H to C) |
|----------|-----------|------------------------------------------|-------|---------------|
| 1 | 145.1 | - | - | - |
| 2 | 115.5 | 6.66 (br s) | 12 | 3, 4, 11a, 12 |
| 3 | 162.4 | - | - | - |
| 4 | 104.7 | 6.66 (br s) | 13 | 2, 3, 4a, 11a |
| 4a | 161.5 | - | - | - |
| 5a | 142.1 | - | - | - |
| 6 | 131.1 | - | - | - |
| 7 | 113.5 | 6.53 (dd, 2.8, 0.7) | - | 5a, 8, 9, 13 |
| 8 | 154.5 | - | - | - |
| 9 | 104.9 | 6.52 (d, 2.8) | - | 5a, 7, 8, 9a |
| 9a | 144.9 | - | - | - |
| 11 | 163.3 | - | - | - |
| 11a | 112.8 | - | - | - |
| 12 | 20.2 | 2.39 (s) | 2 | 1, 2, 11a |
| 13 | 15.1 | 2.37 (s) | 4 | 5a, 6, 7 |
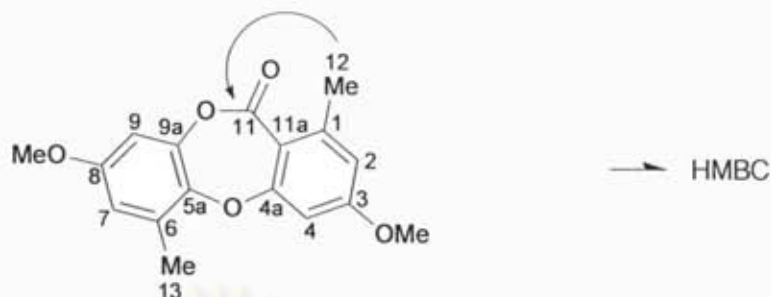
**Figure 43** Long-rang correlation from HMBC spectral data of di-O-methyl derivative (17) from H$_3$-12 to C-11

The NOESY spectrum of di-O-methyl derivative (17) demonstrated correlations from 3-OMe protons to H-2 and H-4; and from 8-OMe protons to H-7 and H-9, readily placing the methoxy groups in di-O-methyl derivative (17) (the hydroxyl groups in corynesidone A 16) (Figure 44). The above NOESY correlations also implied that the two aromatic parts were linked either at C-5a/C-4a and C-9a/C-11 or at C-5a/C-11 and C-9a/C-4a. Fortunately, the key NOESY correlation from H$_3$-13 to H-4 was observed for both corynesidone A (16), as shown above in Figure 41 and its methylated derivative, which indicated the linkage at C-5a/C-4a and C-9a/C-11 in both compounds.
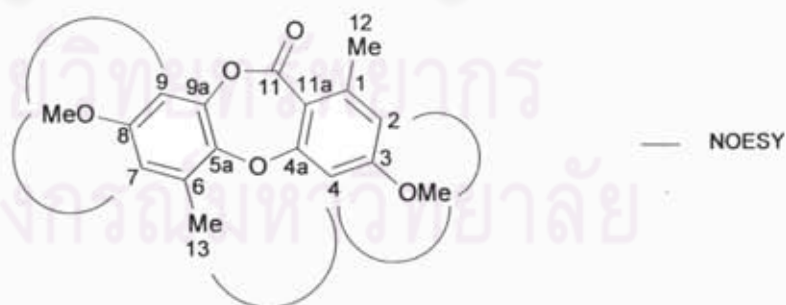


**Figure 44** The correlations NOESY spectrum of di-O-methyl derivative (17)

Upon the basis of these spectroscopic data, the structure of corynesidone A (16) was secured as shown. Protons and carbons in corynesidone A (16) were assigned

by analysis of $^1$H–$^1$H COSY and HMBC spectra (Table 8). It should be noted that di-*O*-methyl derivative (**17**) was synthetically known (Sala and Sargent, 1981), however, comparison of the 60 MHz $^1$H NMR spectroscopic data ambiguously confirmed the structural identity of this derivative. Analysis of NOESY and HMBC spectra assisted the assignment of proton and carbon signals in di-*O*-methyl derivative (**17**) (Table 9). It is worth noting that structural elucidation of hydroxylated depsidones, i.e. corynesidone A (**16**), needs analysis of HMBC and NOESY spectral data of its corresponding methylation product, in order to locate individual substituents (particularly on the hydroxyl positions) and the linkage between the two aromatic parts.
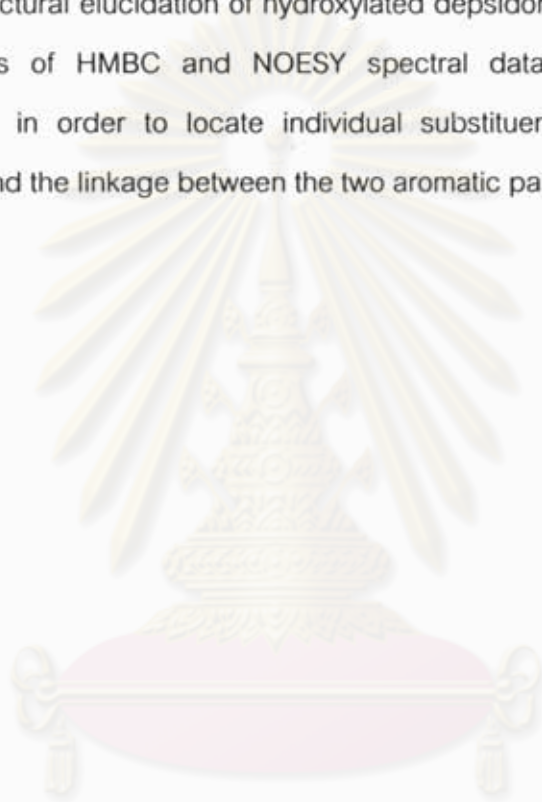
Table 9    The $^1$H, $^{13}$C, NOESY and HMBC spectral data of di-O-methyl derivative (17) in CDCl$_3$
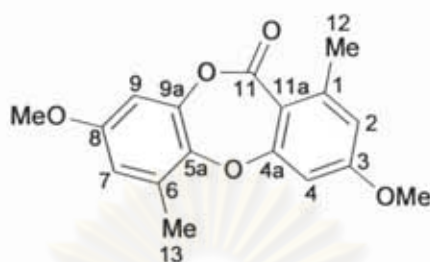


Di-O-methyl derivative 17

| Position | $\delta_C$ | $\delta_H$, multiplicity, $J_{H,H}$ (Hz) | NOESY | HMBC (H to C) |
|---|---|---|---|---|
| 1 | 145.5 | - | - | - |
| 2 | 114.0 | 6.60 (d, 2.4) | 12, 3-OMe | 3, 4, 11a, 12 |
| 3 | 163.0 | - | - | - |
| 4 | 103.5 | 6.60 (d, 2.4) | 13, 3-OMe | 2, 3, 4a, 11a |
| 4a | 163.1 | - | - | - |
| 5a | 142.8 | - | - | - |
| 6 | 131.3 | - | - | - |
| 7 | 112.7 | 6.53 (d, 2.9) | 13, 8-OMe | 5a, 8, 9, 13 |
| 8 | 156.5 | - | - | - |
| 9 | 103.7 | 6.62 (d, 2.9) | 8-OMe | 5a, 7, 8, 9a |
| 9a | 144.8 | - | - | - |
| 11 | 163.3 | - | - | - |
| 11a | 119.5 | - | - | - |
| 12 | 21.5 | 2.50 (s) | - | 1, 2, 11, 11a |
| 13 | 16.2 | 2.43 (s) | - | 5a, 6, 7 |
| 3-OMe | 55.6 | 3.83 (s) | 2, 4 | 3 |
| 8-OMe | 55.7 | 3.74 (s) | 7, 9 | 8 |

### 4.3.2 Structure elucidation of corynesidone B (18)



**18**
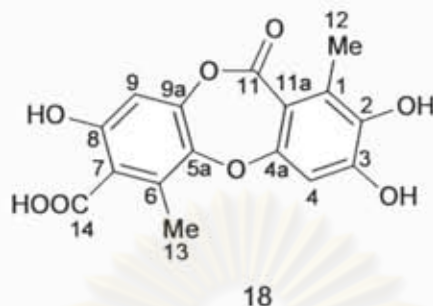
Corynesidone B (**18**) was isolated as pale brown solid, and the ESI-TOF mass spectrum revealed a molecular formula of $C_{16}H_{12}O_8$, showing a protonated molecular ion peak at $m/z$ 331.0454 [M − H]⁻ (Figure P26 in Appendix B). The IR spectrum of corynesidone B (**18**) displayed absorption bands for a carboxylic acid (1703 cm⁻¹) and an aromatic ester carbonyl (1687 cm⁻¹) (Figure P25 of Appendix B).

The 400 MHz $^1H$ NMR spectrum of corynesidone B (**18**) contained only four signals, all singlets: two $sp^2$ singlet methines, $\delta_H$ 6.64 and 6.78 ppm, and two $sp^3$ singlet methyls, $\delta_H$ 2.31 and 2.70 ppm, as shown in Figure P27 (Appendix B).

Analysis of $^{13}C$ NMR, DEPT, and HMQC spectral data (Figure P28 to Figure P30 in Appendix B) established sixteen carbons in the molecule, consisting of two $sp^3$ methyl carbons: $\delta$ 12.5 (C-12), and 14.1 ppm (C-13), two $sp^2$ methine carbons: $\delta$ 104.1 (C-4), and 106.4 ppm (C-9), and twelve quaternary carbons: $\delta$ 110.0 (C-7), 112.9 (C-11a), 128.1 (C-1), 133.5 (C-6), 141.6 (C-2), 142.8 (C-5a), 149.3 (C-3), 149.4 (C-9a), 155.0 (C-a), 160.3 (C-8), 161.6 (C-11), and 172.0 ppm (C-14). The $^{13}C$ NMR resonance at $\delta_C$ 172.0 indicated the presence of a carboxylic acid functionality in corynesidone B (**18**).

The NOESY spectrum (acetone-$d_6$) (Figure P35 of Appendix B) showed the correlation from H-4 to H-13, as demonstrated in Figure 45.
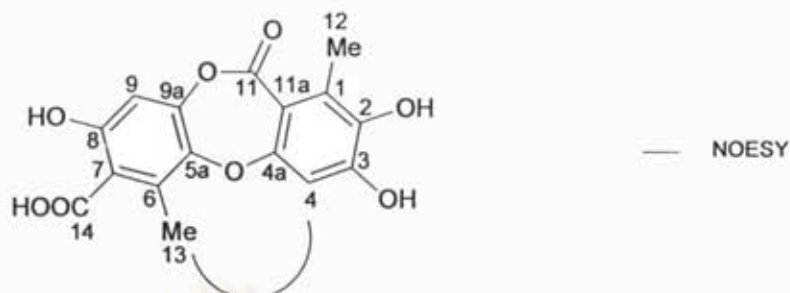
Figure 45    NOESY correlations of corynesidone B (18)

The HMBC experiment of corynesidone B (18) (Figure P31 in Appendix b) showed correlations from H-4 to C-2, C-3, C-4a, and C-11a; H-9 to C-5a, C-7, C-8, and C-9a; $H_3$-12 to C-1, C-2, and C-11a; and $H_3$-13 to C-5a, C-6, and C-7. Similar to the previously reported depsidone, excelsione (Lang *et al.*, 2007), there were no H–H couplings for corynesidone B (18); therefore, it was expected that longer range $^nJ_{CH}$ couplings could be observable in the HMBC spectrum. Indeed, there were $^4J_{CH}$ couplings, e.g., from both H-4 and $H_3$-12 to the C-11 ester carbonyl and from H-9 and $H_3$-13 to C-14 carboxylic acid carbonyl, placing positions of ester and carboxylic acid in each aromatic ring. The $^1$H-$^{13}$C long-range correlations of corynesidone B (18) in acetone-$d_6$ are depicted in Figure 46.
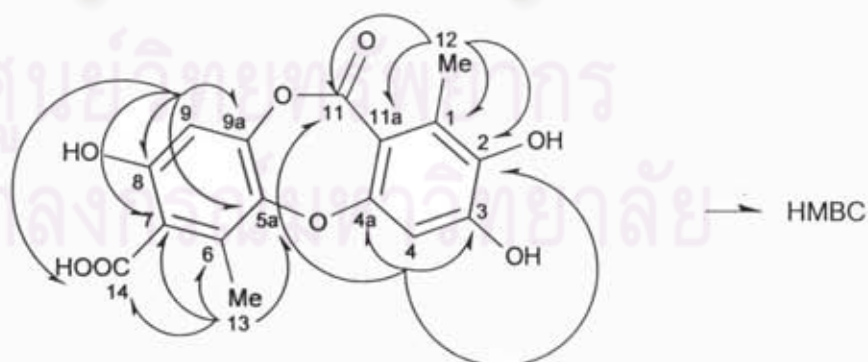


Figure 46    Long-range correlations from HMBC spectral data of corynesidone B (18) in acetone-$d_6$

Assignments of all $^1$H and $^{13}$C NMR spectroscopic signals for corynesidone B (18) were made by analysis of NOESY and HMBC spectra summarized in Table 10.

Table 10　　The $^1$H, $^{13}$C, NOESY and HMBC spectral data of corynesidone B (18) in acetone-$d_6$
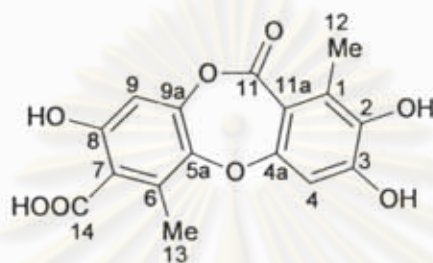


Corynesidone B 18

| Position | $\delta_C$ | $\delta_H$, multiplicity, $J_{H,H}$ (Hz) | NOESY | HMBC (H to C) |
|---|---|---|---|---|
| 1 | 128.1 | - | - | - |
| 2 | 141.6 | - | - | - |
| 3 | 149.3 | - | - | - |
| 4 | 104.1 | 6.78 (br s) | 13 | 2, 3, 4a, 11, 11a |
| 4a | 155.0 | - | - | - |
| 5a | 142.8 | - | - | - |
| 6 | 133.5 | - | - | - |
| 7 | 110.0 | - | - | - |
| 8 | 160.3 | - | - | - |
| 9 | 106.4 | 6.64 (s) | - | 5a, 7, 8, 9a, 14 |
| 9a | 149.4 | - | - | - |
| 11 | 161.6 | - | - | - |
| 11a | 112.9 | - | - | - |
| 12 | 12.5 | 2.31 (s) | - | 1, 2, 11, 11a |
| 13 | 14.1 | 2.70 (s) | 4 | 5a, 6, 7, 14 |
| 14 | 172.0 | - | - | - |

Methylation of corynesidone B (**18**) yielded a tetra-*O*-methyl derivative (**19**) whose molecular formula was established as $C_{20}H_{20}O_8$ by ESI-TOF mass spectrum, as shown Figure P36 in Appendix B.



**4**
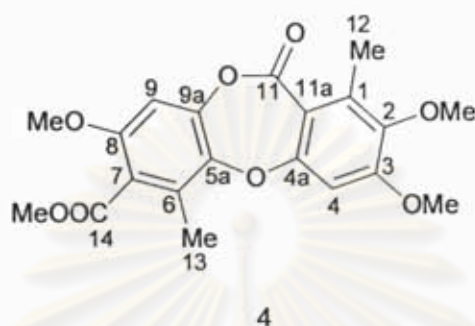
The NOESY spectrum of methyl derivative (**19**) (Figure P41 in Appendix B) displayed correlations between 3-OMe and H-4, between 8-OMe and H-9, and between $H_3$-13 and H-4 showed in Figure 47.
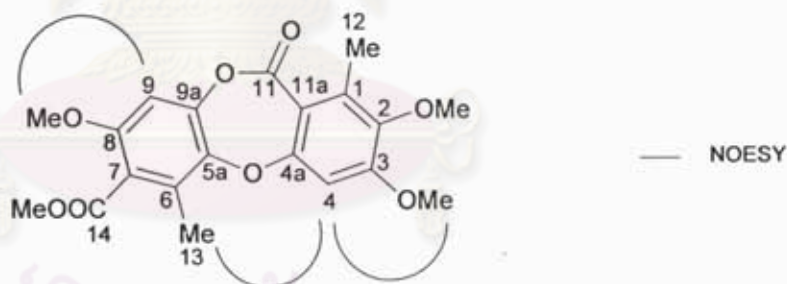


— NOESY

**Figure 47**    NOESY correlations of tetra-*O*-methyl derivative (**19**)

The HMBC correlations in tetra-*O*-methyl derivative (**19**) (Figure P40 in Appendix B) were exhibited from 2-OMe to C-2; 3-OMe to C-3; H-4 to C-3, C-4a, C-11a, and C-11 ($^4J_{CH}$); 8-OMe to C-8; H-9 to C-5a, C-7, C-8, C-9a, and C-14 ($^4J_{CH}$); $H_3$-12 to C-1, C-2, C-11a, and C-11 ($^4J_{CH}$); and $H_3$-13 to C-5a, C-6, C-7, and C-14 ($^4J_{CH}$); COOMe to C-14. The $^1H$-$^{13}C$ long-range correlations from the HMBC spectrum of tetra-*O*-methyl derivative (**19**) in $CDCl_3$ are shown in Figure 48.
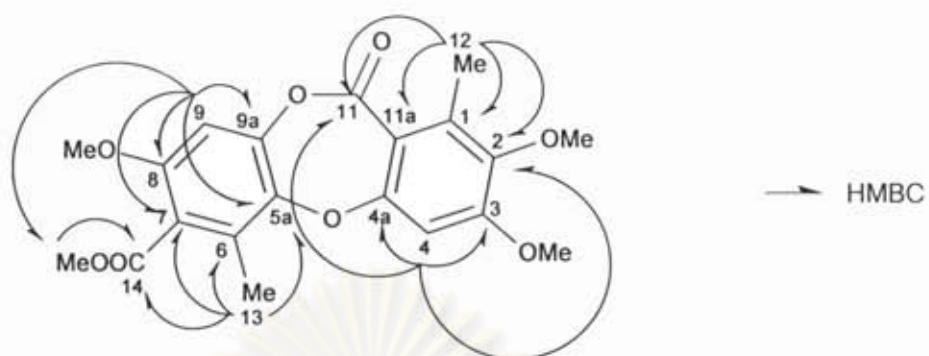
**Figure 48**   Long-range correlations from HMBC spectral data of tetra-*O*-methyl derivative (**19**) in CDCl$_3$

On the basis of these spectroscopic data, the chemical structure of tetra-*O*-methyl derivative (**19**) was successfully established. Assignments of proton and carbon signals for tetra-*O*-methyl derivative (**19**) are summarized in Table 11.

Table 11    The $^1$H, $^{13}$C, NOESY and HMBC spectral data of tetra-$O$-methyl derivative

(19) in CDCl$_3$
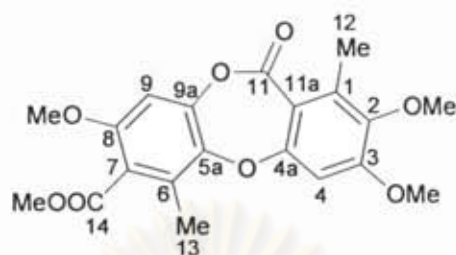


Tetra-O-methyl derivative 19

| Position | $\delta_C$ | $\delta_H$, multiplicity, $J_{H,H}$ (Hz) | NOESY | HMBC (H to C) |
|---|---|---|---|---|
| 1 | 136.5 | - | - | - |
| 2 | 145.2 | - | - | - |
| 3 | 156.8 | - | - | - |
| 4 | 101.7 | 6.62 (br $s$) | 3-OMe, 13 | 2, 3, 4a, 11, 11a |
| 4a | 158.7 | - | - | - |
| 5a | 142.9 | - | - | - |
| 6 | 129.2 | - | - | - |
| 7 | 120.9 | - | - | - |
| 8 | 153.7 | - | - | - |
| 9 | 102.0 | 6.67 ($s$) | 8-OMe | 5a, 7, 8, 9a, 14 |
| 9a | 145.6 | | | - |
| 11 | 162.3 | - | - | - |
| 11a | 113.7 | | | - |
| 12 | 13.3 | 2.41 ($s$) | - | 1, 2, 11, 11a |
| 13 | 13.6 | 2.40 ($s$) | 4 | 5a, 6, 7, 14 |
| 14 | 167.3 | - | - | - |
| 2-OMe | 60.3 | 3.73 ($s$) | - | 2 |
| 3-OMe | 56.0 | 3.90 ($s$) | 4 | 3 |
| 8-OMe | 56.3 | 3.77 ($s$) | 9 | 8 |
| COOMe | 52.4 | 3.91 ($s$) | - | 14 |

### 4.3.3 Structure elucidation of corynether A (20)



20
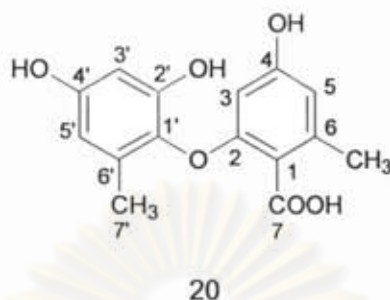
Corynether A (20) was isolated as brown solid, and its molecular formula was determined as $C_{15}H_{14}O_6$ from the ESI-TOF mass spectrum, observed ion peak at $m/z$ 289.0720 [M-H]⁻, calculated for $C_{15}H_{13}O_6$ at $m/z$ 289.0712 (Figure P44 in Appendix B).

The ¹H NMR spectrum (DMSO-$d_6$) of corynether A (20) exhibited signals corresponding to two pairs of meta-coupling aromatic protons ($\delta$ 5.91, 5.96, 6.03 and 6.22 ppm) and two singlet methyls ($\delta$ 2.16 and 2.24 ppm) (Table 12), while the ¹³C NMR, HMQC, and DEPT spectra of this substance revealed the presence two sp³ methyls ($\delta$ 16.7 and 20.5 ppm), four sp² methines ($\delta$ 101.9, 102.4, 106.3 and 111.6 ppm), and nine non-protonated carbons ($\delta$ 123.8, 131.4, 136.8, 137.3, 152.1, 154.8, 156.7, 157, and 173.5 ppm). The ¹³C NMR resonance at $\delta_C$ 173.5 indicated the presence of carboxylic acid in corynether A (20). The ¹H NMR, ¹³C NMR, HMQC, and DEPT spectra are in Figures P45, P46, P47 and P48, respectively, in Appendix B.

The complete ¹³C assignments of corynether A (20) were assigned from the HMBC spectrum (Figure P50 in Appendix B) showing the following long-range correlations; H-3 ($\delta$ 5.91) to C-1 ($\delta$ 123.8), C-2 ($\delta$ 156.7), C-4 ($\delta$ 157.1), and C-5 ($\delta$ 111.6); H-5 ($\delta$ 6.22) to C-1 ($\delta$ 123.8), C-3 ($\delta$ 101.9), C-4 ($\delta$ 157.1), C-6 ($\delta$ 136.8), and C-8 ($\delta$ 20.5); H-3' ($\delta$ 5.96) to C-1' ($\delta$ 137.3), C-2' ($\delta$ 152.1), C-4' ($\delta$ 154.8), and C-5' ($\delta$ 106.3); H-5' ($\delta$ 6.03) to C-1' ($\delta$ 137.3), C-3' ($\delta$ 102.4), C-4' ($\delta$ 154.8), C-6' ($\delta$ 131.4), and C-7' ($\delta$ 16.7); and H₃-7' ($\delta$ 2.16) to C-1'($\delta$ 137.3), C-5' ($\delta$ 106.3), and C-6' ($\delta$ 131.4).

The $^1$H-$^{13}$C long-range correlations from the HMBC spectrum of corynether A (20) in DMSO-$d_6$ are demonstrated in Figure 49.
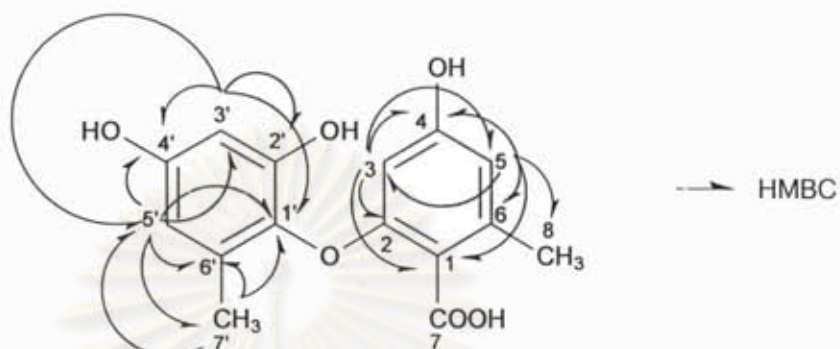


**Figure 49**    Long-range correlations from HMBC spectral data of corynether A (20)

Although the $^{13}$C NMR resonance at $\delta_C$ 123.8 of C-1 implied that the carboxylic acid may be situated at C-1, the available NMR spectroscopic data could not conclusively establish the structure of corynether A (20), particularly on the positions of ether linkage and free hydroxyl groups. Therefore, corynether A (20) was subjected to methylation to yield a tetra-O-methyl derivative (21).
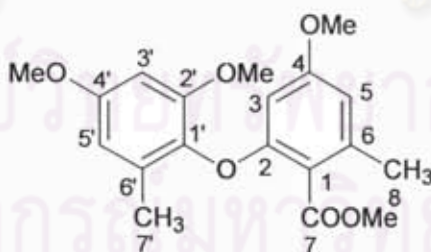


Tetra-O-methyl derivative (21)

Tetra-O-methyl (21) was obtained as yellow viscous oil. The molecular formula was determined to be $C_{19}H_{22}O_6$ by positive ESI-TOF MS (found 369.1309 [M + Na]$^+$, calculated for $C_{19}H_{22}O_6Na$, 369.1314).

The NOESY correlation from 4-OMe to H-3 and H-5; from 2'-OMe to H-3'; and from 4'-OMe to H-3' and H-5' readily indicated the 1'/2 ether linkage in tetra-O-methyl derivative 21 (Figure P60 in Appendix B). The HMBC correlations from $H_3$-8 to C-1, C-5, C-6, and C-7 ($^4J_{CH}$) and from COOCH$_3$ to C-7 and C-1 ($^4J_{CH}$) unambiguously assigned the position of ester carbonyl (C-7) in tetra-O-methyl derivative 21 (Figure P60 in Appendix B), and thus establishing the carboxylic acid position in corynether A (20). Both NOESY and HMBC correlations of tetra-O-methyl derivative 21 are summarized in Figure 50.
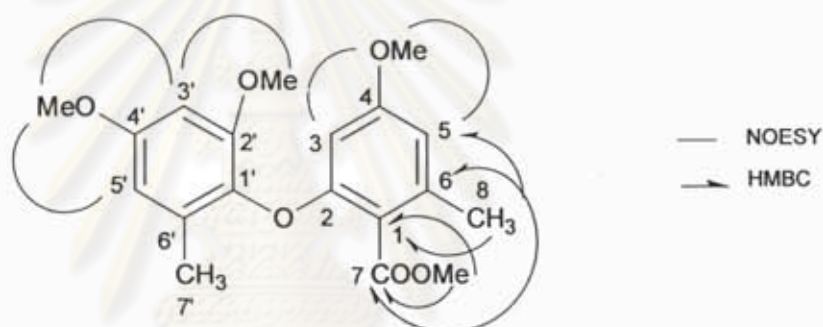


Figure 50    NOESY and HMBC correlations of tetra-O-methyl derivative (21)

The evidence from these spectroscopic data supported the structure of corynether A (20) as shown; proton and carbon signals in corynether A (20) and tetra-O-methyl derivative 21 were assigned by analysis of 2D NMR spectroscopic data Table 12 and Table 13, respectively. It should be noted that analysis of NOESY and HMBC spectra of the corresponding methylated product is crucially necessary for structure elucidation of hydroxylated diaryl ether.

Table 12    The $^1$H, $^{13}$C, NOESY and HMBC spectral data of corynether A (20) in DMSO-$d_6$
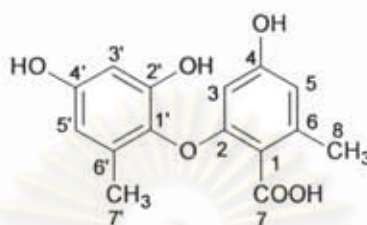


Corynether A 20

| Position | $\delta_C$ | $\delta_H$, multiplicity, $J_{H,H}$ (Hz) | NOESY | HMBC (H to C) |
|---|---|---|---|---|
| 1 | 123.8 | - | - | - |
| 2 | 156.7 | - | - | - |
| 3 | 101.9 | 5.91 (br s) | - | 1, 2, 4, 5 |
| 4 | 157.1 | - | - | - |
| 5 | 111.6 | 6.22 (br s) | - | 1, 3, 4, 6, 8 |
| 6 | 136.8 | - | - | - |
| 7 | 173.5 | - | - | - |
| 8 | 20.5 | 2.24 (s) | - | - |
| 4-OH | - | 12.75 (br s) | - | - |
| 1' | 137.3 | - | - | - |
| 2' | 152.1 | - | - | - |
| 3' | 102.4 | 5.96 (br s) | - | 1', 2', 4', 5' |
| 4' | 154.8 | - | - | - |
| 5' | 106.3 | 6.03 (br s) | - | 1', 3', 4', 6', 7' |
| 6' | 131.4 | - | - | - |
| 7' | 16.7 | 2.16 (s) | - | 1', 5', 6' |
| 2'-OH | - | 9.04 (br s) | - | - |
| 4'-OH | - | 9.37 (br s) | - | - |

Table 13    The $^1$H, $^{13}$C, NOESY and HMBC spectral data of tetra-O-methyl derivative
(21) in CDCl$_3$
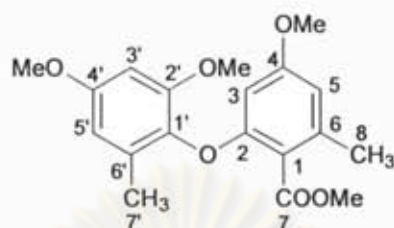


Tetra-O-methyl derivative 21

| Position | $\delta_C$ | $\delta_H$, multiplicity, $J_{H,H}$ (Hz) | NOESY | HMBC (H to C) |
|---|---|---|---|---|
| 1 | 115.9 | - | - | - |
| 2 | 161.2 | - | - | - |
| 3 | 97.6 | 5.85 (d, 2.1) | - | 1, 2, 4, 5 |
| 4 | 157.2 | - | - | - |
| 5 | 107.7 | 6.33 (d, 2.1) | - | 1, 3, 4, 6, 8 |
| 6 | 138.5 | - | - | - |
| 7 | 168.4 | - | - | - |
| 8 | 20.0 | 2.35 (s) | - | 1, 5, 6, 7 |
| COOMe | 51.1 | 3.91 (s) | - | 1, 7 |
| 4-OMe | 55.2 | 3.66 (s) | 3, 5 | |
| 1' | 135.4 | - | - | - |
| 2' | 153.2 | - | - | - |
| 3' | 98.3 | 6.39 (d, 2.1) | - | 1', 2', 4', 5' |
| 4' | 157.3 | - | - | - |
| 5' | 106.7 | 6.34 (d, 2.1) | - | 1', 3', 4', 6', 7' |
| 6' | 133.1 | - | - | - |
| 7' | 16.2 | 2.13 (s) | - | 1', 5', 6' |
| 2'-OMe | 56.1 | 3.72 (s) | 3' | - |
| 4'-OMe | 55.5 | 3.80 (s) | 3', 5' | - |

### 4.3.4 Structure elucidation of diaryl ether (22)
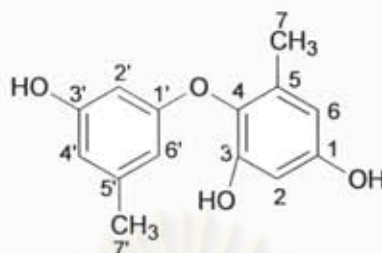


22

Diaryl ether (22) was isolated as pale brown viscous oil and its molecular formula $C_{15}H_{14}O_6$ was deduced from the ESi-TOF-MS spectrum. The IR spectrum of diaryl ether (22) exhibited absorption bands for 3336 cm$^{-1}$ (OH stretching) and 2923 cm$^{-1}$ (CH stretching of aromatic). The ESI-TOF-MS and IR spectroscopic of 22 are shown in Figure P63 and Figure P64 (Appendix B), respectively.

The $^1$H NMR spectrum (acetone-$d_6$) (Figure P65 in Appendix B) of diaryl ether 22 revealed the presence of two coupled aromatic protons ($\delta_H$ 6.25 and 6.35 ppm; $J_{3,5}$ = 2.9 Hz), three aromatic protons ($\delta_H$ 6.03, 6.13 and 6.28 ppm), two singlet methyls ($\delta_H$ 1.98 and 2.17 ppm), and three phenolic protons ($\delta_H$ 8.01, 8.17 and 8.23 ppm). Analyses of the $^{13}$C, DEPT, and HMQC spectra of diaryl ether (22) indicated that this compound possessed 14 carbons attributable to two sp$^3$ methyls, five sp$^2$ methines, and seven non-protonated carbons. The $^{13}$C, DEPT, and HMQC spectra of 22 are demonstrated in Figure P67, Figure P68, and Figure P69 (Appendix B), respectively.

The HMBC spectrum (Figure P71 in Appendix B) of diaryl ether 22 showed correlations from H-2 to C-1, C-3, C-4, and C-6; H-6 to C-1, C-2, C-6, and C-7; H$_3$-7 to C-3 ($^4J_{CH}$), C-4, C-5, and C-6; H-2' to C-1', C-3', C-4', and C-6'; H-4' to C-2', C-3', C-6', and C-7'; H-6' to C-1', C-2', C-4', and C-7'; H$_3$-7' to C-1' ($^4J_{CH}$), C-3' ($^4J_{CH}$), C-4', C-5', and C-6'; 3'-OH to C-2', and C-4', as shown in Figure 51.

Analysis of the $^1$H-$^1$H COSY spectrum of diaryl ether 22 in acetone-$d_6$ (Figure P74 in Appendix B) showed the correlations from H-2 to H-6, H-2' to H-4' and H-6', and H-4' to H-6', while the NOESY spectrum (Figure P75 of Appendix B) demonstrated the

correlations from H-6 to H$_3$-7, and H-7′ to H-4′ and H-6′. Both NOESY and COSY correlations are depicted in Figures 52.
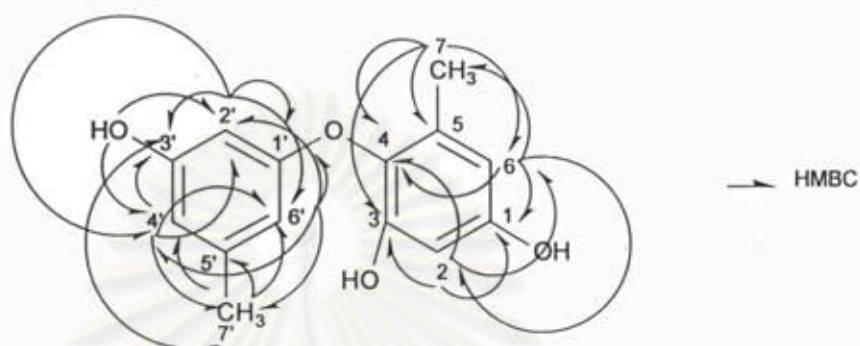


**Figure 51**     Long-range correlations from HMBC spectral data of diaryl ether (**22**) in acetone-$d_6$
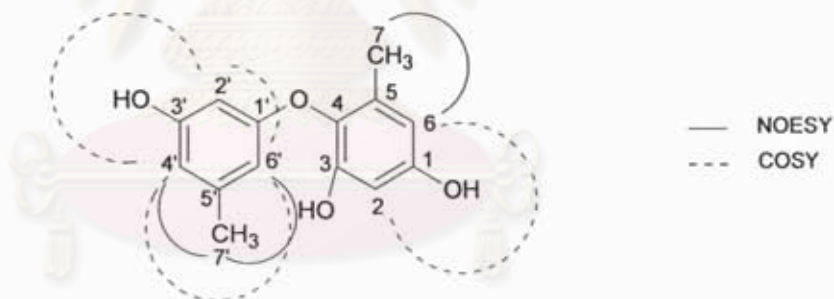


**Figure 52**     The correlations of $^1$H-$^1$H COSY and NOESY spectra of diaryl ether (**22**)

Assignments of $^1$H and $^{13}$C NMR signals for diaryl ether **22** are summarized in Table 14.

Table 14      The $^1$H, $^{13}$C, NOESY and HMBC spectral data of diaryl ether (22) in acetone-$d_6$
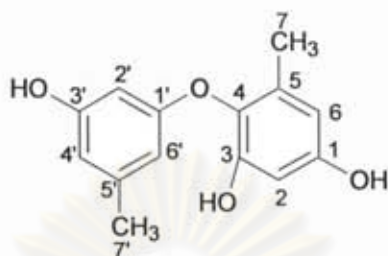


Diaryl ether 22

| Position | $\delta_C$ | $\delta_H$, multiplicity, $J_{H,H}$ (Hz) | NOESY | HMBC (H to C) |
|---|---|---|---|---|
| 1 | 154.8 | - | - | - |
| 2 | 101.4 | 6.35 (d, 2.9) | - | 1, 3, 4, 6 |
| 3 | 150.6 | - | - | - |
| 4 | 133.1 | - | - | - |
| 5 | 132.4 | - | - | - |
| 6 | 108.1 | 6.25 (d, 2.9) | - | 1, 2, 4, 7 |
| 7 | 15.4 | 1.98 (s) | 6 | 4, 5, 6 |
| 1-OH | - | 8.17 (br s) | - | - |
| 3-OH | - | 8.01 (br s) | - | - |
| 1' | 159.7 | - | - | - |
| 2' | 99.1 | 6.25 (dd, 2.1, 2.1) | - | 1', 3', 4', 6' |
| 3' | 158.4 | - | - | - |
| 4' | 109.2 | 6.28 (m) | - | 2', 3', 5', 7' |
| 5' | 139.8 | - | - | - |
| 6' | 106.8 | 6.13 (m) | - | 1', 2', 5', 7' |
| 7' | 20.6 | 2.17 (s) | 4', 6' | 4', 5', 6' |
| 3'-OH | - | 8.23 (br s) | - | 2', 4' |

Diaryl ether **22** was a demethyl derivative of 2-hydroxy-4-methoxy-6-methylphenyl 3-hydroxy-5-methylphenyl ether (Cannon *et al.*, 1972; Sargent *et al.*, 1971), also known as LL-V125a, a fungal metabolite of the order Sphaeropsidales (McGahren *et al.*, 1970). However, LL-V125a was incorrectly identified as 2-hydroxy-6-methoxy-4-methylphenyl 3-hydroxy-5-methylphenyl ether (McGahren *et al.*, 1970); it was subsequently revised, by chemical synthesis, to 2-hydroxy-4-methoxy-6-methylphenyl 3-hydroxy-5-methylphenyl ether (Cannon *et al.*, 1972; Sargent *et al.*, 1971). Diaryl ether **22** was synthetically prepared during the synthesis of LL-V125a, unfortunately, only the 60 MHz $^1$H NMR spectroscopic data of diaryl ether **22** was available in the literature (Cannon *et al.*, 1972; Sargent *et al.*, 1971). Furthermore, comparison of such NMR data was not sufficient to confirm the structural identity of diaryl ether, particularly on the assignment of aromatic substituents. In order to prove the structure of diaryl ether **22**, the corresponding methylated product **23** was prepared and subjected to NOESY analysis.

Methylated derivative (**23**) was obtained as a pale yellow solid. The molecular formula was determined to be $C_{17}H_{20}O_4$ by analysis of its ESI-TOF MS spectrum, as shown in Figure P76 (Appendix B).
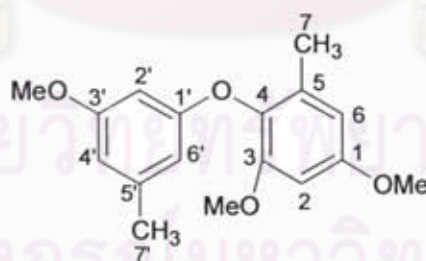


Methylated derivative (23)

The NOESY correlations from 1-OMe to H-2 and H-6; from 3-OMe to H-2; and from 3'-OMe to H-2' and H-4' readily indicated 1'/4 ether linkage in methylated derivative (Figure 53), and thus confirming the structure of diaryl ether **22**. Assignments of $^1$H and $^{13}$C NMR signals in methylated derivative **23** are summarized in Table 15. The 1D NMR

and 2D NMR spectroscopic data of methylated derivative (23) are shown in Figure P77 to Figure P80 of Appendix B.
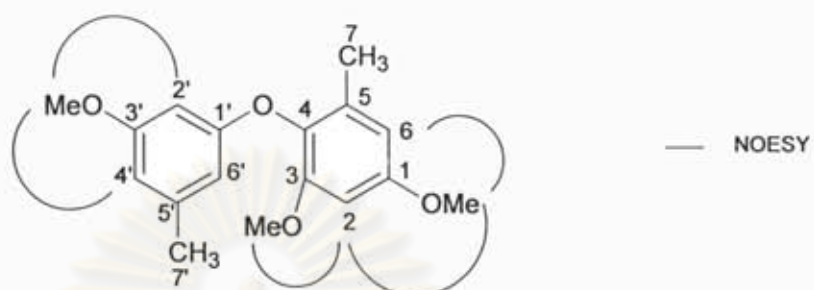


Figure 53    The NOESY correlations of methylated derivative (23)

Table 15   The $^1$H, $^{13}$C, NOESY and HMBC spectral data of methylated derivative (23) in CDCl$_3$
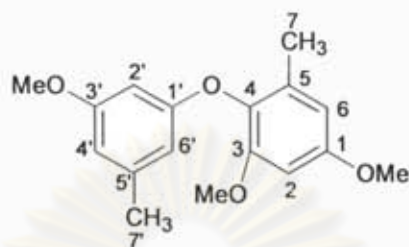


Methylated derivative 23

| Position | $\delta_C$ | $\delta_H$, multiplicity, $J_{H,H}$ (Hz) | NOESY (H to H) | HMBC (H to C) |
|----------|------------|------------------------------------------|----------------|----------------|
| 1 | 157.0 | - | - | - |
| 2 | 97.9 | 6.41 (*d*, 2.8) | - | 1, 3, 4, 6 |
| 3 | 153.0 | - | - | - |
| 4 | 135.3 | - | - | - |
| 5 | 133.1 | - | - | - |
| 6 | 106.2 | 6.36 (*d*, 2.8) | - | 1, 2, 4, 7 |
| 7 | 16.4 | 2.13 (*s*) | - | 4, 5, 6 |
| 1-OMe | 55.5 | 3.81 (*s*) | 2, 6 | 1 |
| 3-OMe | 56.0 | 3.74 (*s*) | 2 | 3 |
| 1' | 159.5 | - | - | - |
| 2' | 98.1 | 6.20 (*dd*, 2.2, 2.2) | - | 1', 3', 4', 6' |
| 3' | 160.6 | - | - | - |
| 4' | 107.6 | 6.34 (*m*) | - | 2', 3', 5', 7' |
| 5' | 140.2 | - | - | - |
| 6' | 107.7 | 6.22 (*m*) | - | 1', 2', 5', 7' |
| 7' | 21.8 | 2.25 (*s*) | - | 4', 5', 6' |
| 3'-OH | 55.2 | 3.73 (*s*) | 2', 4' | 3' |

4.4     Biological activities of the isolated compounds

4.4.1   Bioactivities of metabolites and their derivatives from the endophytic fungus LRUB20

The isolated substances, dothideopyrones A–D (1, 3, 4, and 5), together with seven known compounds, including cis,trans-muconic acid (9), questin (10), asterric acid (11), methyl asterrate (12), sulochrin (13), eugenitin (14), and 6-hydroxymethyleugenitin (15) and acetate derivatives (2) and (6), were tested for biological activities. The biological activities are summarized in Tables 16, 17, and 18.

Table 16     Cytotoxic activity of compounds 1-6 and 9-15 against nine cancer cell lines

| Cell line[a] | Cytotoxic activity ($IC_{50}$, µg/mL); mean (±s.d.), n=3 | | | | | | | | | | | | | |
|---|---|---|---|---|---|---|---|---|---|---|---|---|---|---|
| | 1 | 2 | 3 | 4 | 5 | 6 | 9 | 10 | 11 | 12 | 13 | 14 | 15 | Etoposide[c] Doxorubicin[d] |
| HeLa | >50 | >50 | >50 | ND[b] | 23.0 (±2.1) | 23.0 (±0.7) | >50 | >50 | >50 | >50 | >50 | 18.0 (±4.2) | >50 | 0.04[d] (±0.01) |
| HuCCA-1 | >50 | >50 | >50 | ND | 19.0 (±8.4) | 22.0 (±0.7) | >50 | >50 | >50 | >50 | >50 | >50 | >50 | 0.42[d] (±0.11) |
| HepG2 | >50 | >50 | >50 | ND | 21.0 (±2.6) | 19.5 (±0.7) | >50 | 44.5 (±6.3) | >50 | 45.0 (±4.3) | >50 | 20.8 (±8.4) | >50 | 0.18[d] (±0.00) |
| T47D | >50 | >50 | >50 | ND | 21.0 (±1.4) | 20.0 (±1.4) | >50 | >50 | >50 | >50 | >50 | 44.0 (±1.4) | >50 | 0.04[d] (±0.01) |
| MDA-MB231 | >50 | >50 | >50 | ND | 20.0 (±0.0) | 18.0 (±2.8) | >50 | >50 | >50 | >50 | 35.00 (±0.0) | >50 | >50 | 0.20[d] (±0.00) |
| S102 | >50 | >50 | >50 | ND | 24.0 (±1.4) | 22.5 (±4.9) | >50 | >50 | >50 | >50 | >50 | >50 | >50 | 1.20[d] (±0.00) |
| A549 | >50 | >50 | >50 | ND | 25.0 (±1.5) | 19.0 (±1.4) | >50 | >50 | >50 | >50 | >50 | >50 | >50 | 0.31[d] (±0.01) |
| HL-60 | >50 | 41.2 (±3.4) | >50 | ND | 16.0 (±1.1) | 18.0 (±0.7) | >50 | 23.4 (±3.3) | >50 | 23.40 (±3.37) | 38.9 (±4.3) | >50 | >50 | 0.82[e] (±0.04) |
| MOLT-3 | >50 | 18.9 (±0.3) | 26.3 (±0.9) | ND | 13.8 (±0.9) | 8.6 (±0.4) | >50 | 11.8 (±0.3) | >50 | 11.87 (±0.33) | 16.4 (±0.2) | 14.8 (±1.1) | 31.5 (±1.0) | 0.02[e] (±0.00) |

[a]Cell lines were: HeLa = cervical adenocarcinoma cell line; HuCCA-1 = human lung cholangiocarcinoma cancer cells; HepG2 = human hepatocellular liver carcinoma cell line; T47D = human mammary adenocarcinoma cell line; MDA-MB231 = human breast cell line; S102 = human liver cancer cell line; A549 = human lung carcinoma cell line; HL-60 = human promyelocytic leukemia cell line; MOLT-3 = T-lymphoblast (acute lymphoblastic leukemia) cell line.

[b]ND = Not determined

[c]Etoposide, and [d]doxorubicin were standard drugs.

Table 17　　　Antiviral, antifungal and antimycobacterial activities of compounds 1 and
4

| Biological activity | Compound 1 | Compound 4 |
|---|---|---|
| Antiviral (% inhibition) | | |
| - HSV-1 | 35-50% (moderately active) | Inactive |
| Antifungal (IC$_{50}$, µg/mL) | | |
| - *Candida albicans* | >50 | >50 |
| Antimycobacterial (MIC, µg/mL) | | |
| - *Mycobacterium tuberculosis* | >200 | >200 |

For anti-HSV-1 test, acyclovir was used as positive control; IC$_{50}$ = 0.5 ±0.2 µg/mL.

For antifungal test, amphotericin B was used as positive control; IC$_{50}$ = 0.042-0.058 µg/mL.

For antimycobacterial test, rifampicin (RMP), kanamycin (KM), and isoniazide (INH) were
used as positive control; MIC = 0.05, 2.50, and 0.05 µg/mL, respectively.

Table 18　　　Antimalarial activity (*Plasmodium falciparum*) of compounds 1, 4, 10, 11
and 12

| Compound | Antimalarial (IC$_{50}$, µg/mL) |
|---|---|
| 1 | >50 |
| 4 | >50 |
| 10 | 43.58 (fair) |
| 11 | >50 |
| 12 | >50 |

Dihydroartemisinnine was a positive control (IC$_{50}$ = 4.00- 4.30 µg/mL).

The isolated compounds and derivatives were evaluated for cytotoxicity toward
nine cancer cell lines (Table 16). Compounds 1–4 and 9–15 were either inactive (at 50
µg/mL) or showed only weak activity (14.8–45.0 µg/mL) towards some cell lines (Table
16). Dothideopyrone D (5) and its acetate derivative 6 exhibited moderate cytotoxic
activity (8.6–25.0 µg/mL). In addition, compounds 1, 4, 10, 11, and 12 were found to

exhibit only weak activity or were inactive against other activities tested (Tables 17 and 18). Previous reports have demonstrated that many pyrones are not cytotoxic (Zhan *et al.*, 2007). However, members of this class show phytotoxic activity (Pedras and Chumala, 2005), inhibitory effects on NF-kappaB (Folmer *et al.*, 2008), and interactions with the GABA-A receptor (Boonen and Haberlein, 1998). Questin (**10**) was recently found to be an inhibitor of Cdc25B phosphatase (Choi *et al.*, 2007).

Interestingly, the LRUB20 fungus cultured in M1D medium (supplemented with 0.5 g/L malt extract) produced large quantities of *cis,trans*-muconic acid (**9**), up to 47.8 mg/L. Generally, *cis,cis*-muconic acid and *trans,trans*-muconic acid are known metabolites from the metabolism of benzene and phenol (or derivatives) in living organisms, including humans (Tsai *et al.*, 2005; Xiao *et al.*, 2007; Yoshikawa *et al.*, 1993), and thus are employed as biomarkers for benzene contamination in living organisms (Melikian *et al.*, 2002; Navasumrit *et al.*, 2008; Yardley-Jones *et al.*, 1991). To date, only a monomethyl ester of *cis,cis*-muconic acid isolated from a marine sponge *Plakortis simplex* has been reported as a natural product (Shen *et al.*, 2001). To our knowledge, the present work is the first report on naturally occurring muconic acid. Interestingly, a prior report showed that genetically engineered *Escherichia coli* can catalytically convert D-glucose to *cis,cis*-muconic acid (Draths and Frost, 1994) (Scheme 9). Consequently, such muconic acid production initiated an environmentally compatible synthesis of adipic acid, an important ingredient for the production of nylon 6.6, gelatin, jams, polyamides, polyurethanes, and lubricants (Niu *et al.*, 2002; Thomas *et al.*, 2003). The current industrial production of adipic acid involves benzene, a carcinogen derived from nonrenewable fossil fuels, is the principal starting material. Hydrogenation of benzene to produce cyclohexane is followed by air oxidation to yield a mixture of cyclohexanol and cycclohexanone (Scheme 10). Nitric acid oxidation yields nitrous oxide ($N_2O$) as a byproduct, which contributes to both ozone depletion and global warming. Overproduction of *cis,trans*-muconic acid (**9**) through a genetic manipulation of the LRUB20 fungus, by analogy to that for the genetically engineered *E. coli* (Draths and Frost, 1994), is a challenging research approach to be pursued. Based

upon this investigation, endophytic fungi could prove to be potential sources of industrial chemicals, and may therefore offer potential utility in the field of white biotechnology.
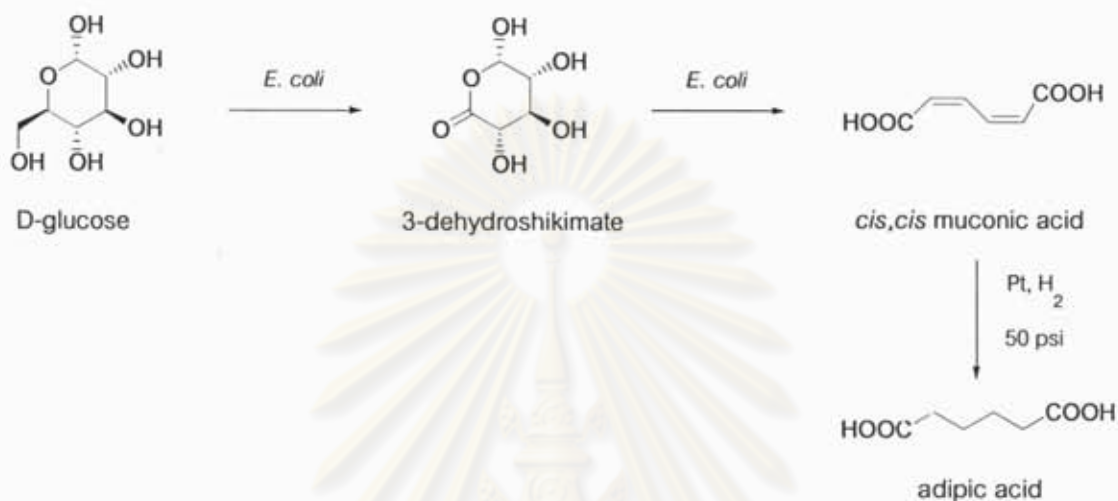


**Scheme 9** Synthesis of adipic acid using D-glucose as a starting material (adapted from: Draths and Frost. 1994 *J. Am. Chem. Soc.* 116: 399)
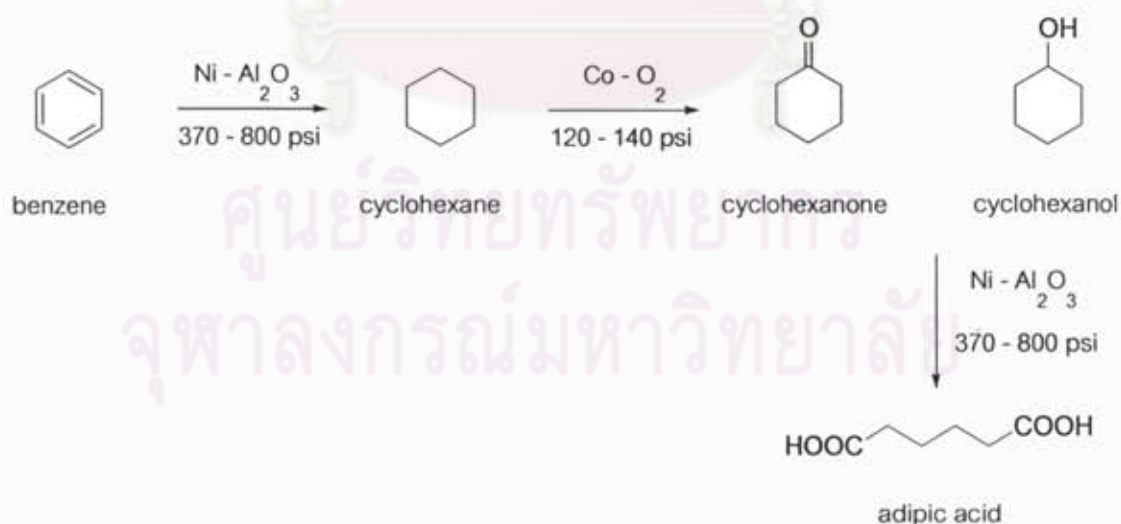


**Scheme 10** Synthesis of adipic acid using benzene as a starting material (adapted from: Draths and Frost. 1994 *J. Am. Chem. Soc.* 116: 399)

4.4.2 Bioactivities of metabolites and their methylated derivatives from the endophytic fungus LPHIL36

The isolated natural substances and their methylated derivatives (16–23) were evaluated for cancer chemopreventive properties (Table 19), i. e. measuring radical scavenging, antioxidant, aromatase (CYP19) inhibitory, and cytotoxic activities (Table 20), and antibacterial activities (Table 21).

Table 19    Radical scavenging, antioxidant, and aromatase inhibitory activities of depsidones and diaryl ethers

| Compound | Radical scavenging and antioxidant activities ($IC_{50}$, µM) | | | | | Aromatase inhibition ($IC_{50}$, µM) |
|---|---|---|---|---|---|---|
| | DPPH | XXO | IXO | HL-60 | ORAC (unit)[a] | |
| 16 | >250 | ND | 19.1 | >100 | 5.9 | 5.30 |
| 18 | 22.4 | ND | 226.5 | >100 | 5.9 | >25 |
| 19 | >250 | ND | >500 | >100 | 0.1 | >25 |
| 20 | 182.4 | >500 | >500 | >100 | 4.3 | >25 |
| 22 | >250 | >500 | 421.4 | >100 | 5.8 | >25 |
| 23 | >250 | >500 | >500 | >100 | 0.0 | ND |

[a] Results were expressed as ORAC units, where one ORAC unit equals the net protection of β-phycoerythrin produced by 1 µM of Trolox.

Among the compounds tested, corynesidone B (18) showed the best activity for the scavenging 2,2-diphenyl-1-picrylhydrazyl (DPPH) free radicals with an $IC_{50}$ value of 22.4 µM (Table 19), comparable to ascorbic acid ($IC_{50}$ 21.2 µM). Compounds 16–23 did not inhibit superoxide anion radical formation in the xanthine/xanthine oxidase (XXO) assay, while corynesidone A (16) inhibited xanthine oxidase (IXO) with an $IC_{50}$ value of 19.1 µM (Table 19). None of the tested compounds could suppress superoxide anion generation (at 100 µM), induced by 12-O-tetradecanoylphorbol-13-acetate (TPA), in differentiated HL-60 human promyelocytic leukemia cells (Table 19). Interestingly, natural products, corynesidones A (16) and B (18), corynether A (20), and the diaryl

ether 22 show potent antioxidant activity, exhibiting oxygen radical absorbance capacity (ORAC) 4.3–5.9 units, while the methylated derivatives 19 and 23 did not showed this activity (Table 19). It is clear that hydroxyl groups in depsidones (16 and 18) and diaryl ethers (20 and 22) are required for antioxidant property. Corynesidone A (16) inhibited aromatase activity with an $IC_{50}$ value of 5.30 µM (Table 19), comparable to that of ketoconazole standard ($IC_{50}$ 2.4 µM). Compounds 16–23 exhibited only weak cytotoxic activity or were inactive (at 50 µg/mL) towards some cell lines (Table 20). However, a derivative 23 exhibited moderate cytotoxicity with $IC_{50}$ values of 1.4–9.0 µg/mL (Table 20).

Moreover, fungal metabolites, corynesidones A (16) and B (18), and diaryl ether (22) had mild antibacterial activities, however compounds 16 and 18 exhibited potent antimethicillin-resistant *Staphylococcus aureus* activity, comparable to ampicillin, as shown in Table 21.

In general, natural compounds, corynesidones A (16) and B (18), corynether A (20), and diaryl ether 22 were relatively non-toxic, but, exhibited antioxidant activities. Corynesidone A (16) exhibited aromatase inhibitory activity with an $IC_{50}$ value of 5.30 µM; this activity magnitude is comparable to the first generation aromatase inhibitor drug, aminoglutethimide. Both anti-aromatase and antioxidant activities of corynesidone A (16) are interesting functions because this dual biological activity may be useful for cancer chemoprevention, particularly for breast cancer. A recent study showed that depsidones and depsides from lichens could prevent UV light and nitric oxide-mediated plasmid DNA damage and induce apoptosis in human melanoma cells, whose mechanism of action was partly involved in the inhibition of reactive oxygen species and reactive nitrogen species (Russo *et al.*, 2008). Some fungal depsidones showed better superoxide anion scavenging activity than quercetin (Lohezic-Le Devehat *et al.*, 2007); however, a few depsidones showed moderate antioxidant activity (Hidalgo *et al.*, 1994). Previous reports also demonstrated that fungal depsidones exhibited cytotoxicity (Bezivin *et al.*, 2004; Pittayakhajonwut *et al.*, 2006) and antibacterial activity against methicillin- and multidrug-resistant *Staphylococcus aureus* (Kokubun *et al.*, 2007).

Several natural products are known to be aromatase inhibitors (Balunas *et al.*, 2008; Paoletta *et al.*, 2008); however, to our knowledge, aromatase inhibitory activity of depsidones has never been reported to date. This is, therefore, the first report on anti-aromatase activity of natural depsidones.

Table 20     Cytotoxic activity of compounds 16-23

| Cell line | Cytotoxic activity ($IC_{50}$, µg/mL); mean (±s.d.), n=3 | | | | | | | | |
|---|---|---|---|---|---|---|---|---|---|
| | 16 | 17 | 18 | 19 | 20 | 21 | 22 | 23 | Etoposide[a]/ Doxorubicin[b] |
| HeLa | 22.50 (±2.21) | 32.70 (±2.08) | >50 | 23.30 (±3.06) | >50 | 29.50 (±0.71) | 35.00 (±3.00) | 2.75 (±1.06) | 0.12 (±0.04)[b] |
| HuCCA-1 | >50 | >50 | >50 | 38.00 (±1.41) | >50 | >50 | >50 | >50 | 0.40 (±0.11)[b] |
| HepG2 | 17.50 (±3.54) | 35.50 (±3.54) | >50 | 35.00 (±0.00) | >50 | 23.50 (±2.12) | >50 | 4.00 (±1.41) | 0.23 (±0.00)[b] |
| T47D | >50 | >50 | >50 | 25.00 (±0.00) | >50 | 41.00 (±5.57) | >50 | >50 | 0.04 (±0.01)[b] |
| MDA-MB231 | >50 | 47.66 (±2.52) | >50 | >50 | >50 | 31.00 (±1.41) | >50 | 9.00 (±0.00) | 0.28 (±0.00)[b] |
| S102 | >50 | 44.00 (±5.66) | >50 | 45.00 (±0.00) | >50 | >50 | >50 | 25.00 (±0.00) | 1.40 (±0.00)[b] |
| A549 | >50 | >50 | >50 | 35.00 (±0.67) | >50 | 46.30 (±4.73) | >50 | >50 | 0.39 (±0.03)[b] |
| HL-60 | 14.72 (±1.73) | 19.38 (±1.52) | >50 | 17.83 (±0.26) | >50 | 17.54 (±1.86) | 43.61 (±1.55) | 2.19 (±0.10) | 0.61 (±0.05)[a] |
| MOLT-3 | 12.26 (±0.06) | 14.71 (±0.54) | >50 | 12.49 (±0.33) | >50 | 9.61 (±0.21) | 34.62 (±1.22) | 1.41 (±0.04) | 0.02 (±0.00)[a] |
| MRC-5 | >50 | >50 | >50 | >50 | >50 | >50 | >50 | >50 | >50[a, b] |

[a]Etoposide and [b]doxorubicin were standard drugs.

Table 21       Antibacterial activities of corynesidones A (16) and B (18), and diaryl ether
22

| Compound | Antibacterial (MIC, mM) | | |
|---|---|---|---|
| | *Enterococcus faecalis* | Methicillin-resistant *S. aureus* | *S. aureus* |
| Corynesidones A (16) | 0.50 | 0.25 | 0.25 |
| Corynesidones B (18) | 0.50 | 0.50 | 1.0 |
| Diaryl ether (22) | 2.0 | 2.0 | 2.0 |
| [a]Ampicillin (µM) | 2.50 | 800 | 3.13 |

[a]Ampicillin was standard drugs.

4.5　Classification of the endophytic fungi isolate LRUB20 and isolate LPHIL36

Conventional and molecular methods were applied to classify the isolate LRUB20 and isolate LPHIL36.

### 4.5.1　Conventional method

The endophytic fungus isolate LRUB20 grown on potato dextrose agar (PDA) had a gray velvety colony and produced characteristic brown spores, as shown Figure 54. However, this fungus isolate LRUB20 did not develop any fruiting body when grown for 2 months on water agar and small pieces of banana leaves, a condition suggested for promoting fruiting body production (Smith and Onions, 1990).
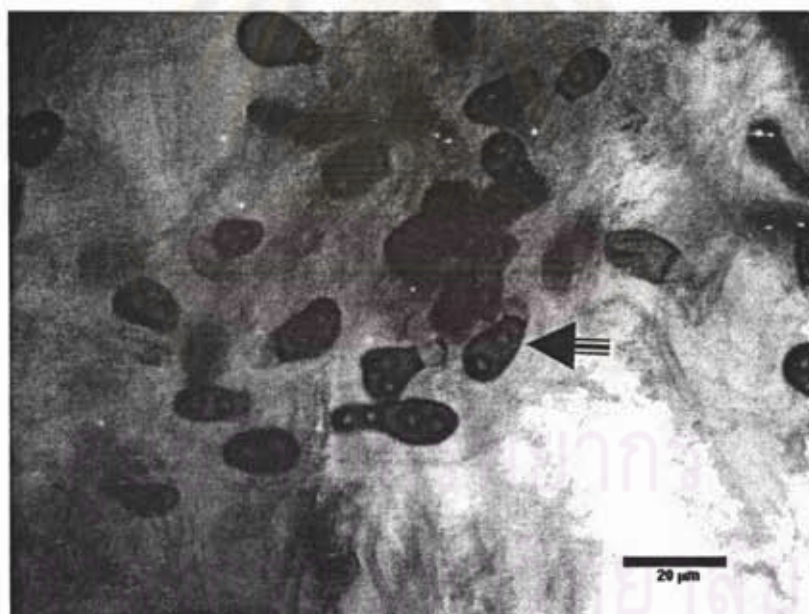


Figure 54　Conidia (arrow) of endophytic fungus isolate LRUB20

Endophytic fungus isolate LPHI L36 grew on PDA as brown velvety colony. Conidiophores were pale brown and formed singly with successive cylindrical

proliferations. Conidia (52–124 × 7–10 µm) were in chains, obclavate to subcylindrical with 4–10 pseudosepta. These correspond well with the characteristics of *Corynespora cassiicola* (Ellis, 1971) (Figure 55).
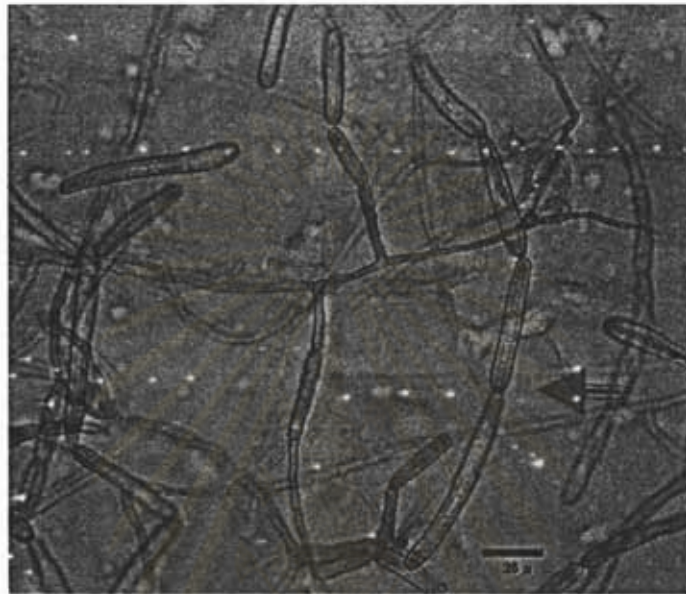


**Figure 55**     Conidia (arrow) of endophytic fungus isolate LPHIL36

### 4.5.2  Molecular method

Further efforts to taxonomically classify the endophytic fungal isolates LRUB20 and LPHIL36 were carried out with molecular method by determining the nucleotide sequences of 18S and ITS1-5.8S-ITS2 regions of rRNA gene. Nucleotide sequences of 18S and 5.8S region is highly conserved, and it is used for the phylogenetic analysis at higher taxonomic levels (Phylum and Class), while the highly variable internal transcribed spacers (ITS1 and ITS2) were used for phylogenetic analysis at lower taxonomic levels (order to species) (Mitchell *et al.*, 1995).

4.5.2.1 The PCR product of 18S and ITS1-5.8S-ITS2 region of rRNA gene

PCR conditions were optimized to amplify rRNA gene of the isolates LRUB20 and LPHIK36. The primers NS1 and NS8 (White *et al.*, 1990) were used to amplify the 18S rRNA gene from total DNA extracts of the isolate LRUB20. While the oligonucleotide primers ITS5 and ITS4 (White *et al.*, 1990) were used to amplify a DNA fragment at 3' end of 18S, ITS1-5.8S-ITS2, and 5' end of 28S rRNA genes of the isolate LPHIL36. The optimized PCR condition was previously described in the material and method section. The sizes of PCR products were compared with λ*Pst*1 molecular markers. The PCR products amplified from chromosomal DNA of isolate LRUB20 and isolate LPHIL36 were found as single band approximately 1800 bp and 600 bp, respectively.

4.5.2.2 Nucleotide sequence of partial 18S rRNA gene of isolate LRUB20 and phylogenetic analysis

Sequencing of the NS1-NS8 PCR product amplified from chromosomal DNA of isolate LRUB20 resulted in 1713 bp. This comprised partial 18S rRNA gene sequence, as shown in Figure 56.

The partial 18S sequences of isolate the LRUB20 was used as the query sequence to search for similar sequences from GenBank. It was found that *Acrospermum compressum* and *Acrospermum gramineum* were the closest matches. A total of 20 known species (Table 22) with relative high % identity (92-96%) were selected for phylogenetic analysis.

```
          ....|....| ....|....| ....|....| ....|....| ....|....|
                10        20        30        40        50
   1     GTCTAAGTAT AAGCACTCAT ACTGTGAAAC TGCGAATGGC TCATTAAATC      50
         AGTTATCGTT TATTTGATAG TACCTTACTA CATGGATACC CGTGGTAATT
 101     CTAGAGCTAA TACATGCCAA AAACCCCGAC TTCGGAAGGG GTGTGTTTAT     150
         TAGATAAAAA ACCAATGCCC TTCGGGGCTG CTTGGTGATT CATGATAACC
 201     AAACGAATCG CATGGCCTTG AGCCGGCGAT GGTTCATTCA AATTTCTGCC     250
         CTATCAACTT TCGATGGTAG GATCTGGGCC TACCATGGTA TCAACGGGTA
 301     ACGGGGAATT AGGGTTCGAT TCCGGAGAGG GAGCCTGAGA AACGGCTACC     350
         ACATCCAAGG AAGGCAGCAG GCGCGCAAAT TACCCAATCC CGACGCGGGG
 401     AGGTAGTGAC AATAAATACT GATACAGGGC TCTTTAGGGT CTTGTAATTG     450
         GAATGAGTAC AATTTAAACC CCTTAACGAG GAACAATTGG AGGGCAAGTC
 500     TGGTGCCAGC AGCCGCGGTA ATTCCAGCTC CAATAGCGTA TATTAAAGTT     550
         GTTGCAGTTA AAAAGCTCGT AGTTGAACCT TGGGCCAGGC TGACCGGTCC
 601     GCCTTACCGC GTGCACTGGT TCGGCCGGGC CCTTTCCTCT GGCAAACCGC     650
         ATGCCCTTCA CTGGGCGTGC CGGGGAACCA GGACTTTTAC TTTGAAAAAA
 701     TTAGAGTGTT CAAAGCAGGC CT-TTGCTCG GATACATTAG CATGGAATAA     750
         TAGAATAGGA CGCGTGGTTC TATTTTGTTG GTTTCTAGAA CCGCCGTAAT
 801     GATTAATAGG GACAGTCGGG GGCATCAGTA TTCAGACGCG AGAGGTGAAA     850
         TTCTTAGACC GTCTGAAGAC TAACTACTGC GAAAGCATTT GCCAAGGATG
 901     TTTTCATTAA TCAGTGAACG AAAGTTGGGG GATCGAAGAC GATCAGATAC     950
         CGTCGTAGTC TCAACCGTAA ACTATGCCGA CTAGGGATCG GGCGACGTTC
1001     CAATTATGAC TCGCCCGGCA CCTTACGAGA AATCAAAGTC TTTGGGTTCT    1050
         GGGGGGAGTA TGGTCGCAAG GCTGAAACTT AAAGAAATTG ACGGAAGGGC
1101     ACCACCAGGC GTGGAGCCTG CGGCTTAATT TGACTCAACA CGGGGAAACT    1150
         CACCAGGTCC AGTACACAAC GAGGATTGAC AGATTGAGAG CTCTTTCTTG
1201     ATTTTGTGGG TGGTGGTGCA TGGCCGTTCT TAGTTGGTGG AGTGATTTGT    1250
         CTGCTTAATT GCGATAACGA ACGAGACCTT CCCCTGCTAA ATAGCCAGGC
1301     TCGCTTTGGC GGGTCGCAGG CTTCTTAGAG GGACAGTCGG CTCAAGCCGA    1350
         TGGAAGTTGG AGGCAATAAC AGGTCTGTGA TGCCCTTAGA TGTTCTGGGC
1401     CGCACGCGCG CTACACTGAC GGAGCCAACG AGTTTAACCA CCTTGTTCCG    1450
         AGAGGTCTGG GTAATCTTGT TAAACTCCGT CGTGCTGGGG ATAGAGCATT
1501     GCAATTATCG CTCTTCAACG AGGAATGCCT AGTAAGCGCA TGTCATCAGC    1550
         ATGCGTTGAT TACGTCCCTG CCCTTTGTAC ACACCGCCCG TCGCTACTAC
1601     CGATCGAATG GCTCAGTGAG GCGTTCGGAC TGGCTTAGGG AGGTTGGCAA    1650
         CGACCACCCG GAGCCGGAAA GTTCGTCAAA CTTGGTCATT TAGAGGAAGT
         AAAAGTCGTA ACA
```

**Figure 56**   Nucleotide sequence of the partial 18S rRNA gene of the LRUB20 fungus

Table 22    Twenty known species (taxa) with relatively high sequence similarity to
isolate LRUB20 selected for phylogenetic analysis

| Known species | Taxa (GenBank) | Accession number |
|---|---|---|
| 1 | *Acrospermum compressum* | AF242258 |
| 2 | *Acrospermum gramineum* | AF242259 |
| 3 | *Jahnula siamensiae* strain SS0081 | AF438180 |
| 4 | *Hyphozyma variabilis* | AJ496241 |
| 5 | *Heyderia abietis* strain HMAS71954 | AY789295 |
| 6 | *Hyphozyma variabilis* var. *odora* | AJ496240 |
| 7 | *Thelebolus stercoreus* | AY942193 |
| 8 | *Thelebolus globosus* strain CBS 113940 | AY942187 |
| 9 | *Thelebolus microsporus* strain dH12783 | AY942191 |
| 10 | *Blastomyces dermatitidis* ATCC 26199 | M63096 |
| 11 | *Goniopila monticola* strain FNP 1 | AY357277 |
| 12 | *Paracoccidioides brasiliensis* 63265 | AF238302 |
| 13 | *Sporobolomyces lactosus* JCM 8510 | AB021676 |
| 14 | *Ajellomyces capsulatus* ATCC26032 | AF320009 |
| 15 | *Ascozonus woolhopensis* ARO 2535 | AF010590 |
| 16 | *Rhynchosporium secalis* isolate 788 | AY038583 |
| 17 | *Sagenomella verticillata* CBS 414.78 | AB024594 |
| 18 | *Sagenomella griseoviridis* CBS 426.67 | AB024591 |
| 19 | *Paecilomyces variotii* IAM 13428 | AB023948 |
| 20 | *Talaromyces byssochlamydoides* IAM 13445 | AB023950 |

Figure 57 shows % identity between partial 18S region of LRUB20 and the 20
reference taxa. It was found that the isolate LRUB20 had relatively higher sequence
similarity to those of *Acrospermum compressum* and *A. gramineum* in the family

Acrospermaceae, subphylum Pezizomycotina, phylum Ascomycota with 96% identity than with other sequences.

LRUB 20

| 96 | | | | | | | | | | | | | | | | | | | | *A. compressum* |
| 96 | 97 | | | | | | | | | | | | | | | | | | | *A. gramineum* |
| 93 | 92 | 93 | | | | | | | | | | | | | | | | | | *J. siamensiae* |
| 93 | 93 | 95 | 94 | | | | | | | | | | | | | | | | | *H. variabilis* |
| 94 | 94 | 95 | 94 | 97 | | | | | | | | | | | | | | | | *H. abietis* |
| 93 | 94 | 95 | 94 | 98 | 97 | | | | | | | | | | | | | | | *H. variabilis* |
| 93 | 93 | 95 | 94 | 99 | 97 | 99 | | | | | | | | | | | | | | *T. stercoreus* |
| 93 | 93 | 95 | 94 | 99 | 97 | 99 | 99 | | | | | | | | | | | | | *T. globosus* |
| 93 | 93 | 95 | 94 | 99 | 97 | 99 | 99 | 99 | | | | | | | | | | | | *T. microsporus* |
| 93 | 93 | 94 | 92 | 95 | 95 | 95 | 95 | 95 | 95 | | | | | | | | | | | *B. dermatitidis* |
| 93 | 93 | 94 | 94 | 97 | 97 | 96 | 96 | 96 | 96 | 94 | | | | | | | | | | *G. monticola* |
| 93 | 93 | 94 | 92 | 95 | 94 | 95 | 95 | 95 | 95 | 99 | 94 | | | | | | | | | *P. brasiliensis* |
| 93 | 93 | 95 | 94 | 98 | 97 | 99 | 99 | 99 | 99 | 95 | 96 | 95 | | | | | | | | *S. lactosus* |
| 93 | 93 | 94 | 92 | 95 | 94 | 95 | 94 | 94 | 94 | 99 | 94 | 99 | 94 | | | | | | | *A. capsulatus* |
| 93 | 93 | 94 | 94 | 98 | 96 | 98 | 98 | 98 | 99 | 94 | 96 | 94 | 98 | 94 | | | | | | *A. woolhopensis* |
| 93 | 93 | 94 | 93 | 96 | 96 | 96 | 96 | 96 | 96 | 94 | 97 | 94 | 96 | 93 | 96 | | | | | *R. secalis* |
| 93 | 93 | 94 | 92 | 94 | 94 | 94 | 94 | 94 | 94 | 97 | 93 | 97 | 94 | 97 | 94 | 93 | | | | *S. verticillata* |
| 93 | 93 | 94 | 92 | 94 | 94 | 94 | 94 | 94 | 94 | 97 | 93 | 97 | 94 | 97 | 94 | 93 | 99 | | | *S. griseoviridis* |
| 93 | 93 | 93 | 92 | 94 | 93 | 94 | 94 | 94 | 94 | 97 | 93 | 97 | 94 | 97 | 94 | 93 | 98 | 98 | | *P. variotii* |
| 92 | 93 | 94 | 92 | 94 | 93 | 94 | 94 | 94 | 94 | 97 | 93 | 97 | 94 | 97 | 94 | 93 | 99 | 99 | 99 | *T. byssochlamydoides* |

**Figure 57**     The alignment scores (% identity) of partial 18S rRNA gene sequence of the isolate LRUB20 and 20 reference taxa from GenBank

Alignment of 18S sequences of LRUB20, 20 reference taxa and 2 outgroup species by ClustalW multiple alignment program and by manually were used to analyze phylogenetic relationship. The inferred phylogenetic tree was 50% majority rule consensus trees with 655 steps tree length, with consistency index (CI), retention index (RI) and rescaled consistency index (RC) of 0.0678, 0.7494, and 0.5034, respectively. Evolution of isolate LRUB20 was found to be most closely related to *A. compressum* and *A. gramineum* with 99% bootstrap support, as shown in Figure 58.
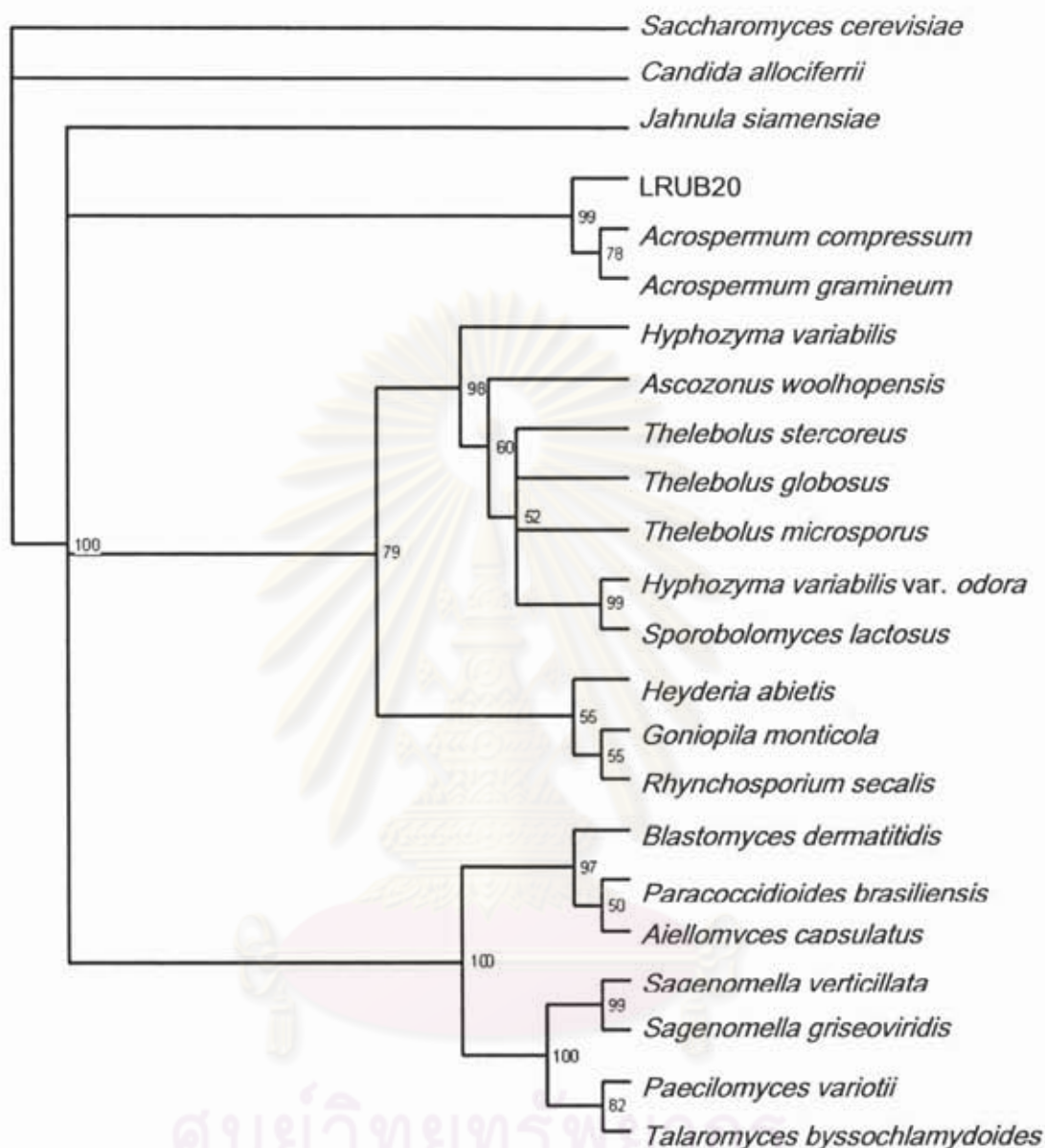
Figure 58    Maximum-parsimony tree (50% majority-rule consensus tree) generated from the 18S rRNA gene sequences of 23 taxa [consistency index (CI) = 0.6718, retention index (RI) = 0.7494, rescaled consistency index (RC) = 0.5034, tree length = 655 steps) showing the evolutionary relationship of LRUB20 with *Acrospermum compressum* and *A. gramineum*. The numbers at internal node indicate the percentages of trees from 1,000 bootstrap replications. *Saccharomyces cerevisiae* and *Candida allociferrii* were used as outgroups.

It is to be noted that microscopic morphology of LRUB20 differs apparently from that of *Dactylaria* (the anamorph of *A. compressum*) and *Virgariella* (the anamorph of *A. gramineum*) (Webster, 1956; Tubaki, 1958). On the basis of the current Ascomycota systematics (Eriksson, 2006), LRUB20 is tentatively classified as a mitosporic species member of Dothideomycetes et Chaetothyriomycetes incertae sedis, class Dothideomycetes, subphylum Pezizomycotina. In an attempt to classify LRUB20 to lower taxonomic level, the ITS1-5.8S-ITS2 sequence was used as query sequence. The highest ITS sequence similarity to known species hit was only 78% to *Mycoleptodiscus terrestris*, a mitosporic Magnaporthaceae, Sordariomycetes incertae sedis, subphylum Pezizomycotina (Chomcheon, 2004; in Master's thesis), suggesting that LRUB20 is potentially a new species. The 18S rRNA gene sequence and ITS sequence of LRUB20 have been submitted to GenBank with accession number DQ381536 and DQ384608, respectively. The culture of isolate LRUB20 has been deposited at the MIM Laboratory, Department of Microbiology, Mahidol University, Thailand.

4.5.2.3 Nucleotide sequence of partial 18S and 28S sequences and complete ITS1-5.8S-ITS2 sequences of isolate LPHIL36 and phylogenetic analysis

Sequencing of the PCR product amplified from chromosomal DNA of isolate LPHIL36 resulted in a 497 bp. This comprised partial of the 18S sequence, complete ITS1-5.8S-ITS2 sequences, and partial of the 28S sequence, as shown in Figure 59.

A GenBank search for DNA sequence similarity revealed that ITS1-5.8S-ITS2 of the isolate LPHIL36 was 100% homology to those of *Corynespora cassiicola* reference strains (CBS1, GenBank Accession No. EU364555; ATCC64204, GenBank Accession No. AY238606).

```
    ....|....| ....|....| ....|....| ....|....| ....|....|
        10        20        30        40        50
      18S                                     ITS1
    CTGCGGAAGG ATCATTATCG TAGGGGCCTC -GCCCCCTTCG AGATAGCACC
                                    ITS1
    GTTTGTTTAT GAGCACCTCT CGTTTCCTCG GCAGGCTCGC CTGCCAACGG
                                    ITS1
    GGACCCACCA CAAACCCATT GTAGTACAAG AAGTACACGT -CTGAACAAAA
      ITS1                                    5.8S
    CAAAACAAAC TATTTACAAC TTTCAACAAC GGATCTCTTG GTTCTGGCAT
                                    5.8S
    CGATGAAGAA CGCAGCGAAA TGCGATAAGT AGTGTGAATT GCAGAATTCA
                                    5.8S
    GTGAATCATC GAATCTTTGA ACGCACATTG CGCCCTTTGG TATTCCTTAG
        5.8S                                  ITS2
    GGCATGCCTG TTCGAGCGTC ATTTCAACCC TCAAGCCTAG CTTGGTGTTG
                                    ITS2
    GGCGTCTGTC CCGCCTCCGC GCGCCTGGAC TCGCCTCAAA AGCATTGGCG
                                    ITS2
    GCCGGTTCCC AGCAGGCCAC GAGCGCAGCA. GAGCAAGCGC TGAAGTGGCT
           ITS2                             28S
    GCGGGTCGGC GCACCATGAG CCCCCCCACA CCAGAATTTT GACCTCG
```

**Figure 59**    Nucleotide sequences of the partial 18S sequence, complete ITS1-5.8S-ITS2 sequences, and partial 28S sequence of the isolate LPHIL36

Based on microscopic morphological characteristics and DNA sequence of the ribosomal RNA gene region, this endophytic fungus is identified as *Corynespora cassiicola* LPHIL36 in class Dothideomycetes, subclass Pleosporomycetidae, order Pleosporales, and family Corynesporascaceae. The ITS1-5.8S-ITS2 DNA sequence of the isolate LPHIL36 fungus has been submitted to GenBank with the Accession number of FJ225970. The culture of *C. cassiicola* LPHI L36 has been deposited at the MIM Laboratory, Department of Microbiology, Mahidol University, Thailand.

*C. cassiicola* is of world-wide distribution and is known to be plant pathogens to many crop plants including tomato (*Lycopersicon esclentum* Mill) in Australia, India, Cuba, and Romania (Oluma and Amuta, 1999). The fungus has also been cited as a serious pathogen of soyabean (*Glycine max* L.), *Phaseolus* spp. in Canada (Seaman *et. al.*, 1965), cassava (*Manihot esculenta* L.), rubber (*Hevea braziliensis* L.) in Brazil and Indonesia (Janqueira *et. al.*, 1985) and attacks the leaf, stem and root of *Vigna sinensis* L., *Arachis hypogea* L., and *Sesamum indicum* L. in the USA. Despite the fact that these

evidences of plant pathogenic nature of *C. cassiicola*, the LPHIL36 is considered to be an endophytic fungus because it is capable of living as a symptomless endophyte for prolonged periods within its host plant, *Lindenbergia philippensis* (Cham.) Benth. [H]. (family Scrophulariaceae).

# CHAPTER V

# CONCLUSION

The endophytic fungus isolate LRUB20 was isolated from the surface-sterilized stem of *Leea rubra* Blume Ex Spreng. (Leeaceae). In the present investigation, eleven metabolites were obtained from this fungal isolate including four new pyrone derivatives, dothideopyrones A–D (**1**, **3**, **4**, and **5**), and seven known compounds, *cis,trans*-muconic acid (**9**), questin (**10**), asterric acid (**11**), methyl asterrate (**12**), sulochrin (**13**), and eugenitin (**14**), and 6-hydroxymethyleugenitin (**15**) when the fungus was fermented on both CzYA culture broth and modified M1D medium. This is the first report on a naturally occurring muconic acid, a biomarker in environments after exposure to benzene and phenol. Dothideopyrone D (**5**) and its acetate derivative **6** exhibited moderate cytotoxic activity. Although the cytotoxic properties of the isolated compounds are not promising, the LRUB20 fungus can produce muconic acid (**9**) at high yield (47.8 mg/L). The latter is an important reference compound in environmental studies. The fungus LRUB20 could also produce a gram scale of 2-hydroxymethyl-3-methyl-cyclopent-2-enone, a useful scaffold for organic synthesis (Chomcheon *et al.*, 2006). The LRUB20 fungus is a potential fungal candidate for the use in the field of white biotechnology. Microscopic morphologically, the LRUB20 fungus produced unique brown spore. DNA sequences of the 18S and ITS1-5.8S-ITS2 ribosomal RNA genes did not match with any known fungi in the GenBank database. Accordingly, the LRUB20 fungus may represent a new species and it was tentatively characterized as mitosporic Dothideomycete LRUB20.

The endophytic fungus LPHIL36 was separated from the apparently healthy leaves of a Thai medicinal plant, *Lindenbergia philippensis* (Cham.) Benth. [H]. (family Scrophulariaceae). Three new compounds, corynesidones A (**16**) and B (**18**), and corynether A (**20**), together with a known diaryl ether **22**, were isolated from this fungal endophyte cultivated on MEB medium. Corynesidone B (**18**) could scavenge DPPH free

radicals at the same activity as that of ascorbic acid. All isolated natural products (**16, 18, 20,** and **22**) showed potent antioxidant activity, as revealed by ORAC assay. However, the isolated metabolites and their methylated derivatives (**16-23**) neither inhibited superoxide anion radical formation in the XXO assay nor suppressed TPA-induced superoxide anion generation in HL-60 cell line. In addition, corynesidone A (**16**) was found to be an aromatase inhibitor, showing comparable activity to the first generation aromatase inhibitor drug, aminoglutethimide. The LPHIL36 fungus produced the cylindrical pale brown conidia on PDA. Based on microscopic morphology and analysis of the DNA sequences of the ITS1-5.8S-ITS2 ribosomal RNA gene region, this fungal isolate was identified as *Corynespora cassiicola* in the family Corynesporascaceae.

# REFERRENCES

Altschul, S. F., Madden, T. L., Schaffer, A. A., Zhang, J., Miller, W. and Lipman, D. J. 1997. Gapped BLAST and PSI-BLAST: a new generation of protein database search programs. Nucleic Acids Res. 25: 3389-3402.

Arnold, A. E., Maynard, Z., Gilbert, G. S., Coley, P.D. and Kursar, T. A. 2000. Are tropical fungi endophytes hyperdiverse?. Ecology Letters. 3: 267-274.

Azevedo, J. L., Maccheroni, Jr. W., Pereira., J. O. and Araujo., W. L. 2000. Endophytic Microorganisms: a review on insect control and recent advances on tropical plants. J. Biot. 3: 40-65.

Balunas, M.J., Su, B., Brueggemeier, R. W. and Kinghorn, A. D. 2008. Natural products as aromatase inhibitors. Anticancer Agents Med. Chem. 8: 646–682.

Bezivin, C., Tomasi, S., Rouaud, I., Delcros, J. G. and Boustie, J. 2004. Cytotoxic activity of compounds from the lichen: *Cladonia convoluta*. Planta Med. 70: 874–877.

Bill, G. F. 1996. Isolation and analysis of endophytic fungal communities from woody plants. In: Redlin, S. C. and Carris, L. M. editors. Endophytic fungi in grasses and woody plants. Minnesota: APS Press: 31-65.

Boonen, G. and Haberlein, H. 1998. Influence of genuine kavapyrone enantiomers on the GABA-A binding site. Planta Med. 64: 504–506.

Cannon, J. R., Cresp, T. M., Metcalf, B. W., Sargent, M. V. and Elix, J. A. 1972. Structure and synthesis of 2-hydroxy-4-methoxy-6-methylphenyl 3-hydroxy-5-methylphenyl ether (LL- V125a), a fungal diaryl ether. J. Chem. Soc., Perkin Trans. 1, 1200–1203.

Carmichael, J., DeGraff, W. G., Gazdar, A. F., Minna, J. D. and Mitchell, J. B. 1987. Evaluation of a tetrazolium-based semiautomated colorimetric assay: assessment of chemosensitivity testing. Cancer Res. 47: 936–942.

Cao, G. and Prior, R. L. 1999. Measurement of oxygen-radical absorbing capacity in biological samples. Meth Enzymol. 299: 50-62.

Chanway, C. P. 1996. Endophytes: they're not just fungi. Can. J. Bot. 74: 321-322.

Charlie, M. J. and Watkinson, S. C. 2001. The Fungi: Fungi Diversity . p.11 . London: Academic Press.

Chinworrungsee, M., Wiyakrutta, S., Sriubolmas, N., Chuailua, P. and Suksamrarn, A. 2008. Cytotoxic activities of trichothecenes isolated from an endophytic fungus belonging to order Hypocreales. Arch. Pharm. Res. 31(5): 611-616.

Choi, S. G., Kim, J., Sung, N. D., Son, K. H., Cheon, H. G., Kim, K. R. and Kwon, B. M. 2007. Anthraquinones, Cdc25B phosphatase inhibitors, isolated from the roots of *Polygonum multiflorum* Thunb. Nat. Prod. Res. 21: 487–493.

Chomcheon, P. 2004. Bioactive compounds from endophytic fungi *Phomopsis* sp. from *Urobotrya siamensis* and isolate LRUB20 from *Leea rubra*. Master's Thesis. Program of Biotechnology, Faculty of Science, Graduate School, Chulalongkorn University.

Chomcheon, P., Wiyakrutta, S., Sriubolmas, N., Ngamrojanavanich, N., Isarangkul, D. and Kittakoop, P. 2005. 3-Nitropropionic Acid (3-NPA), a potent antimycobacterial agent from endophytic fungi: Is 3-NPA in some plants produced by    endophytes?. J. Nat. Prod. 68: 1103-1105.

Chomcheon, P., Sriubolmas, N., Wiyakrutta, S., Ngamrojanavanich, N., Chaichit, N., Mahidol, C., Ruchirawat., S. and Kittakoop, P. 2006. Cyclopentanones, scaffolds for organic syntheses produced by the endophytic fungus, mitosporic Dothideomycete sp. LRUB 20. J. Nat. Prod. 69(5): 1351-1353.

Christensen, M. J., Ball, O. J. P., Bennett, R and Schardi, C. L. 1997. Fungi and host geno-ype effects on compatibility and vascular colonisation by *Epichloë festucae*. Mycol. Res. 101: 493-501.

Chuakul, W., Saralamp, P., Paonil, W., Temsiririkkul, R. and Clayton, T. 1997. Medicinal Plants in Thailand Volume II. P. 147. Bangkok: Amarin Printing and Publishing Public Co., Ltd.

Dale, J. A. and Mosher, H. S. 1973. Nuclear magnetic resonance enantiomer reagents. Configurational correlations via nuclear magnetic resonance chemical shifts of diastereomeric mandelate, O-methylmandelate, and α-methoxy-α-trifluoromethylphenylacetate (MTPA) esters. J. Am. Chem. Soc. 95: 512–519.

Demain, A. L. 1981. Industrial microbiology. Science. 214: 987-994.

Doyle, A. and Griffiths, J. B. 1997. Mammalian Cell Culture: Essential Techniques. John Wiley and Sons.

Draths, K. M. and Frost, J. W. 1994. Environmentally compatible synthesis of adipic acid from D-glucose. J. Am. Chem. Soc. 116, 399–400.

Dreyfuss, M. M. and Chapela, I. H. 1994. In Gullo, V.P. (ed.), The discovery of natural products with therapeutic potential. pp. 49-80. Boston, MA: Butterworth-Heinemann.

Ellis, M. B. 1971. Dematiaceous Hyphomycetes. CAB International, Kew, UK.

Eriksson, O. 2000. Notes on ascomycete systematics. Myconet. 5: 1–35.

Feng, Y., Blunt, J. W., Anthony, L., Cole, J., Murray, H. and Munro, G. 2002. The isolation of two new chromone derivatives from the New Zealand fungus Tolypocladium extinguens. J. Nat. Prod. 65: 1681-1682.

Folmer, F., Harrison, W. T., Tabudravu, J. N., Jaspars, M., Aalbersberg, W., Feussner, K., Wright, A. D., Dicato, M. and Diederich, M. 2008. NF-kappaB-inhibiting naphthopyrones from the Fijian echinoderm Comanthus parvicirrus. J. Nat.Prod. 71: 106–111.

Fox, C. H. 1969. The formation of roccellic acid, eugenitol, eugenetin, and rupicolon by the mycobiont Lecanora Rupicola. Phytochemistry. 8: 1301-1304.

Freeman,S., and Rodriguez, R. J. 1993. Genetic conversion of a fungal plant pathogen to a nonpathogenic, endophytic mutualist. Science 260:75.

Fujimoto, H., Satoh, Y., Nakayama, M., Takayama, T. and Yamazaki, M. 1995. Isolation of some immunosuppressive components from an ascomycete, Gelasinospora multiforis. Chem. Pharm. Bull. 43: 547–552.

Gerhauser, C., Klimo, K., Heiss, E., Neumann, I., Gamal-Eldeen, A., Knauft, J., Liu, G. Y., Sitthimonchai, S. and Frank, N., 2003.  Mechanism-based in vitro screening of potential cancer chemopreventive agents. Mutat. Res. 523–524: 163–172.

Griesinger, C., Schwalbe, H., Schleucher, J. and Sattler, M. 1994. Proton-detected heteronuclear and multidimensional NMR. In: Croasmun, W.R., Carlson, R.M.K. (Eds.), Two-Dimensional NMR Spectroscopy. Applications for Chemists and Biochemists. VCH, New York, pp. 457–480.

Guo, B., Dai, J. R., Ng, S., Huang, Y., Leong, C., Ong, W. and Karte, B. K. 2000. Cytonicacids A and B: novel tridepside inhibitors of hCMV protease from the endophytic fungus Cytonaema species. J. Nat. Prod. 63: 602-604.

Guo, L. D., Huang, G. R., Wang, Y., He, W. Y., Zheng, W. H. and Hyde, K. D. 2003. Molecular identification of white morphotype strains of endophytic fungi from Pinus tabulaeformis. Mycol. Res. 107(6): 680-688.

Harper, J. K., Barich, D. H., Hu, J. Z., Strobel, G. A., and Grant, D. M. 2003a. Stereochemical analysis by solid-state NMR: structural predictions in ambuic acids. J. Org. Chem. 68: 4609-4614.

Harper, J. K., Ford, E. J., Strobel, G. A., Arif, A., Grant, D. M., Porco, J., Tomer, D. P. and O'neill, K. 2003b.  Pestacin: a 1,3-dihydro isobenzofuran from Pestalotiopsis microspora possessing antioxidant and antimycotic activities. Tetrahedron 59: 2471-2476.

Hawksworth, D. L. 1991.  The fungal dimention of biodiversity: magnitude, significance, and conversation. Mycol. res. 95: 641-655.

Hidalgo, M. E., Fernandez, E., Quilhot, W. and Lissi, E. 1994.  Antioxidant activity of depsides and depsidones. Phytochemistry. 37: 1585–1587.

Hu, Y., Chaomin, L., Kulkarni, B., Strobel, G. A., Lobkovsky, E., Torczynski, R., and Porco, J. 2001.  Exploring chemical diversity of epoxyquinoid natural products: synthesis and biological activity of jesterone and related molecules. Org. Lett. 3: 1649-1652.

Isaac, S. 1992.  Fungal-plant interactions. London: Chapman & Hall.

Jaih, H., Ja-on, P., Emilio, L. G., Sivasithamparam, K., Brian, W. S. and Allan, H. W. 2002. New Chlorinated Diphenyl Ethers from an *Aspergillus* Species. J. Nat. Prod. 65. 65: 7-10.

Janqueira, N. T. V., Gasparotto, L., Morae, V. H. F., Silv, H. M. and Lim, T. M. 1985. New diseases caused by virus, fungi and also bacterium on rubber from Brazil and their impact on International Quarantine. Proc. Reginal Conf. on Plant Quarantine. 253-260.

Kimura, Y., Kozawa, M., Baba, K. and Hata, K. 1983. New constitutents of roots of *Polygonum cuspidatum*. J. of Medicinal Plant Research. 48: 164-168.

Kokubun, T., Shiu, W. K. and Gibbons, S. 2007. Inhibitory activities of lichen-derived compounds against methicillin- and multidrug-resistant *Staphylococcus aureus*. Planta Med. 73: 176–179.

Kongsaeree, P., Prabpai, S., Sriubolmass, N., Vongvein, C. and Wiyakrutta, S. 2003. Antimalarial dihydroisocoumarins produced by *Geotrichum* sp., an endophytic fungus of *Crassocephalum crepidiodes*. J. Nat. Prod. 66: 709-711.

Lambros, C. and Vanderberg, J. P. (1979). Synchronization of *Plasmodium falciparum* erythrocytic stages in culture. J. Parasitol. 65(3): 418-20.

Lang, G., Cole, A. L., Blunt, J. W., Robinson, W. T. and Munro, M. H. 2007. Excelsione, a depsidone from an endophytic fungus isolated from the New Zealand endemic tree *Knightia excelsa*. J. Nat. Prod. 70: 310–311.

Lee, J. C., Lobkovsky, E., Pliam, N. B., Strobel, G. and Clardy, J. 1995. Subglutinols A and B; immunosuppressive compounds from the endophytic fungus *Fusarium subglutinans*. J. Org. Chem. 60: 7076-7077.

Lee, S. and Taylor, J. W. 1990. Isolation of DNA from fungal mycelia and single spores. In: Innis, M. A., Gelfand, D. H., Sninsky, J. J. and White, T. J., eds. PCR Protocols: a guide to method and applications, pp. 282-287. London: Academic Press.

Li, J., Sidhu, R. S., Bollon, A. and Strobel, G. A. 1998a. Stimulation of taxol production in liquid cultures of *Pestalotiopsis microspora*. Mycol. Res. 102(4): 461-464.

Li, J., Sidhu, R. S., Ford, E. J., Long, D. M., Hess, W. M. and Strobel, G. A. 1998b. The induction of taxol production in the endophytic fungus *Periconia* sp. from *Torreya grandifolia*. Journal of Industrial Microbiology and Biotechnology 20: 259-264.

Li, J. Y. and Strobel, G. A. 2001. Jesterone and hydroxy-jesterone antioomycetes cyclohexenone epoxides from the endophytic fungus *Pestalotiopsis jesteri*. Phytochemistry 57: 261-265.

Li, J. Y., Strobel, G. A., Harper, J. K., Lobkovsky, E. and Clardy, J. 2000. Cryptocin, a potent tetramic acid antimycotic from the endophytic fungus *Cryptosporiopsis* cf *quercina*. Org.Lett. 2: 767-770.

Lohezic-Le Devehat, F., Tomasi, S., Elix, J. A., Bernard, A., Rouaud, I., Uriac, P. and Boustie, J. 2007. Stictic acid derivatives from the lichen *Usnea articulate* and their antioxidant activities. J. Nat. Prod. 70: 1218–1220.

Lumyong, S., Lumyong, P., Pongsomboon, S. and Hyde, K. Endophytic fungi from Indigenous dicotyledonous plants at Doi Suthep-Pui area, Thailand. p. 89. Abstract of the International Union of Pure and Applied Chemistry (IUPAC). International conference on biodiversity & bioresources-conservation & utilization.

McGahren, W. J., Andres, W. W. and Kunstmann, M. P. 1970. Novel diaryl ether, LLV125a, from a fungus of the order Sphaeropsidales. J. Org. Chem. 35: 2433–2435.

Meinkoth, J. and Wahl, G. 1988. Hybridization of nucleic acids immobilized on solid supports. Anal. Biochem. 138: 267-284.

Melikian, A. A., Qu, Q., Shore, R., Li, G., Li, H., Jin, X., Cohen, B., Chen, L., Li, Y., Yin, S., Mu, R., Zhang, X. and Wang, Y. 2002. Personal exposure to different levels of benzene and its relationships to the urinary metabolites Sphenylmercapturic acid and *trans,trans*-muconic acid. J. Chromatogr. B. 778: 211–221.

Mitchell, J. I., Roberts, P. J. and Moss, S. T. 1995. Sequence or structure? A short review on the application of nucleic acid sequence information to fungal taxonomy. Mycologist. 9(2): 129-132.

Mosmann, T. 1983. Rapid colorimetric assay for cellular growth and survival: Application to proliferation and cytotoxicity assays. J. Immunol. Methods. 65(1-2): 55-63.

Nagao, A., Seki, M. and Kobayashi, H. 1999. Inhibition of xanthine oxidase by flavonoids. Biosci. Biotechnol. Biochem. 63(10): 1787-1790.

Navasumrit, P., Arayasiri, M., Hiang, O. M., Leechawengwongs, M., Promvijit, J., Choonvisase, S., Chantchaemsai, S., Nakngam, N., Mahidol, C. and Ruchirawat, M. 2008. Potential health effects of exposure to carcinogenic compounds in incense smoke in temple workers. Chem. Biol. Interact. 173: 19–31.

Niu, W., Draths, K. M. and Frost, J. W. 2002. Benzene-free synthesis of adipic acid. Biotechnol. Prog. 18: 201–211.

Oluma, H. O. A. and Amuta, E. U. 1999. *Corynespora cassiicola* leaf spot of pawpaw (*Carica papaya* L.) in Nigeria. Mycopathologia. 145: 23-27.

Paoletta, S., Steventon, G. B., Wildeboer, D., Ehrman, T. M., Hylands, P. J. and Barlow, D. J. 2008. Screening of herbal constituents for aromatase inhibitory activity. Bioorg. Med. Chem. 16: 8466–8470.

Pedras, M. S. and Chumala, P. B. 2005. Phomapyrones from blackleg causing phytopathogenic fungi: isolation, structure determination, biosyntheses and biological activity. Phytochemistry. 66: 81–87.

Pick, E. and Mizel, D. 1981. Rapid microassays for the measurement of superoxide and hydrogen peroxide production by macrophages in culture using an automatic enzyme immunoassay reader. J. Immunol. Methods. 46(2):211-226.

Pittayakhajonwut, P., Dramae, A., Madla, S., Lartpornmatulee, N., Boonyuen, N. and Tanticharoen, M. 2006. Depsidones from the endophytic fungus BCC 8616. J. Nat. Prod. 69: 1361–1363.

Prachya, S., Wiyakrutta, S., Sriubolmas, N., Ngamrojanavanich, N., Mahidol, C., Ruchirawat., S. and Kittakoop, P. 2007. Cytotoxic mycoepoxydiene derivatives from an endophytic fungus *Phomosis* sp. isolated from *Hydnocarpus anthelminthicus*. Planta. Med. 73: 1418-1420.

Puri, S. C., Verma, V., Amna, T., Qazi, G. N. and Spiteller, M. 2005. An endophytic fungus from *Nothapodytes foetida* that produces camptothecin. J. Nat. Prod. 68: 1717-1719.

Russo, A., Piovano, M., Lombardo, L., Garbarino, J. and Cardile, V. 2008. Lichen metabolites prevent UV light and nitric oxide-mediated plasmid DNA damage and induce apoptosis in human melanoma cells. Life Sci. 83: 468–474.

Saikkonen, K., Wali, P., Helander, M. and Stanley, H. F. 2004. Evolution of endophyte-plant symbioses. Trends in Plant Science. 9: 275-280.

Sappapan, R., Sommit, D., Ngamrojanavanich, N., Pengpreecha, S., Wiyakrutta, S., Sriubolmas, N. and Pudhom, K. 2008. 11-Hydroxymonocerin from the plant endophytic fungus *Exserohilum rostratum*. J. Nat. Prod. 71: 1657-1659.

Sala, T. and Sargent, M. V. 1981. Depsidone synthesis. Part 16. Benzophenone-grisa-30, 50-diene-20 , 3-dione-depsidone interconversion: a new theory of depsidone biosynthesis. J. Chem. Soc., Perkin Trans 1. 855–869.

Sargent, M. V., Cannon, J. R., Cresp, T. M., Metcalf, B. W. and Elix, J. A. 1971. Structural revision and synthesis of a novel fungal diaryl ether. Chem. Commun. 473.

Schardl, C. L., Leuchtmann, A. and Spiering, M. J. 2004. Symbioses of grasses with seedborne fungal endophytes. Annu. Rev. Plant. Biol. 55: 315-340.

Seaman, W. L., Shoemaker, R. A. and Peterson, E. A. 1965. Pathogenicity of *Corynespora cassiicola* on soybean. Can. J. Bot. 43(1): 1469.

Shen, Y. C., Prakash, C. V. and Kuo, Y. H. 2001. Three new furan derivatives and a new fatty acid from a Taiwanese marine sponge *Plakortis simplex*. J. Nat. Prod. 64: 324–327.

Shimada, A., Shiokawa, C., Kusano, M., Fujioka, S. and Kimura, Y. 2003.
Hydroxysulochrin, a tea pollen growth inhibitor from the fungus *Aureobasidium*
sp. Biosci. Biotechnol. Biochem. 67: 442–444.

Smith, D. and Onions, A. H. S. 1990. IMI Technical Handbooks No.2 The preservation
and maintenance of living fungi. 2$^{nd}$ ed. International Mycological Institute: CAB
international.

Sriubolmas N., Tung, A., Sawatchupong, R., Ruangrungsi, N. and Wiyakrutta, S. 2001.
Antimicrobial activities of endophytic fungi isolated from selected Thai medicinal
plants. p. 228-237. *In* C. T. Hedreyda, and M. E. A. Zabat (ed.), Proceeding of
the 4$^{th}$ Asia-Pacific Biotechnology Congress & 30$^{th}$ Annual PSM Convention.
Philippine Society for Microbiology, Inc., Philippine.

Stresser, D. M., Turner, S. D., McNamara, J., Stocker, P., Miller, V. P., Crespi, C. L. and
Patten, C. J., 2000. A high-throughput screen to identify inhibitors of aromatase
(CYP19). Anal. Biochem. 284: 427–430.

Strobel, G. 2003. Endophytes as sources of bioactive products. Microbes and
Infection 5: 535-544.

Strobel, G. and Daisy, B. 2003. Bioprospecting for microbial endophytes and their
natural products. Microbiol. Mol. Biol. Rev. 67(4): 491-502.

Strobel, G., Hess, W. M., Li, J., Ford, E. and Sears, J. 1997. *Pestalotiopsis guepinii*, a
taxol producing endophytic of the Wollemi Pine, *Wollemia nobilis*. Aust.J. Bot.
45: 1073-1082.

Strobel, G., Hess, W. M., Baird, G., Ford, E., Li, J. Y. and Sidhu, R. S. 2001. *Stegolerium
kukenani* gen. et sp. nov. an endophytic, taxol producing fungus from the
Roraima and Kukenan tepuis of Venezuela. Mycotaxon LXXVIII: 353-361.

Strobel, G., Miller, R. V., Martinez-Miller, C., Condron, M. M., Teplow, D. B. and Hess, W.
M. 1999. Cryptocandin, a potent antimycotic from the endophytic fungus
*Cryptosporiopsis* cf. *quercina*. Microbiology 145: 1919-1926.

Strobel, G. and Stierle, A. 1993. *Taxomyces andreanae*, a proposed new taxon for a bulbilliferous hyphomycete associated with Pacific Yew (*Taxus brevifolia*). Mycotaxon XLVII: 71-80.

Strobel, G., Yang, X., Sears, J. and Kramer, R. 1996. Taxol from *Pestalotiopsis microspora*, an endophytic fungus of *Taxus wallachiana*. Microbiology 142: 435-440.

Suffness, M. 1995. Taxol, science and applications. Boca Raton, Fla : CRC Press.

Swofford, D. L. 2003. Phylogenetic Analysis Using Parsimony (PAUP). Version 4 Sinauer Associates. Sunderland. MA.

Tan, R. X. and Zou, W. X. 2001. Endophytes: a rich source of functional metabolites. Natural Product Reports. 18: 448-459.

Takeuchi, T., Nakajima, M. and Morimoto, K. (1994). Establishment of a human system that generates $O_2^-$ and induces 8-hydroxydeoxyquanosine, typical of oxidative DNA damage, by a tumor promotor. Cancer Res. 54(22): 5837-5840.

Thompson, J. D., Gibson, T. J., Plewniak, F., Jeanmougin, F. and Higgins, D. G. 1994. The Clustal X windows interface: flexible strategies for multiple sequence alignment aided by quality analysis tools. Nucleic Acids Res. 24: 4876-4882.

Trager, W., and Jensen, J. B. (1976). Human malaria parasites in continuous culture. Science. 193(4254): 673-675.

Tominaga, H., Ishiyama, M., Ohseto, F., Sasamoto, K., Hamamoto, T., Suzuki, K. and Watanabe, M. 1999. A water-soluble tetrazolium salt useful for colorimetric cell viability assay. Anal. Commun. 36: 47–50.

Thomas, J. M., Raja, R., Johnson, B. F., O'Connell, T. J., Sankar, G. and Khimyak, T. 2003. Bimetallic nanocatalysts for the conversion of muconic acid to adipic acid. Chem. Commun. 1126–1127.

Tsai, S. C., Tsai, L. D. and Li, Y. K. 2005. An isolated Candida albicans TL3 capable of degrading phenol at large concentration. Biosci. Biotechnol. Biochem. 69: 2358–2367.

Tubaki, K. 1958. Studies on Japanese hyphomycetes. J. Hattori Bot. Lab. 20, 142–244.

Ukeda, H., Maeda, S., Ishii, T. and Sawamura, M. 1997. Spectrophotometric assay for superoxide dismutase based on tetrazolium salt 3′-{1-[(phenylamino)-carbonyl]-3,4-tetrazolium}-bis(4-methoxy-6-nitro)benzenesulfonic acid hydrate reduction by xanthine/xanthine oxidase. Anal. Biochem. 251(2): 206-209.

Wagenaar, M. M., Corwin, J., Strobel, G. and Clardy, J. 2000. Three new cytochalasins produced by an endophytic fungus in the Genus *Rhinocladiella*. J. Nat. Prod. 63: 1692-1695.

Wang, J., Li, G., Lu, H., Zheng, Z., Huang, Y. and Su, W. 2000. Taxol from *Tubercularia* sp. strain TF5, an endophytic fungus of *Taxus mairei*. FEMS Microbiology Letters 193:249-253.

Wang, C., Wu, J. and Mei, X. 2001. Enhancement of taxol production and excretion in*Taxus chinensis* cell culture by fungal elicitation and medium renewal. Appl. Microbiol. Biotechnol. 55: 404-410.

Webster, J. 1956. Conidia of *Acrospermum compressum* and *A. Gramineum*. Trans. Br. Mycol. Soc. 39: 361–366.

White, T. J., Bruns, T., Lee, S. and Taylor, J. W. 1990. Amplification and direct sequencing of fungal ribosomal RNA gene for phylogenetics. In:Innis, M.A., Gelfand, D.H., Sninsky, J.J. and White, T.J., eds. PCR Protocols: a guide to method and applications, pp. 315-322. London: Academic Press.

Wiyakrutta, S., Sriubolmas, N., Panphut, W., Thongon, N., Danwisetkanjana, K., Ruangrungsi, N. and Meevootisom, V. 2004. Endophytic fungi with anti-microbial, anti-cancer and anti-malarial activities isolated from Thai medicine plants. World J. Microbiol. Biotechnol. 20: 265-272.

Xiao, Y., Zhang, J. J., Liu, H. and Zhou, N. Y. 2007. Molecular characterization of a novel ortho-nitrophenol catabolic gene cluster in Alcaligenes sp. strain NyZ215. J. Bacteriol. 189: 6587–6593.

Yardley-Jones, A., Anderson, D. and Parke, D. V. 1991. The toxicity of benzene and its metabolism and molecular pathology in human risk assessment. Br. J. Ind. Med. 48: 437–444.

Yoshikawa, N., Ohta, K., Mizuno, S. and Ohkishi, H. 1993. Production of cis,cis-muconic acid from benzoic acid. Bioprocess Technol. 16: 131–147.

Zhan, J., Gunaherath, G. M., Wijeratne, E. M. and Gunatilaka, A. A. 2007. Asperpyrone D and other metabolites of the plant-associated fungal strain Aspergillus tubingensis. Phytochemistry. 68: 368–372.

Zhang, B., Salituro, G., Szalkowski, D., Li, Z., Zhang, Y., Royo, I., Vilella, D., Dez, M., Pelaez, F., Ruby, C., Kendall, R. L., Mao, X., Griffin, P., Calaycay, J., Zierath, J. R., Heck, J. V., Smith, R. G. and Moller, D. E. 1999. Discovery of small molecule insulin mimetic with antidiabetic activity in mice. Science 284 : 974-981.

# APPENDICES

# APPENDIX A

## 1. Media

### 1.1 Yeast Extract Sucrose Agar (YEA)

| | |
|---|---|
| Yeast extract | 20 g |
| Sucrose | 150 g |
| Agar | 15 g |
| Distilled water up to | 1 L |

### 1.2 Malt Czapek Broth (MCzA)

| | |
|---|---|
| Czapek stock solution A | 50 ml |
| Czapek stock solution B | 50 ml |
| Sucrose | 30 g |
| Malt Extract | 40 g |
| Agar | 15g |
| Distilled water up to | 1 L |

**Czapek stock solution A**

| | |
|---|---|
| $NaNO_3$ | 4.0 g |
| KCL | 1.0 g |
| $MgSO_4.7H_2O$ | 1.0 g |
| $FeSO_4.7H_2O$ | 0.02 g |
| Dissolved in distilled water up to | 100 ml |
| Keep in a refrigerator | |

**Czapek stock solution B**

| | |
|---|---|
| $K_2HPO_4$ | 2.0 g |
| A solution | 1.0 g |

| B solution | 1.0 g |
| Dissolved in distilled water up to | 100 ml |
| Keep in a refrigerator | |
| **A solution** | |
| $ZnSO_4.7H_2O$ | 1.0 g |
| Dissolved in distilled water up to | 100 ml |
| **B solution** | |
| $CuSO_4.5H_2O$ | 1.0 g |
| Dissolved in distilled water up to | 100 ml |

### 1.3 Sabouraud's Dextrose Agar (SDA)

| Dextrose | 40 g |
| Neopeptone | 10 g |
| Agar | 15 g |
| Distilled water up to | 1 L |

### 1.4 Potato Dextrose Agar (PDA)

| Potato | 200 g |
| Dextrose | 20 g |
| Agar | 15g |
| Distilled water up to | 1 L |

### 1.5 Czapek Yeast Autolysate Agar (CzYA)

| Czapek solution agar | 49 g |
| Yeast extract | 20 g |
| Agar | 15g |
| Distilled water up to | 1 L |

### 1.6 Malt Extract Agar (MEB)

| Malt extract | 20.0 g |
| Peptone | 1.0 g |

| Glucose | 20.0 g |
|---|---|
| Distilled water up to | 1 L |

### 1.7 M1D Medium (Pinkerton and Strobel, 1976)

| | |
|---|---|
| $Ca(NO_3)_2$ | 1.2 mM |
| $KNO_3$ | 0.79 mM |
| KCl | 0.87 mM |
| $MgSO_4$ | 3.0 mM |
| $NaH_2PO_4.H_2O$ | 0.007mM |
| $FeCl_3$ | 0.0074 mM |
| $MnSO_4$ | 0.03 mM |
| $ZnSO_4.H_2O$ | 0.0087 mM |
| $H_3BO_3$ | 0.0022 mM |
| KI | 0.0045 mM |
| Sucrose | 87.6 mM |
| Ammonium Tartrate | 27.1 mM |
| Yeast Extract | 0.5 g |
| Soytone | 1.0 g |
| Distilled water up to | 1 L |

M1D medium was supplemented with 0.5 g/L malt extract.

### 1.8 Czapek Yeast Autolysate (CYA)

| | |
|---|---|
| $K_2HPO_4$ | 1.0 g |
| Czapek concentrate | 10.0 mL |
| Yeast extract | 5.0 g |
| Sucose | 30.0 g |
| Agar | 15g |
| Distilled water up to | 1 L |
| **Czapek concentrate** | |
| $NaNO_3$ | 30.0 g |
| KCl | 5.0 g |

| | |
|---|---|
| MgSO$_4$.7H$_2$O | 5.0 g |
| FeSO$_4$.7H$_2$O | 0.1 g |
| Dissolved in distilled water up to | 100 ml |
| Keep in a refrigerator | |

## 1.9 Water Agar

| | |
|---|---|
| Agar | 15 g |
| Distilled water up to | 1 L |

## 2. Reagent and buffer for DNA amplification by PCR

### 2.1 Lysis buffer

| | |
|---|---|
| Tris-HCl (pH 7.2) | 50 mM |
| EDTA | 50 mM |
| SDS | 3% |
| 2-mercaptoethanol | 1% |

### 2.2 Chlorofrom : TE-saturated phenol      1:1,v/v

### 2.3 TE for resuspending pellet

| | |
|---|---|
| Tris-HCl | 10 mM |
| EDTA | 0.1 mM |

### 2.4 Gel loading buffer

| | |
|---|---|
| Bromophenol blue | 0.25% |
| Sucrose in water | 40% (w/v) |
| Store temperature at 4$^0$C | |

### 2.5 5-X Tris-Borate-EDTA (TBE)

| | |
|---|---|
| Tris base | 54 g |
| Boric acid | 27.5 g |
| 0.5 M EDTA pH 8.0 | 20 ml |

The working solution was 1X TBE, diluted with four volume of distilled water.

### 2.6 10X Buffer

| | |
|---|---|
| Tris HCl pH 9.0 | 100 ml |
| KCL | 500 mM |
| Triton X-100 | 1% |

### 2.7 2mM dNTP (dATP, dCTP, dGTP, dTTP mix)

| | |
|---|---|
| dATP | 100 mM |
| dCTP | 100 mM |
| dGTP | 100 mM |
| dTTP | 100 mM |

Mixed equal volume of each dNTP to get 25 mM dNTP, then dilute to 2 mM dNTP with sterile double distilled water.

# APPENDIX B
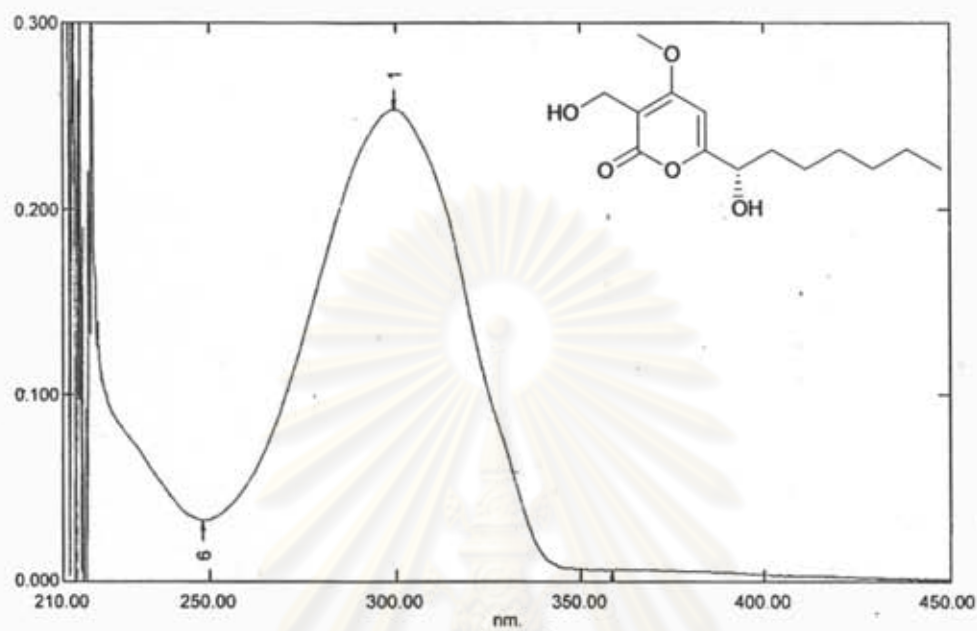


Figure L1　UV spectrum of dothideopyrone A (**1**)
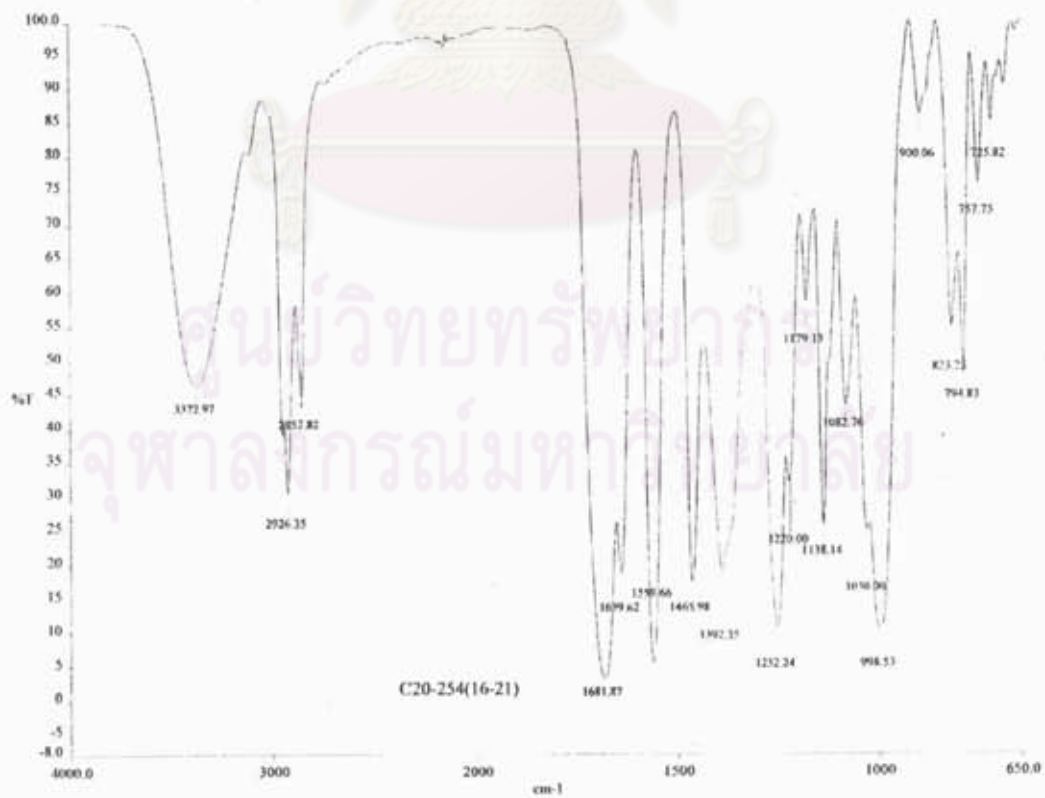


Figure L2　IR spectrum of dothideopyrone A (**1**)
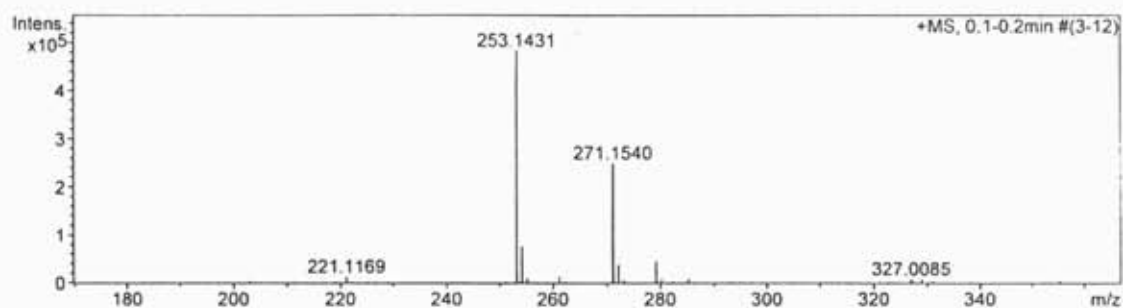
Figure L3   ESI-TOF spectrum of dothideopyrone A (1)
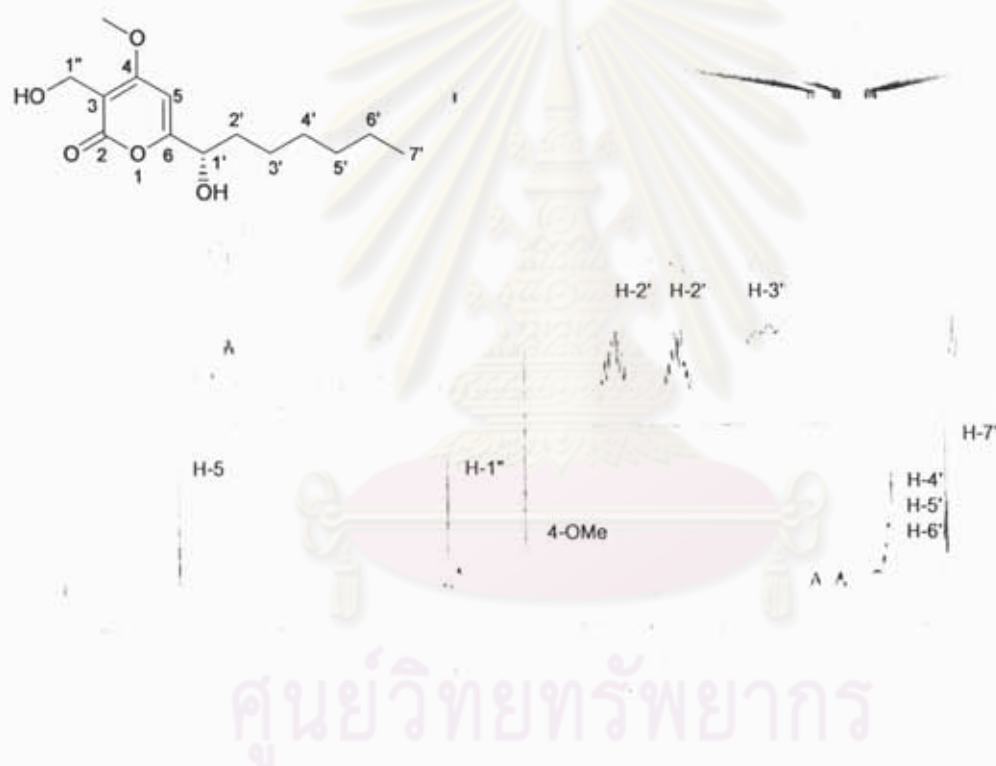


Figure L4   500 MHz $^1$H NMR (CDCl$_3$) spectrum of dothideopyrone A (1)
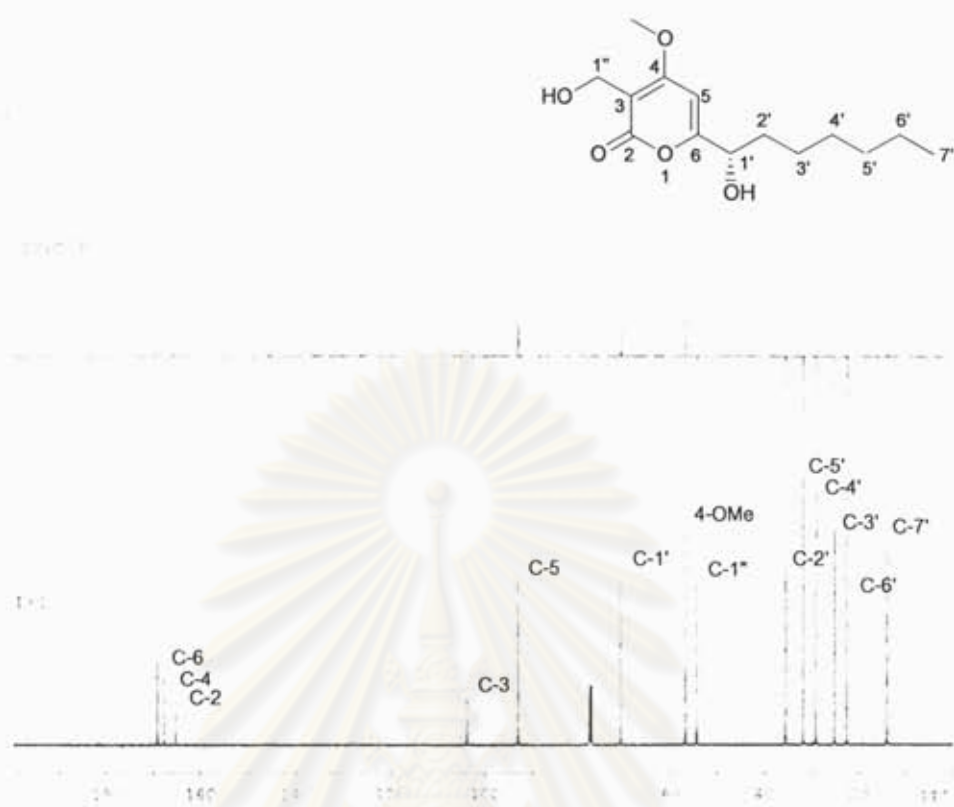
**Figure L5** $^{13}$C NMR (CDCl$_3$) and DEPT spectra of dothideopyrone A (1)



**Figure L6** HMQC spectrum of dothideopyrone A (1)
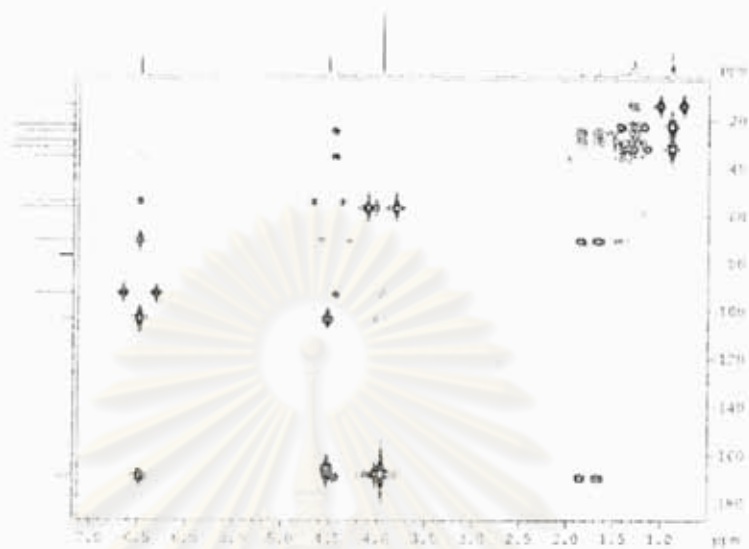
Figure L7    HMBC spectrum of dothideopyrone A (1)
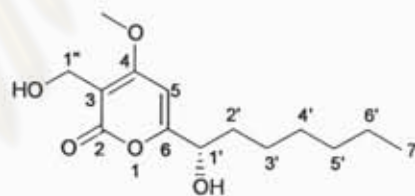


Figure L8    Expansion of Figure L7
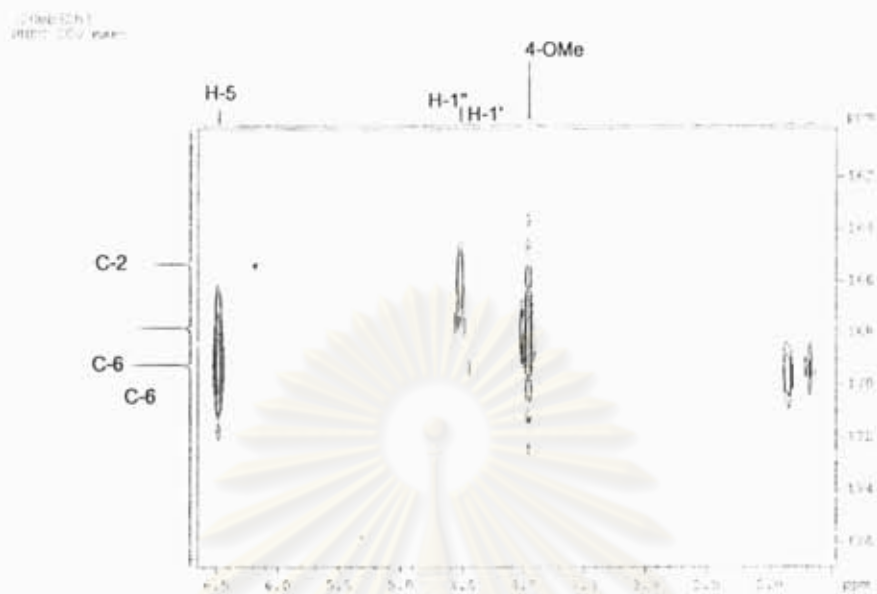
**Figure L9** Expansion of Figure L7



**Figure L10** $^1$H-$^1$H COSY spectrum of dothideopyrone A (1)
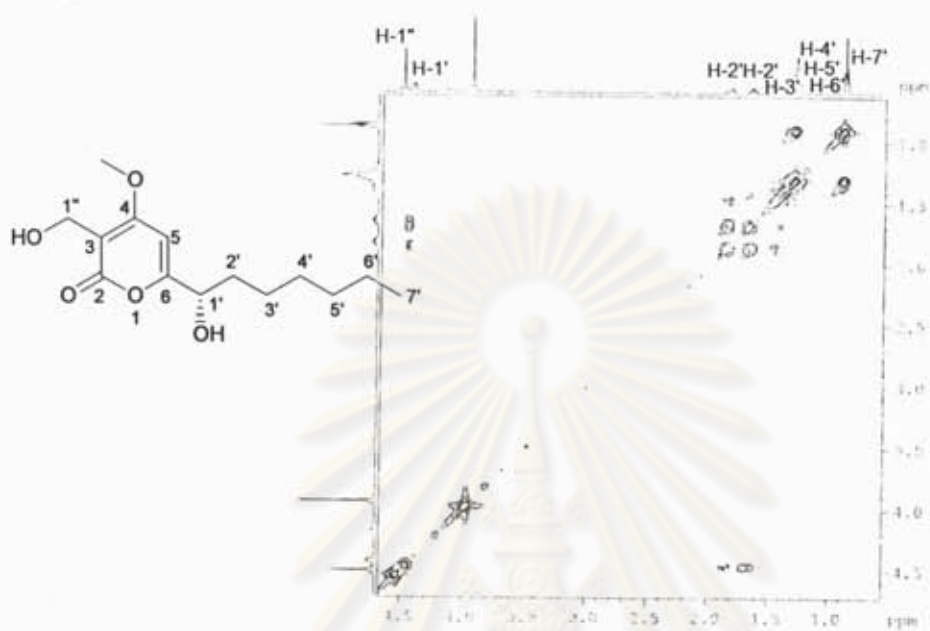
Figure L11    Expansion of Figure L10
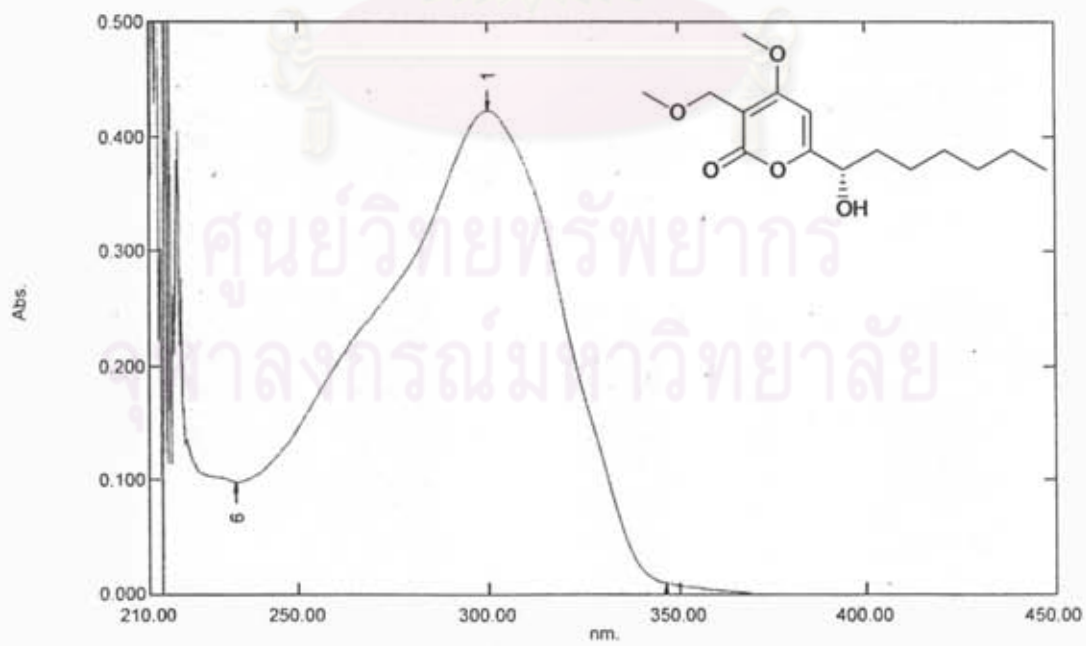


Figure L12    UV spectrum of dothideopyrone B (3)
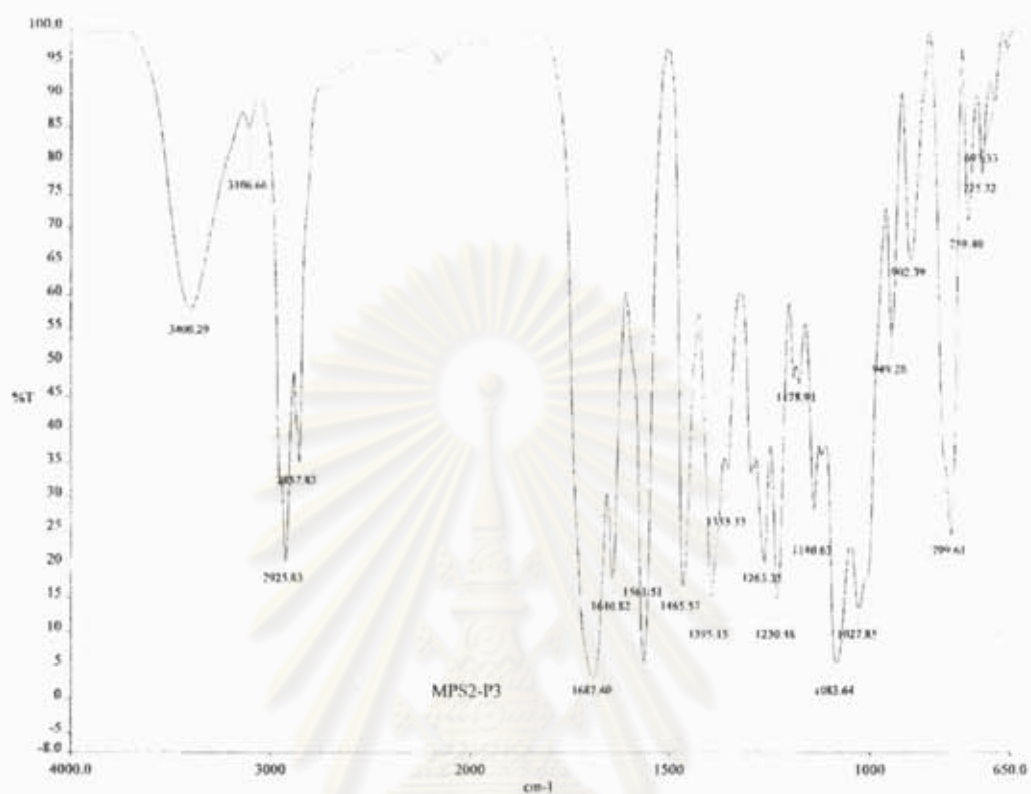
**Figure L13**   IR spectrum of dothideopyrone B (3)
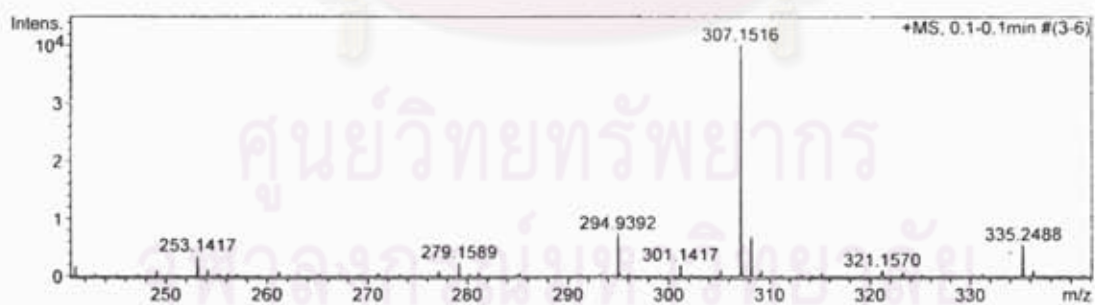


**Figure L14**   ESI-TOF spectrum of dothideopyrone B (3)
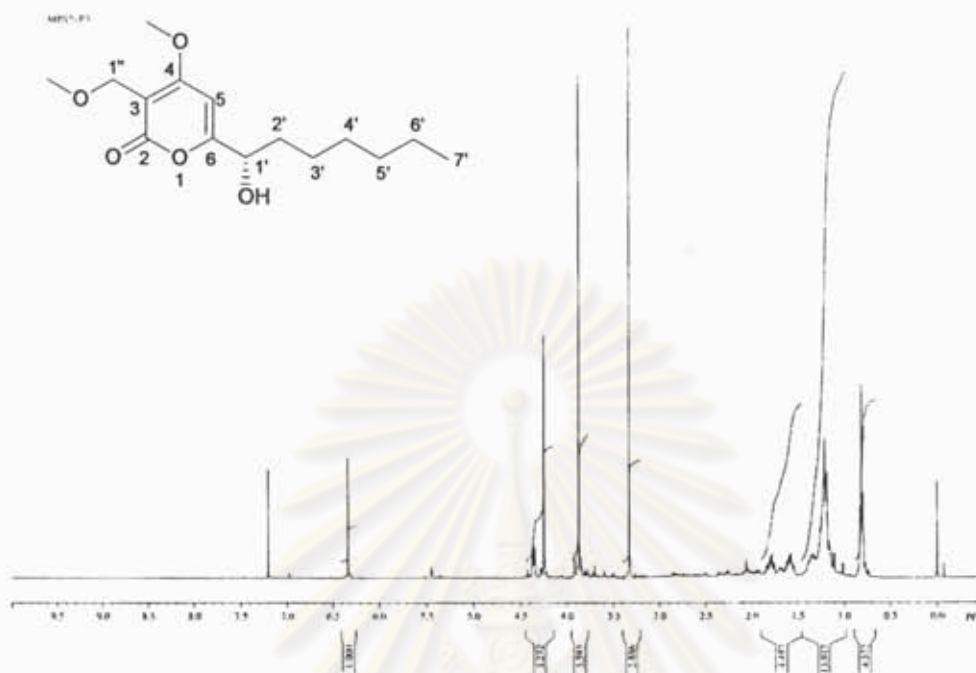
**Figure L15** 400 MHz $^1$H NMR (CDCl$_3$) spectrum of dothideopyrone B (3)
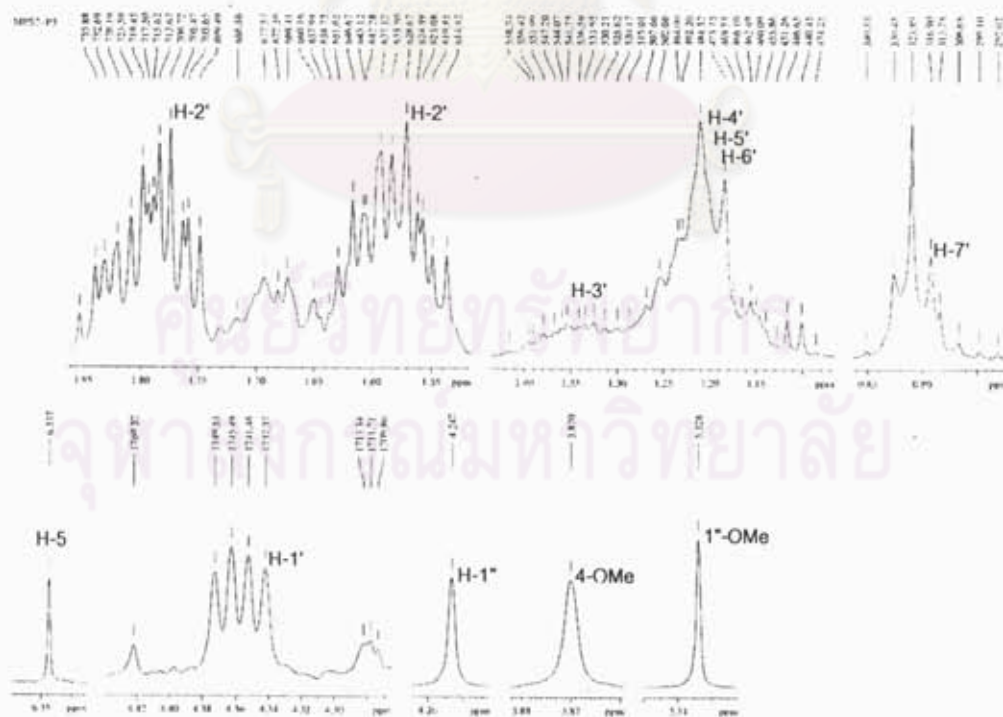


**Figure L16** Expansion of Figure L15
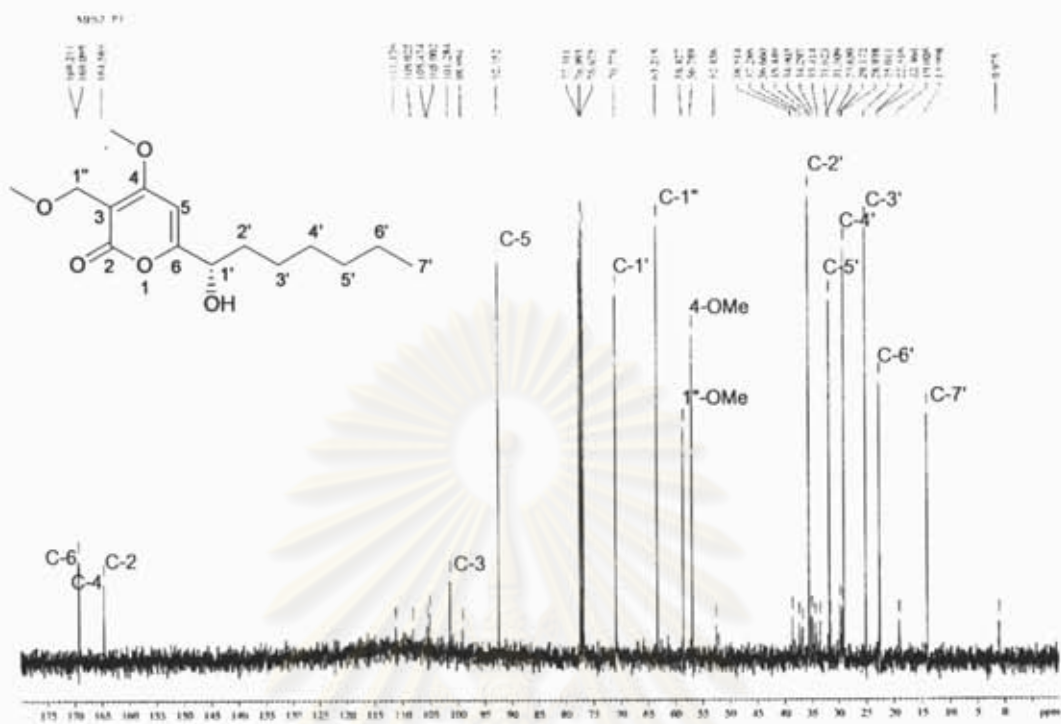
Figure L17   $^{13}$C NMR (CDCl$_3$) spectrum of dothideopyrone B (3)
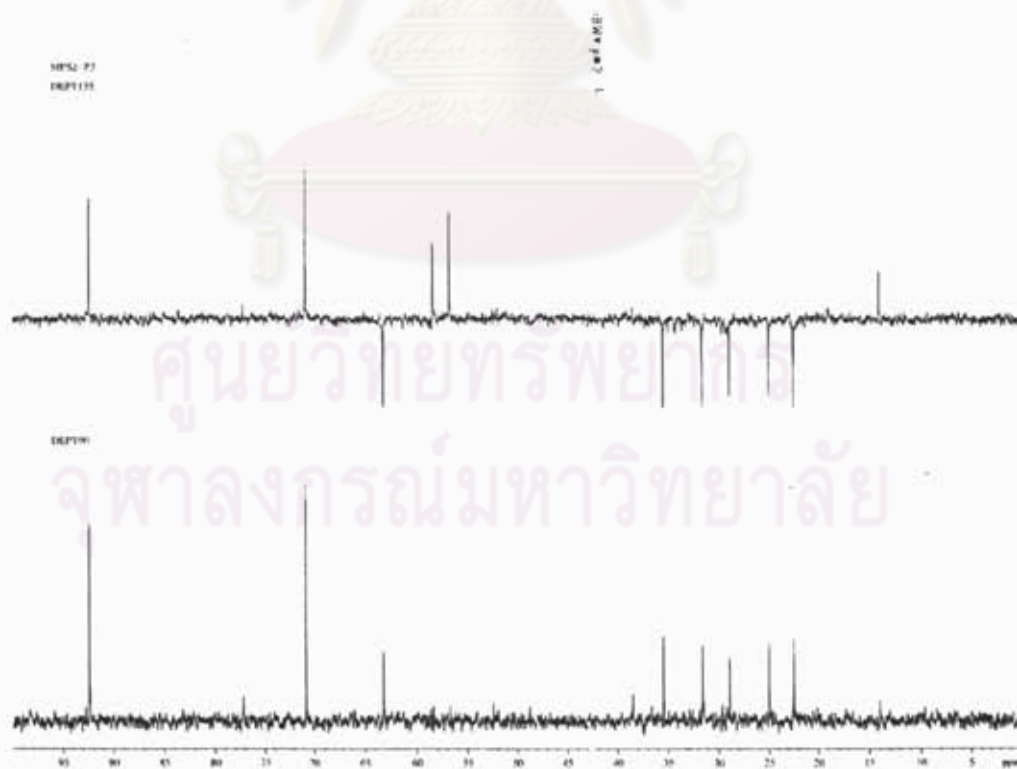


Figure L18   DEPT spectrum of dothideopyrone B (3)
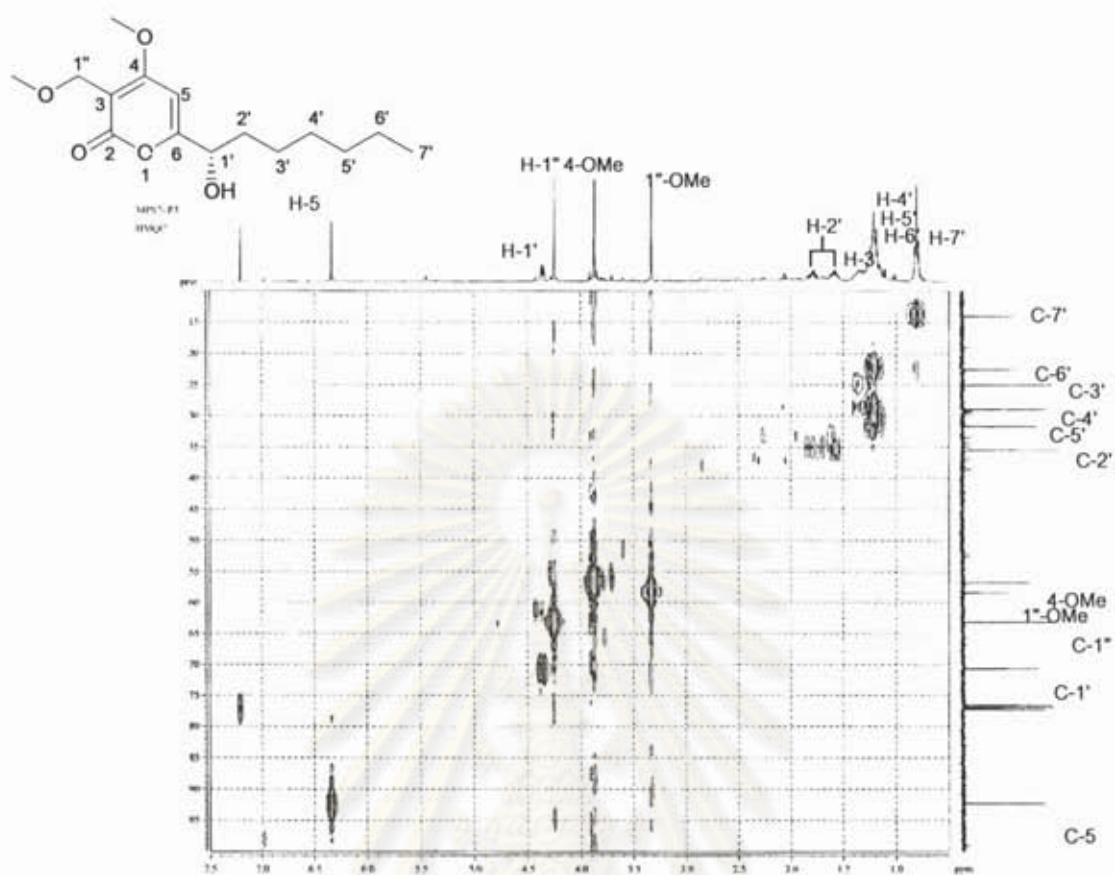
Figure L19    HMQC spectrum of dothideopyrone B (3)
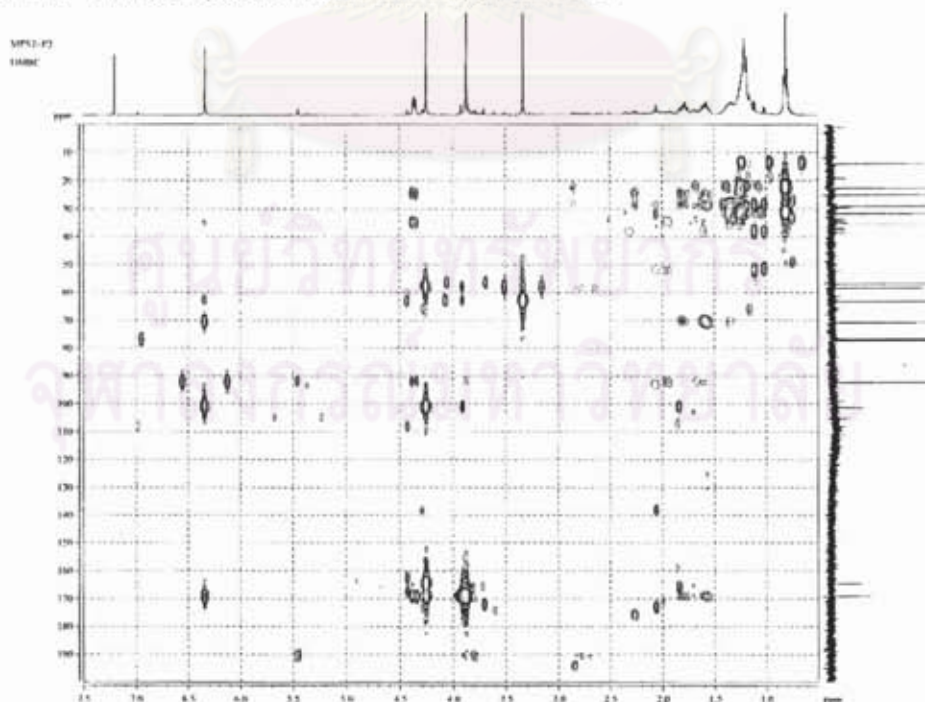


Figure L20    HMBC spectrum of dothideopyrone B (3)
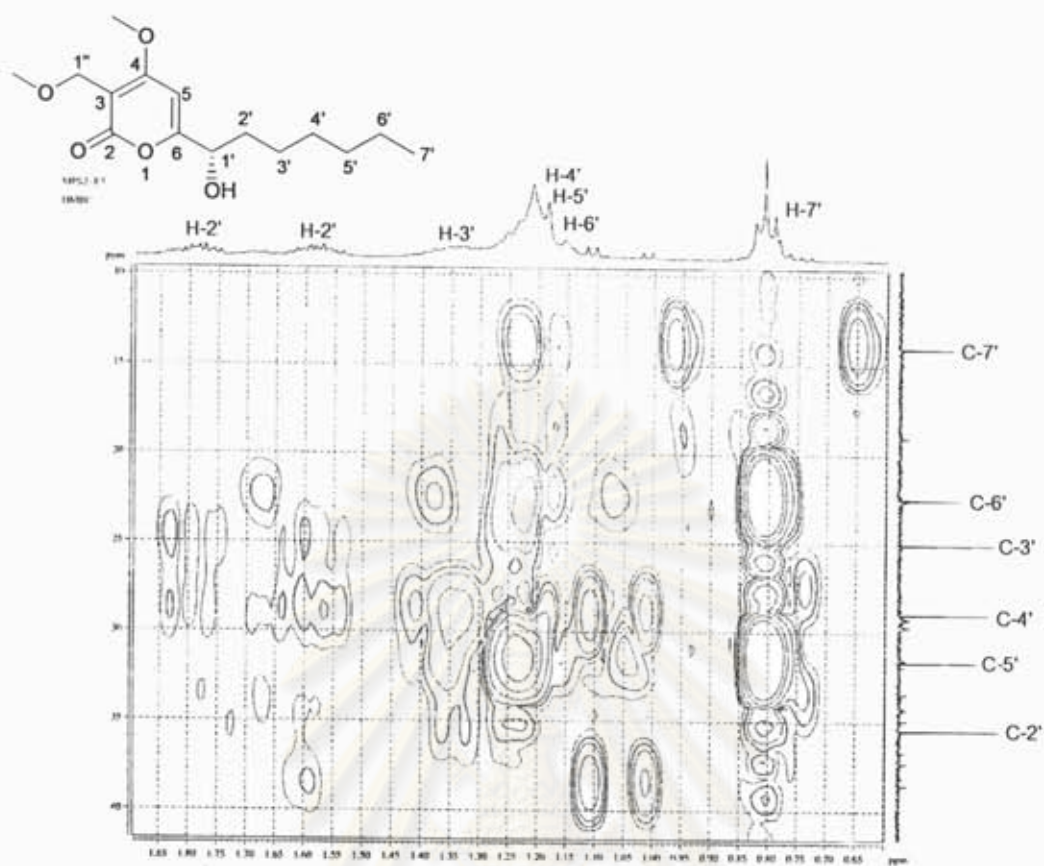
Figure L21  Expansion of Figure L20
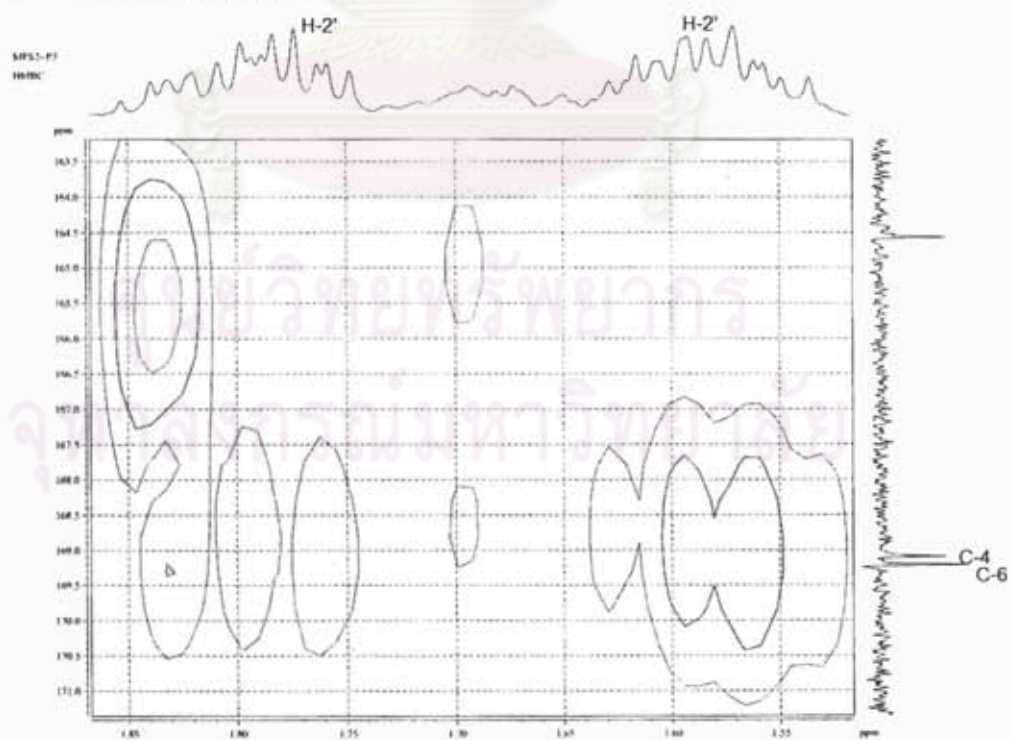


Figure L22  Expansion of Figure L20
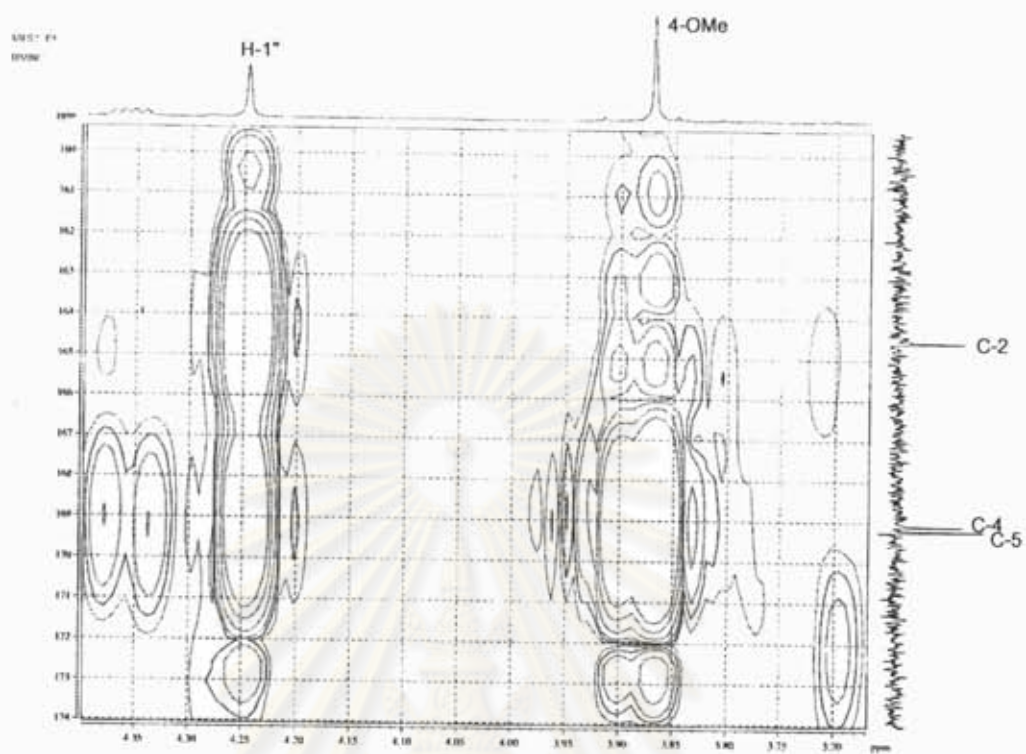
Figure L23    Expansion of Figure L20
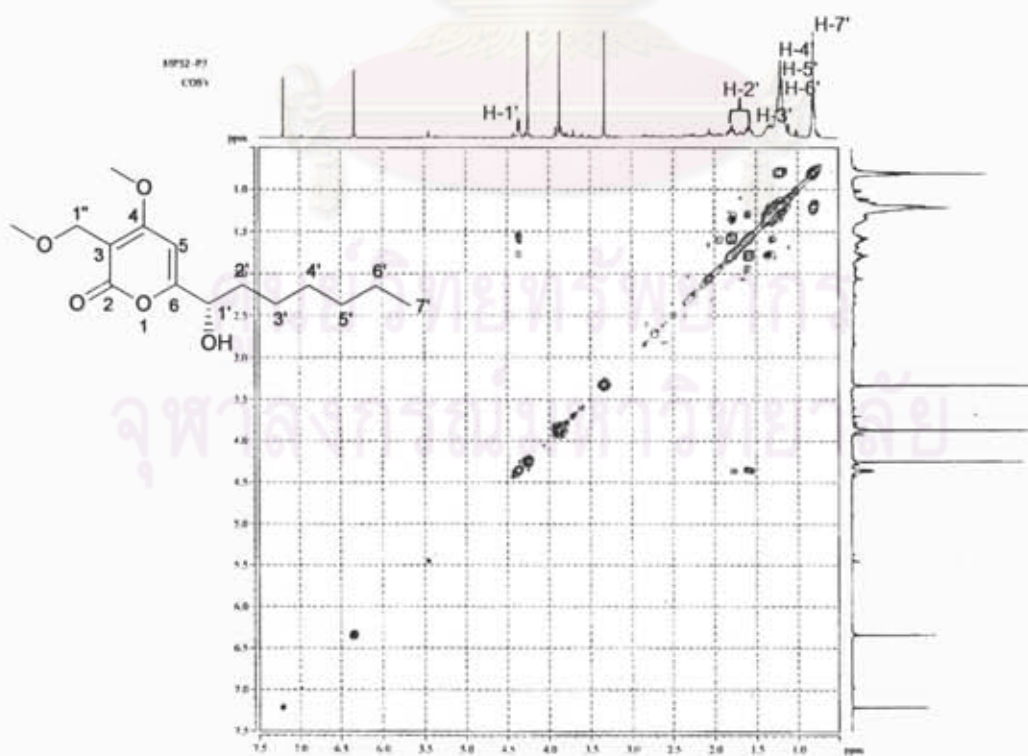


Figure L24    ${}^1$H-${}^1$H COSY spectrum of dothideopyrone B (3)
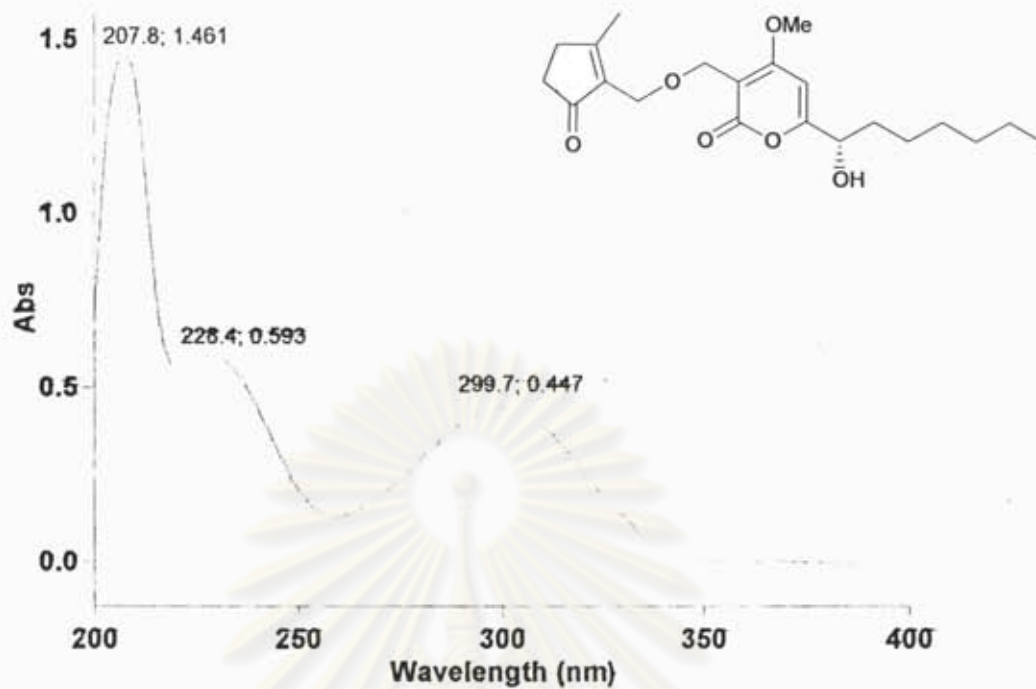
Figure L25    UV spectrum of dothideopyrone C (4)
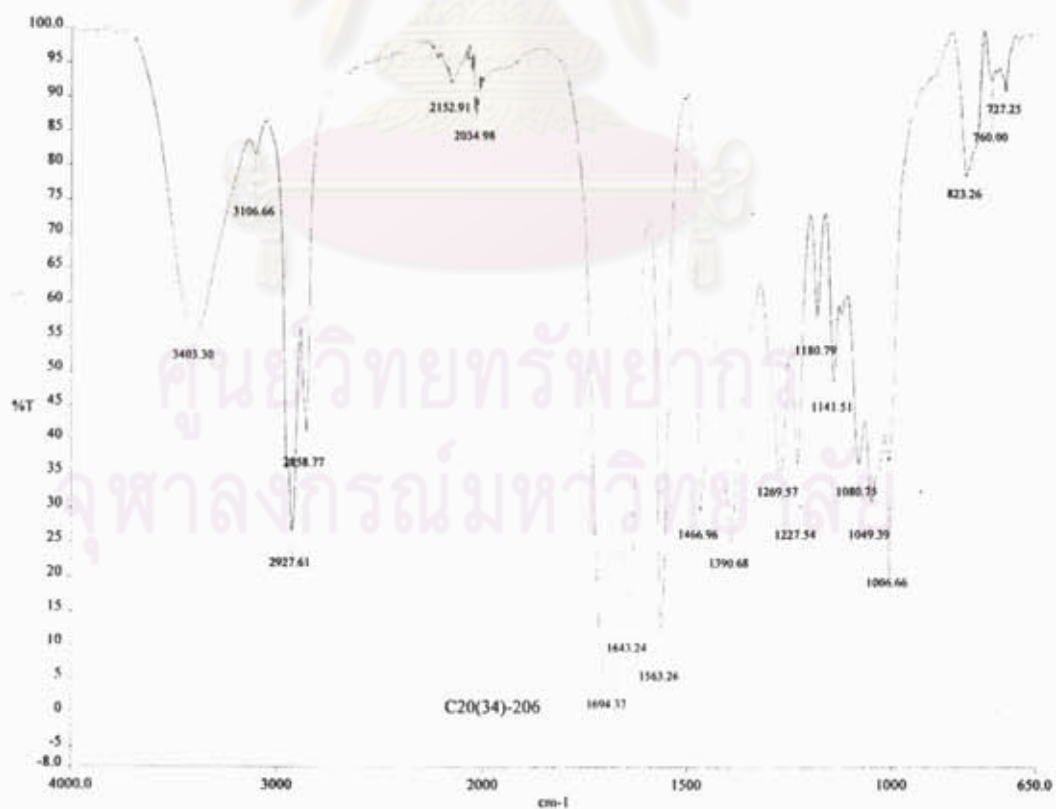


Figure 26    IR spectrum of dothideopyrone C (4)
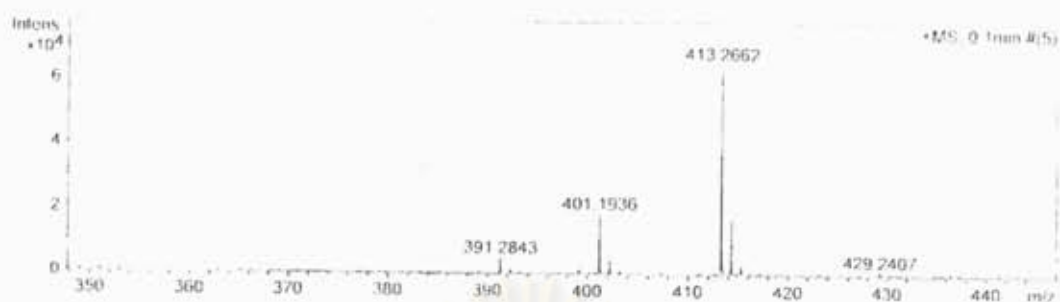
**Figure L27**   ESI-TOF spectrum of dothideopyrone C (4)
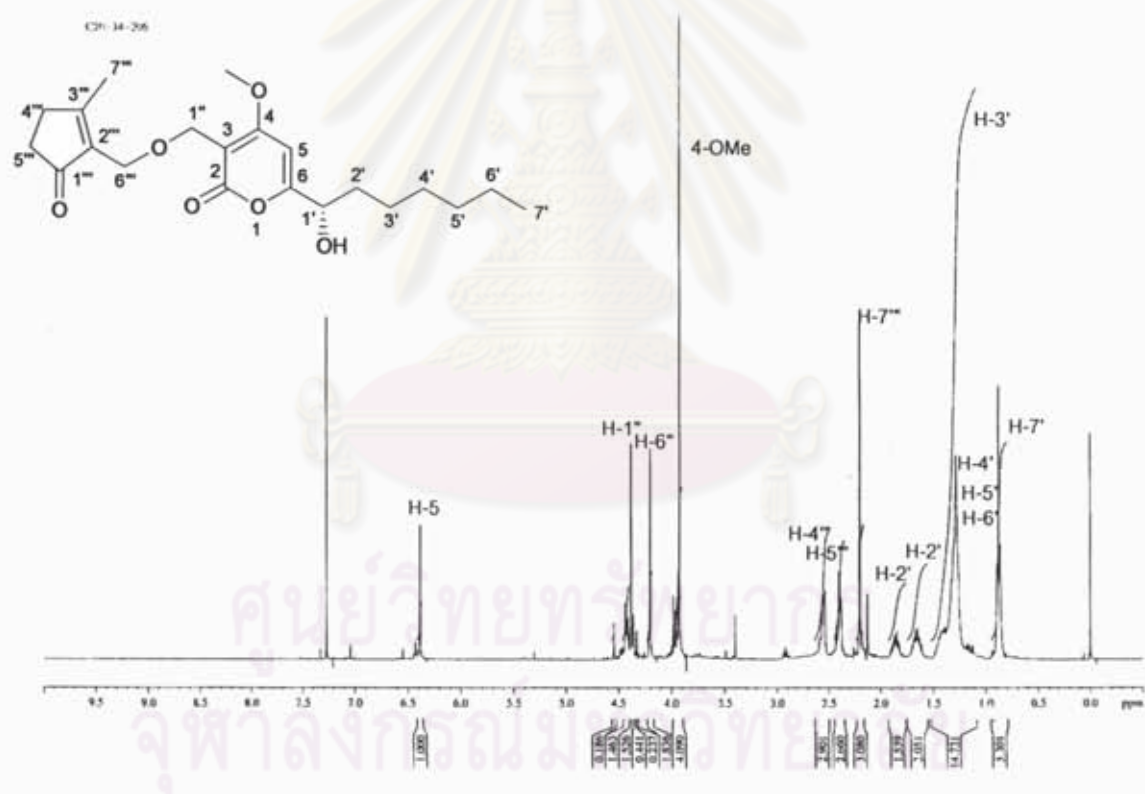


**Figure L28**   400 MHz $^1$H NMR (CDCl$_3$) spectrum of dothideopyrone C (4)
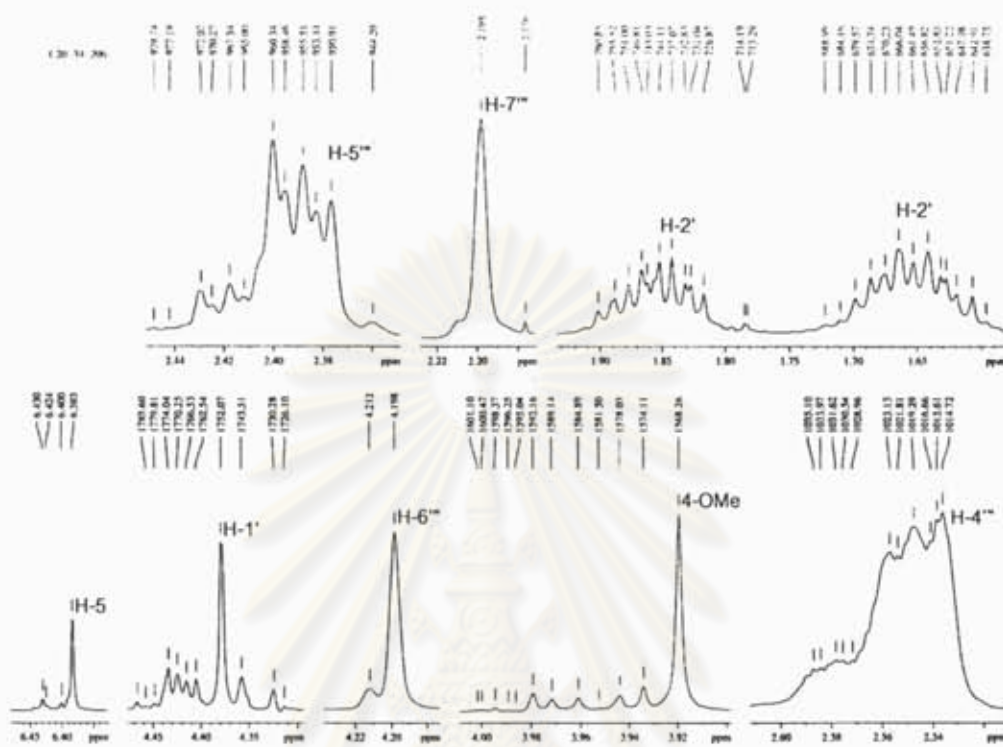
**Figure L29**  Expansion of Figure L28
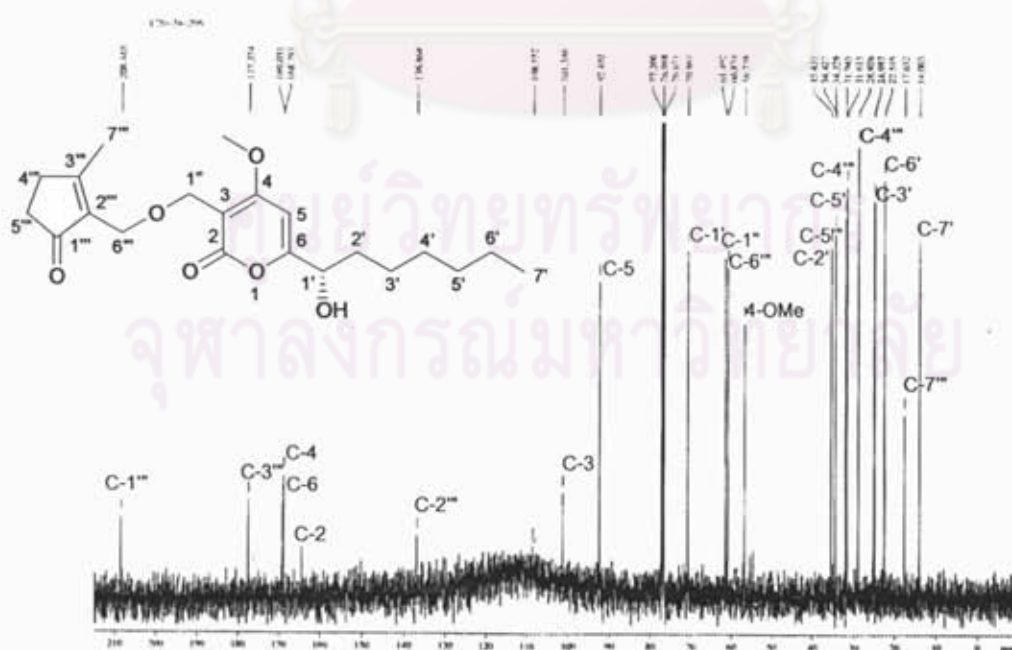


**Figure L30**  $^{13}$C NMR spectrum of dothideopyrone C (4)
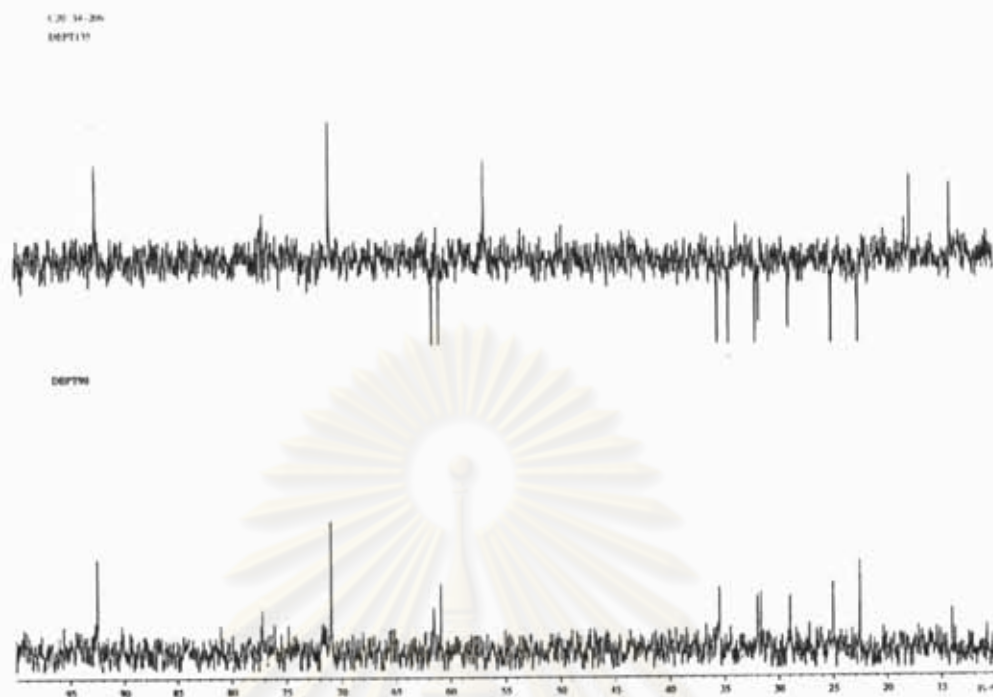
Figure L31　DEPT spectrum of dothideopyrone C (4)
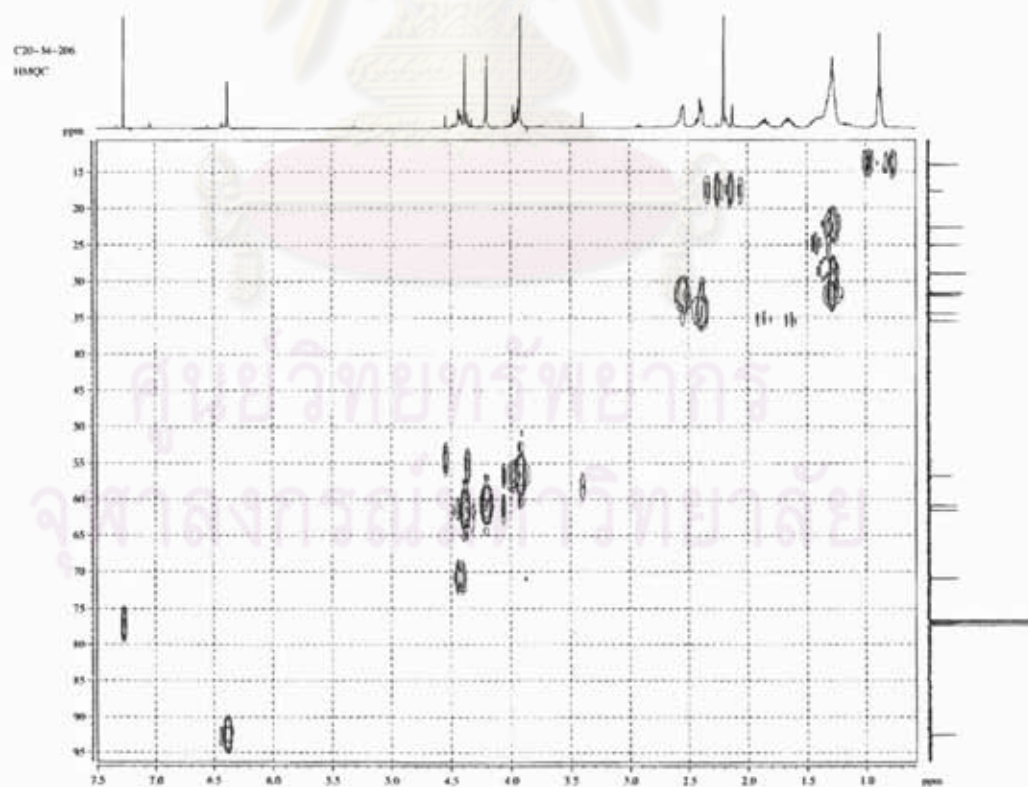


Figure L32　HMQC spectrum of dothideopyrone C (4)
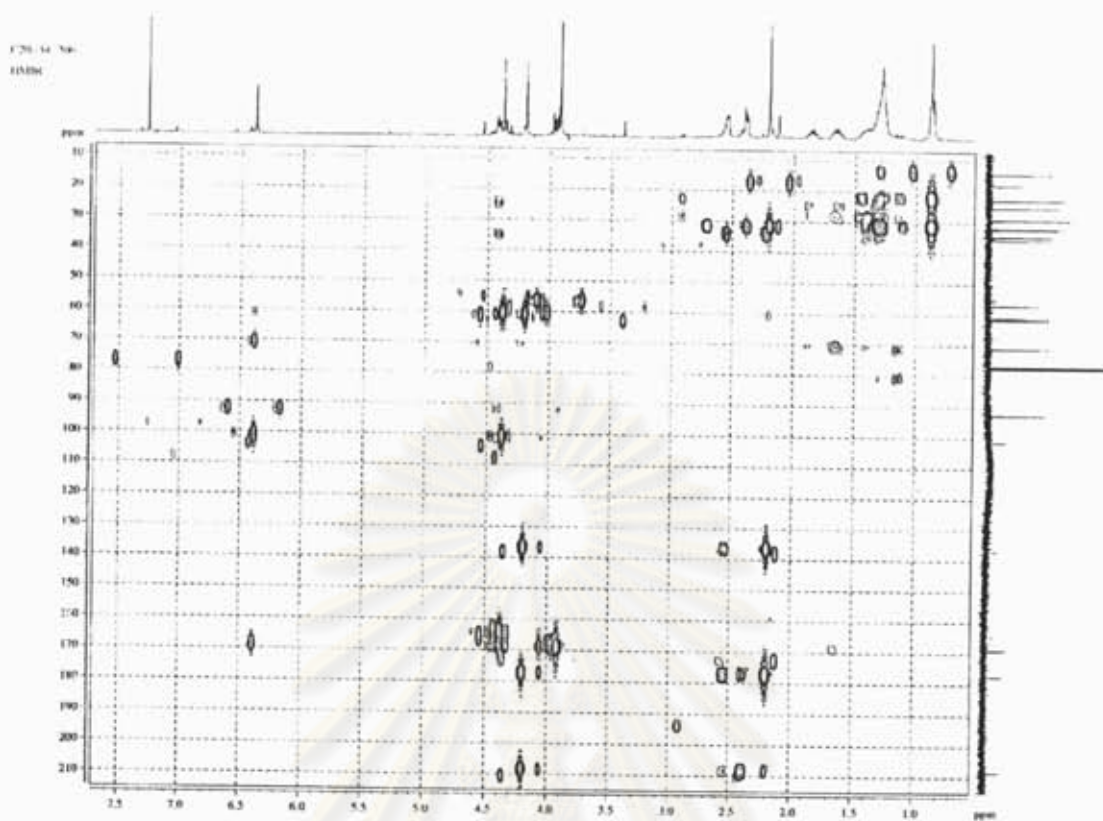
**Figure L33** HMBC spectrum of dothideopyrone C (4)
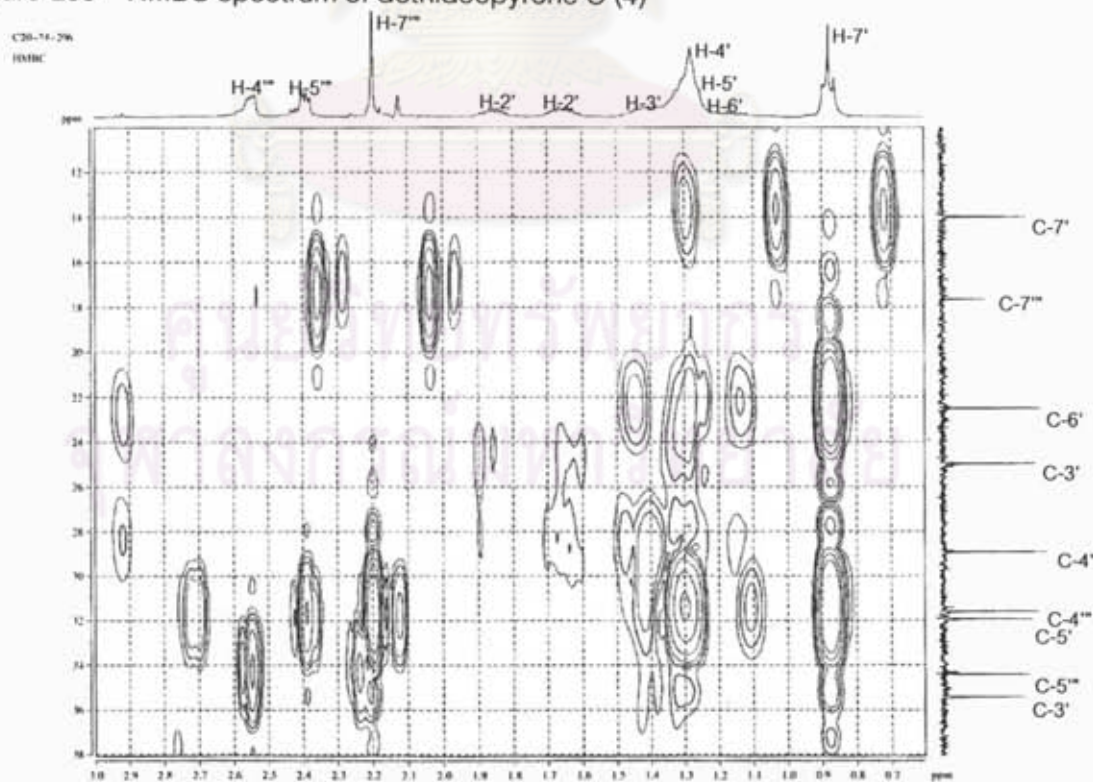


**Figure L34** Expansion of Figure L33
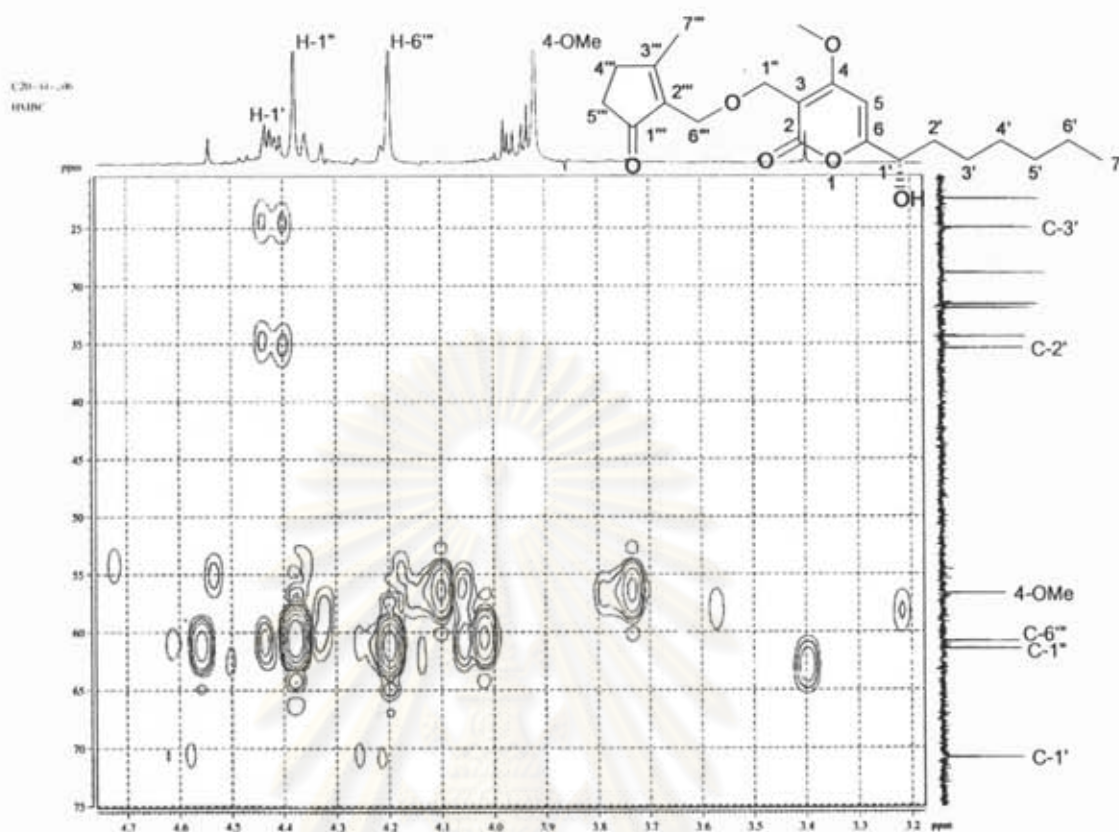
**Figure L35**  Expansion of Figure L33
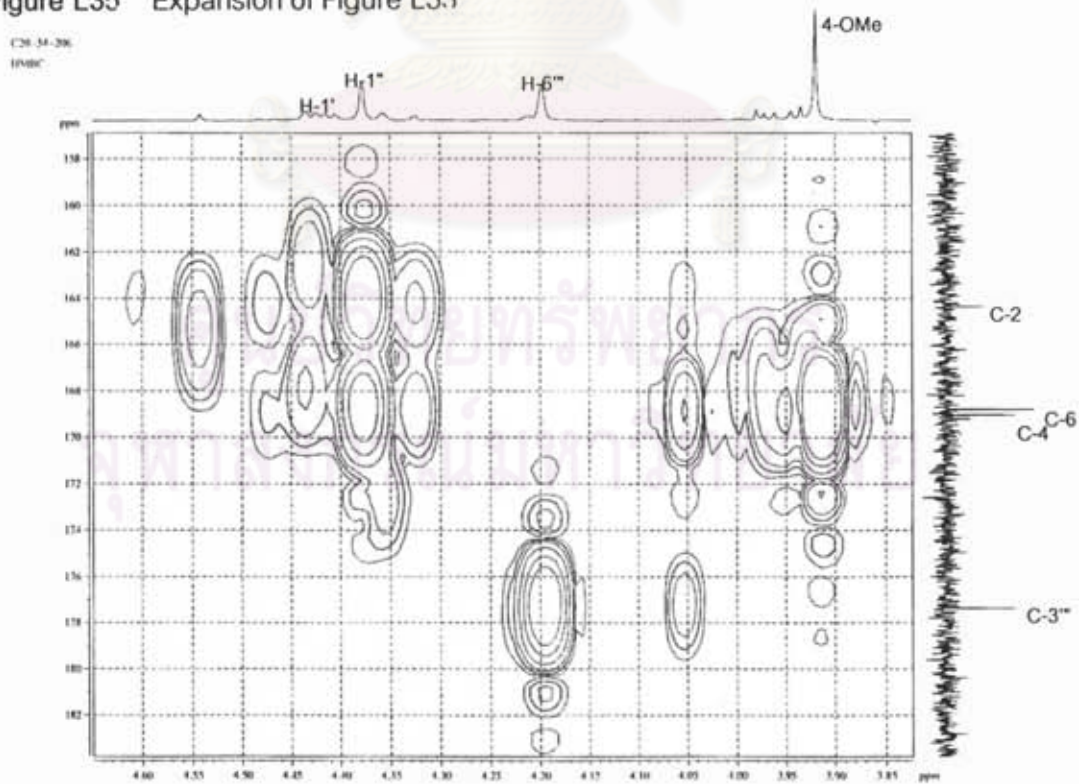


**Figure L36**  Expansion of Figure L33
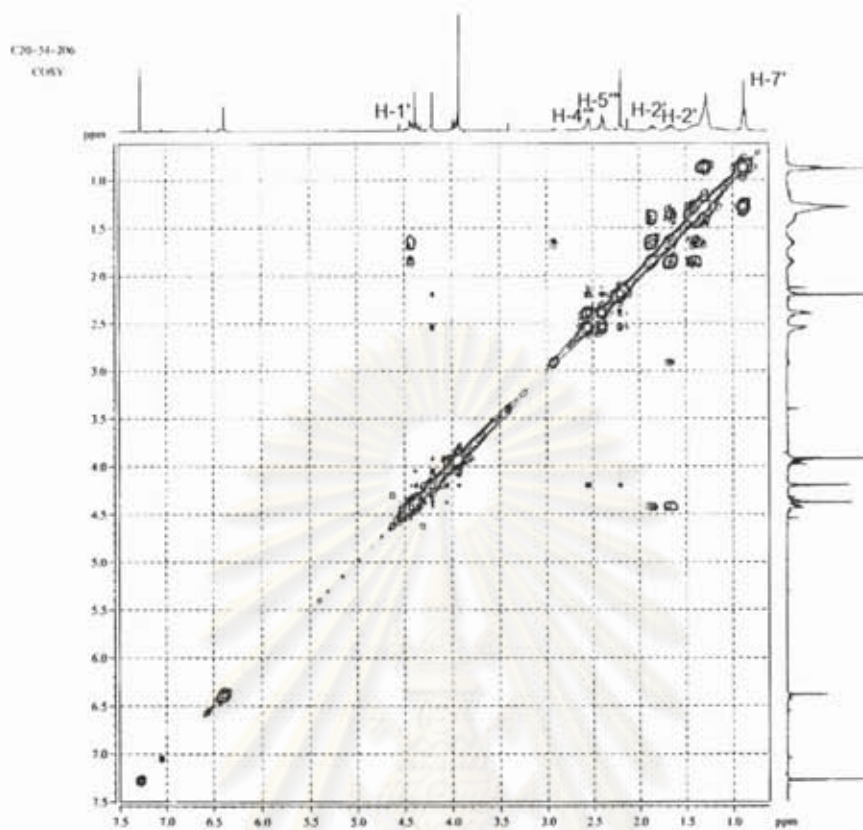
Figure L37    $^1$H-$^1$H COSY spectrum of dothideopyrone C (**4**)
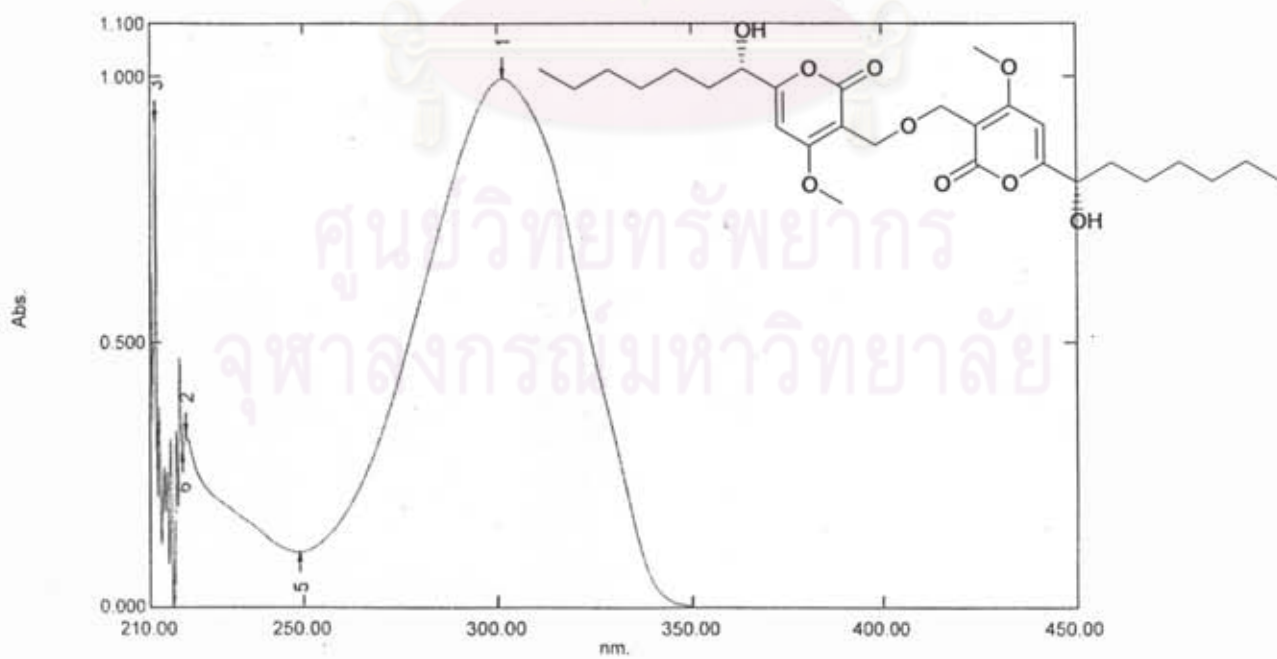


Figure L38    UV spectrum of dothideopyrone D (**5**)
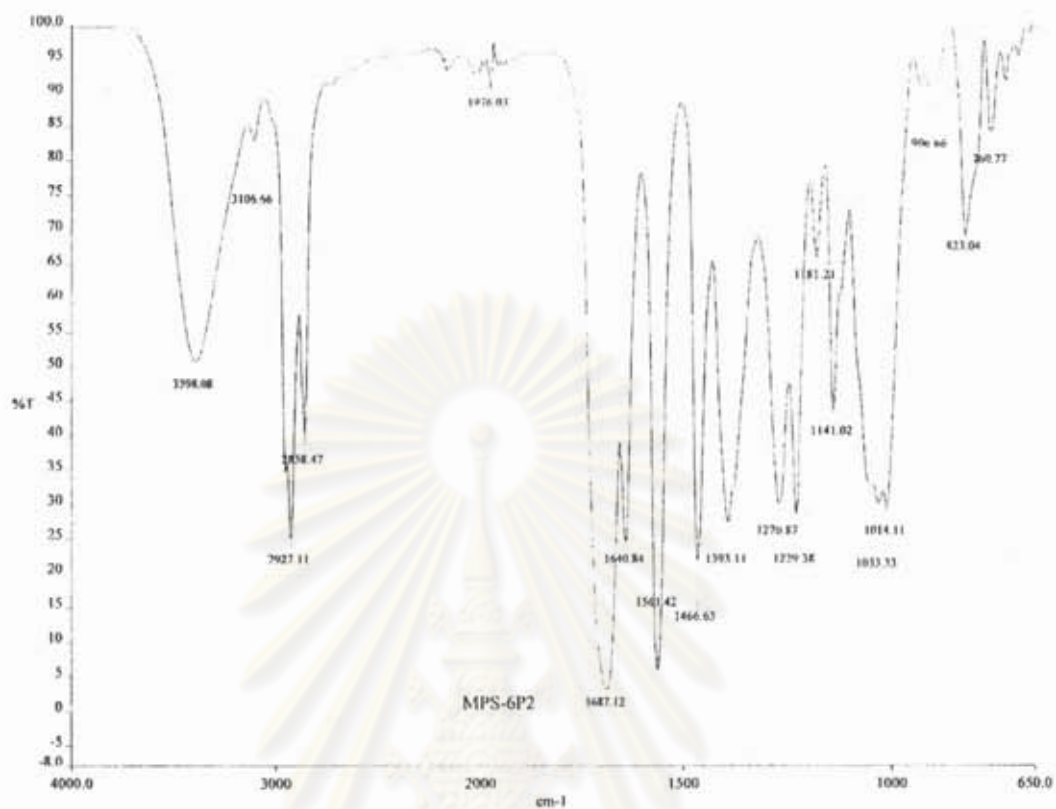
Figure L39    IR spectrum of dothideopyrone D (5)
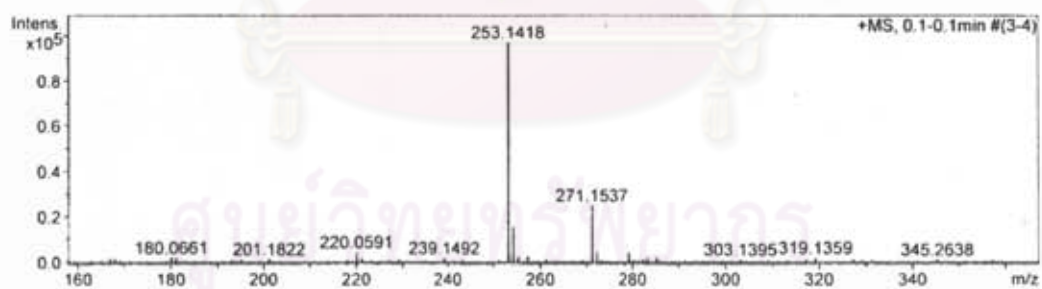


Figure L40    ESI-TOF spectrum of dothideopyrone D (5)
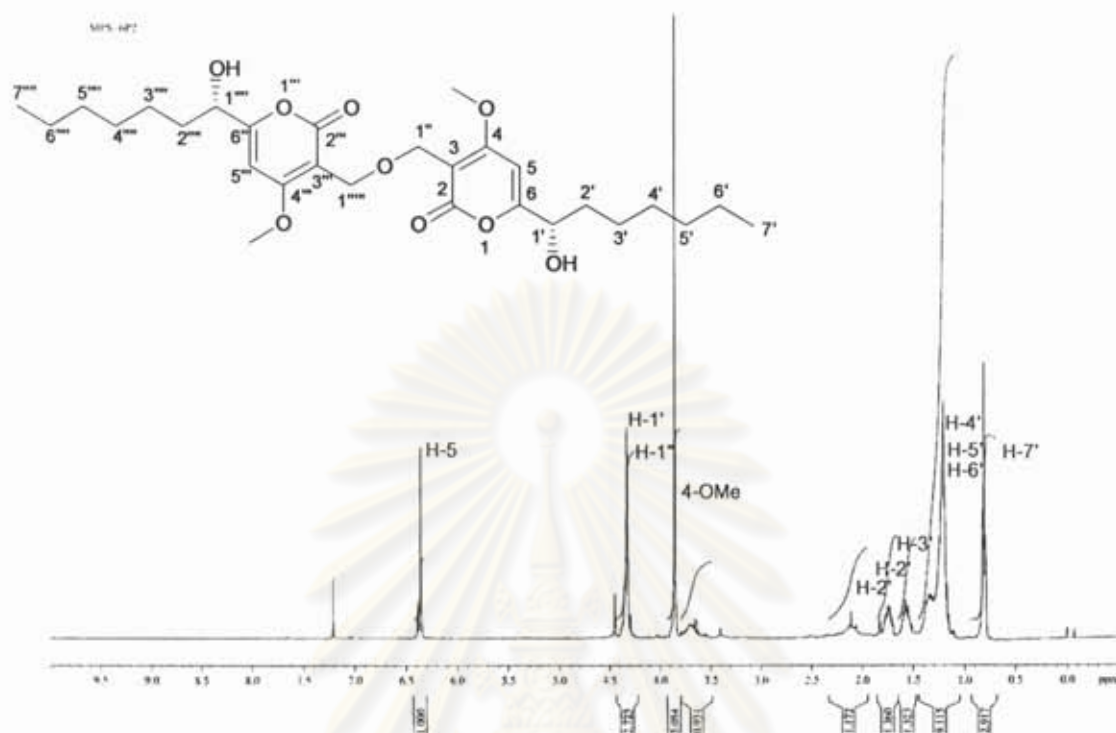
Figure L41    400 MHz $^1$H NMR (CDCl$_3$) spectrum of dothideopyrone D (5)
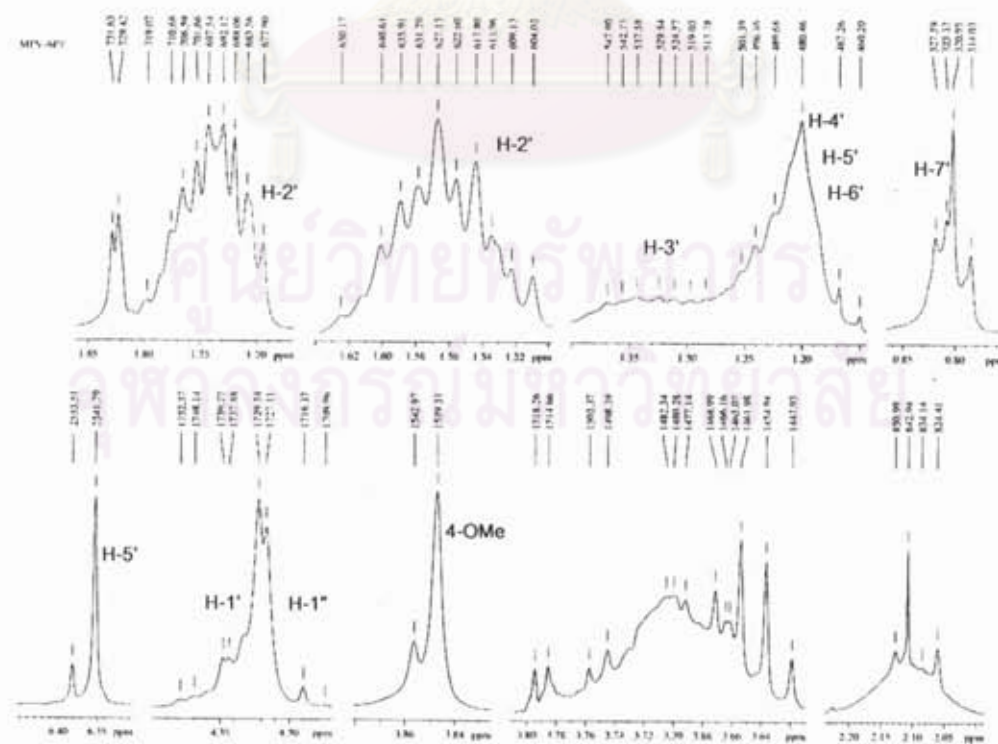


Figure L42    Expansion of Figure L41
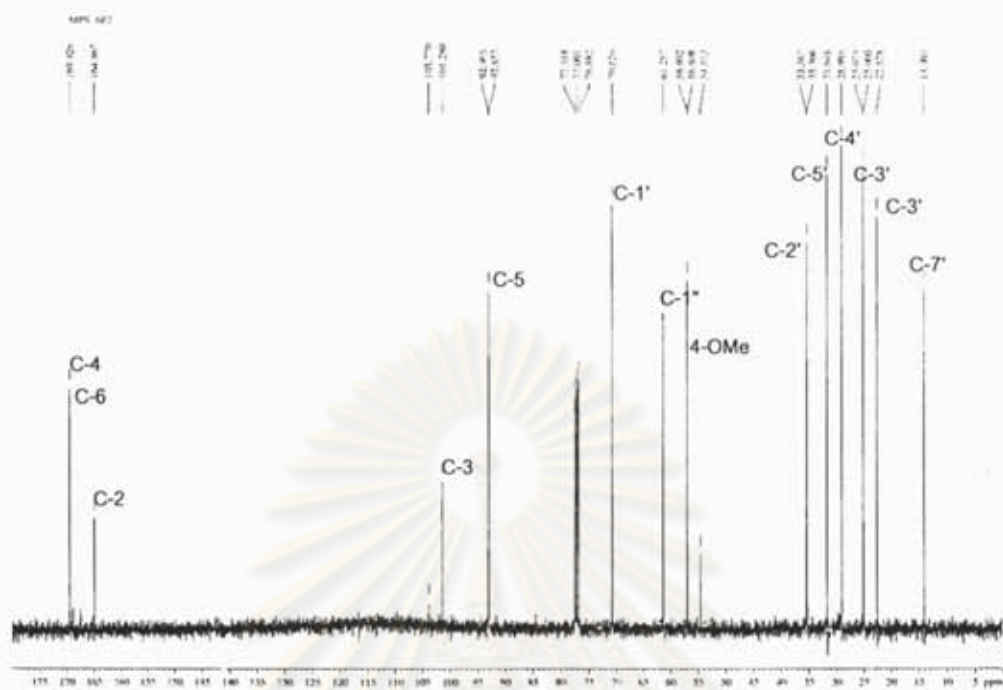
**Figure L43** $^{13}$C NMR (CDCl$_3$) spectrum of dothideopyrone D (5)
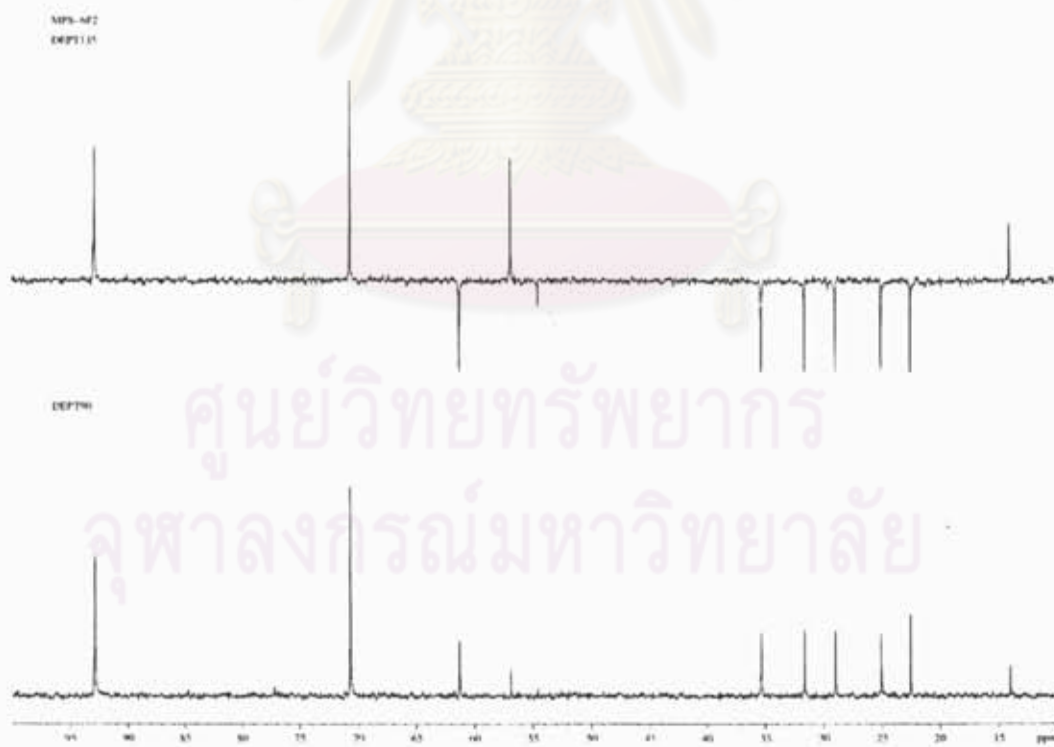


**Figure L44** DEPT spectrum of dothideopyrone D (5)
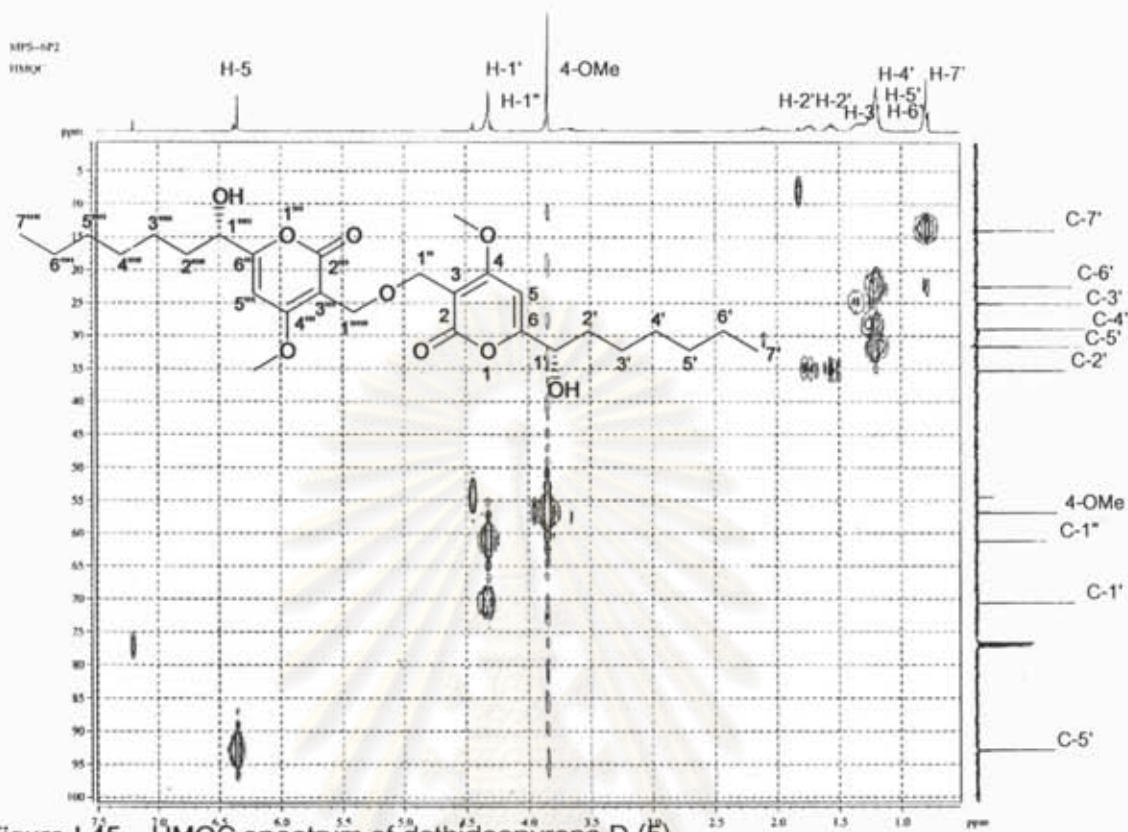
Figure L45  HMQC spectrum of dothideopyrone D (5)
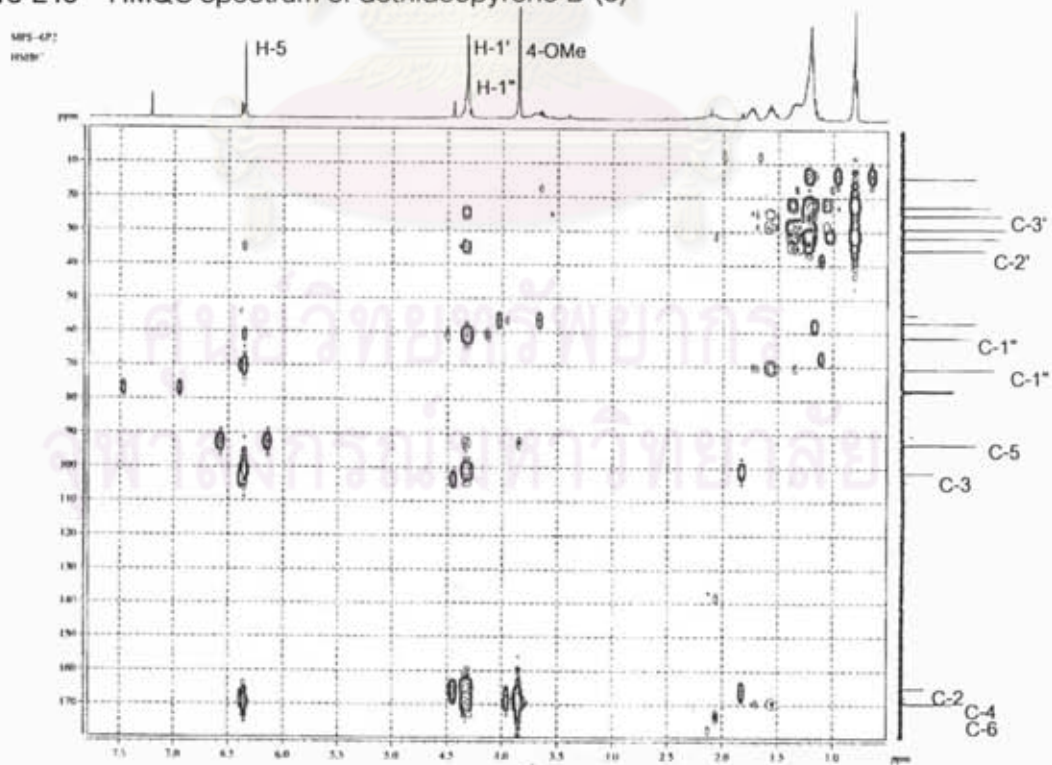


Figure L46  HMBC spectrum of dothideopyrone D (5)
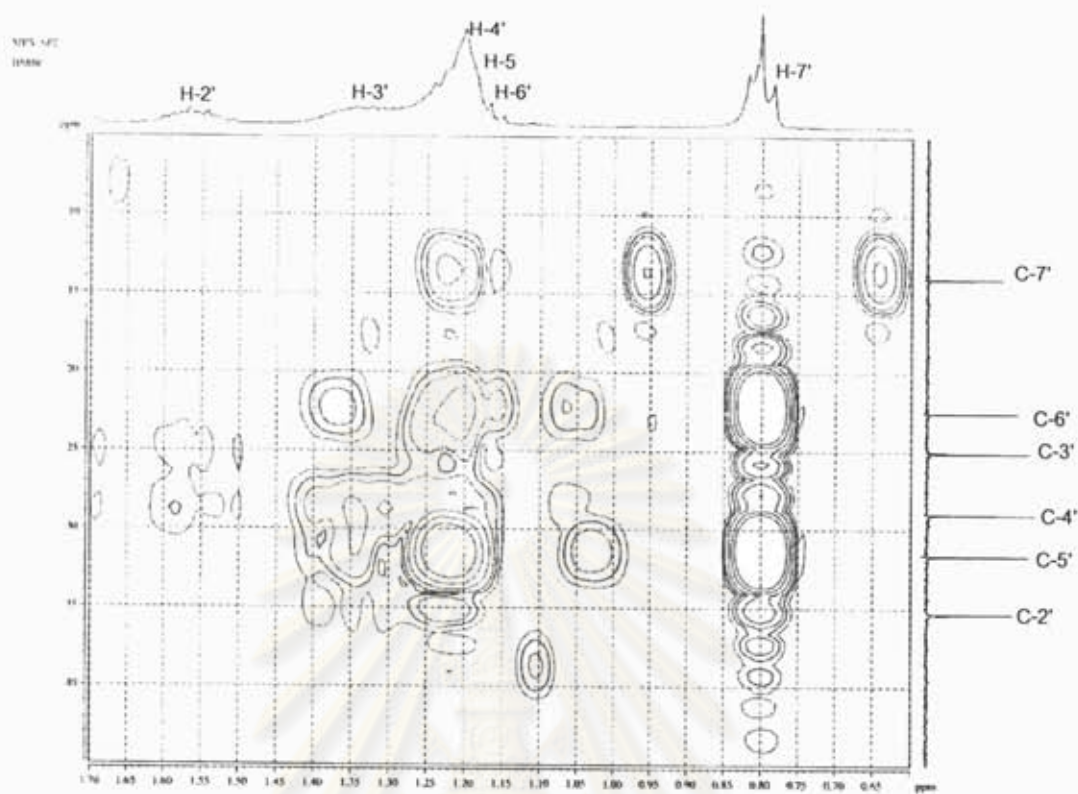
**Figure L47**  Expansion of Figure L46
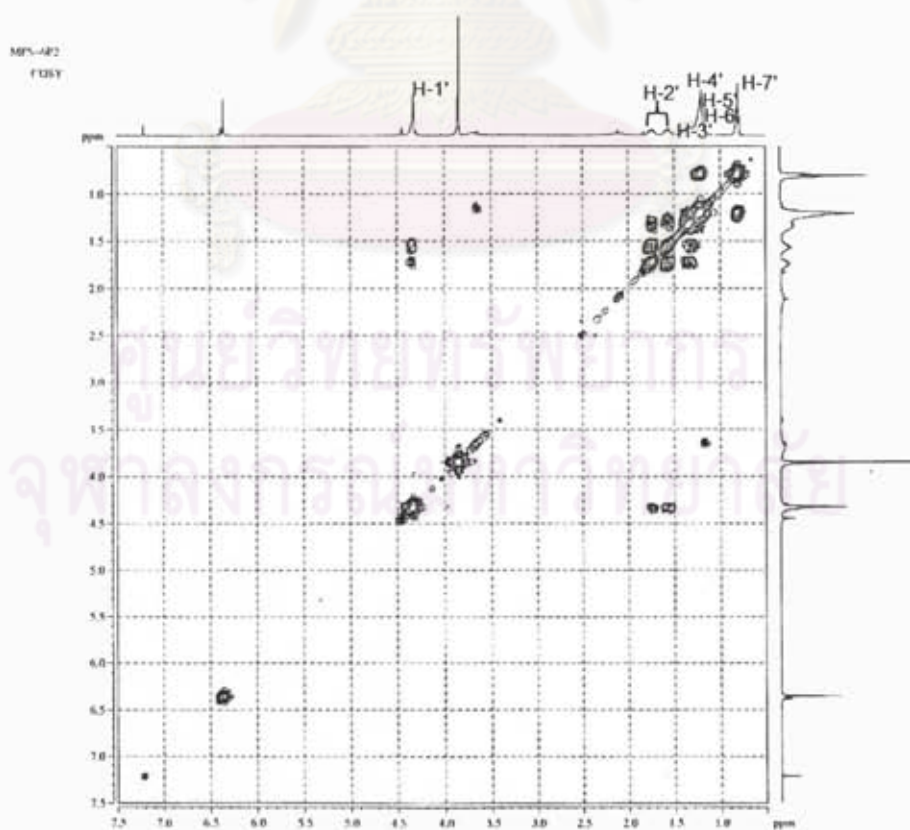


**Figure L48**  $^{1}$H-$^{1}$H COSY spectrum of dothideopyrone D (5)
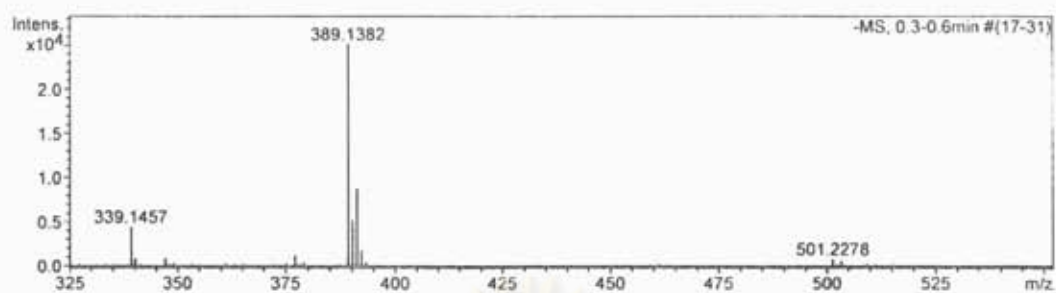
**Figure L49**  The ESI-TOF spectrum of diacetate derivative (2)
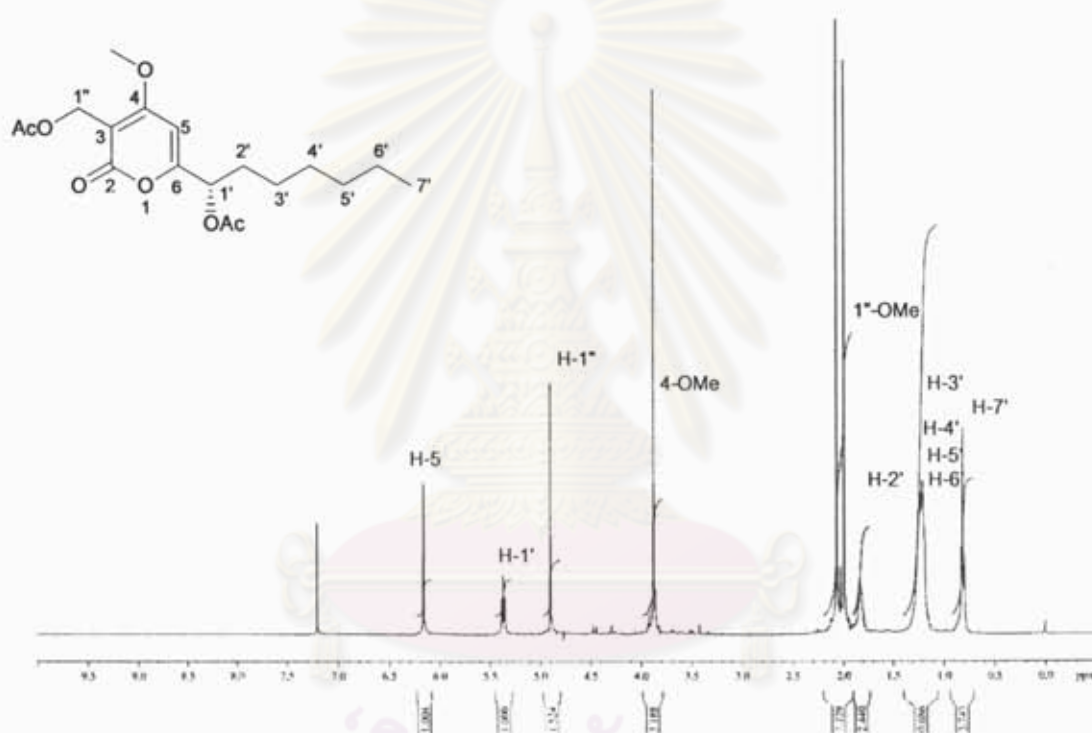


**Figure L50**  400 MHz $^1$H NMR (CDCl$_3$) spectrum of diacetate derivative (2)
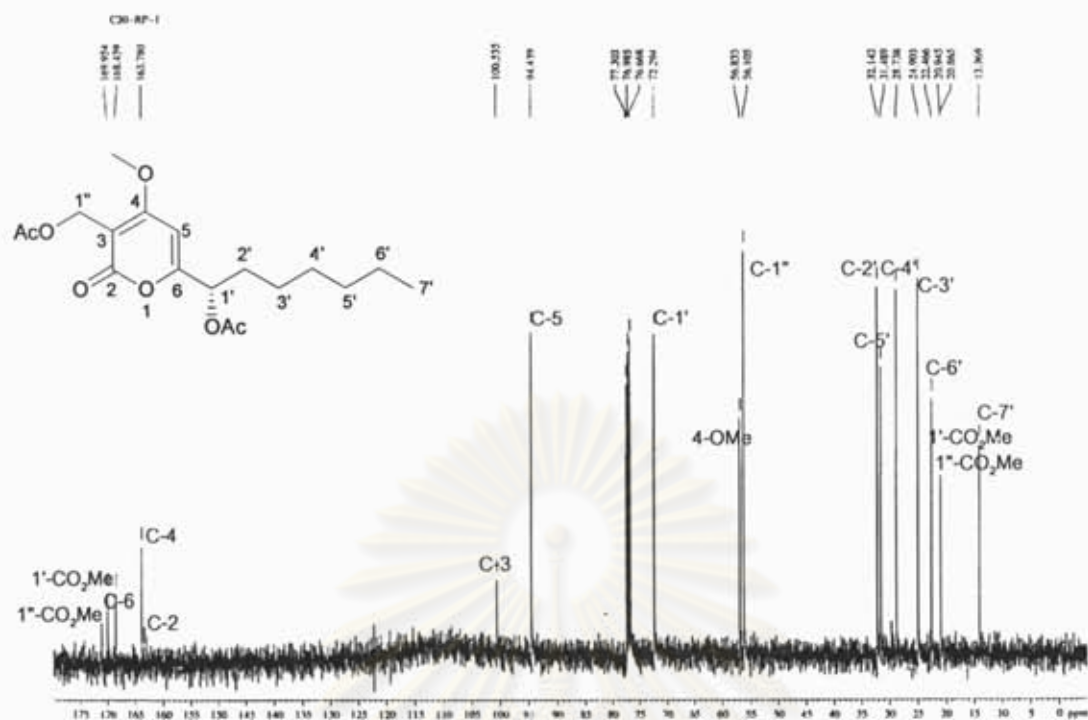
Figure L51    $^{13}$C NMR spectrum of diacetate derivative (2)
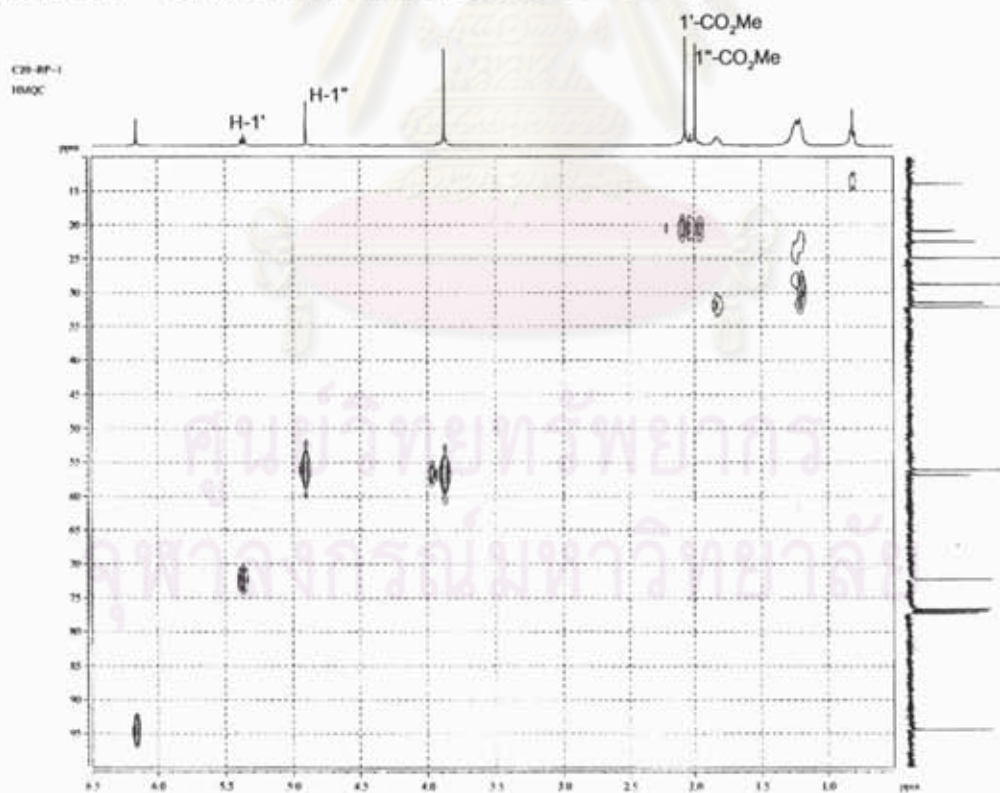


Figure L52    HMQC spectrum of diacetate derivative (2)
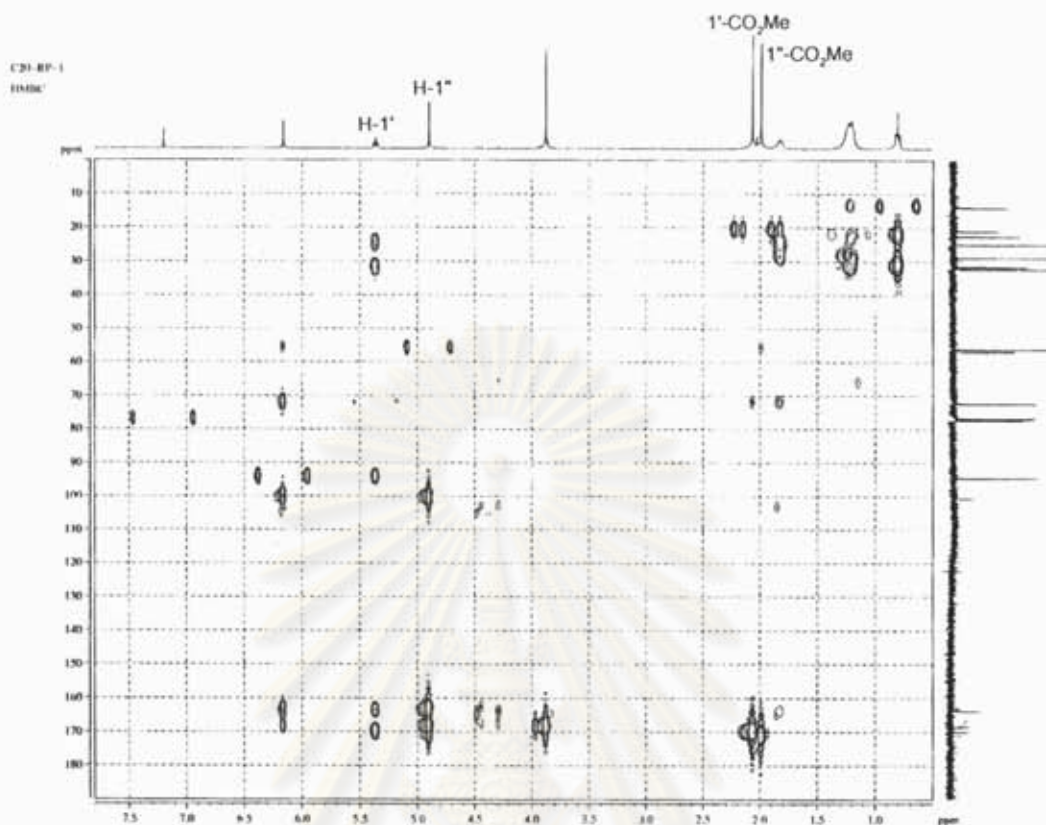
Figure L53  HMBC spectrum of diacetate derivative (2)
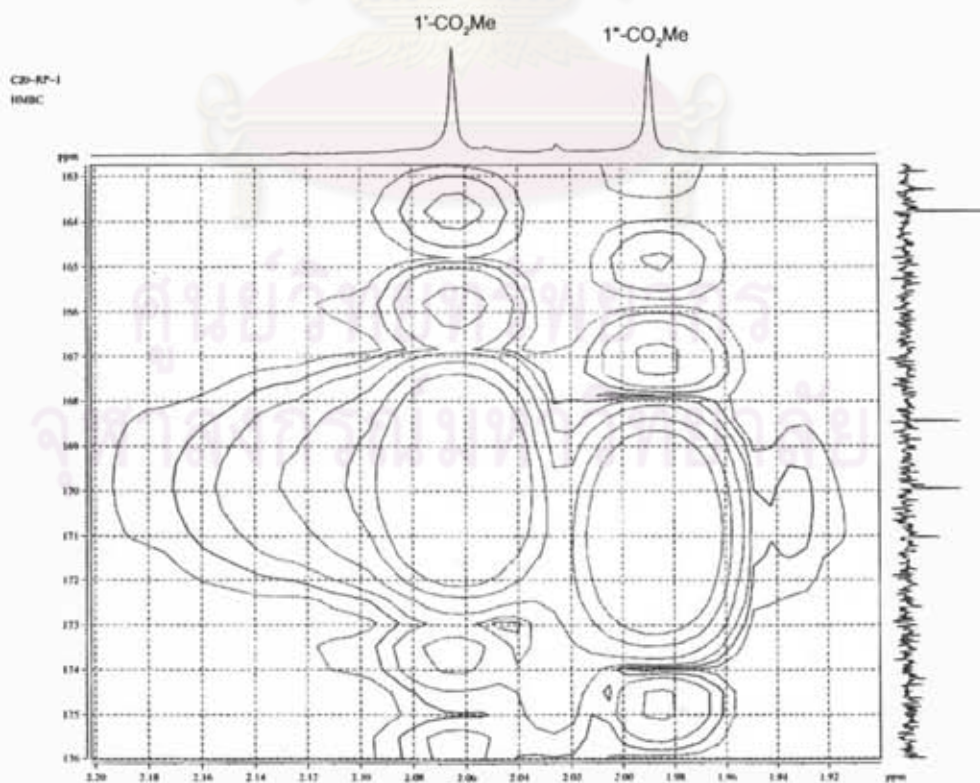


Figure L54  Expansion of Figure L53
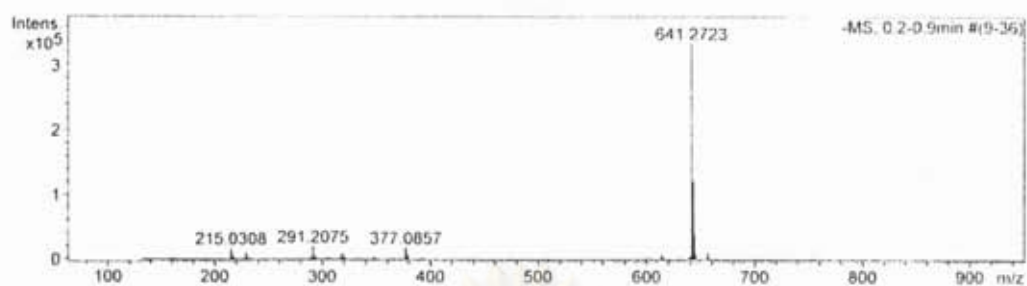
**Figure L55** ESI-TOF spectrum of diacetate derivative (6)
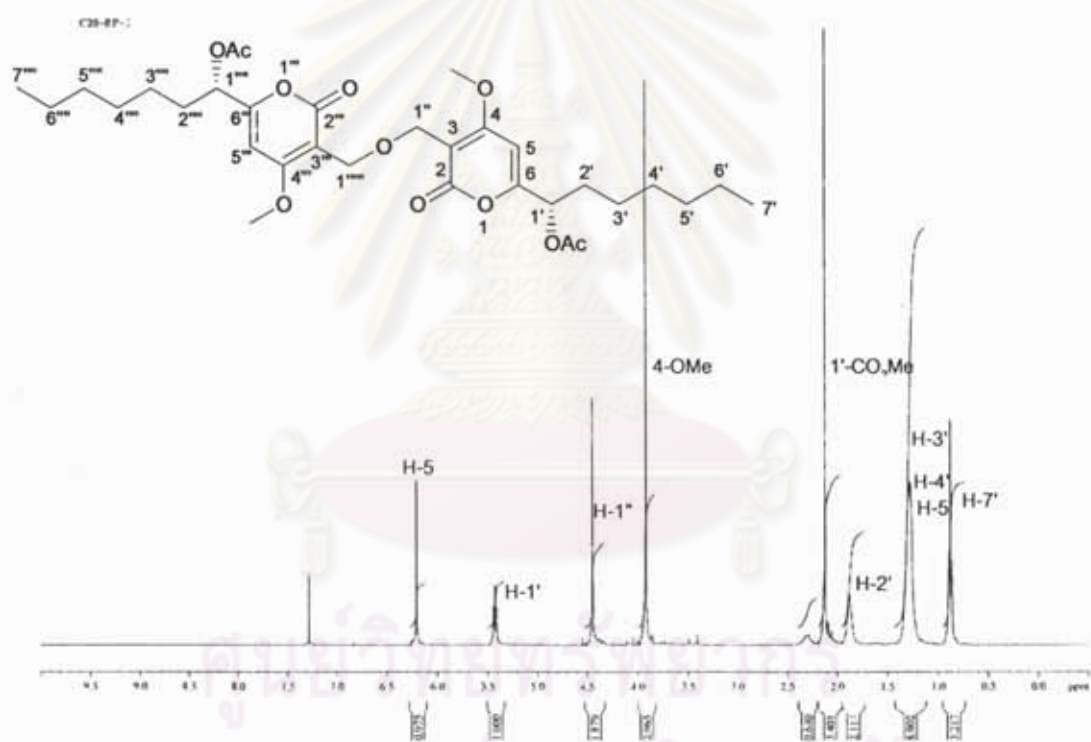


**Figure L56** 400 MHz $^1$H NMR (CDCl$_3$) spectrum of diacetate derivative (6)
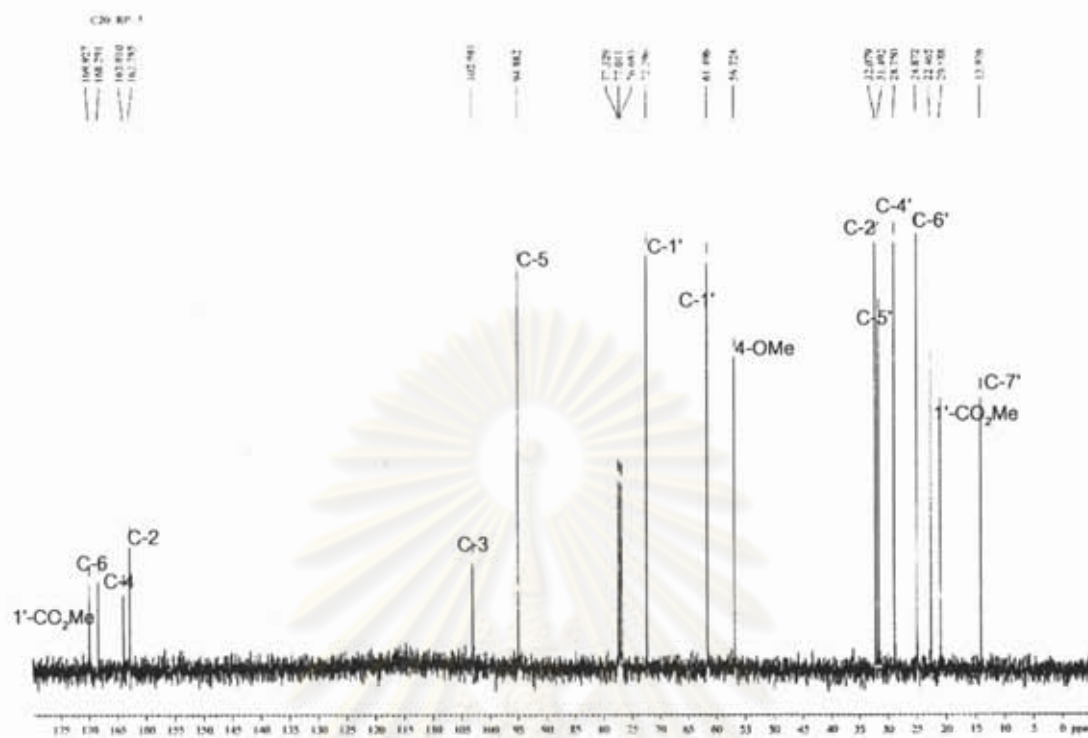
Figure L57    $^{13}$C NMR spectrum of diacetate derivative (6)
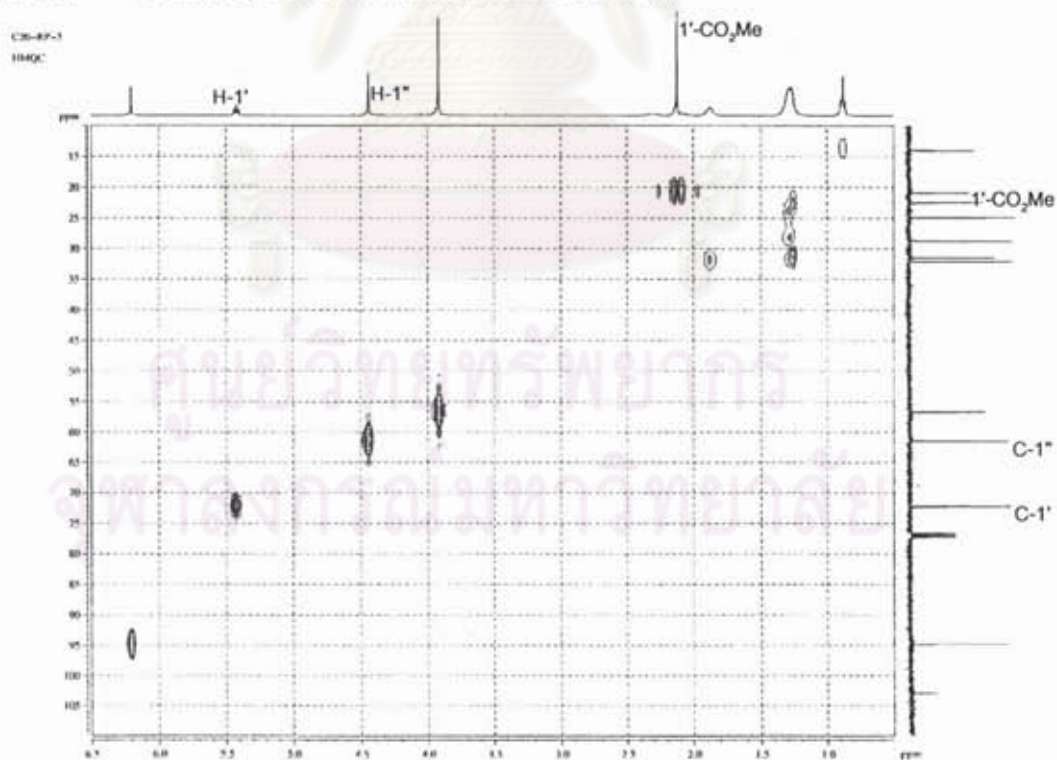


Figure L58    HMQC spectrum of diacetate derivative (6)
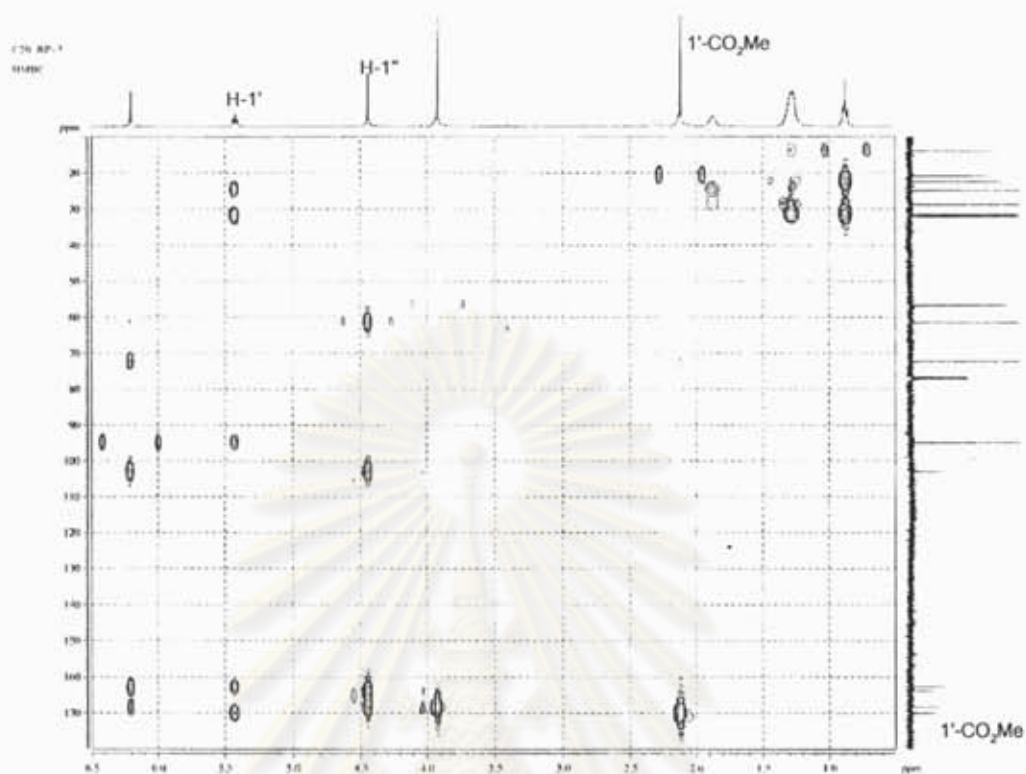
Figure L59    HMBC spectrum of diacetate derivative (6)
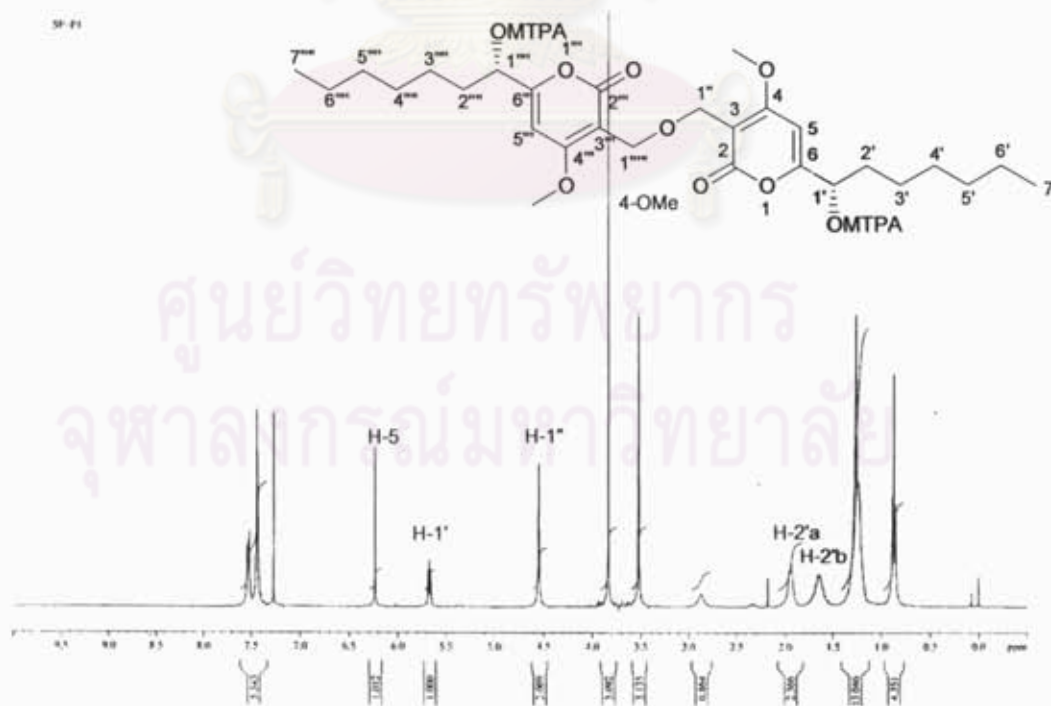


Figure L60    400 MHz $^1$H NMR spectrum (CDCl$_3$) of S-MTPA (7) of diacetate derivative 5
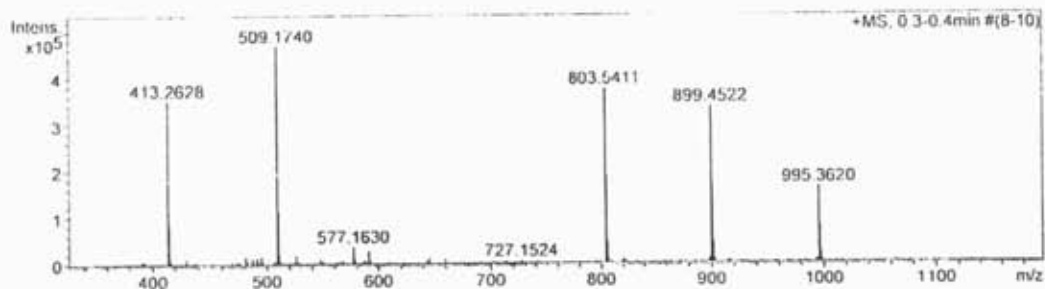
Figure L61    ESI-TOF spectrum of S-MTPA (7) of diacetate derivative 5
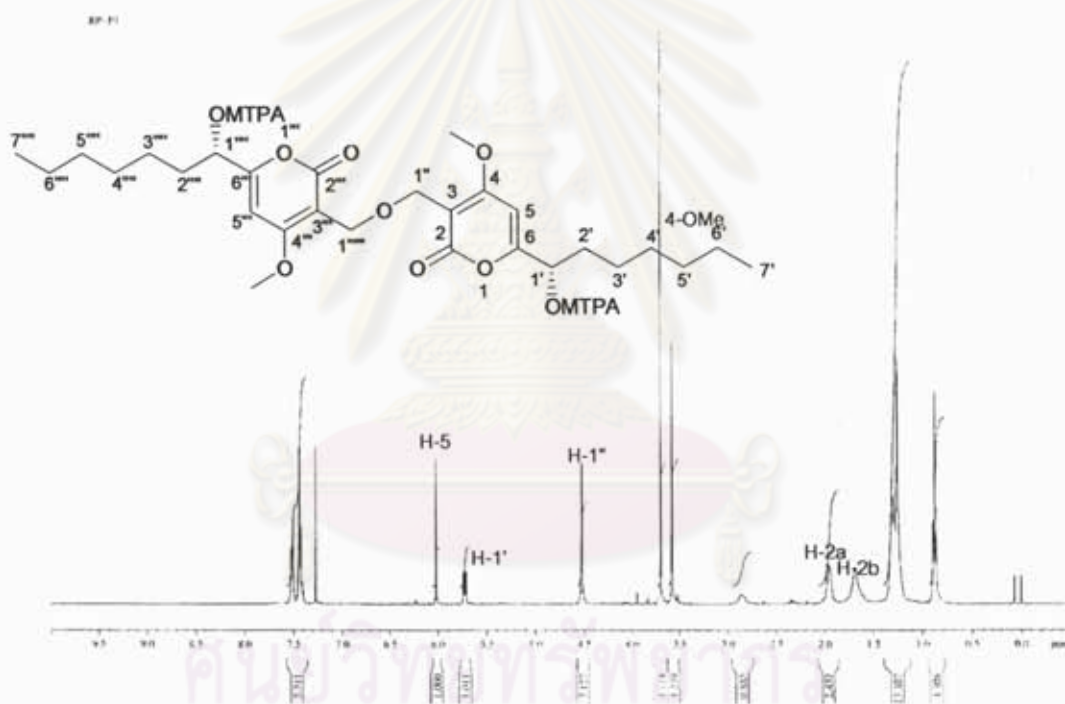


Figure L62    400 MHz $^1$H NMR spectrum (CDCl$_3$) of R-MTPA (8) of diacetate derivative 5
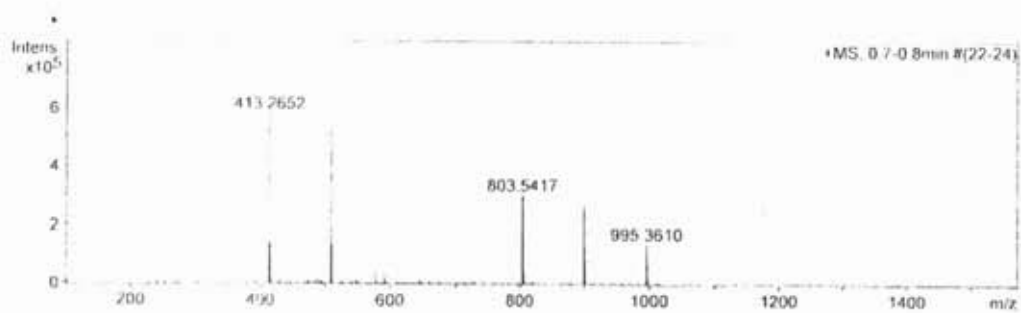
Figure L63    ESI-TOF spectrum of R-MTPA (8) of diacetate derivative 5
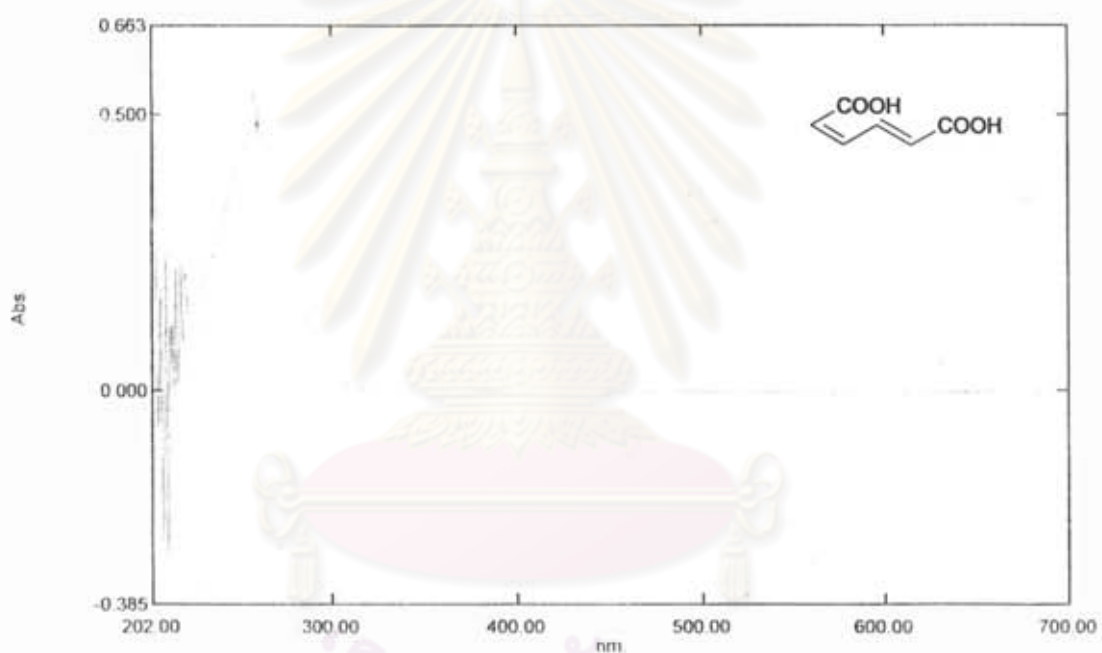


Figure L64    UV spectrum of *cis,trans*-muconic acid (9)
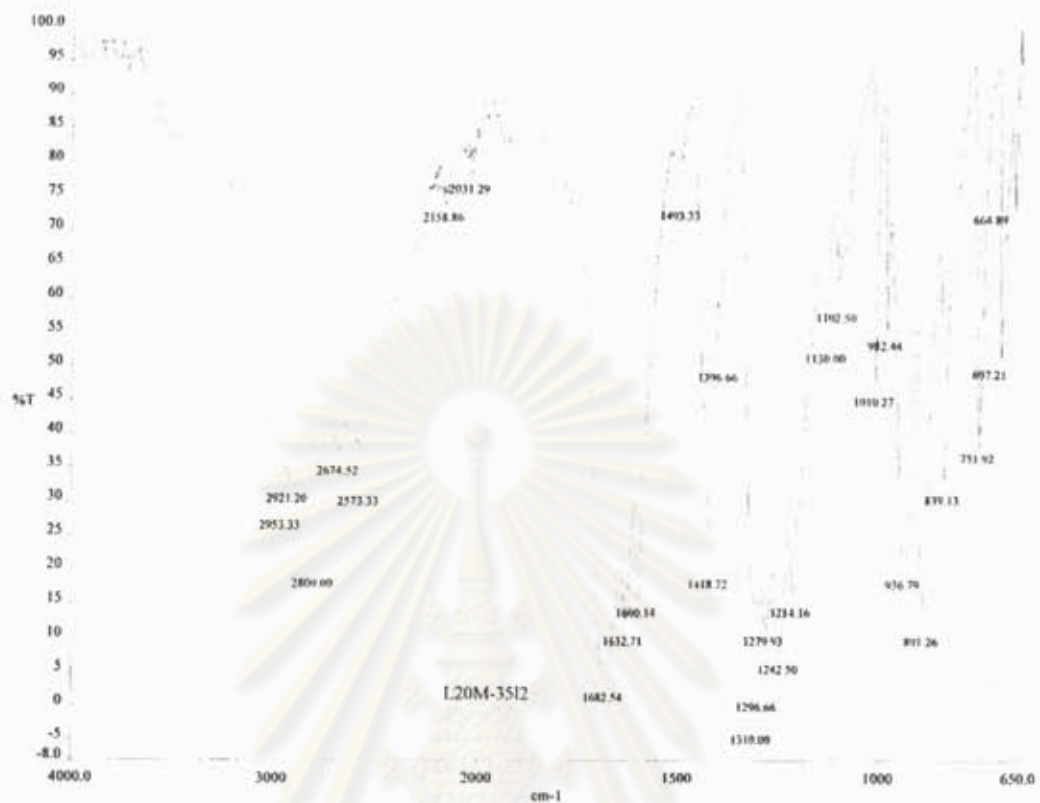
**Figure L65**  IR spectrum of *cis,trans*-muconic acid (9)



**Figure L66**  The ESI-TOF spectrum of *cis,trans*-muconic acid (9)
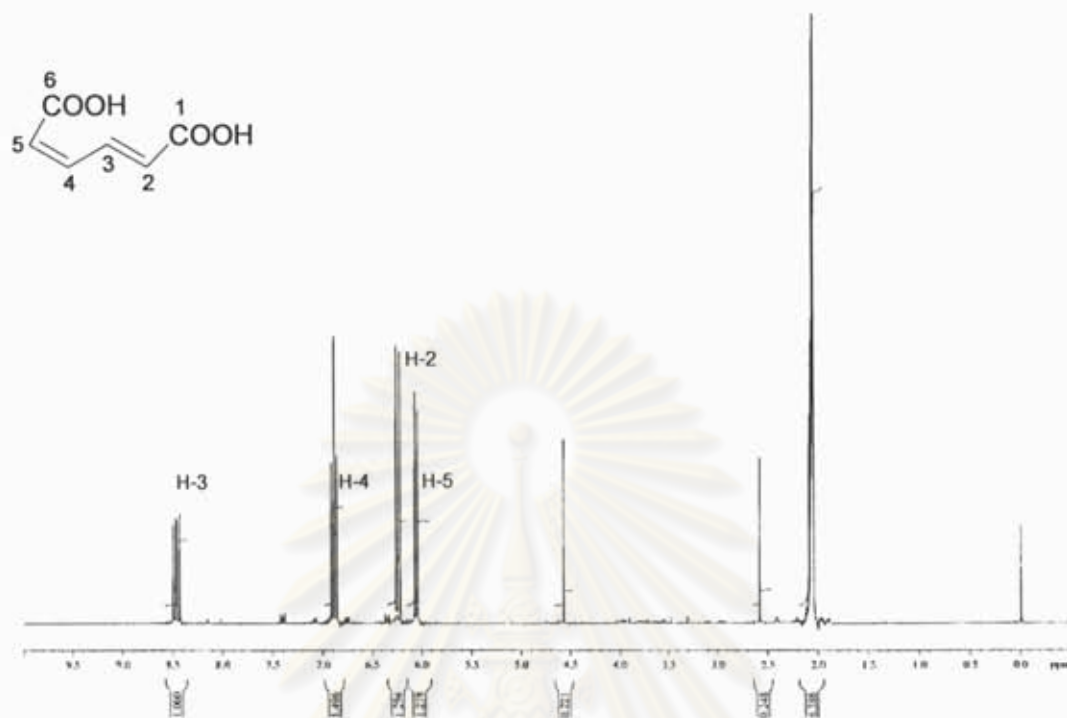
**Figure L67**   400 MHz $^1$H NMR (CDCl$_3$) spectrum of *cis,trans*-muconic acid (9)
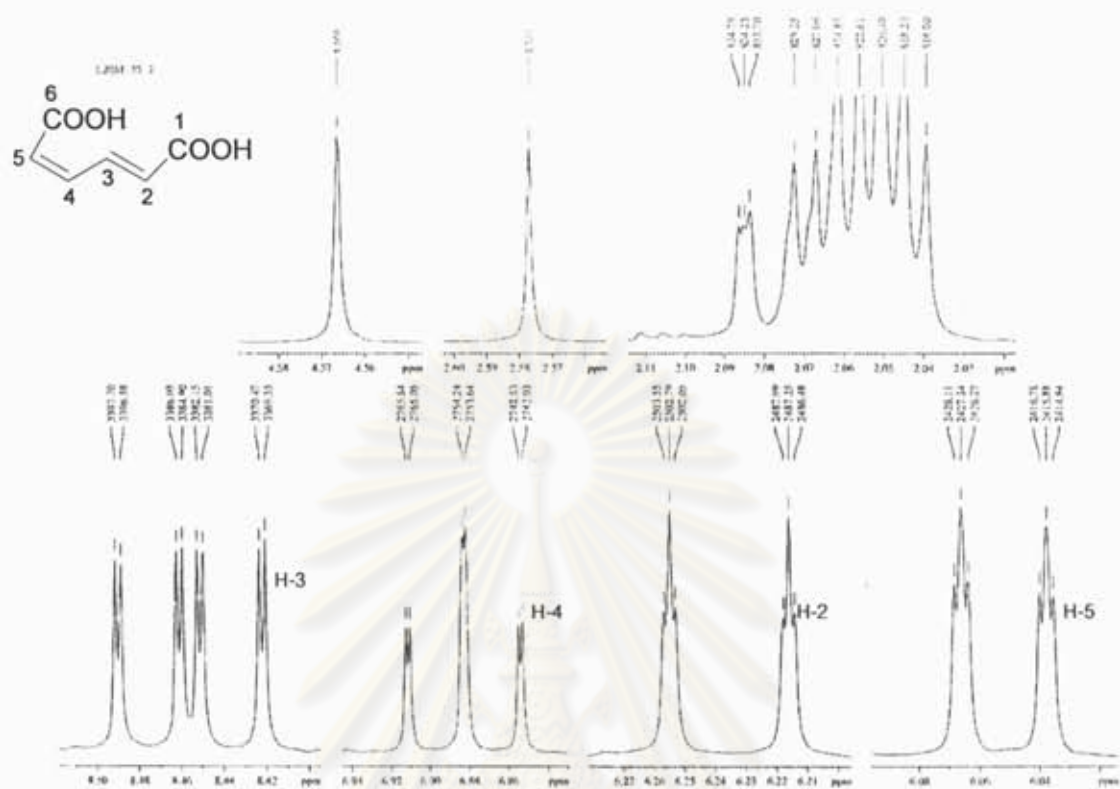
Figure L68    Expansion of Figure L66
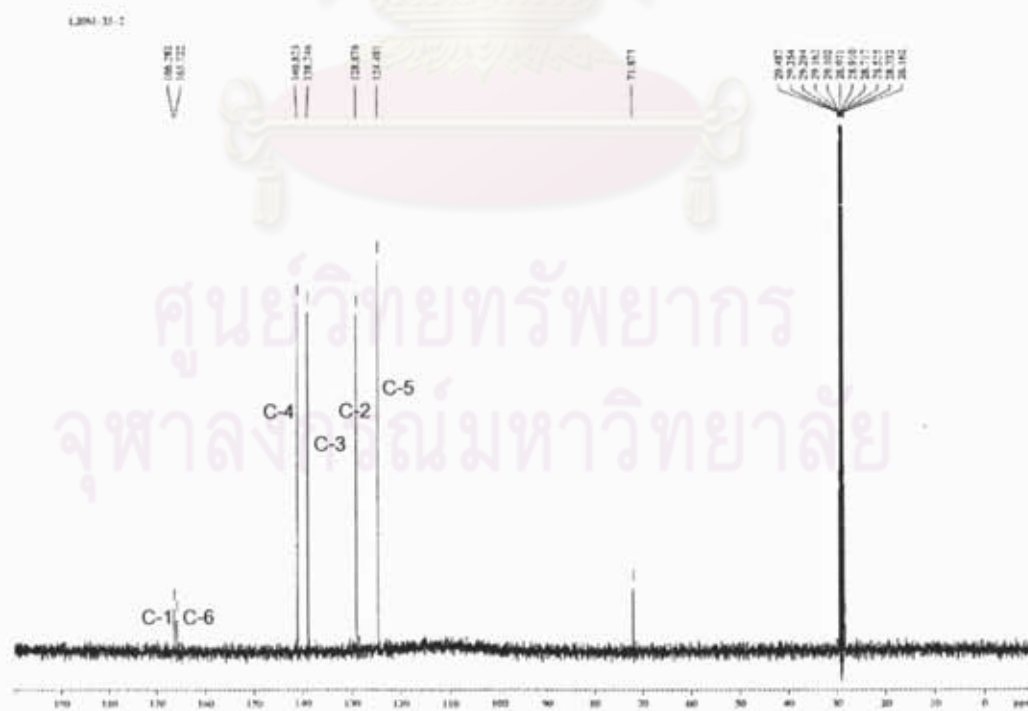


Figure L69    $^{13}$C NMR spectrum of *cis,trans*-muconic acid (9)
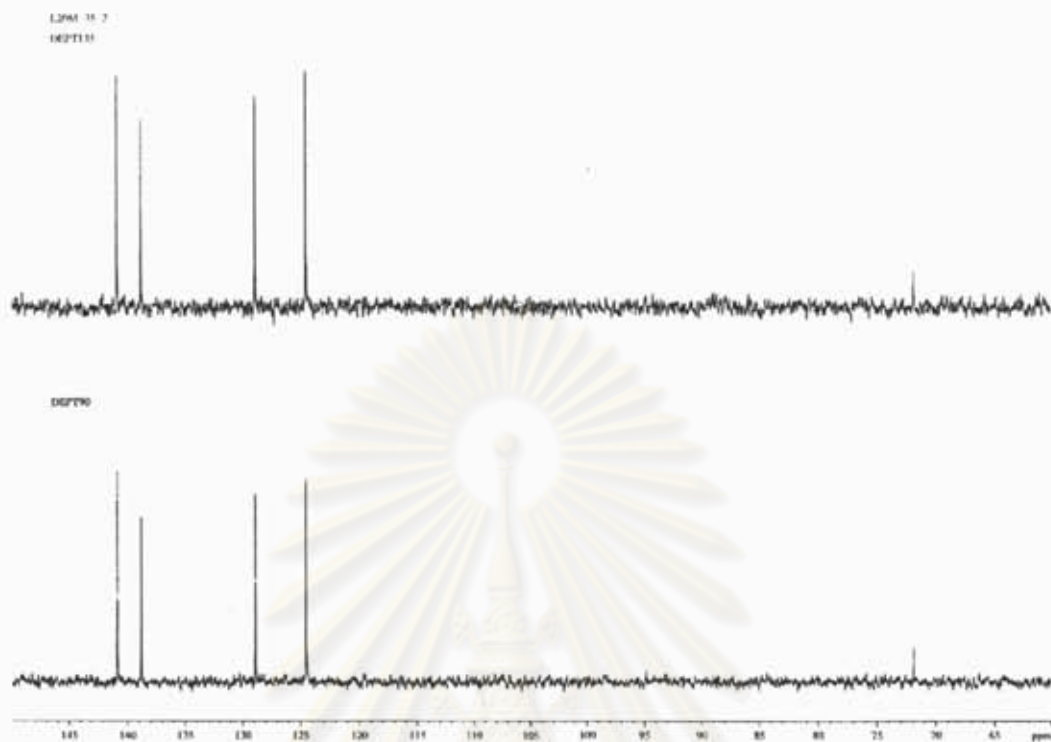
**Figure L70** DEPT spectrum of *cis,trans*-muconic acid (**9**)
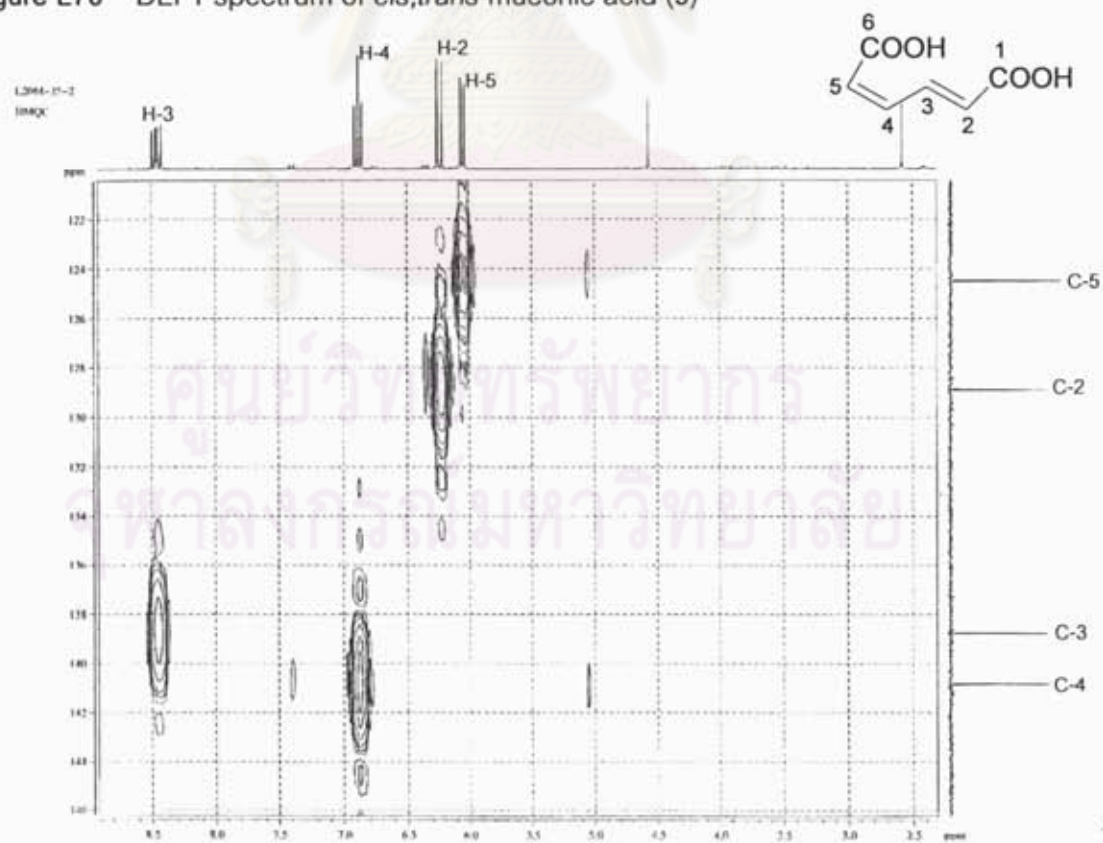


**Figure L71** HMQC spectrum of *cis,trans*-muconic acid (**9**)

**Figure L72** HMBC spectrum of *cis,trans*-muconic acid (9)
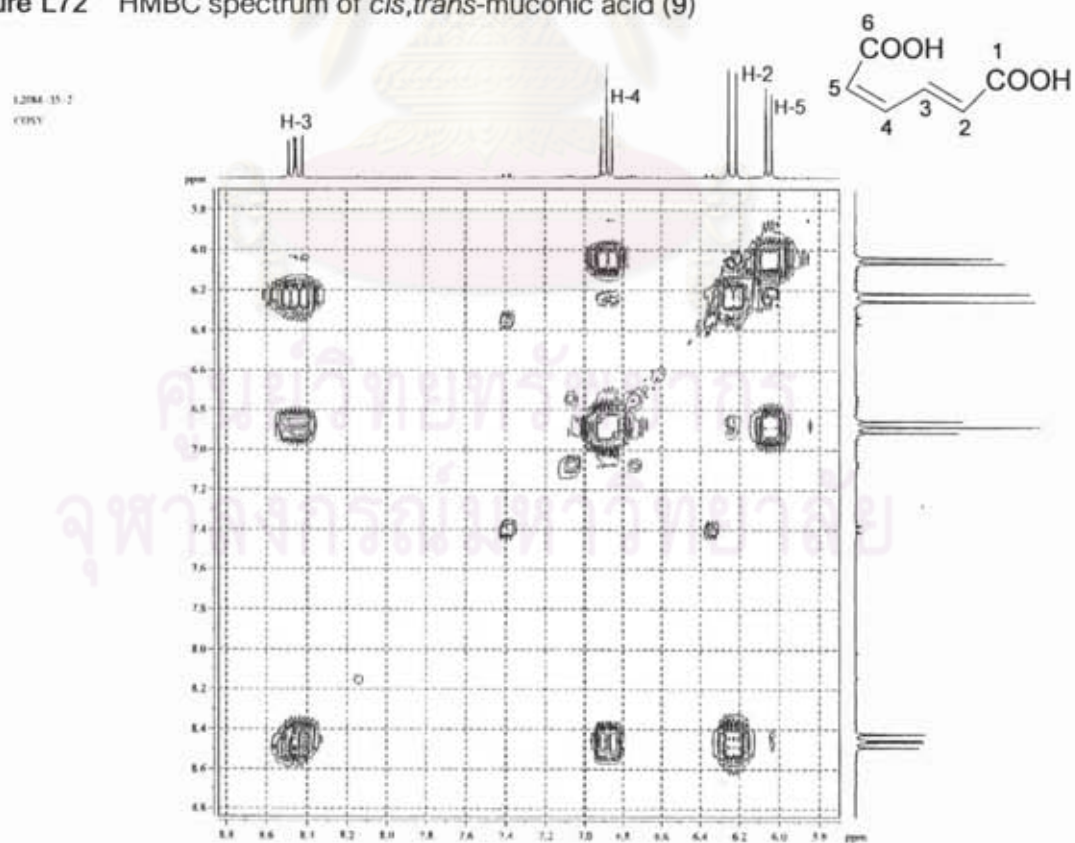


**Figure L73** ¹H-¹H COSY spectrum of *cis,trans*-muconic acid (9)
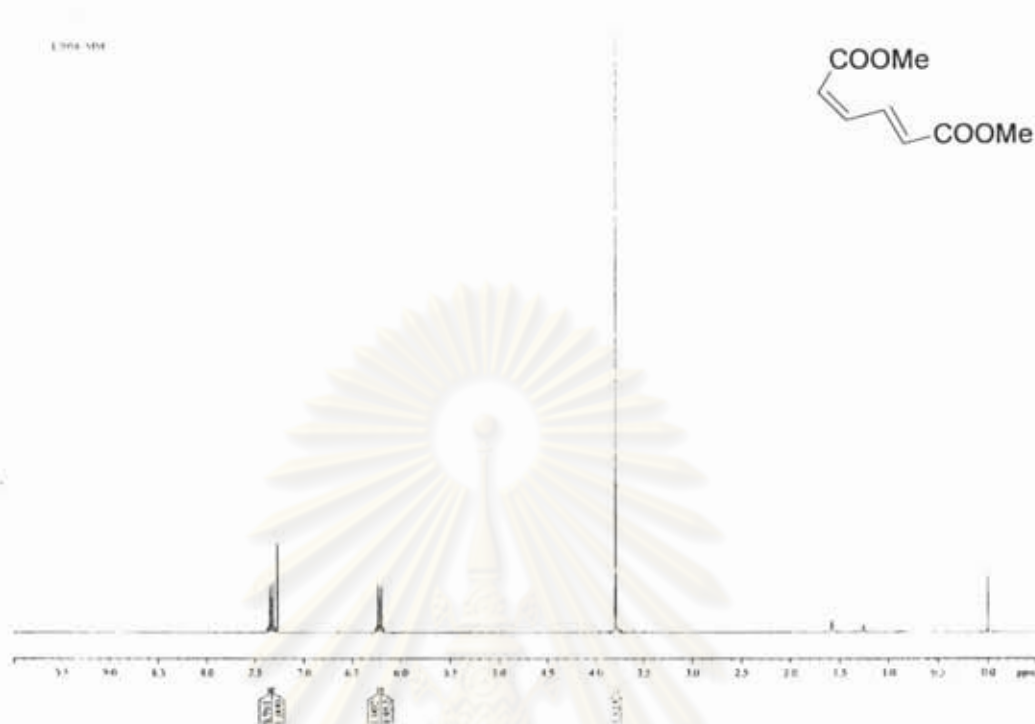
**Figure L74**   400 MHz $^1$H NMR (CDCl$_3$) spectrum of dimethyl derivative of *cis,trans*-muconic acid **9**



**Figure L75**   ESI-TOF spectrum of dimethyl derivative of *cis,trans*-muconic acid **9**
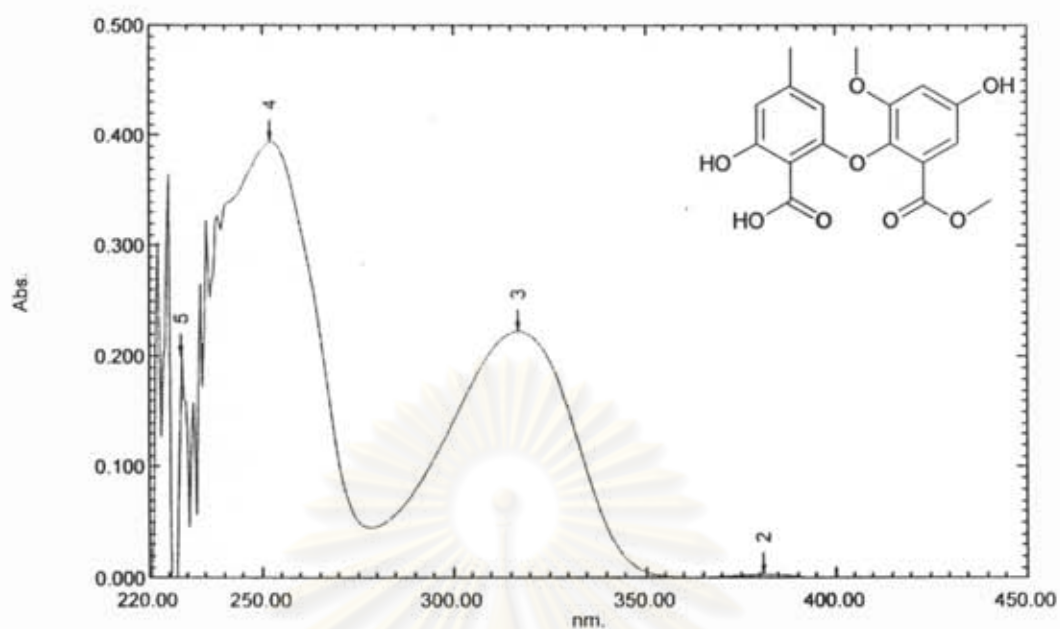
Figure L76    UV spectrum of asterric acid (11)
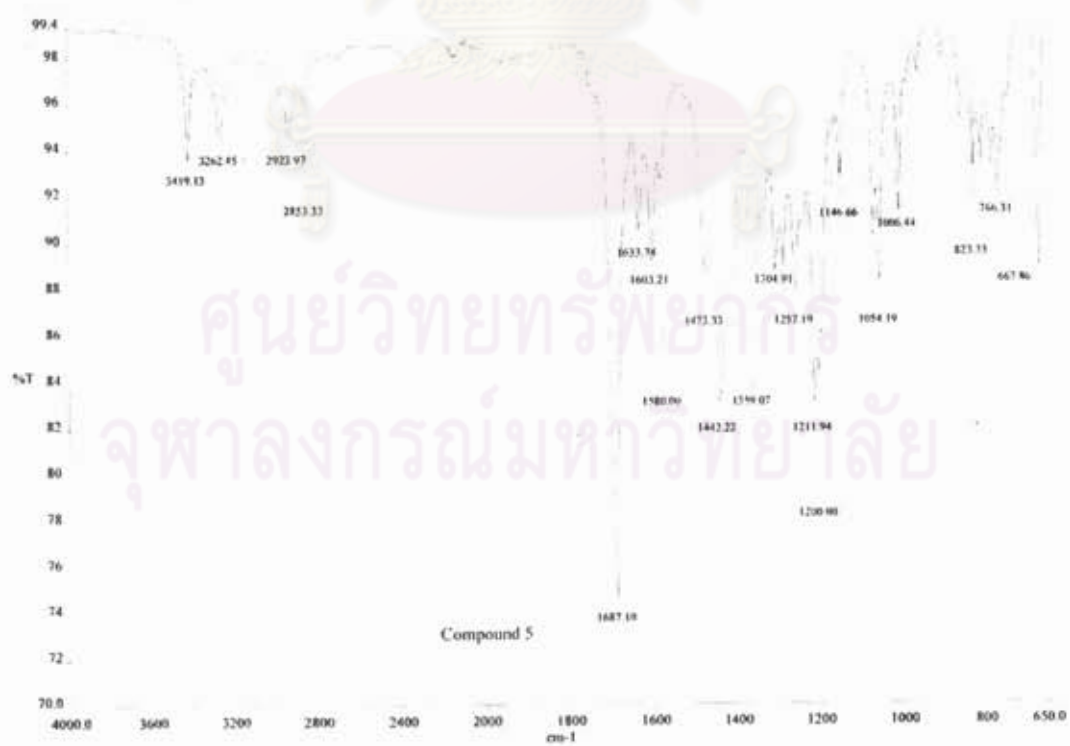


Figure L77    IR spectrum of asterric acid (11)
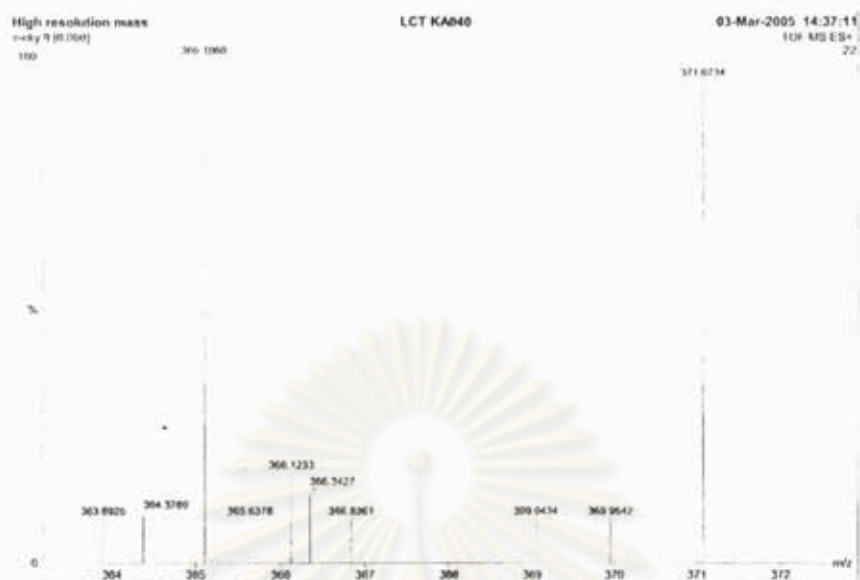
**Figure L78**  The ESI-TOF spectrum of asterric acid (11)
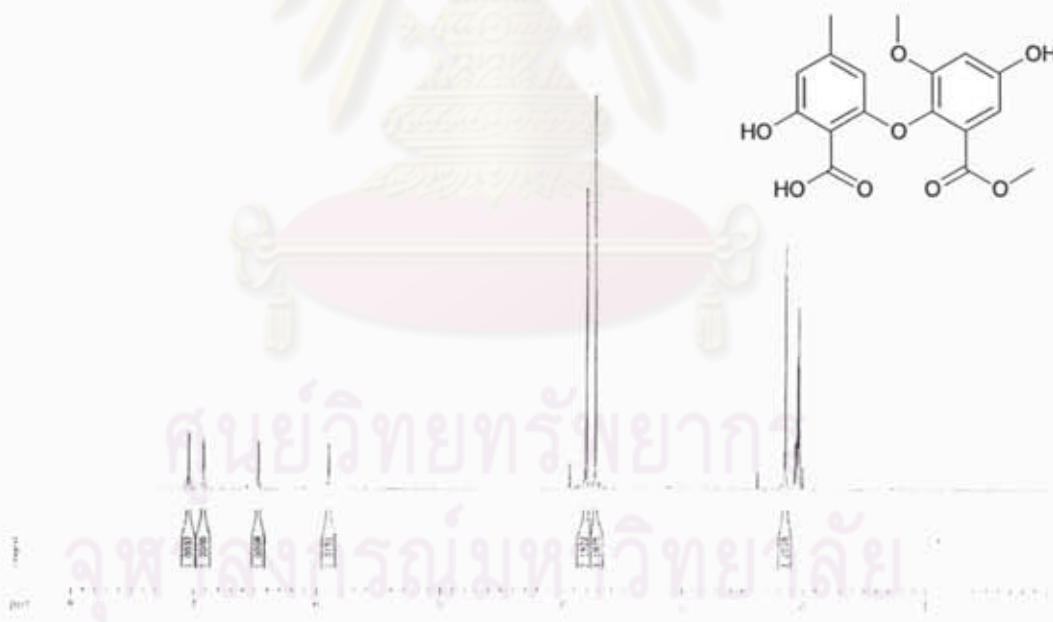


**Figure L79**  500 MHz $^1$H-NMR (acetone–$d_6$) spectrum of asterric acid (11)
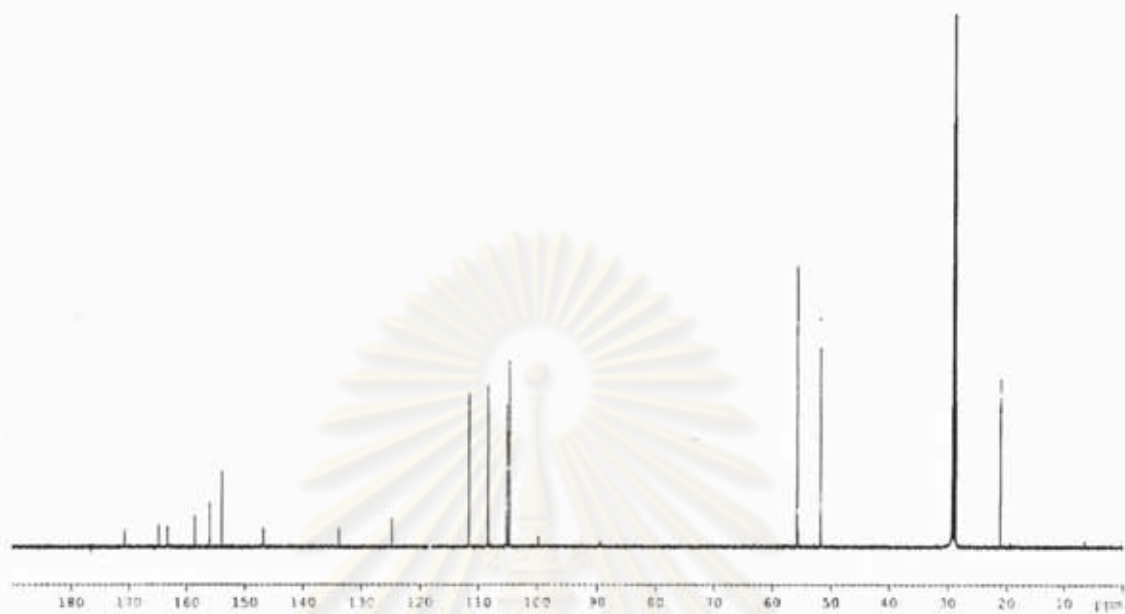
**Figure L80** $^{13}$C NMR spectrum of asterric acid (11)
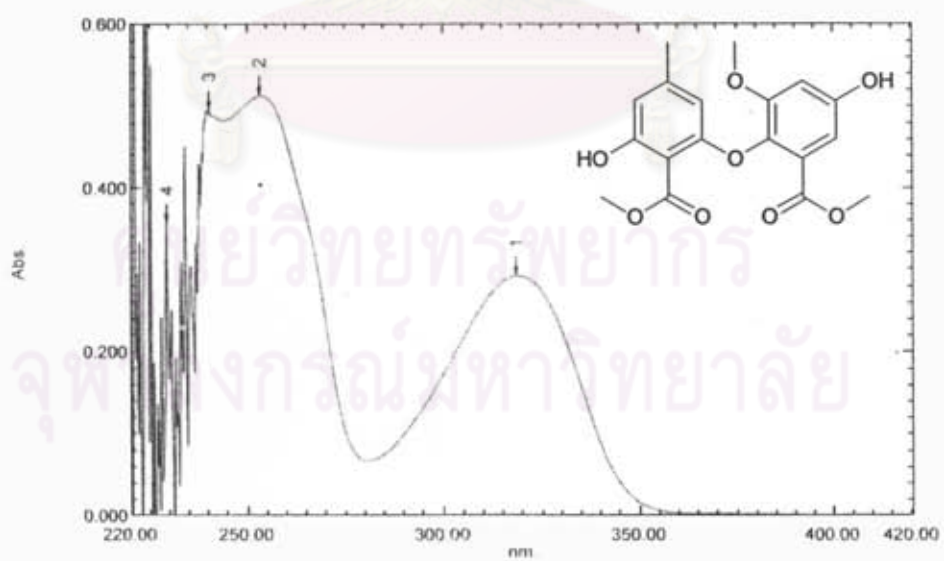


**Figure L81** UV spectrum of methyl asterrate (12)

**Figure L82** IR spectrum of methyl asterrate (12)
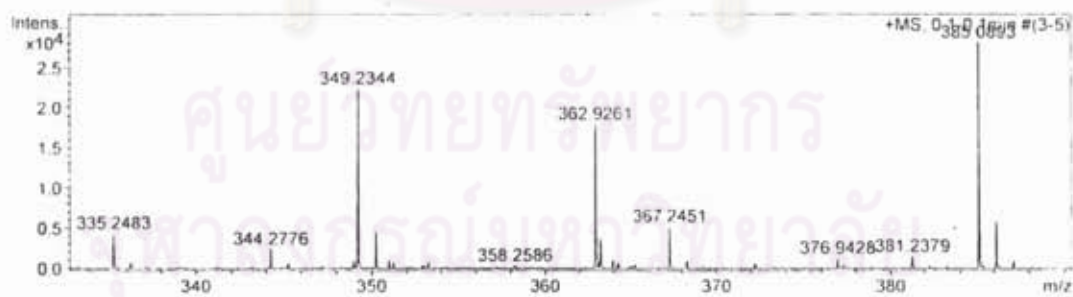


**Figure L83** ESI-TOF spectrum of methyl asterrate (12)
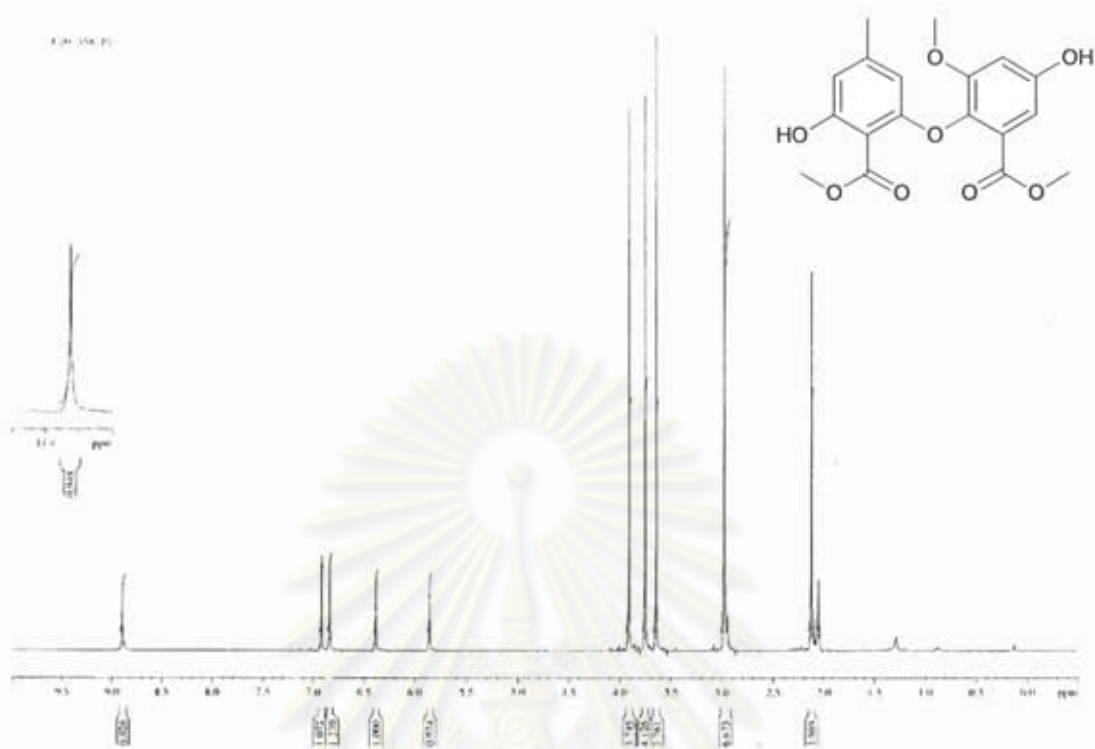
Figure L84  400 MHz $^1$H NMR (acetone–$d_6$) spectrum of methyl asterrate (12)
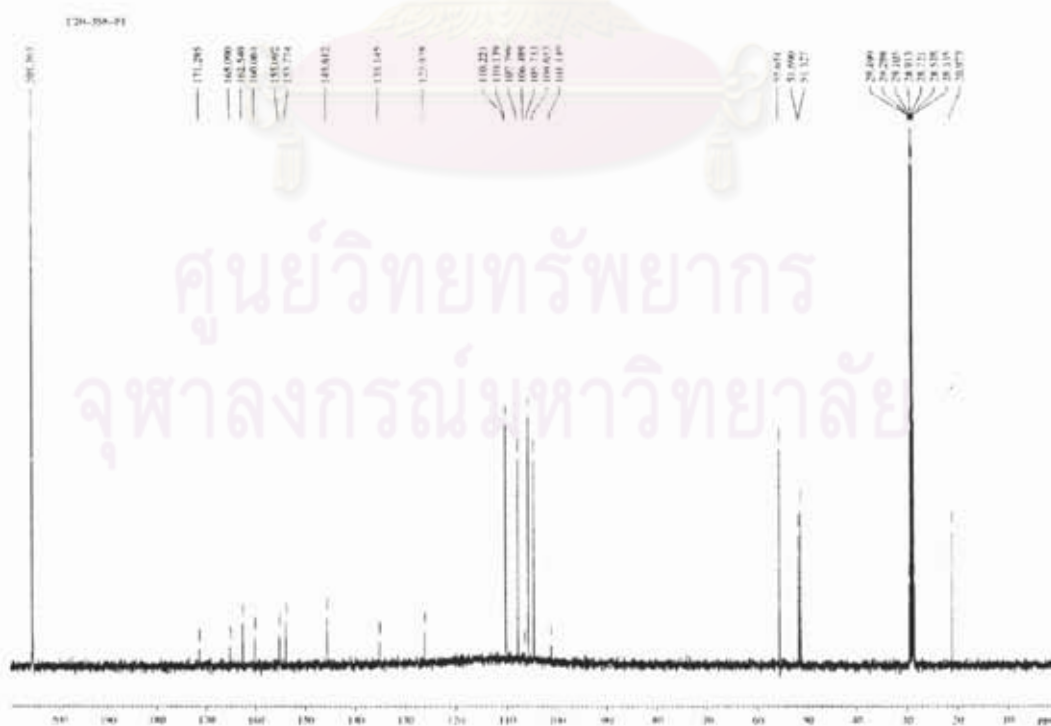


Figure L85  $^{13}$C NMR spectrum of methyl asterrate (12)
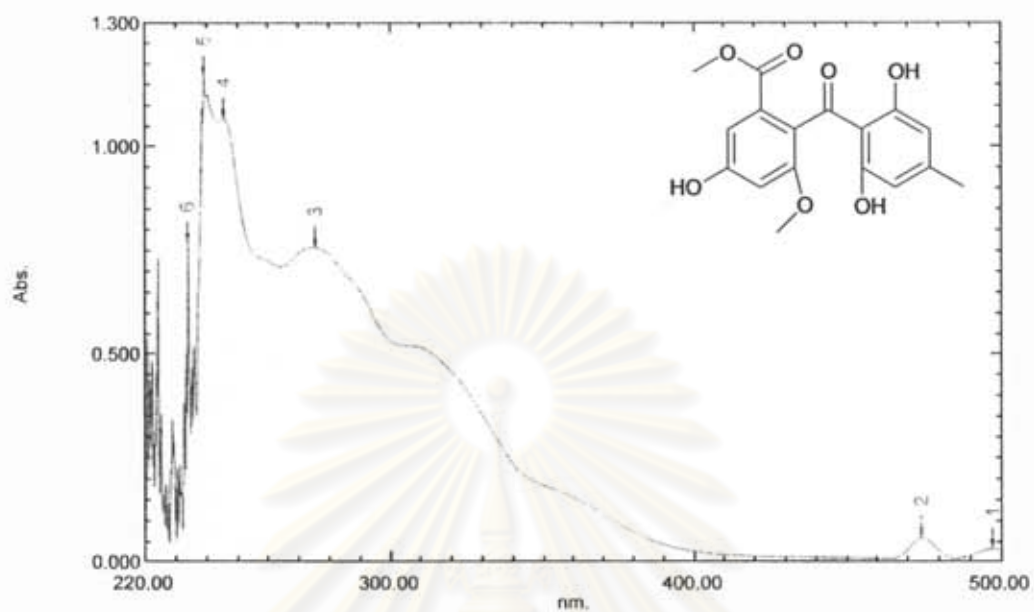
**Figure L86**    UV spectrum of sulochrin (13)



**Figure L87**    IR spectrum of sulochrin (13)
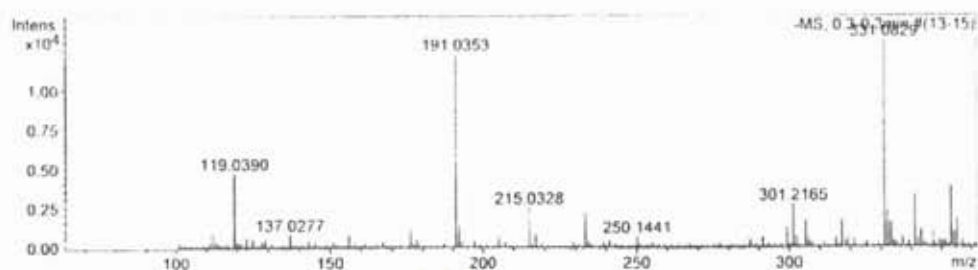
**Figure L88** ESI-TOF spectrum of sulochrin (**13**)
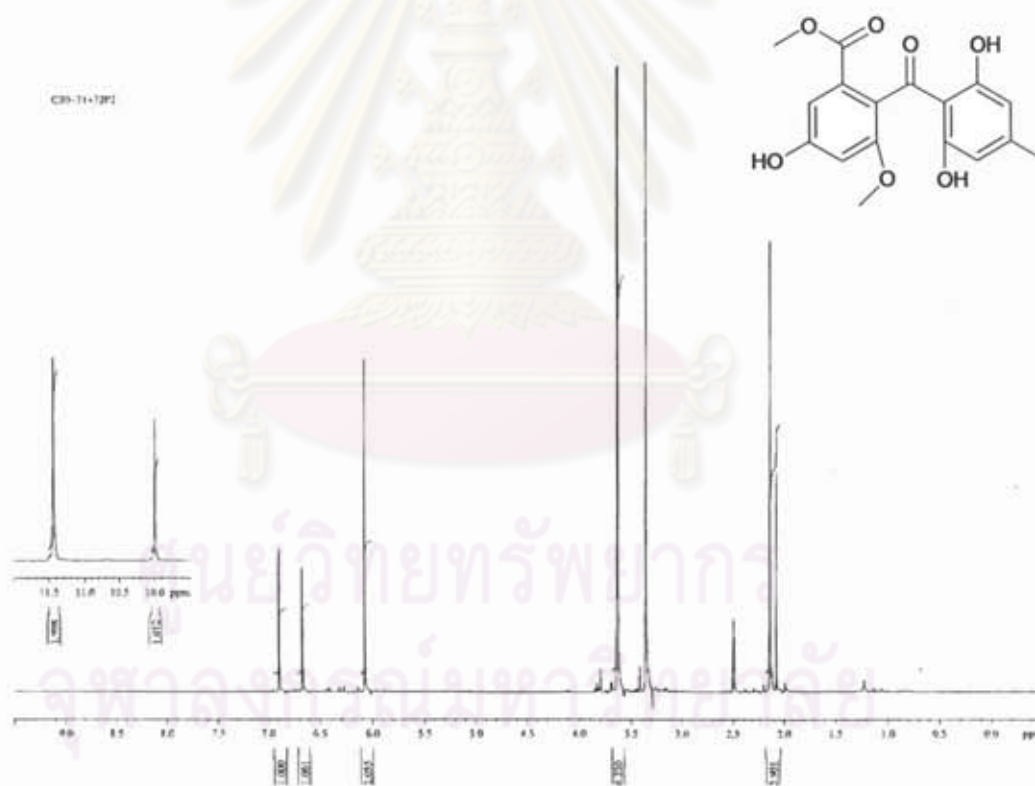


**Figure L89** 400 MHz $^1$H NMR (DMSO-$d_6$) spectrum of sulochrin (**13**)

Figure L90    $^{13}$C NMR spectrum of sulochrin (13)



Figure L91    UV spectrum of questin (10)

**Figure L92** IR spectrum of questin (**10**)
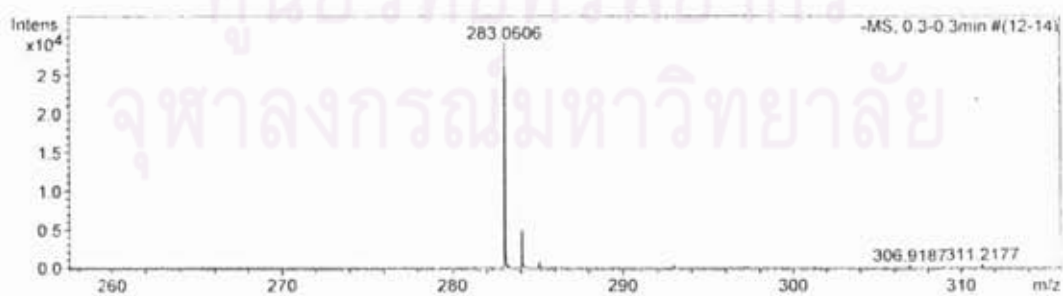


**Figure L93** The ESI-TOF spectrum of questin (**10**)
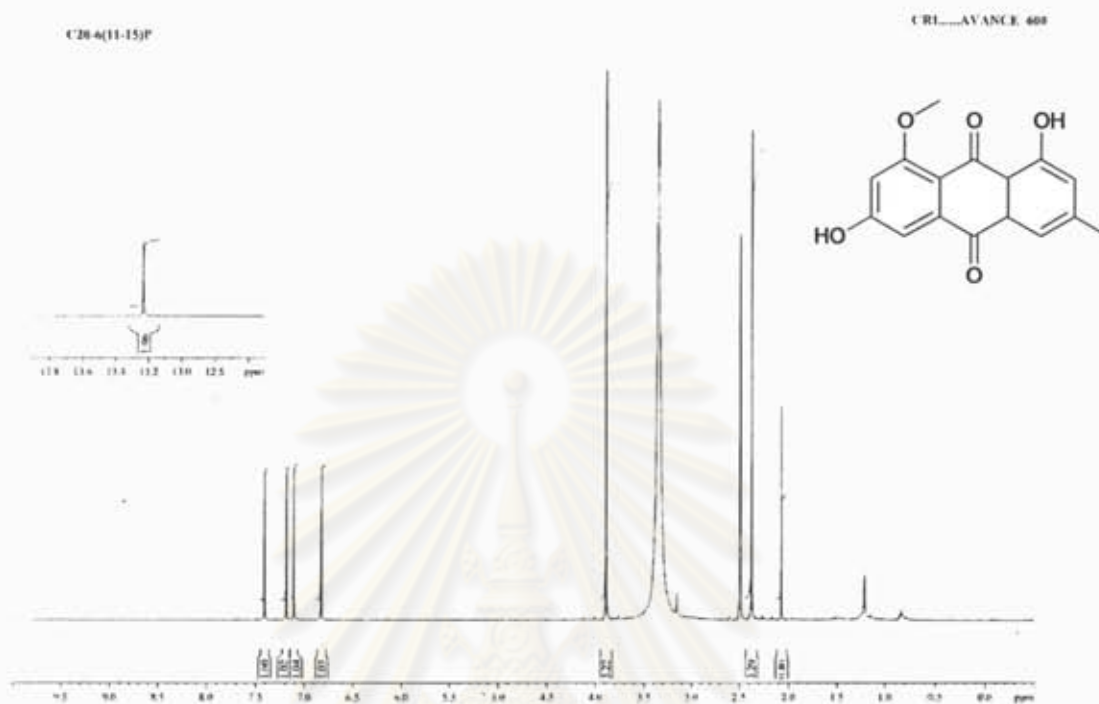
Figure L94    600 MHz $^1$H NMR (DMSO-$d_6$) spectrum of questin (10)
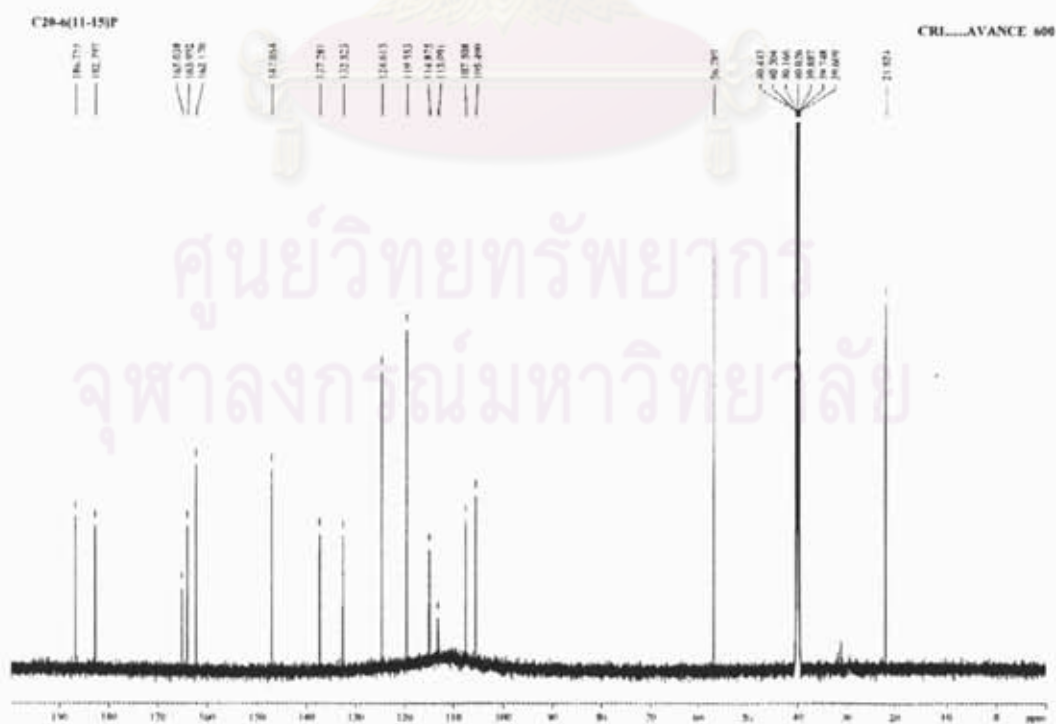


Figure L95    $^{13}$C NMR spectrum of questin (10)

190
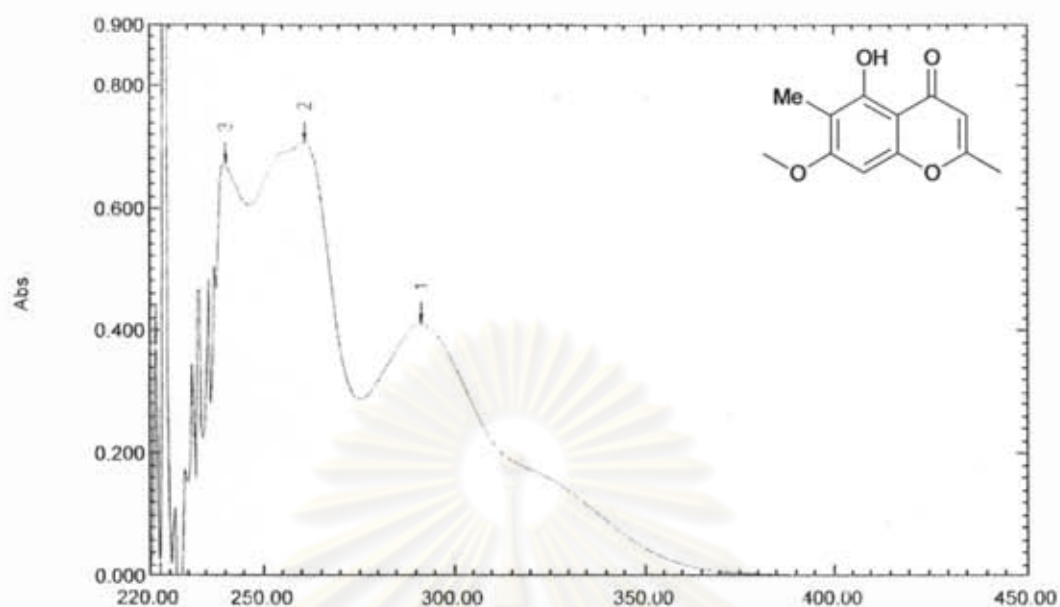


Figure L96    UV spectrum of eugenitin (14)
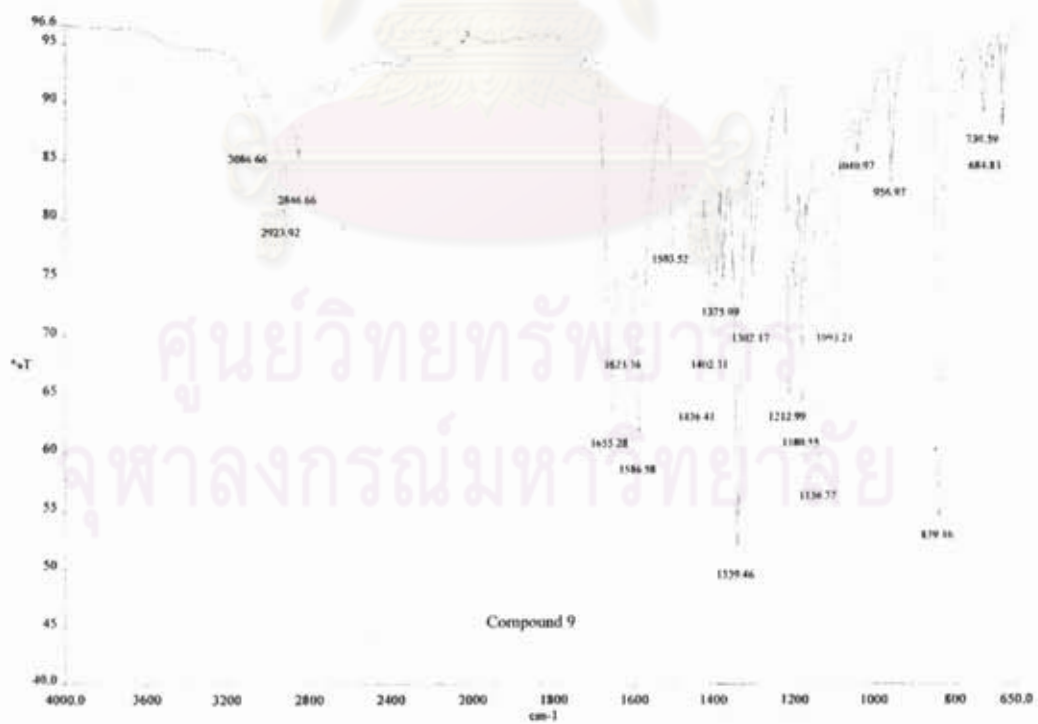


Figure L97    IR spectrum of eugenitin (14)
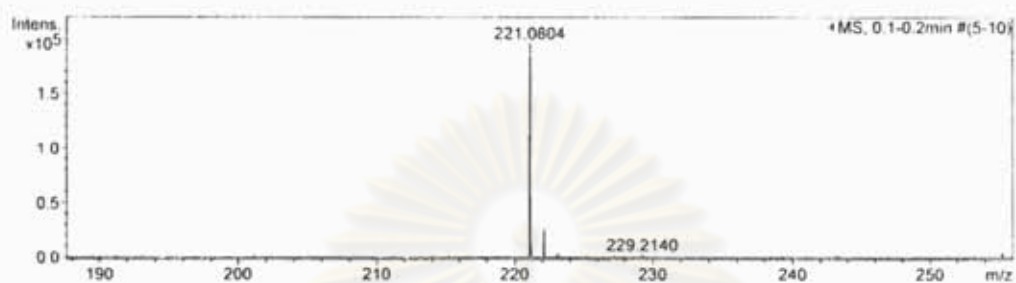
**Figure L98** Mass spectrum of eugenitin (**14**)
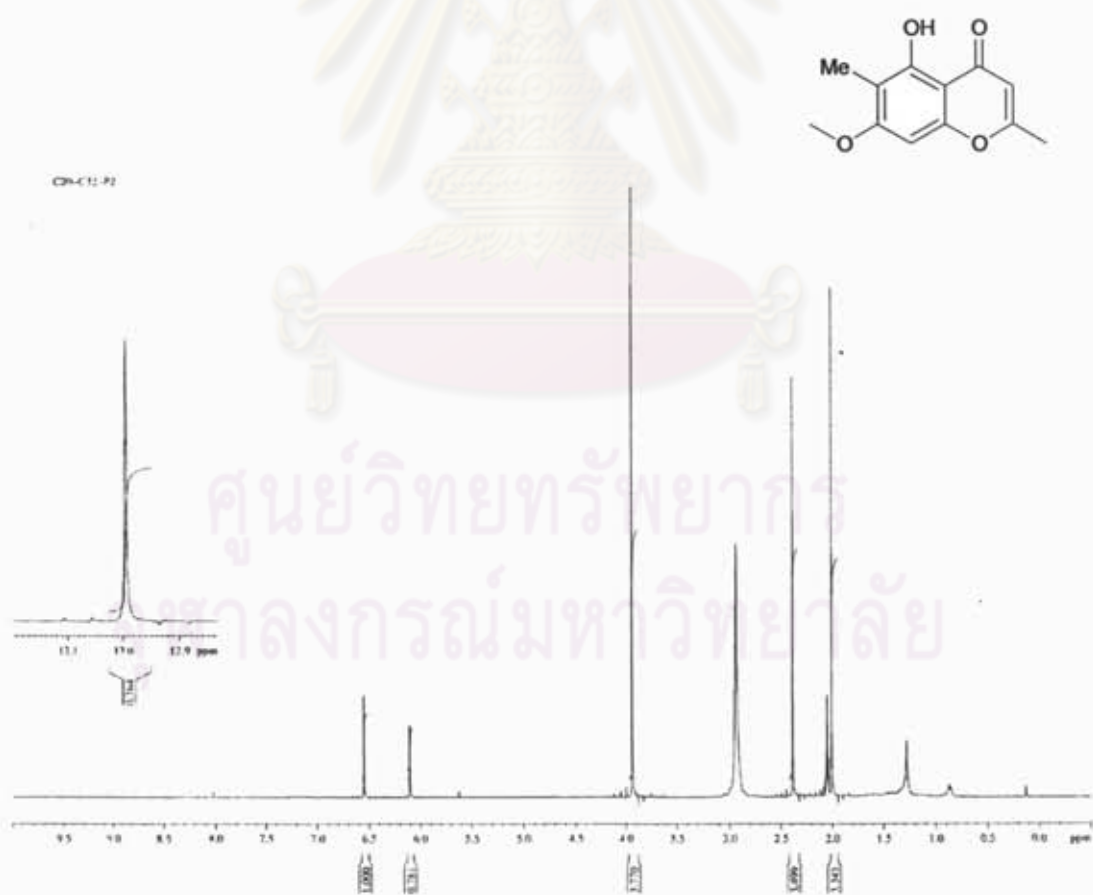


**Figure L99** 400 MHz $^1$H NMR (Acetone-$d_6$) spectrum of eugenitin (**14**)
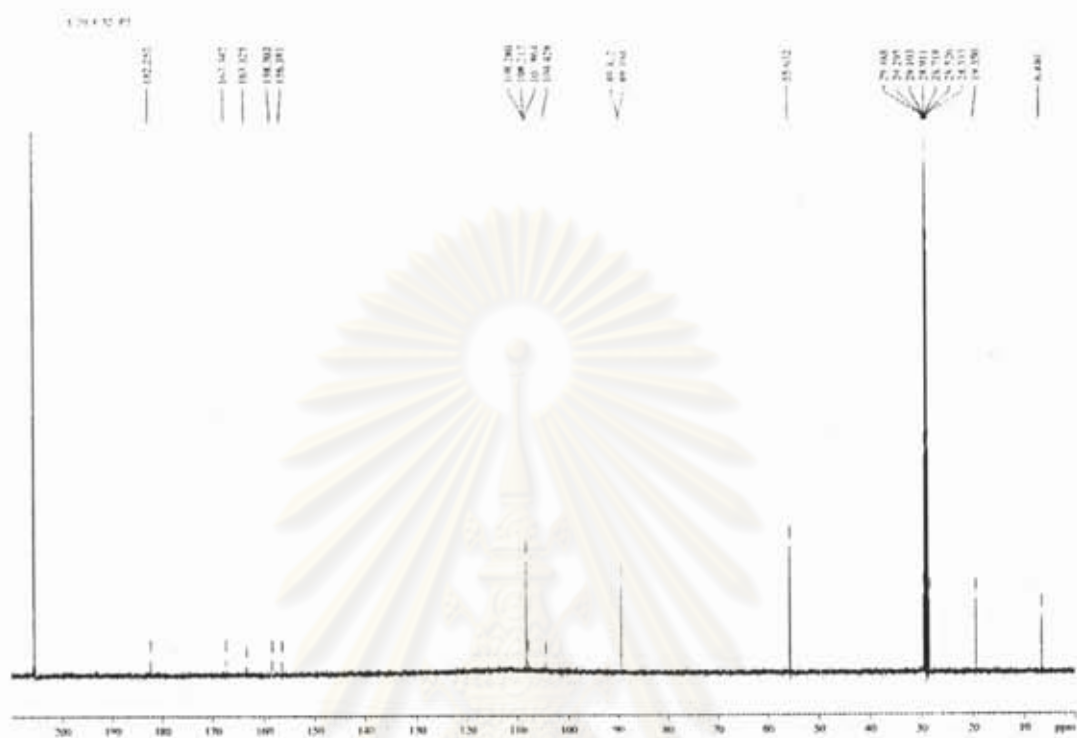
Figure L100    $^{13}$C NMR spectrum of eugenitin (14)
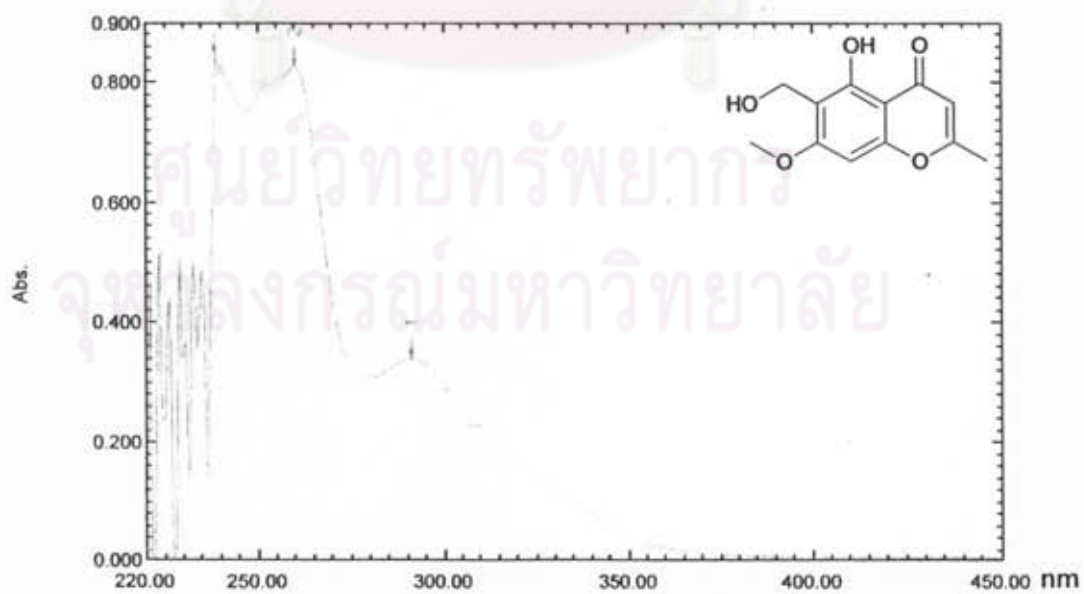


Figure L101    UV spectrum of 6-hydroxymethyleugenitin (15)
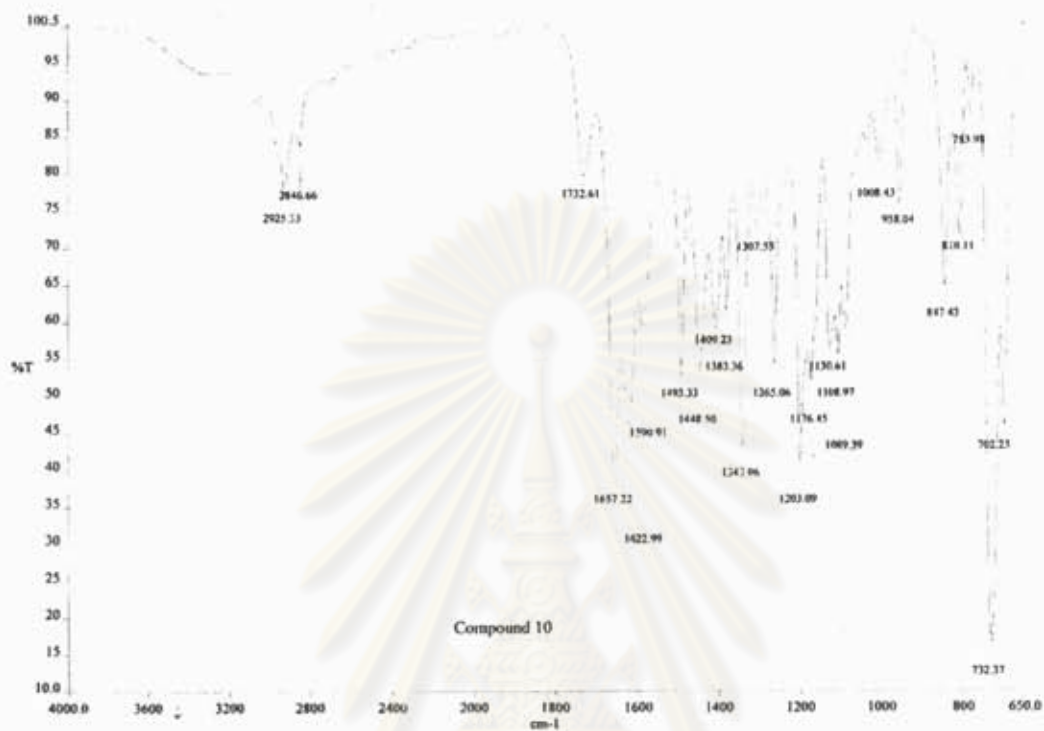
**Figure L102**   IR spectrum of 6-hydroxymethyleugenitin (**15**)
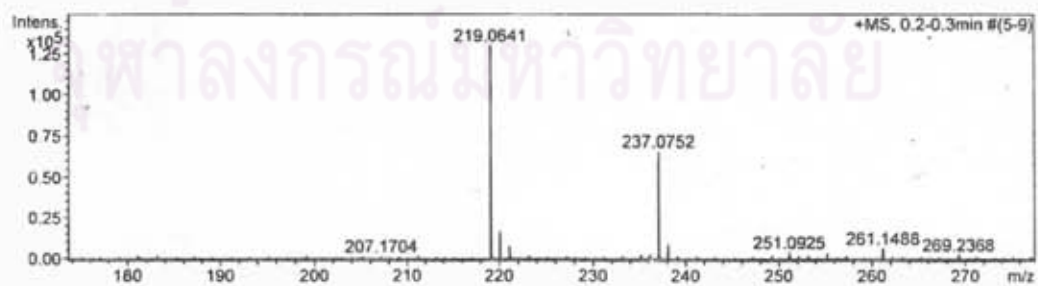


**Figure L103**   The ESI-TOF spectrum of 6-hydroxymethyleugenitin (**15**)
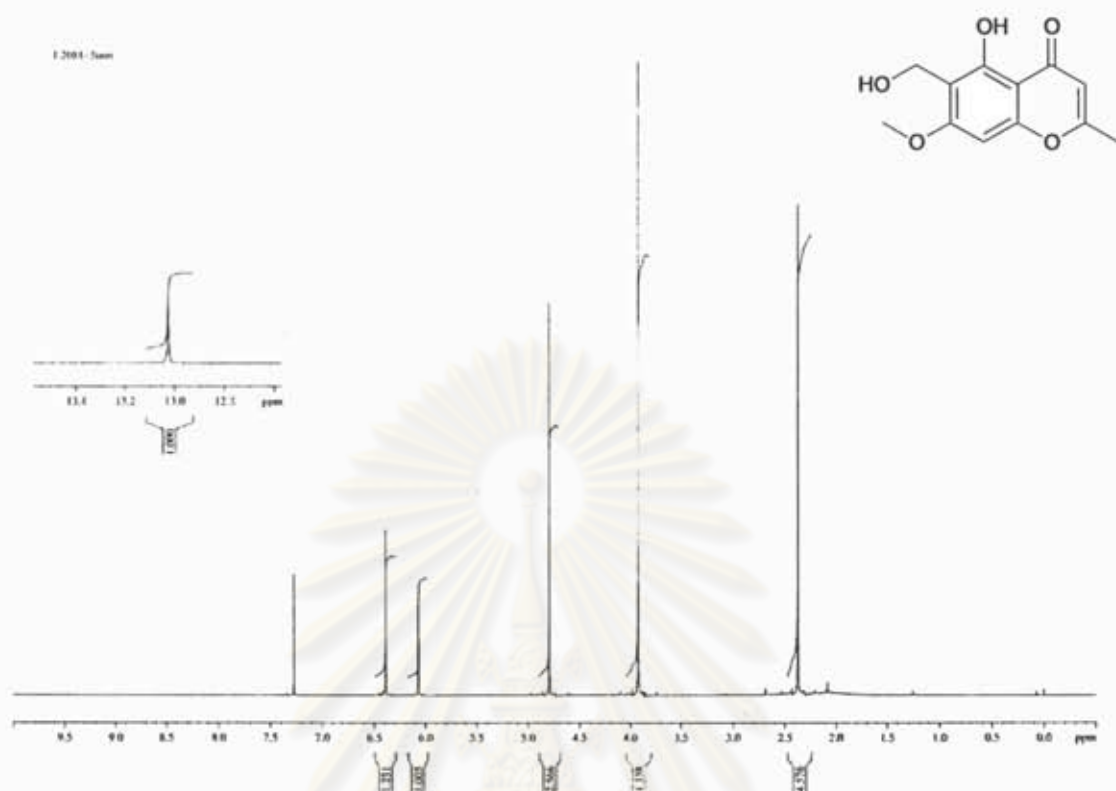
Figure L104   400 MHz $^1$H NMR (CDCl$_3$) spectrum of 6-hydroxymethyleugenitin (15)
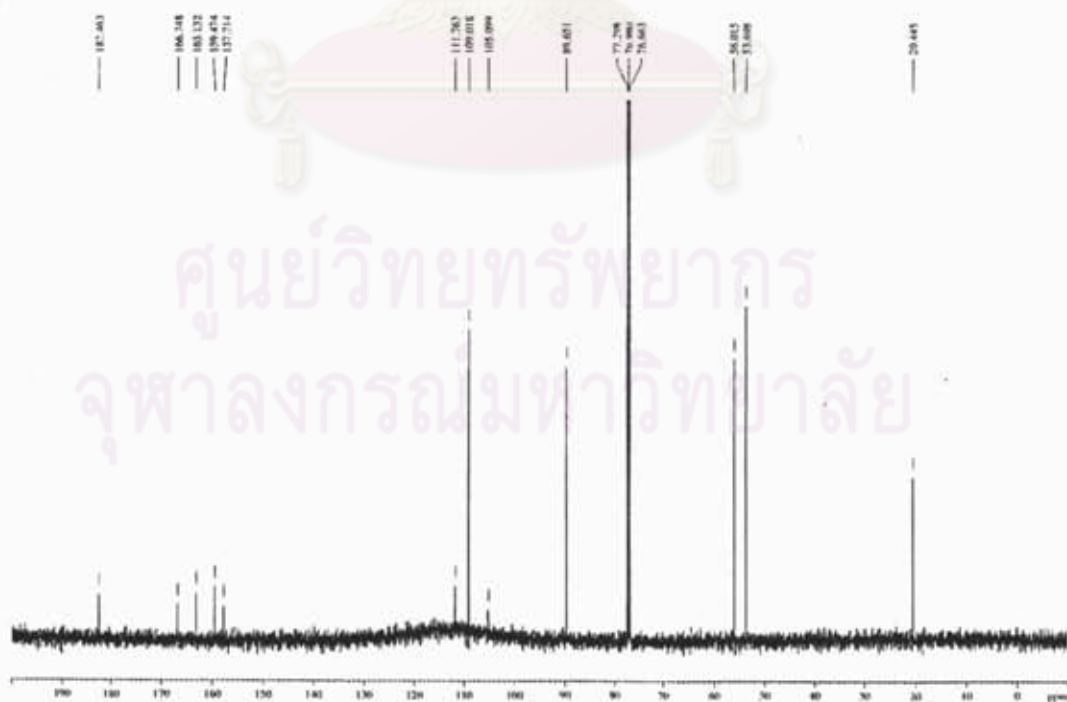


Figure L105   $^{13}$C NMR spectrum of 6-hydroxymethyleugenitin (15)
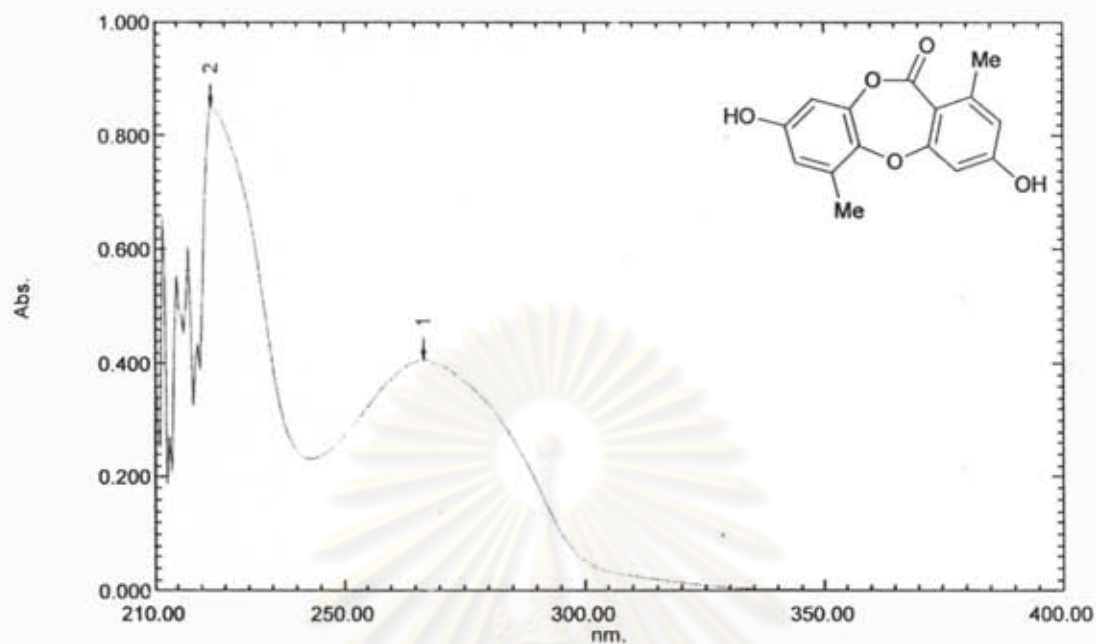
Figure P1        UV spectrum of corynesidone A (16)
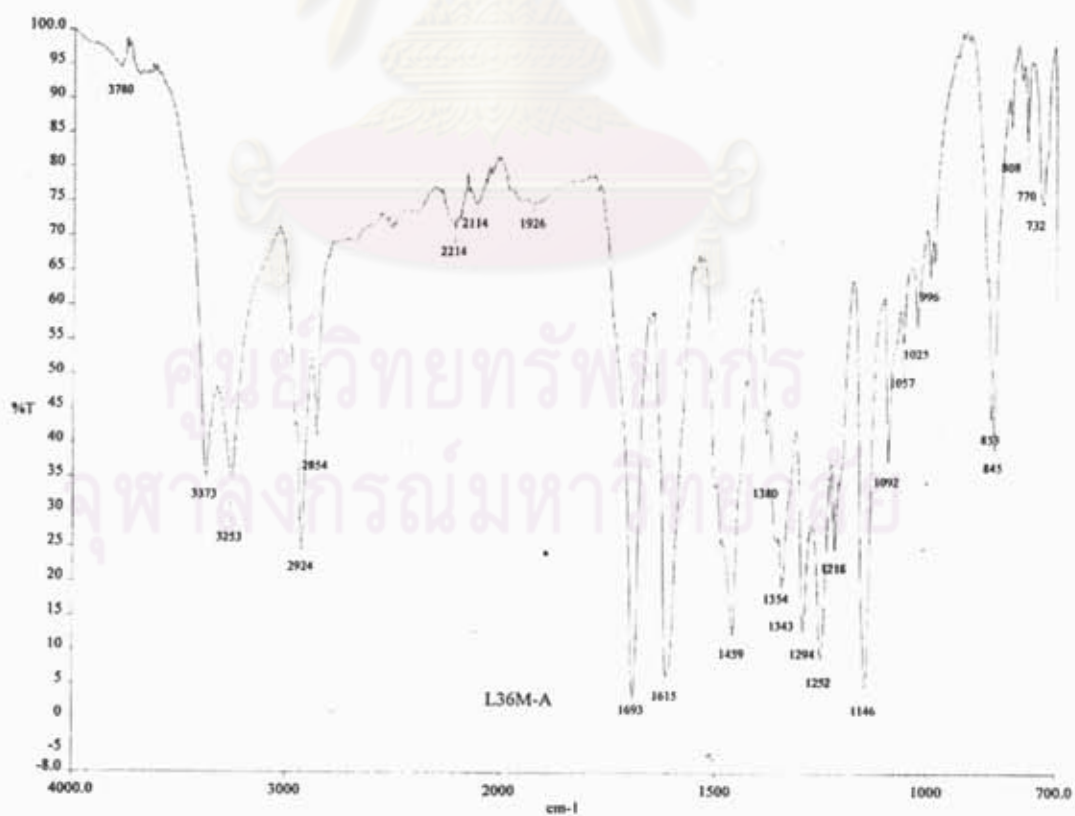


Figure P2        IR spectrum of corynesidone A (16)
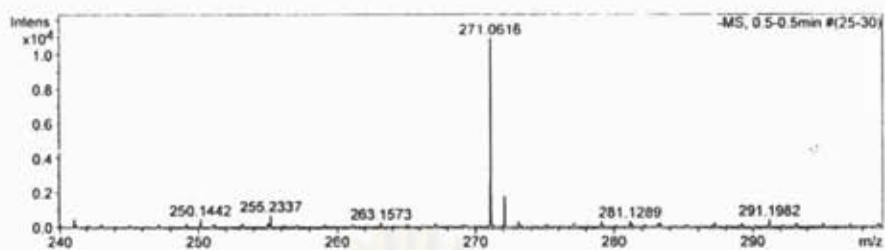
Figure P3    ESI-TOF spectrum of corynesidone A (**16**)
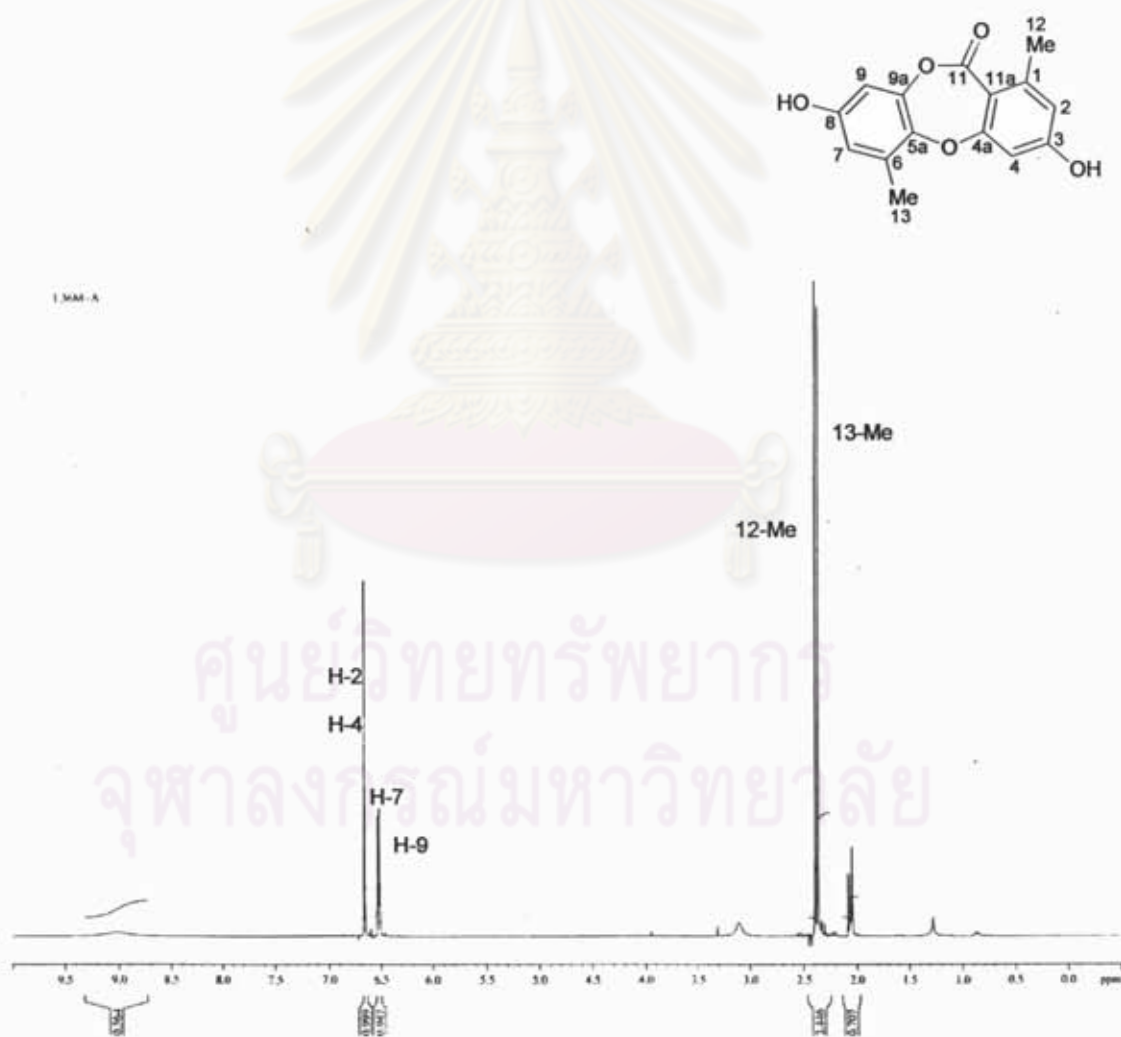


Figure P4    400 MHz $^{1}$H NMR (Acetone-$d_6$) spectrum of corynesidone A (**16**)

Figure P5    Expansion of Figure P4

Figure P6    $^{13}$C NMR (Acetone-d$_6$) spectrum of corynesidone A (16)

L.36M-A
DEPT135

DEPT90
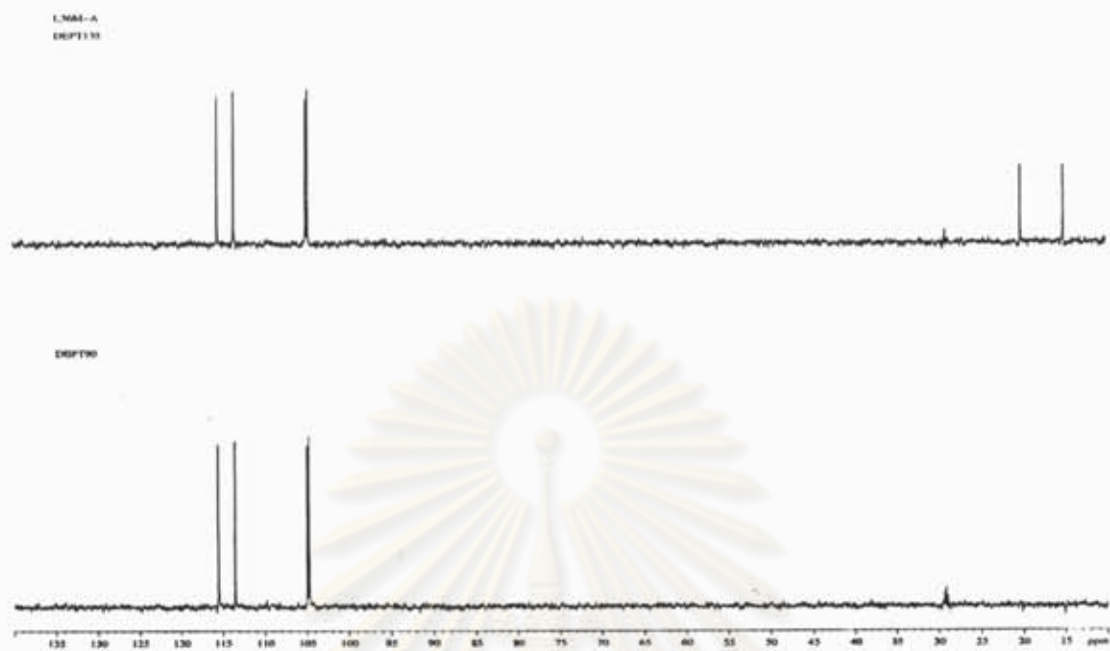
**Figure P7**  DEPT spectrum of corynesidone A (16)

L.36M-A
HMQC
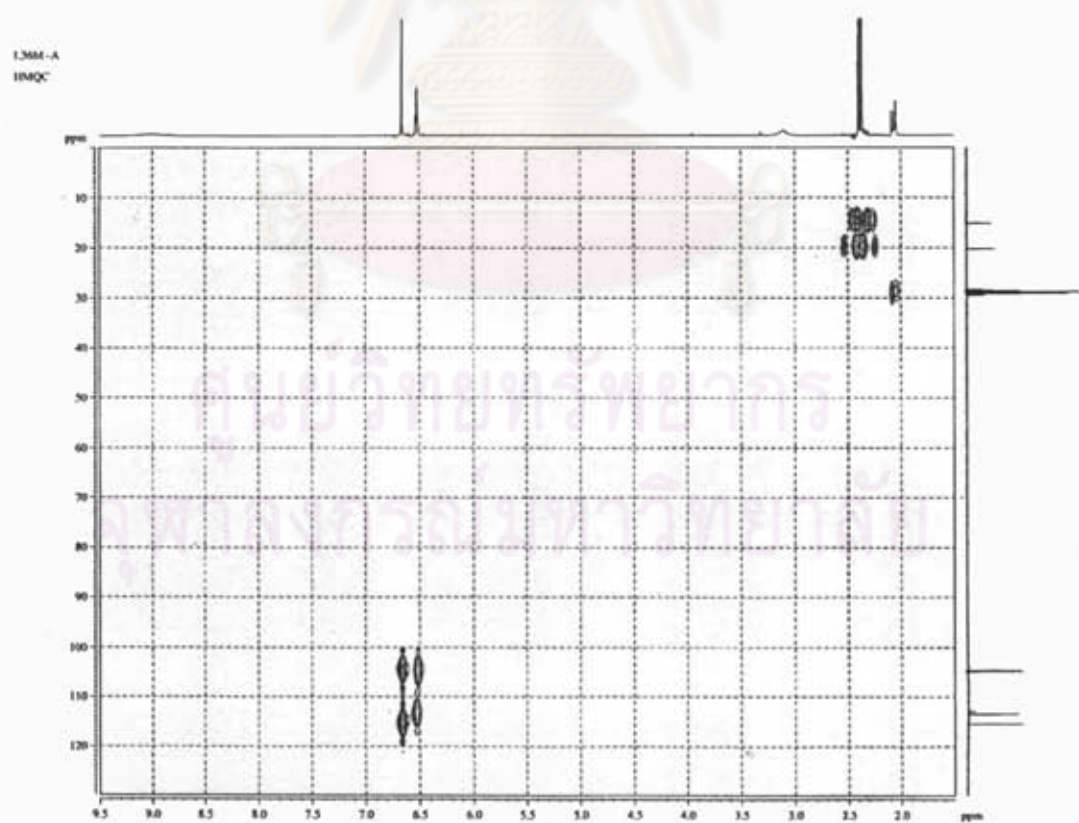
**Figure P8**  HMQC spectrum of corynesidone A (16)
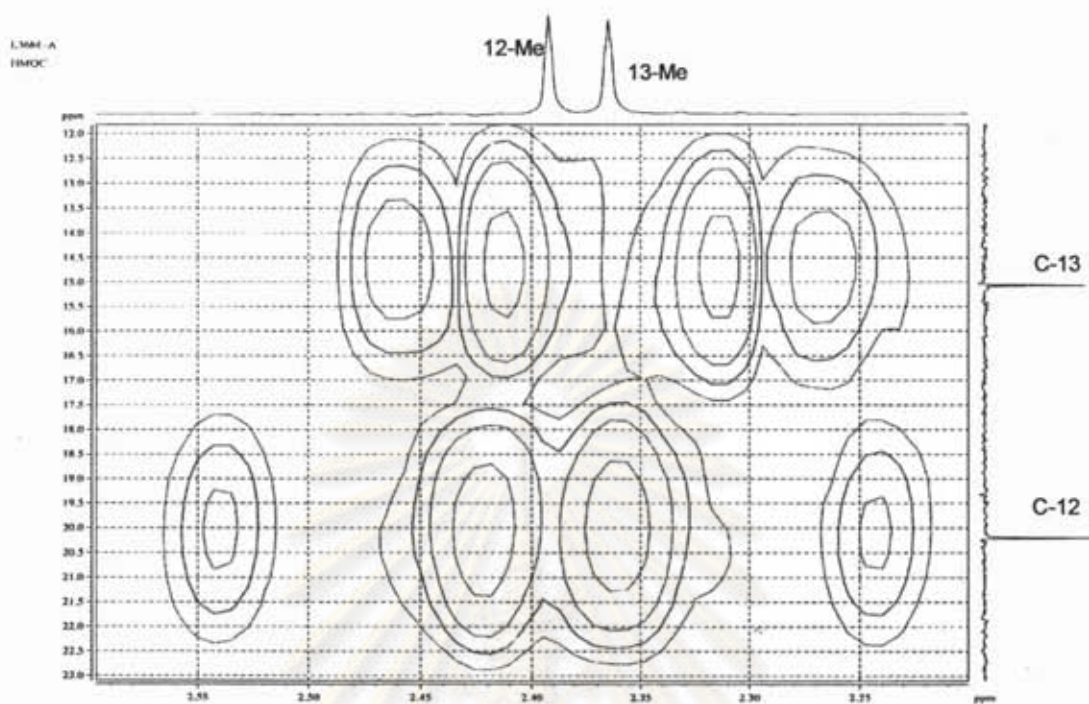
Figure P9    Expansion of Figure P8
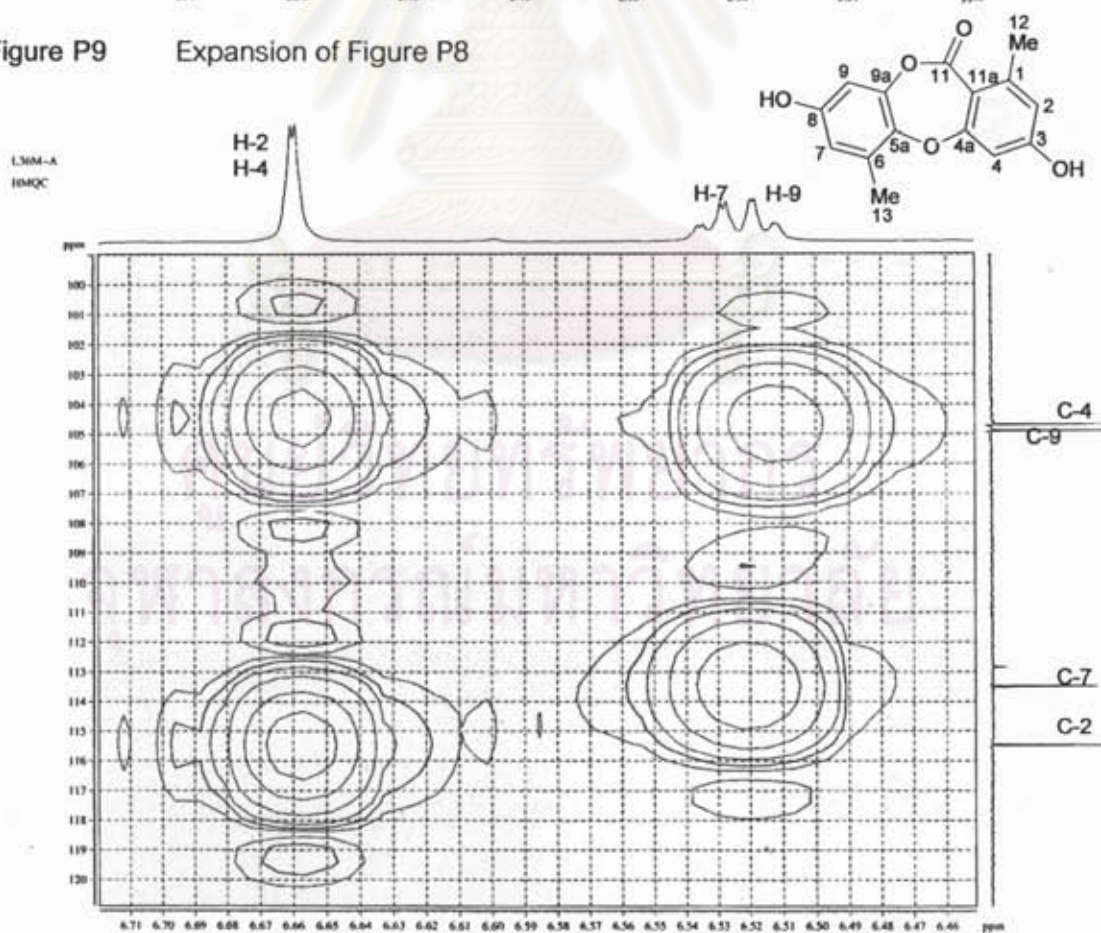


Figure P10    Expansion of Figure P8
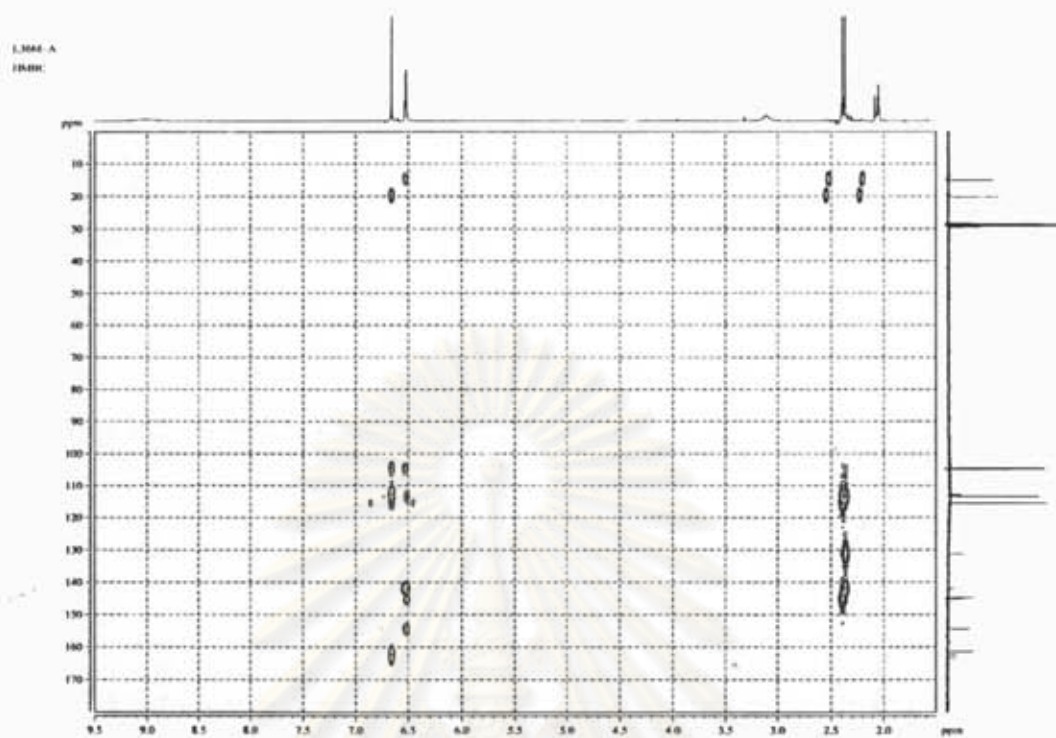
**Figure P11** HMBC spectrum of corynesidone A (16)
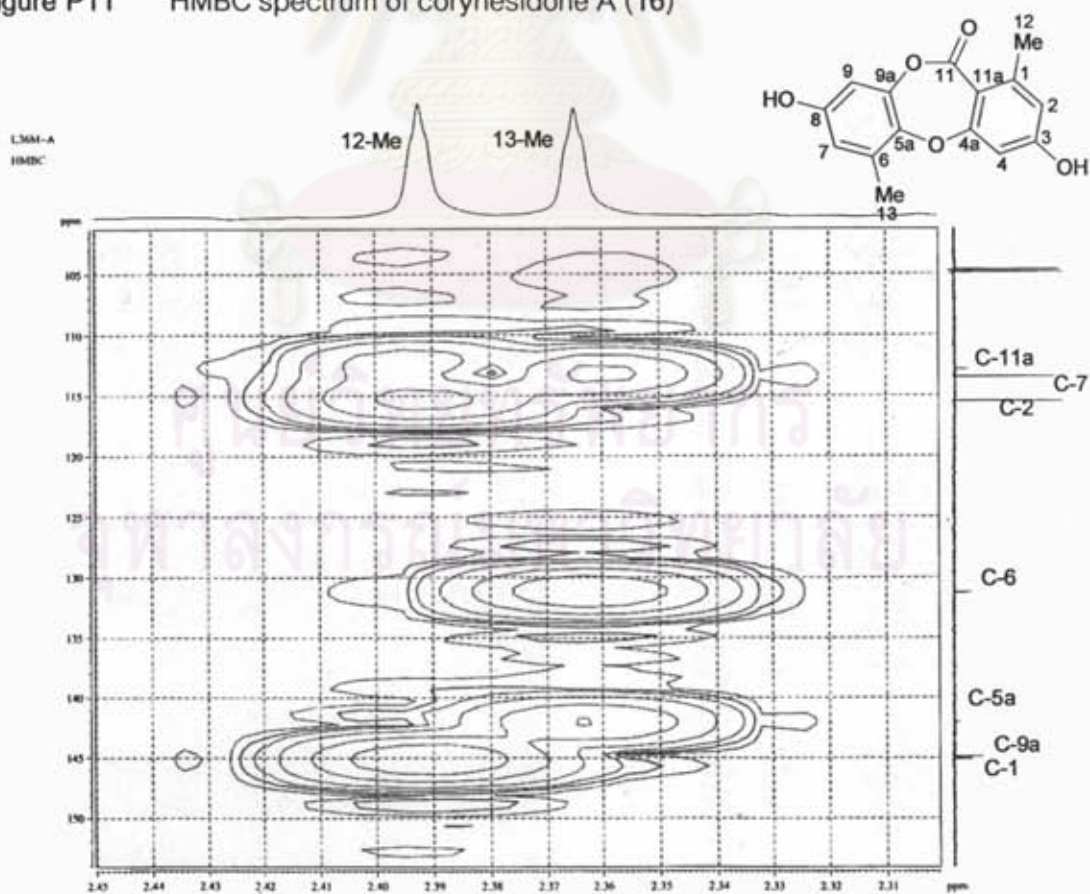


**Figure P12** Expansion of Figure P11
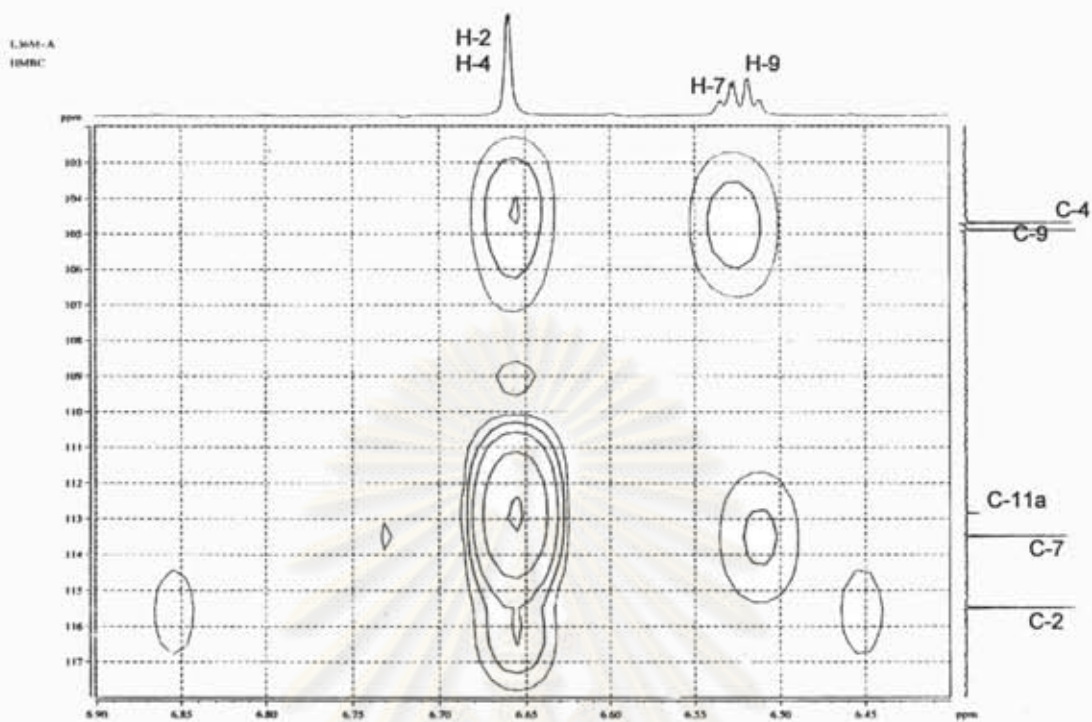
Figure P13    Expansion of Figure P11
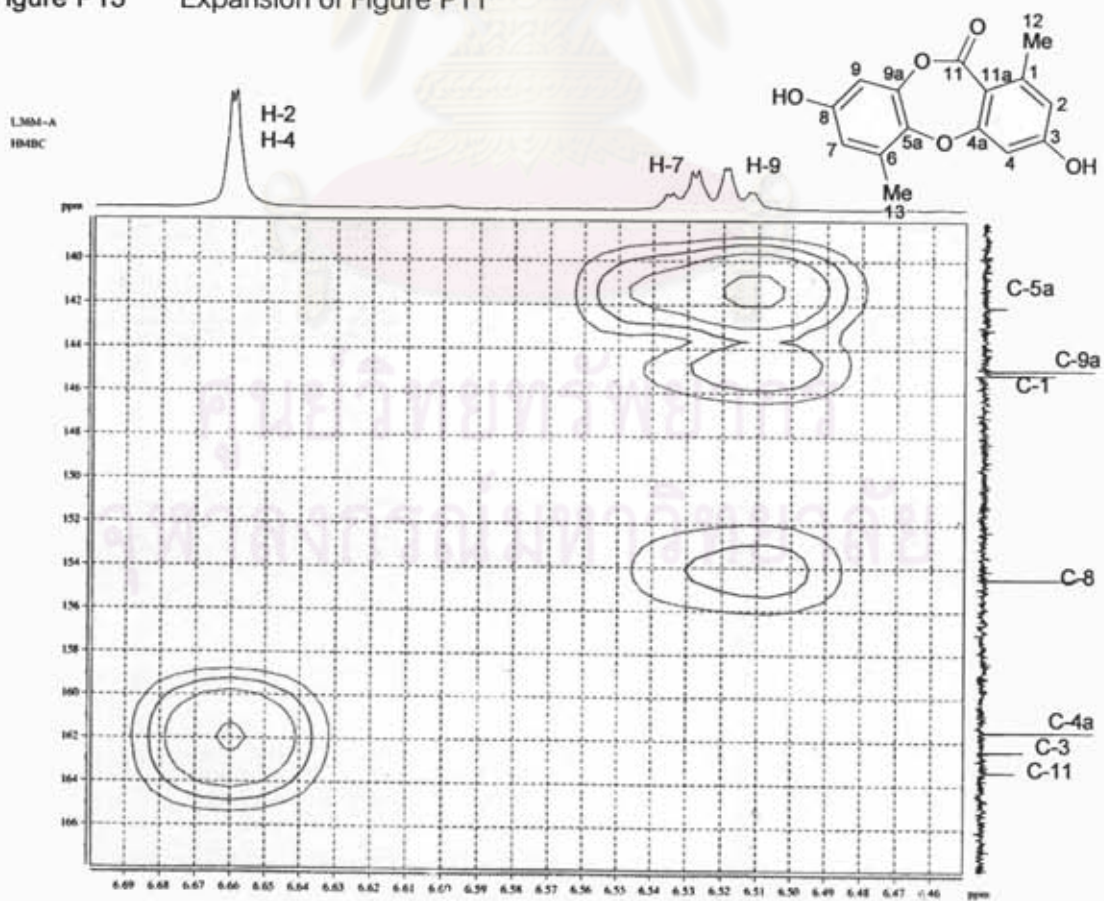


Figure P14    Expansion of Figure P11
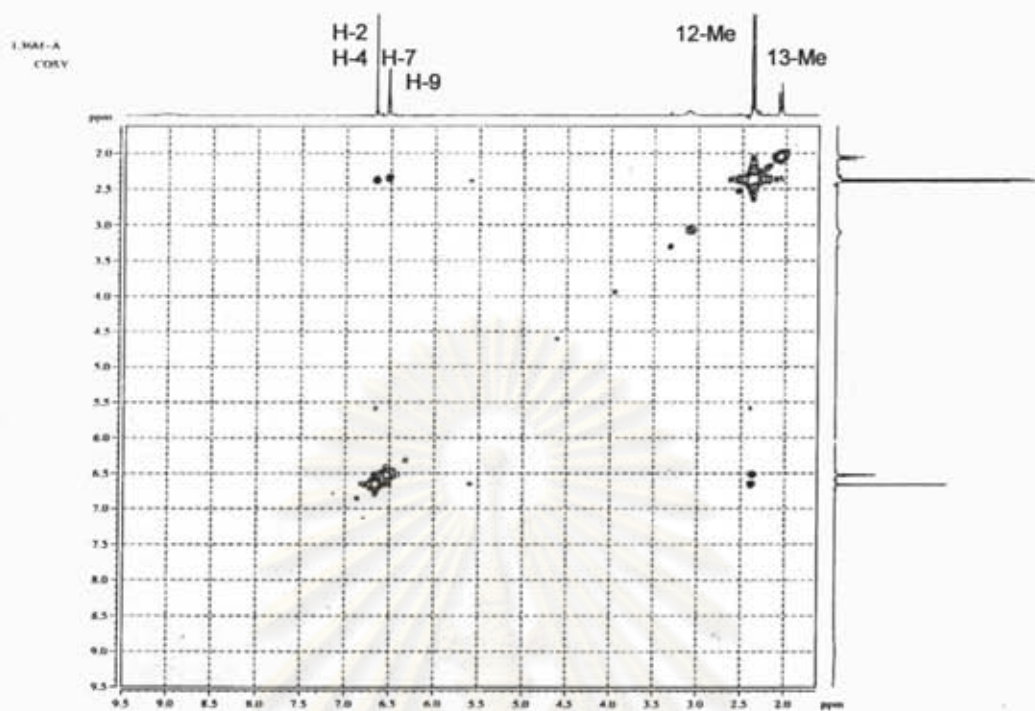
Figure P15    $^1$H-$^1$H COSY spectrum of corynesidone A (16)
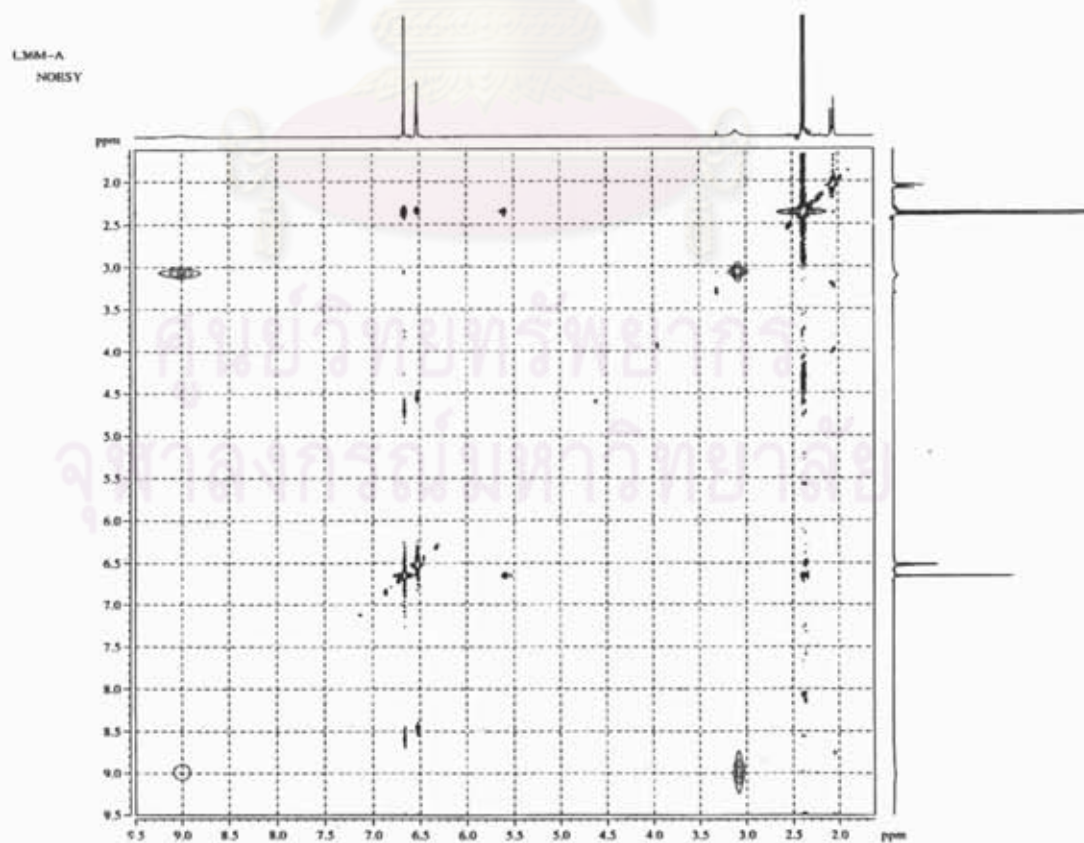


Figure P16    NOESY spectrum of corynesidone A (16)
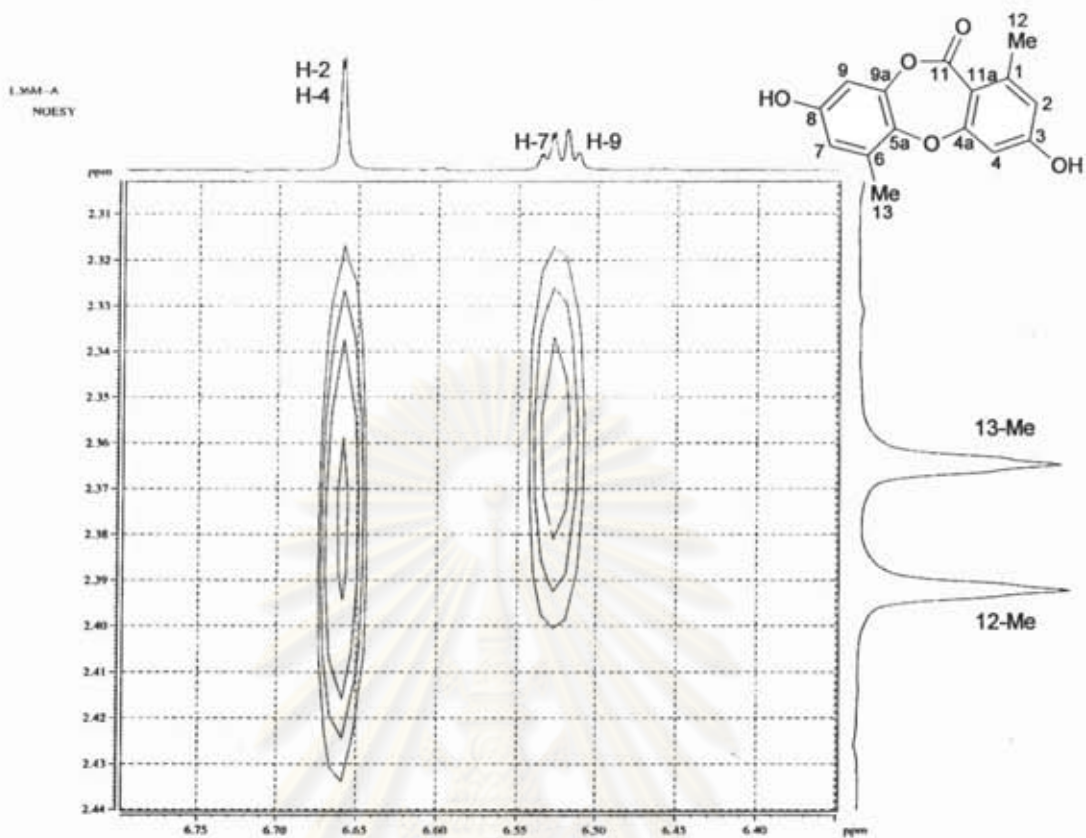
**Figure P17**     Expansion of Figure P16
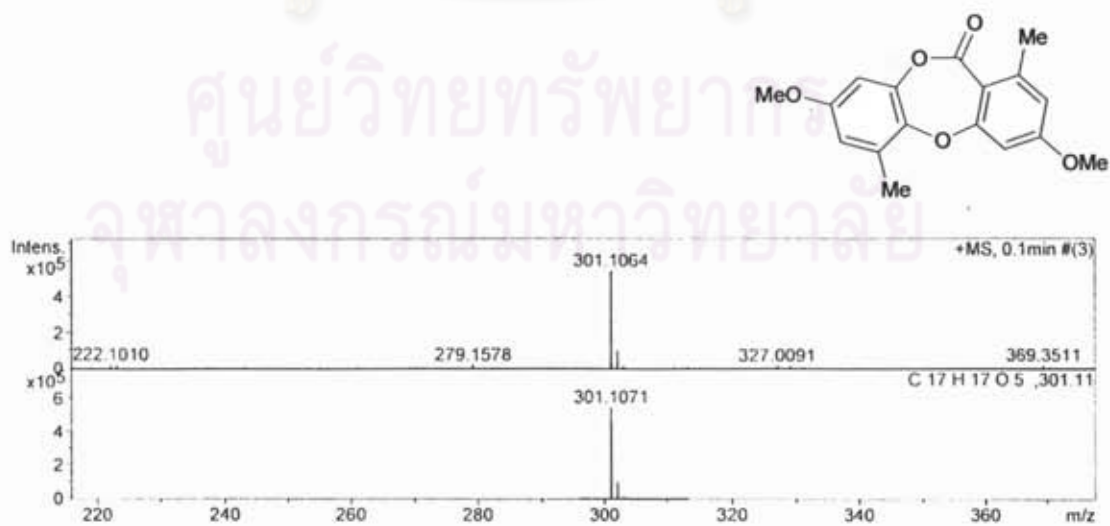


**Figure P18**     ESI-TOF spectrum of di-O-methyl derivative (17)
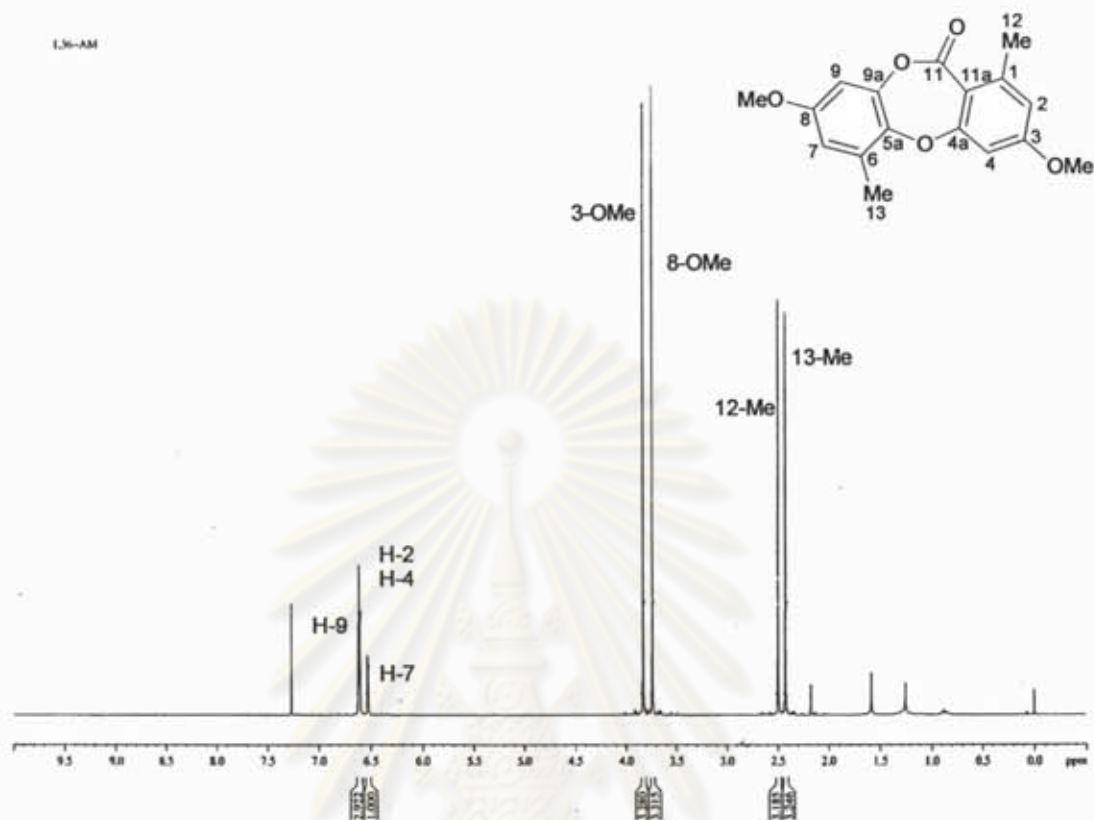
**Figure P19**  400 MHz ¹H NMR (CDCl₃) spectrum of di-O-methyl derivative (17)
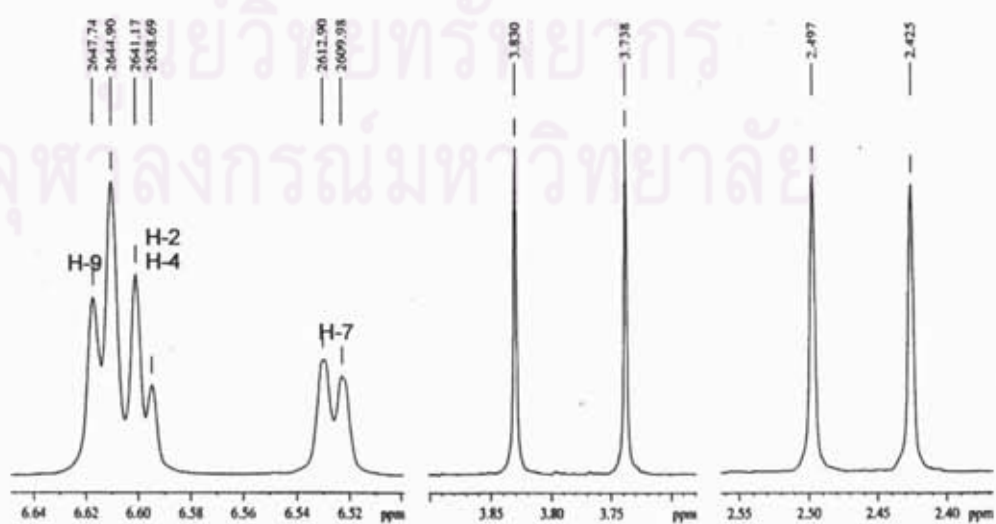


**Figure P20**  Expansion of Figure P19

Figure P21     $^{13}$C NMR (CDCl$_3$) spectrum of di-O-methyl derivative (17)



Figure P22     HMBC spectrum of di-O-methyl derivative (17)
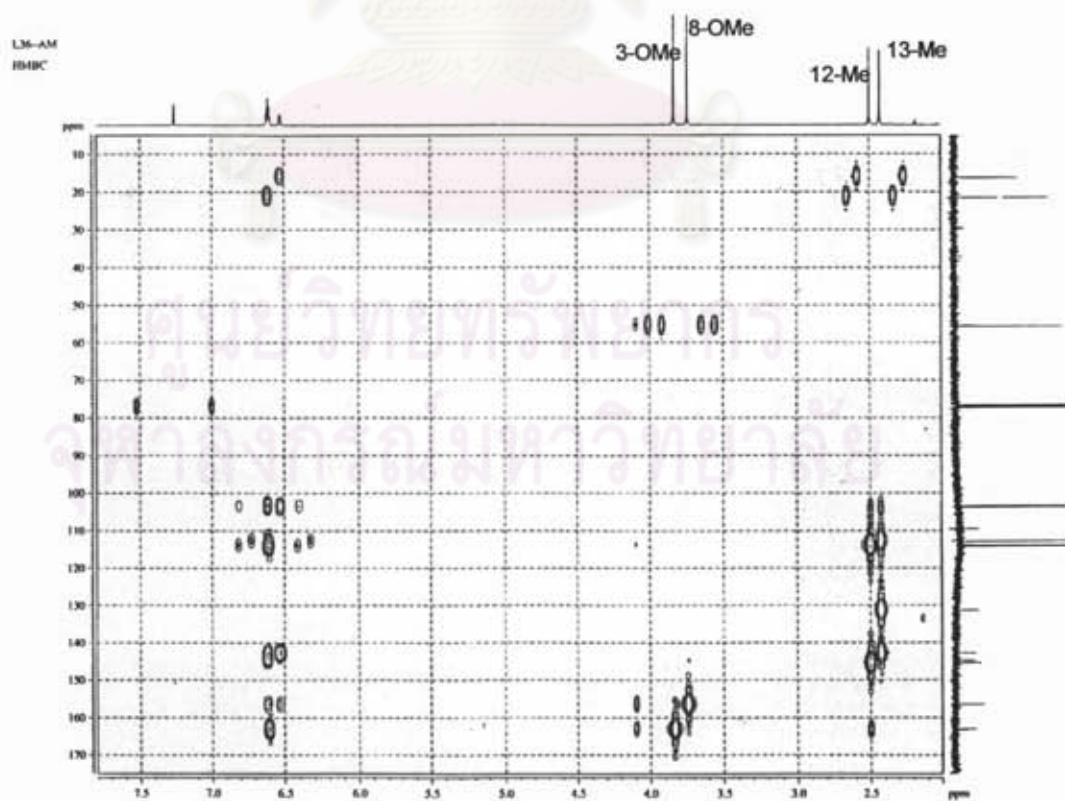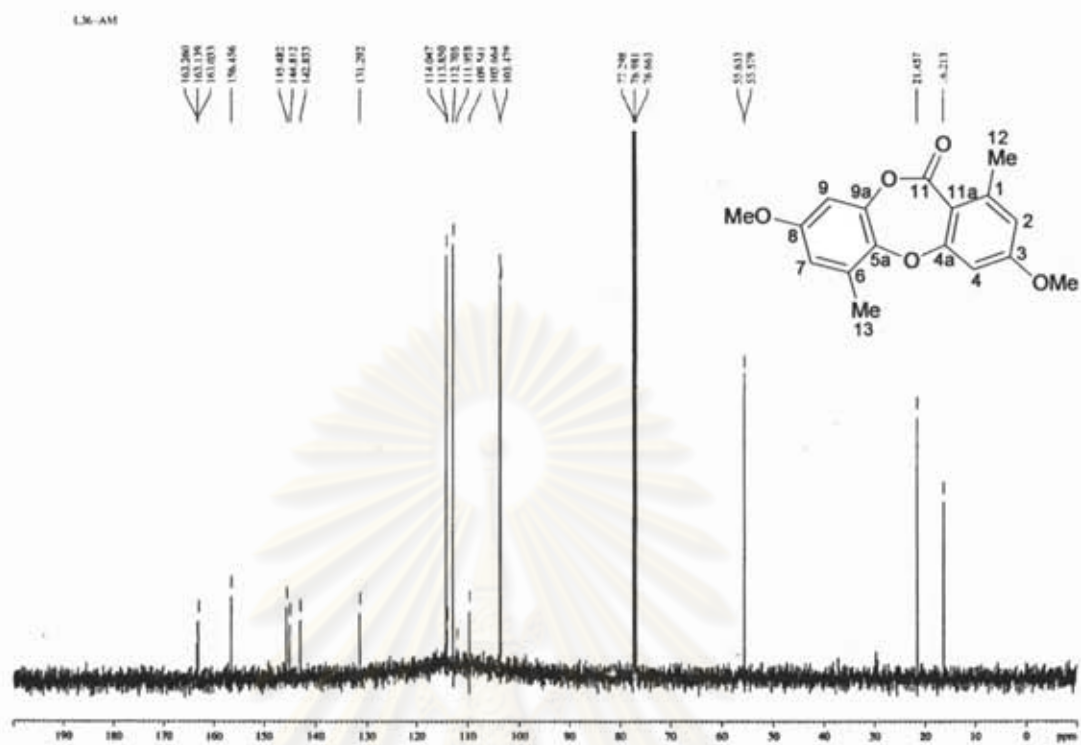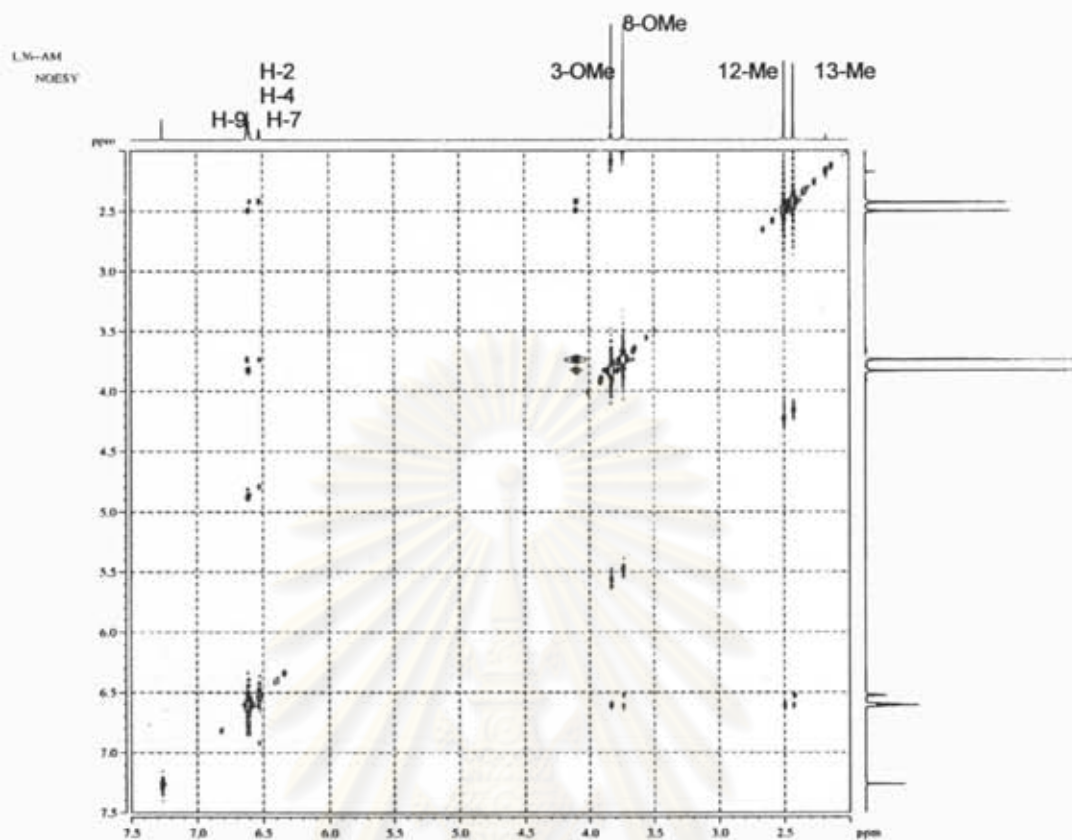
Figure P23    NOESY spectrum of di-O-methyl derivative (17)
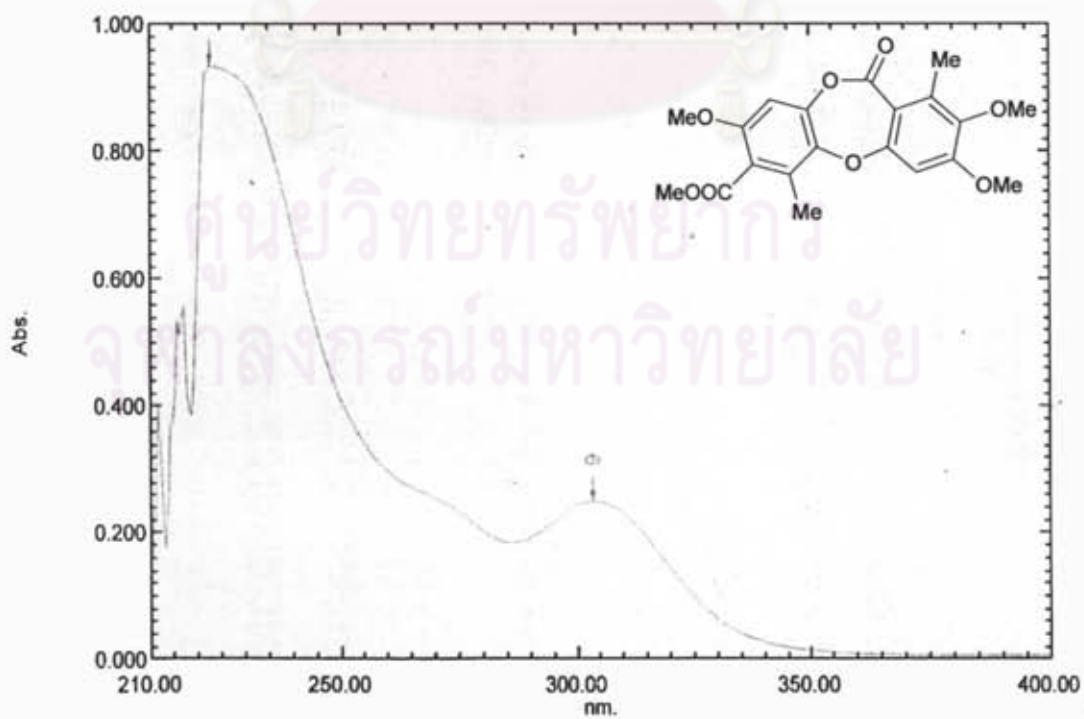


Figure P24    UV spectrum of corynesidone B (18)
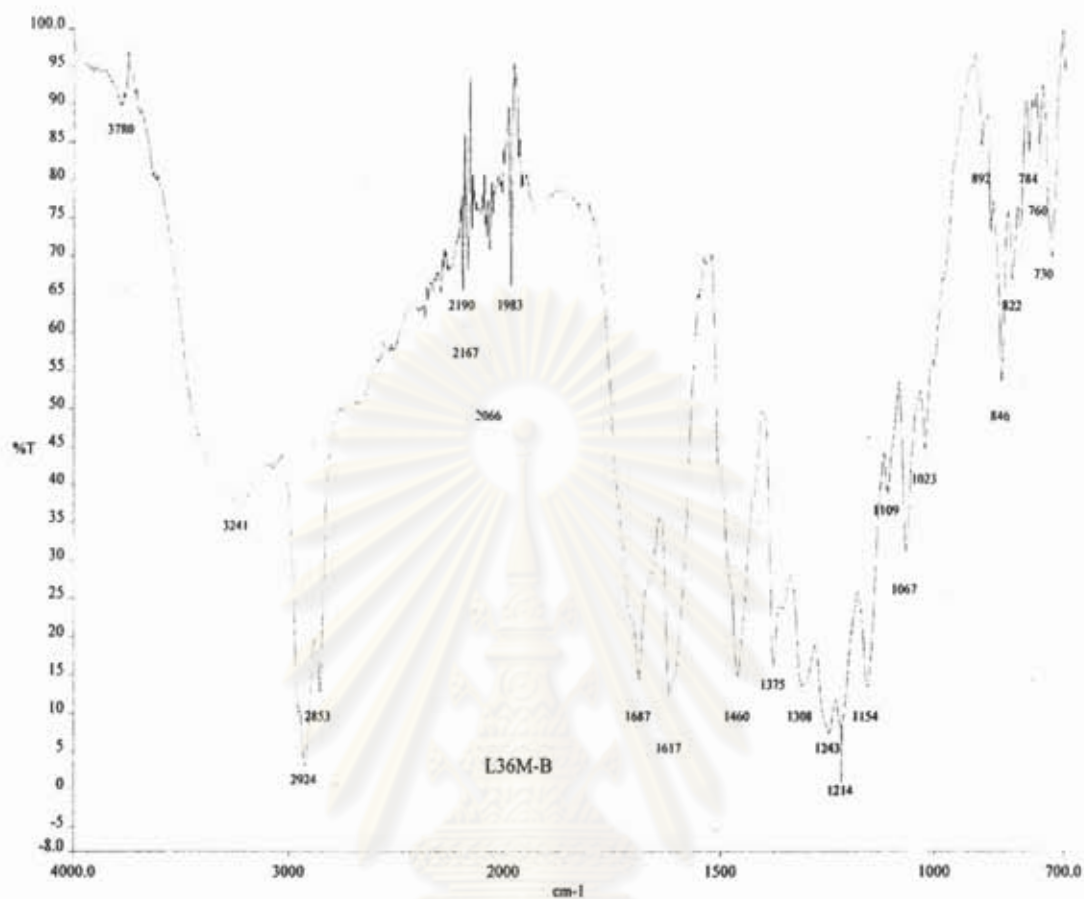
Figure P25    IR spectrum of corynesidone B (18)
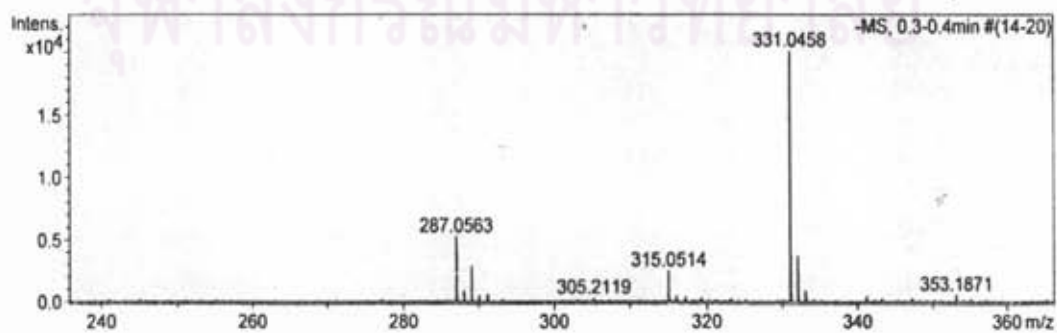


Figure D26    ESI-TOF spectrum of corynesidone B (18)
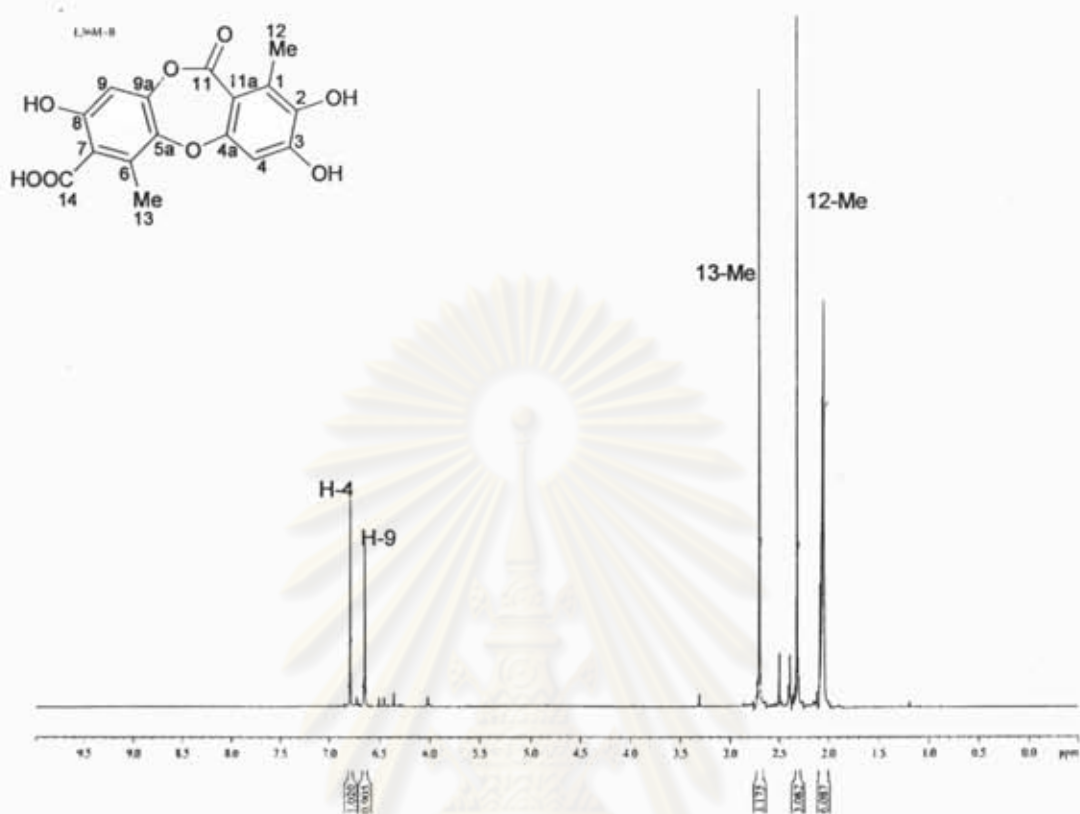
**Figure P27**     400 MHz ¹H NMR (Acetone-$d_6$) spectrum of corynesidone B (18)
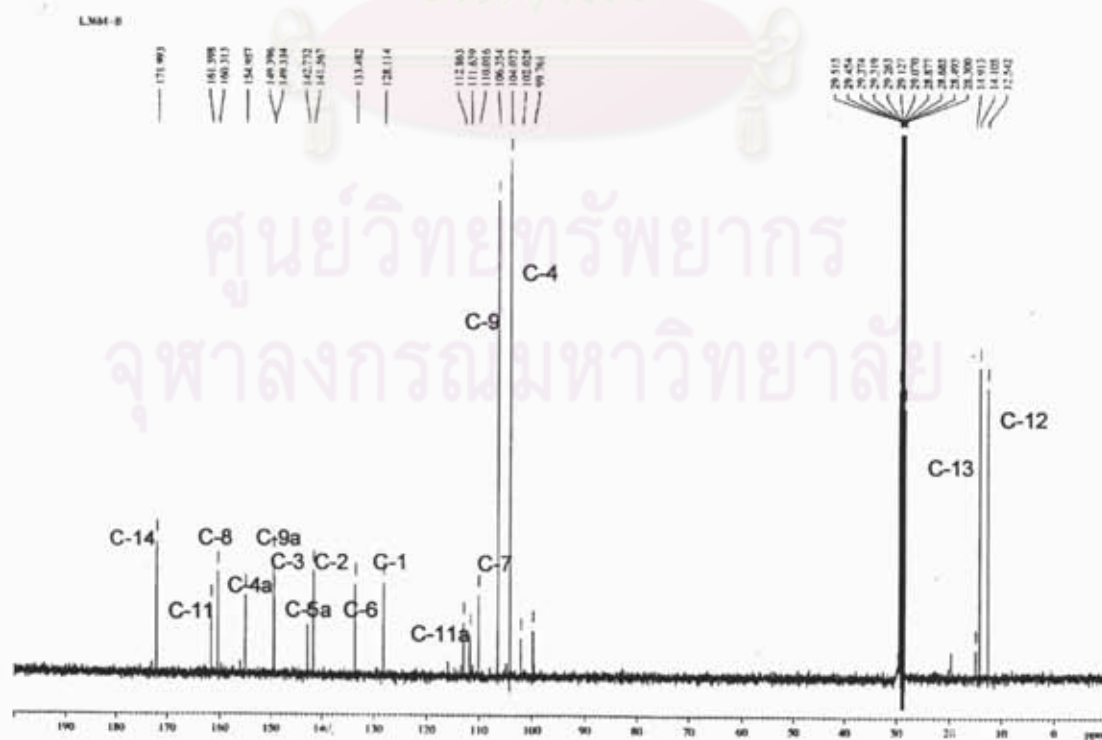


**Figure P28**     ¹³C NMR (Acetone-$d_6$) spectrum of corynesidone B (18)
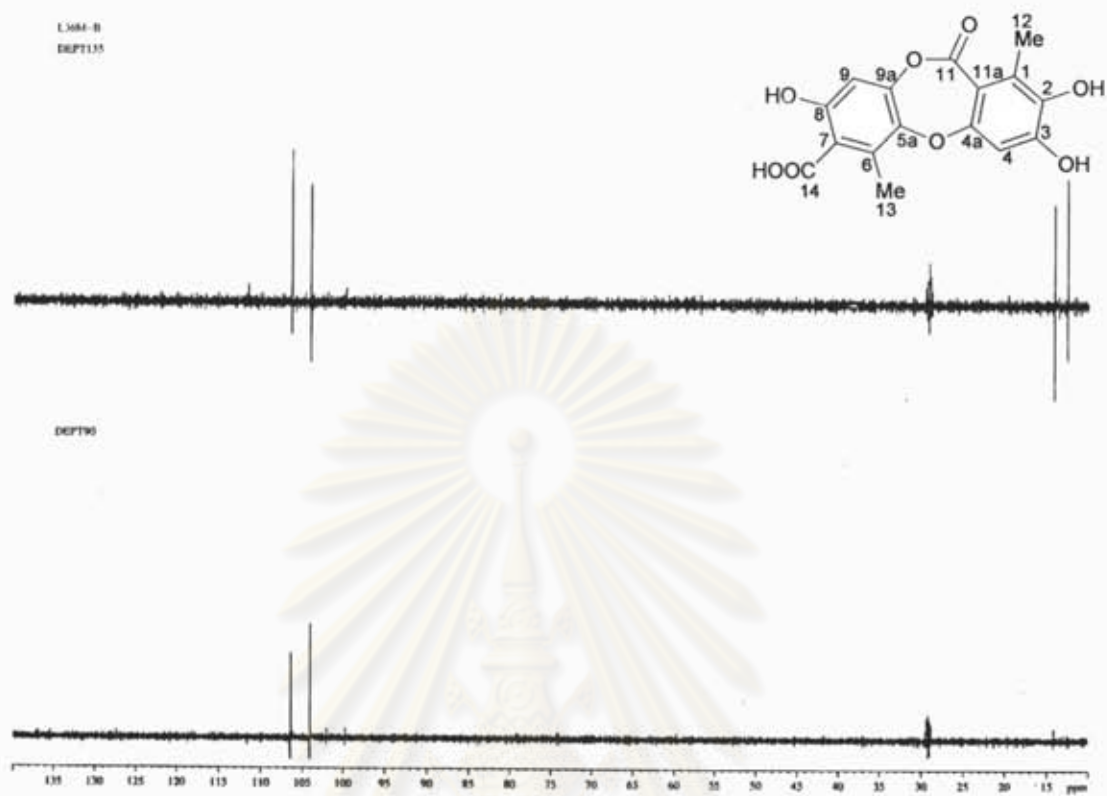
Figure P29    DEPT spectrum of corynesidone B (18)
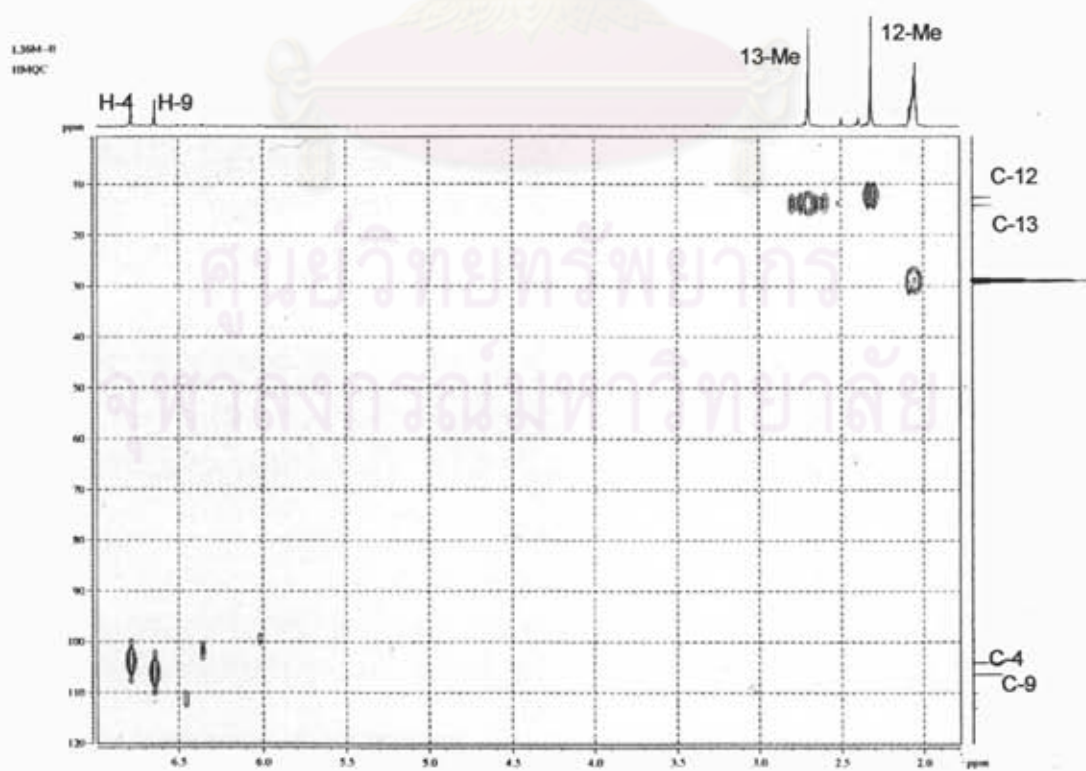


Figure P30    HMQC spectrum of corynesidone B (18)
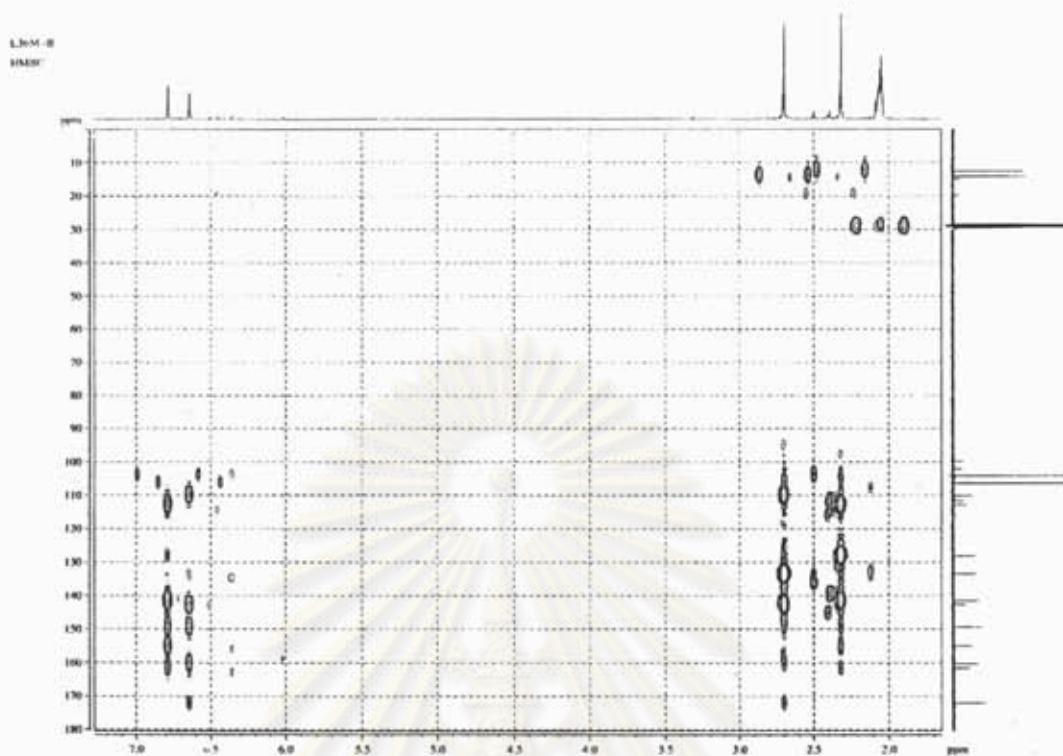
Figure P31    HMBC spectrum of corynesidone B (18)
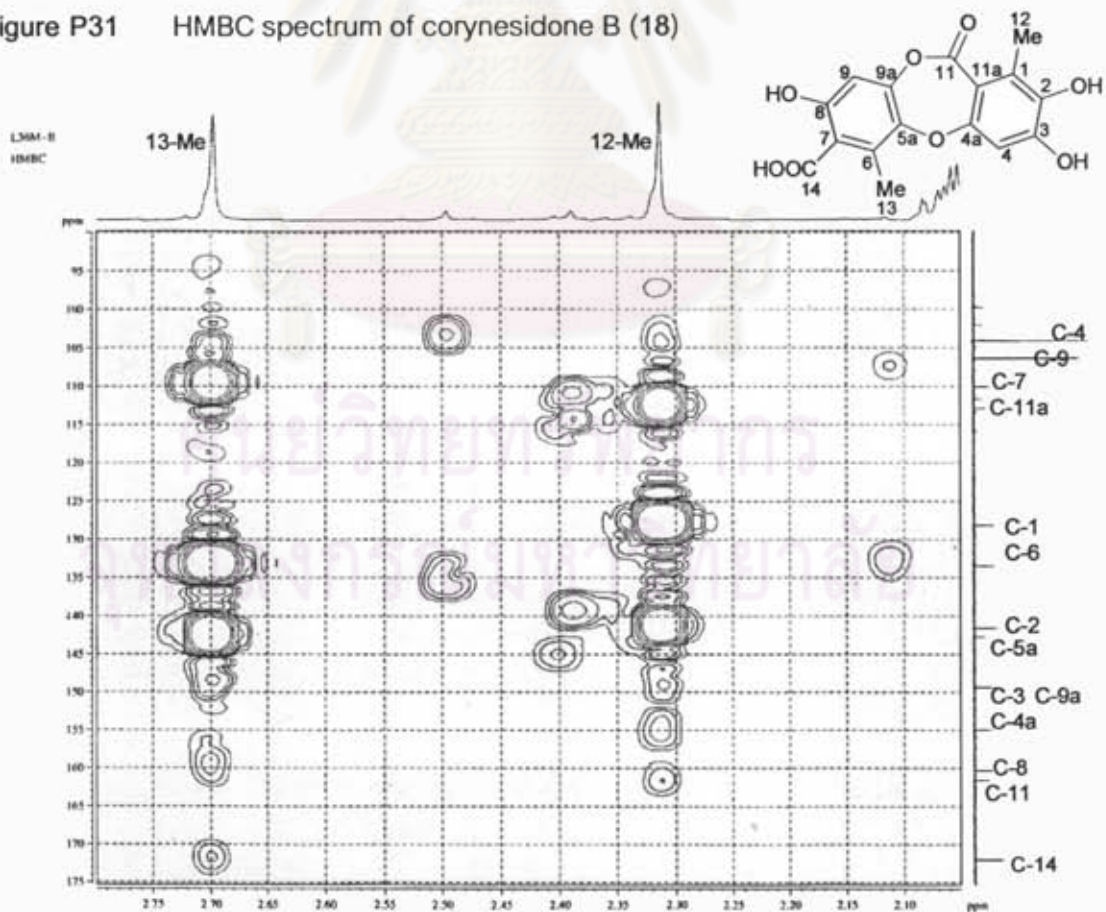


Figure P32    Expansion of Figure P31
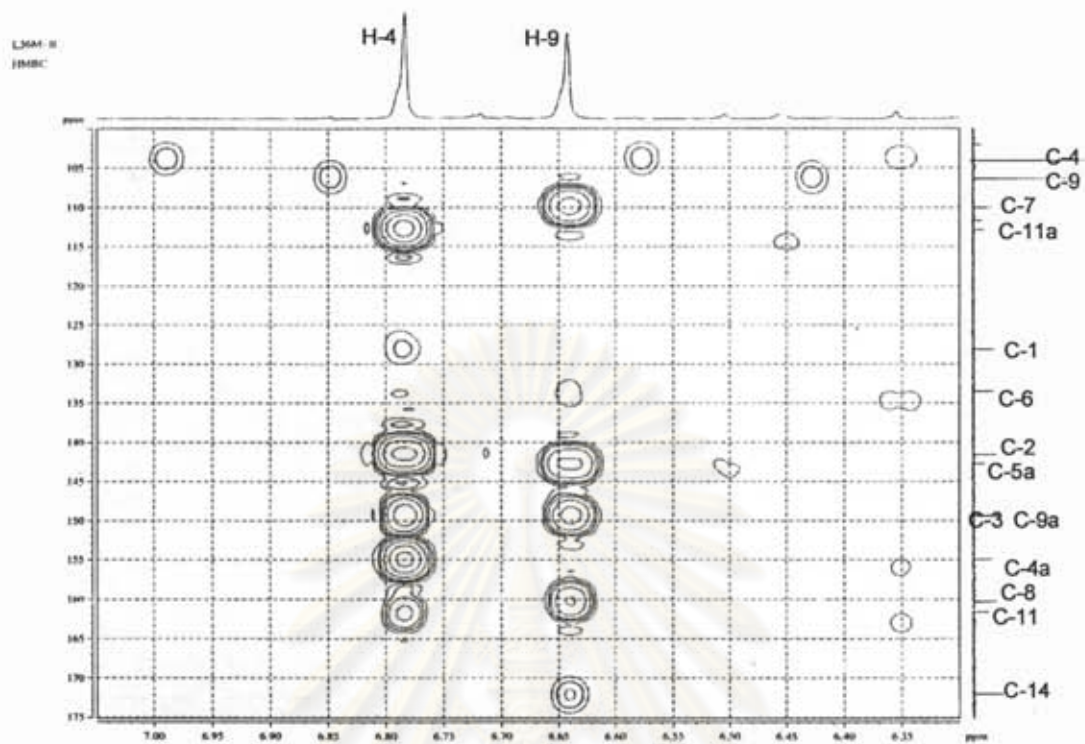
Figure P33   Expansion of Figure P31
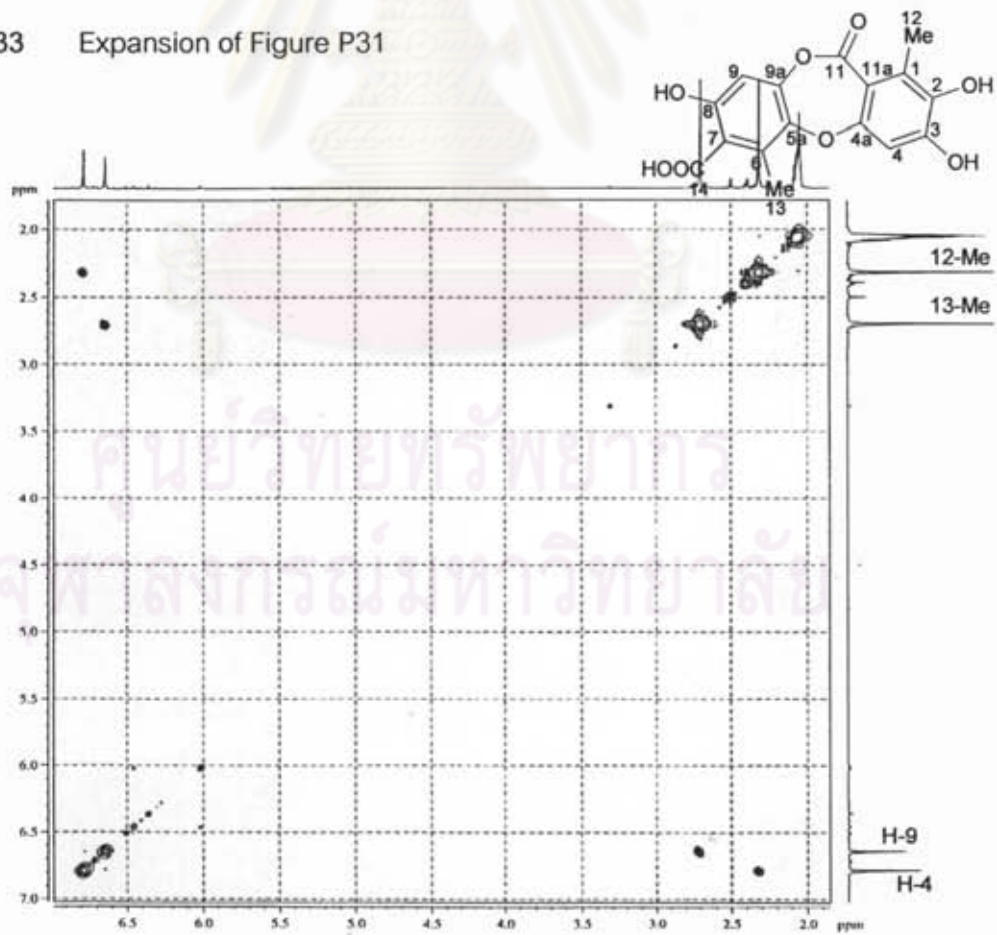


Figure P34   COSY spectrum of corynesidone B (18)
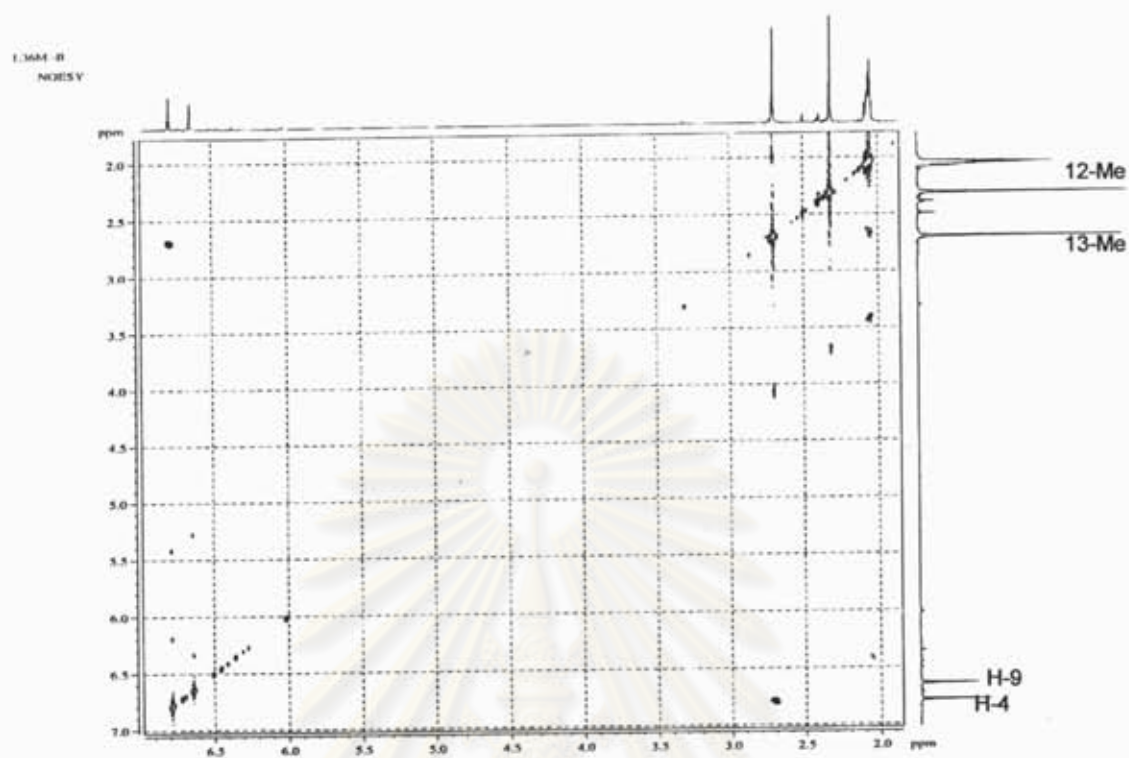
**Figure P35**     NOESY spectrum of corynesidone B (18)
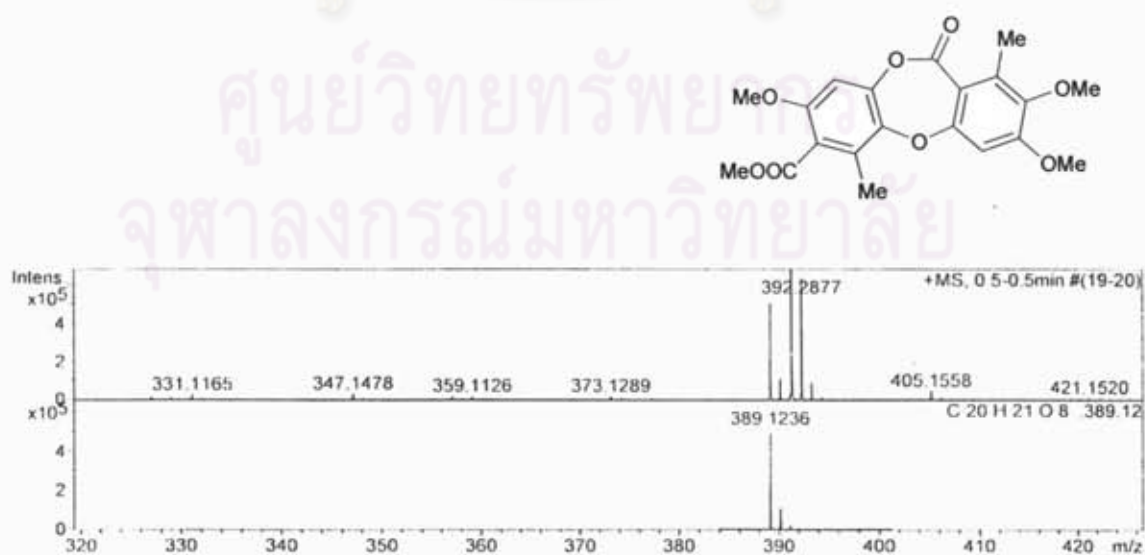


**Figure P36**     ESI-TOF spectrum of tetra-O-methyl derivative (19)
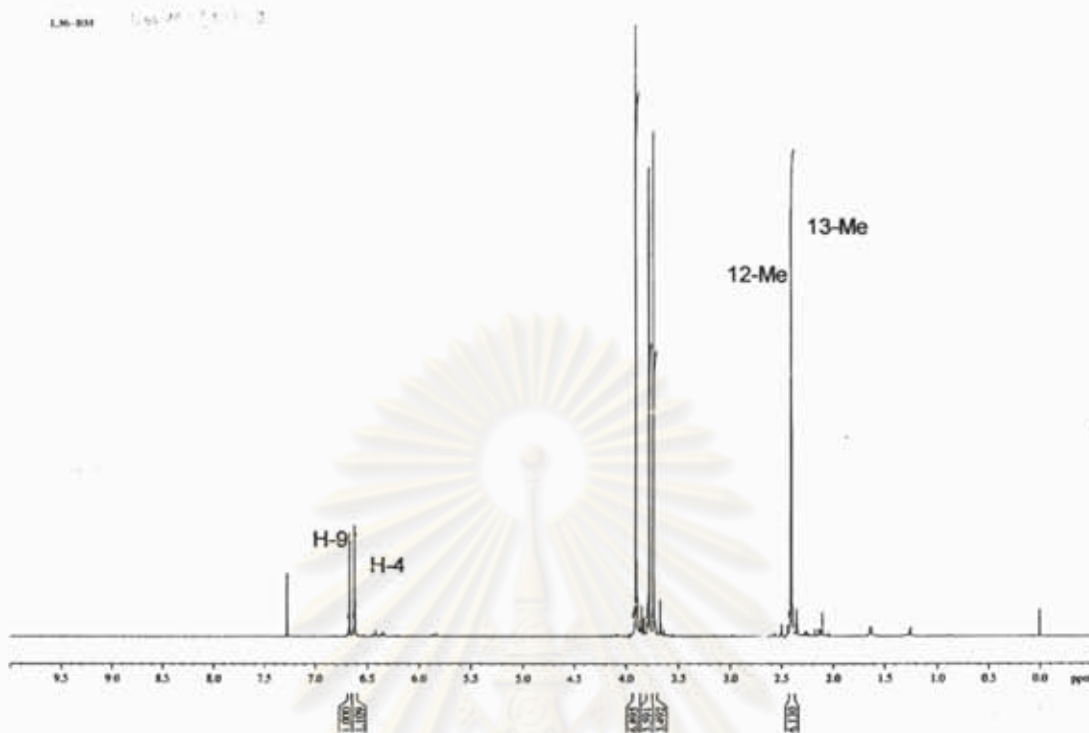
Figure P37     400 MHz $^{1}$H NMR (CDCl$_3$) spectrum of tetra-O-methyl derivative (19)
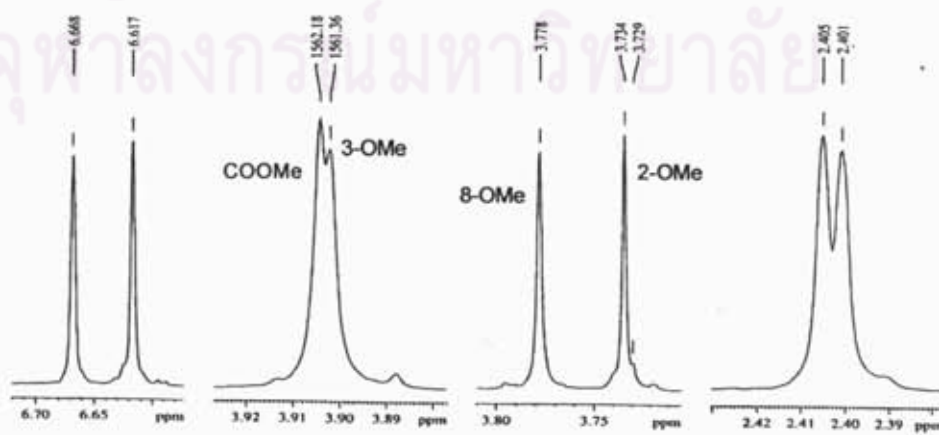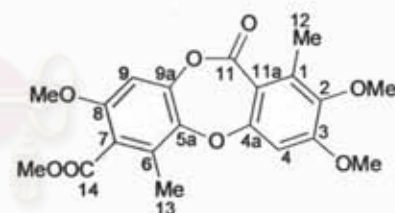




Figure P38     Expansion of Figure P37
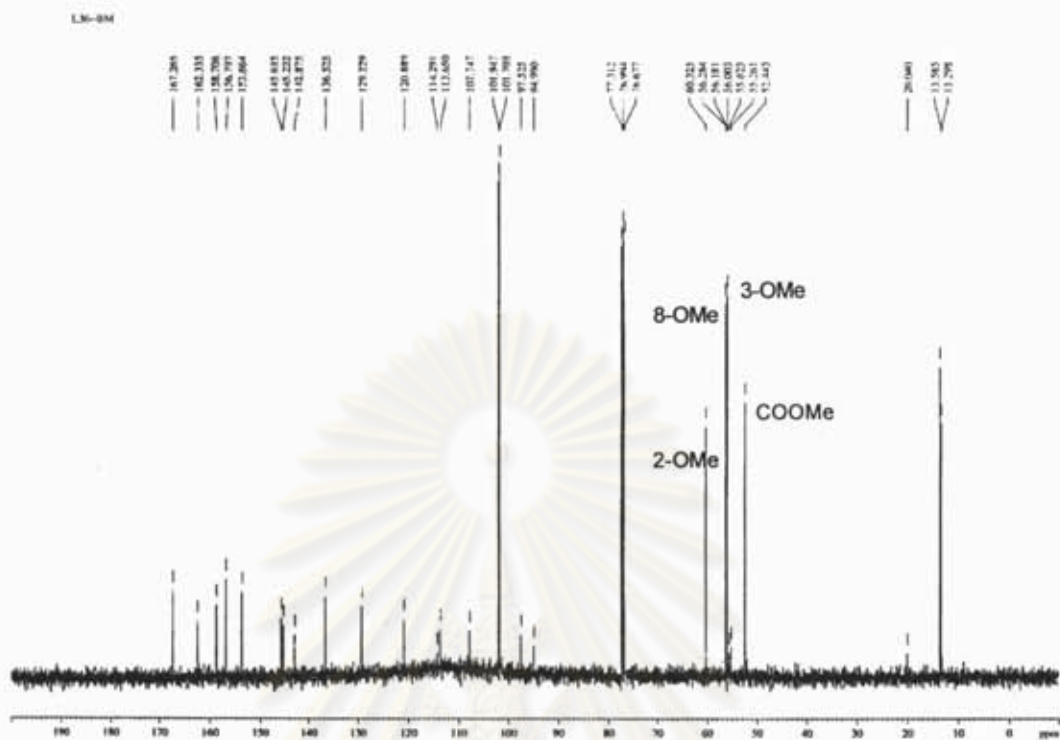
Figure P39    $^{13}$C NMR (CDCl$_3$) spectrum of tetra-O-methyl derivative (19)
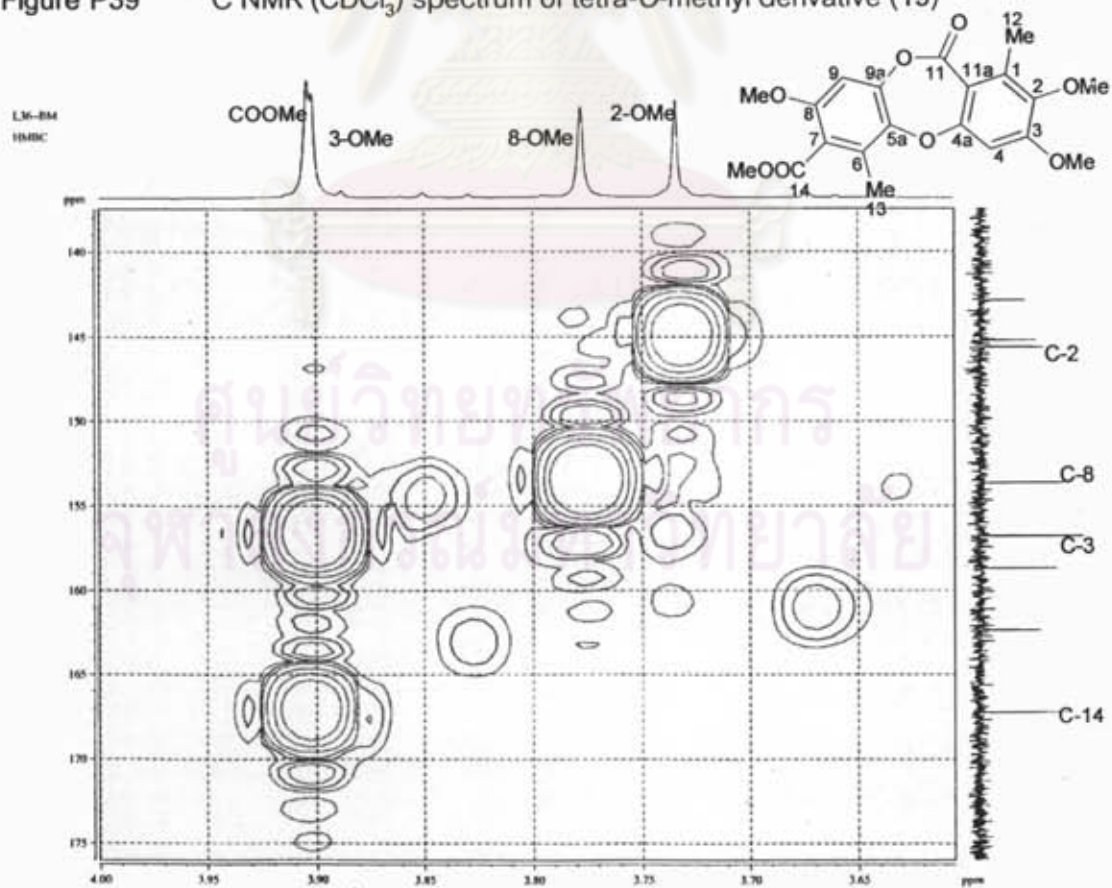


Figure P40    HMBC spectrum of tetra-O-methyl derivative (19)
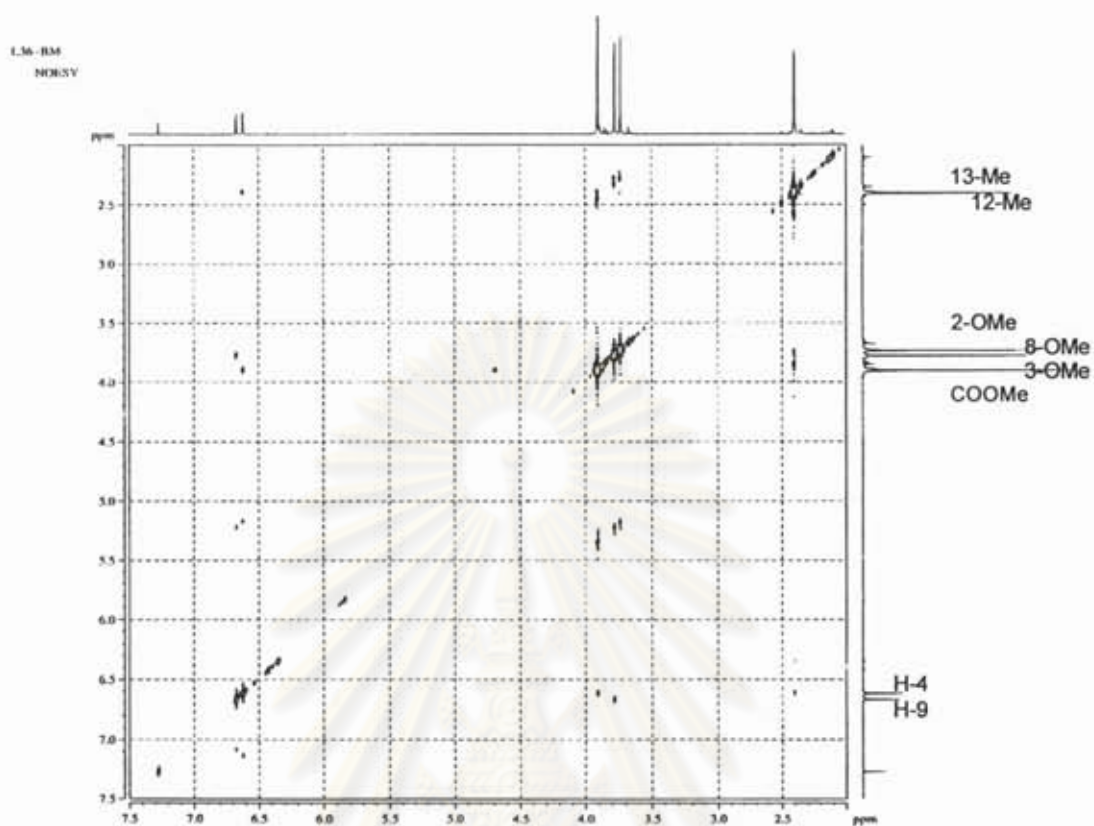
**Figure P41**    NOESY spectrum of tetra-*O*-methyl derivative (**19**)
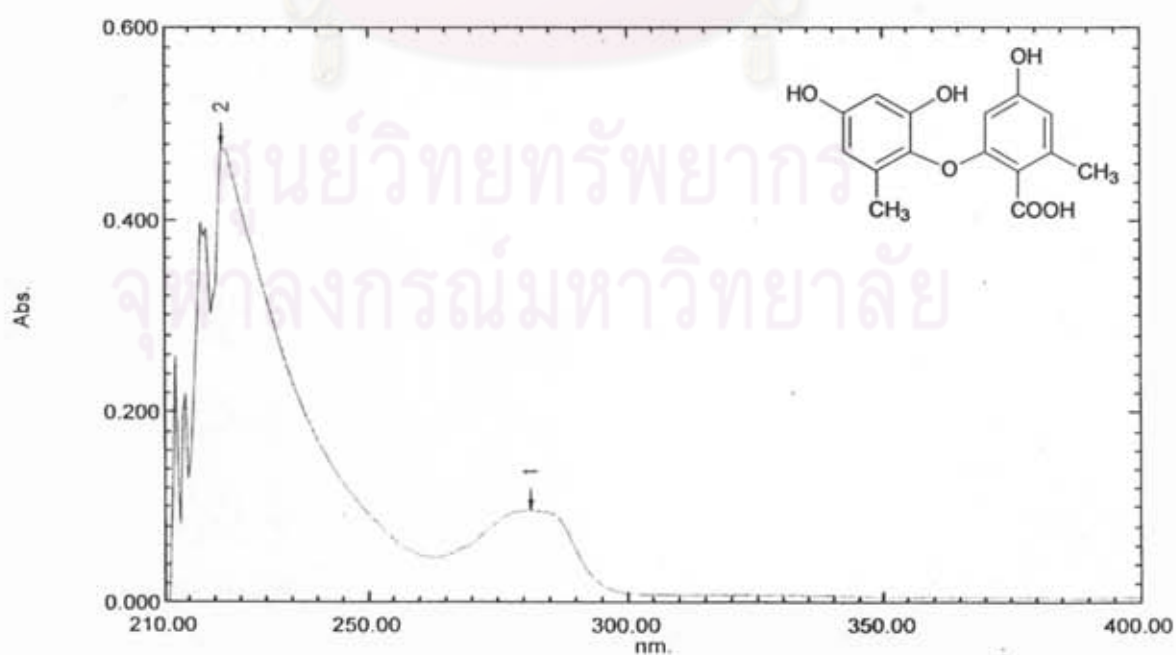


**Figure P42**    UV spectrum of corynether A (**20**)
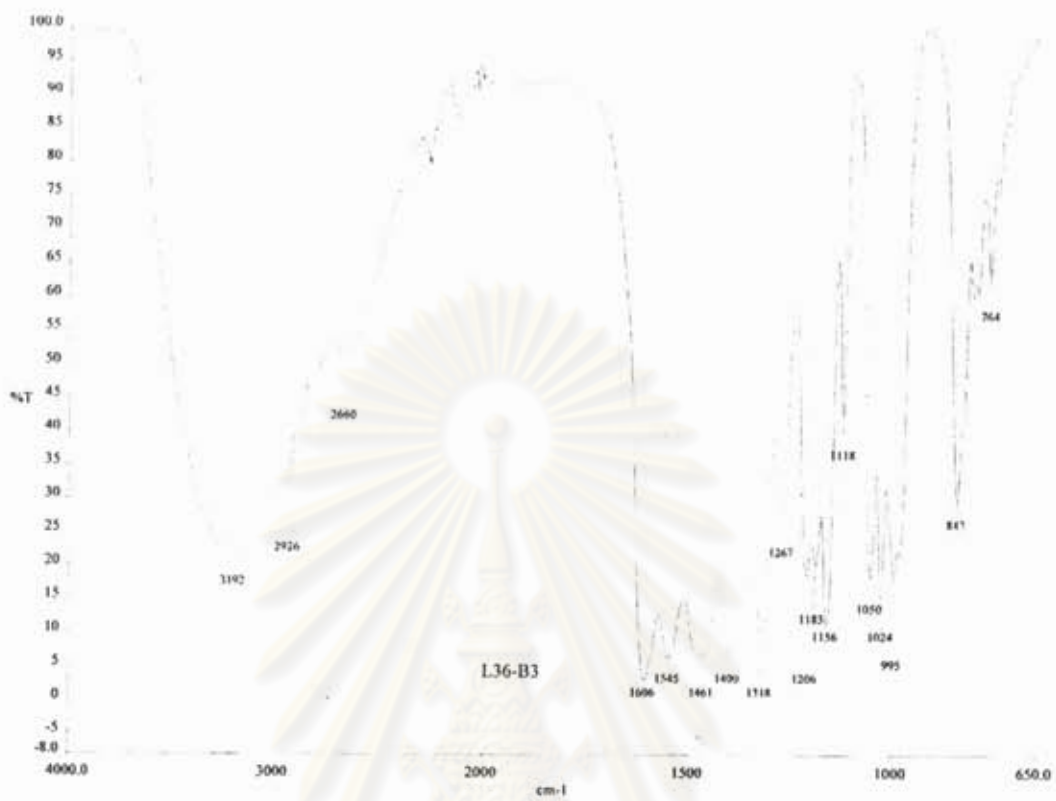
Figure P43     IR spectrum of corynether A (20)
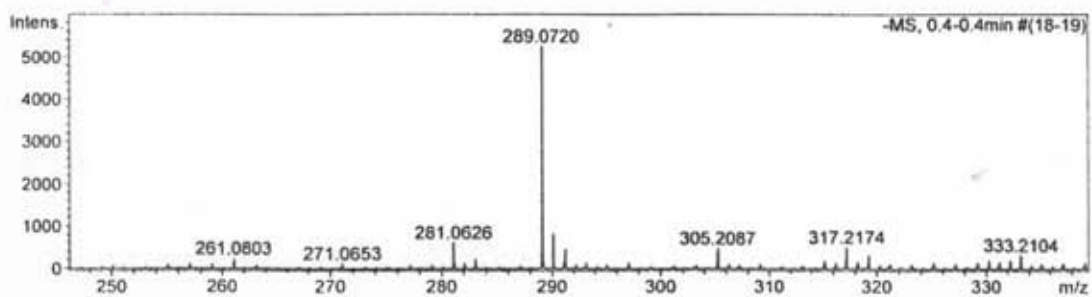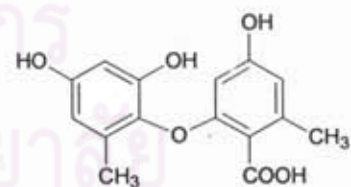


Figure P44     ESI-TOF spectrum of corynether A (20)
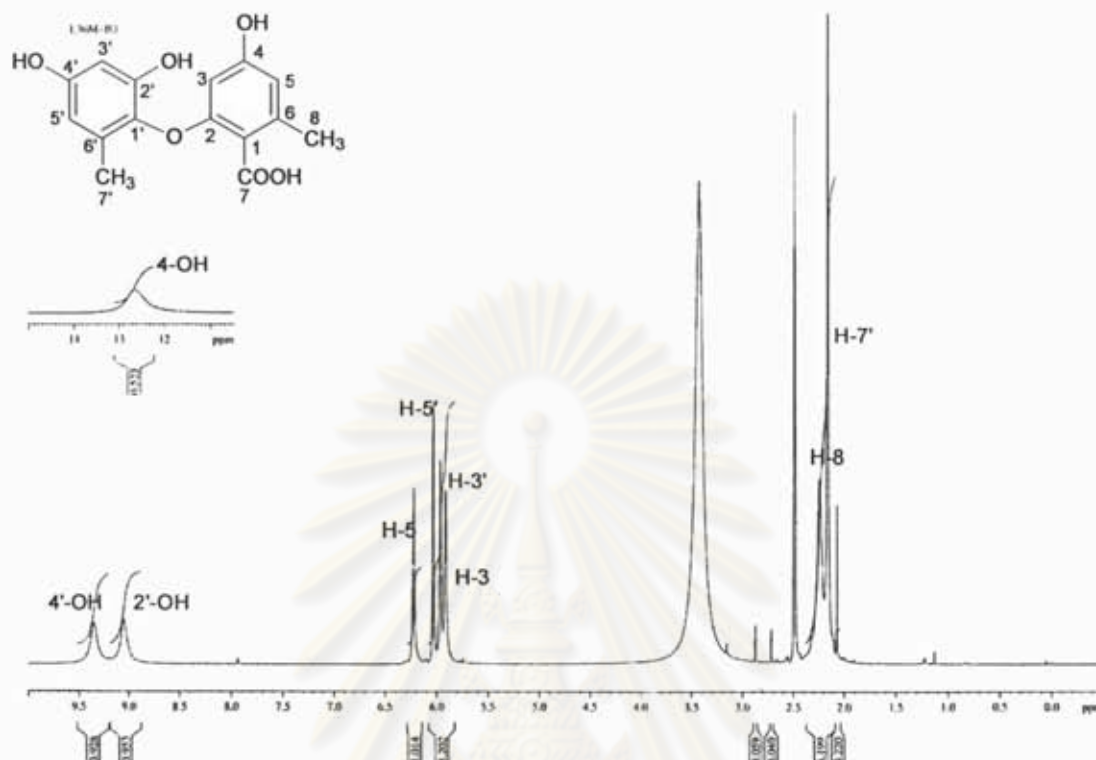
Figure P45    400 MHz $^1$H NMR (Acetone-$d_6$) spectrum of corynether A (20)
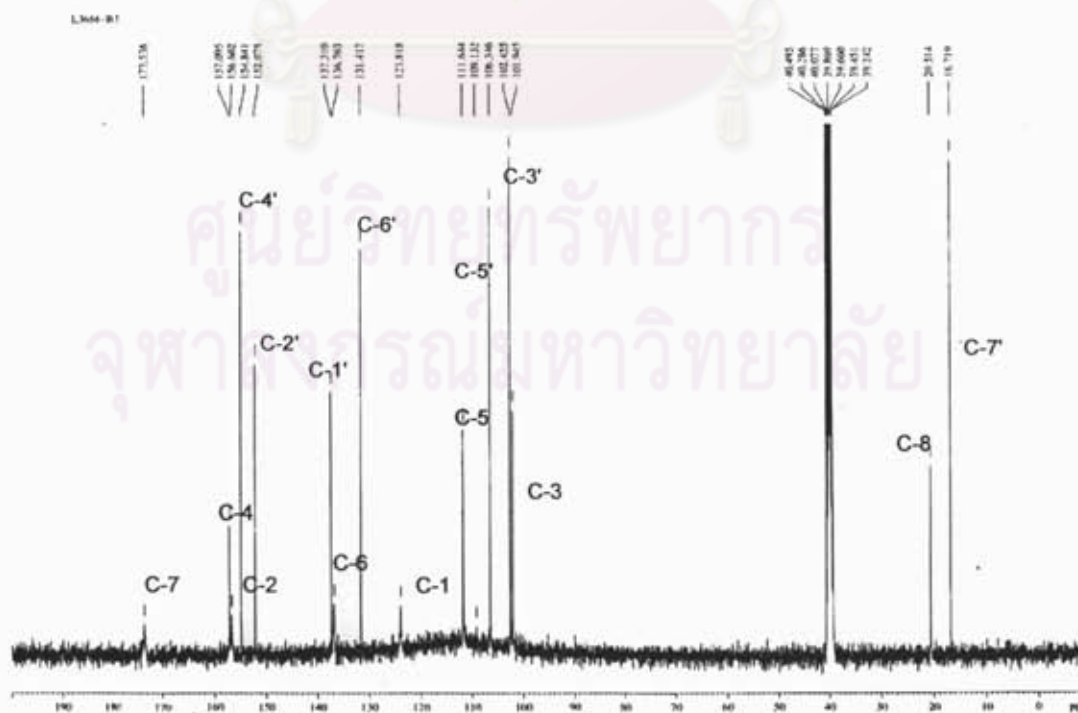


Figure P46    $^{13}$C NMR (Acetone-$d_6$) spectrum of corynether A (20)
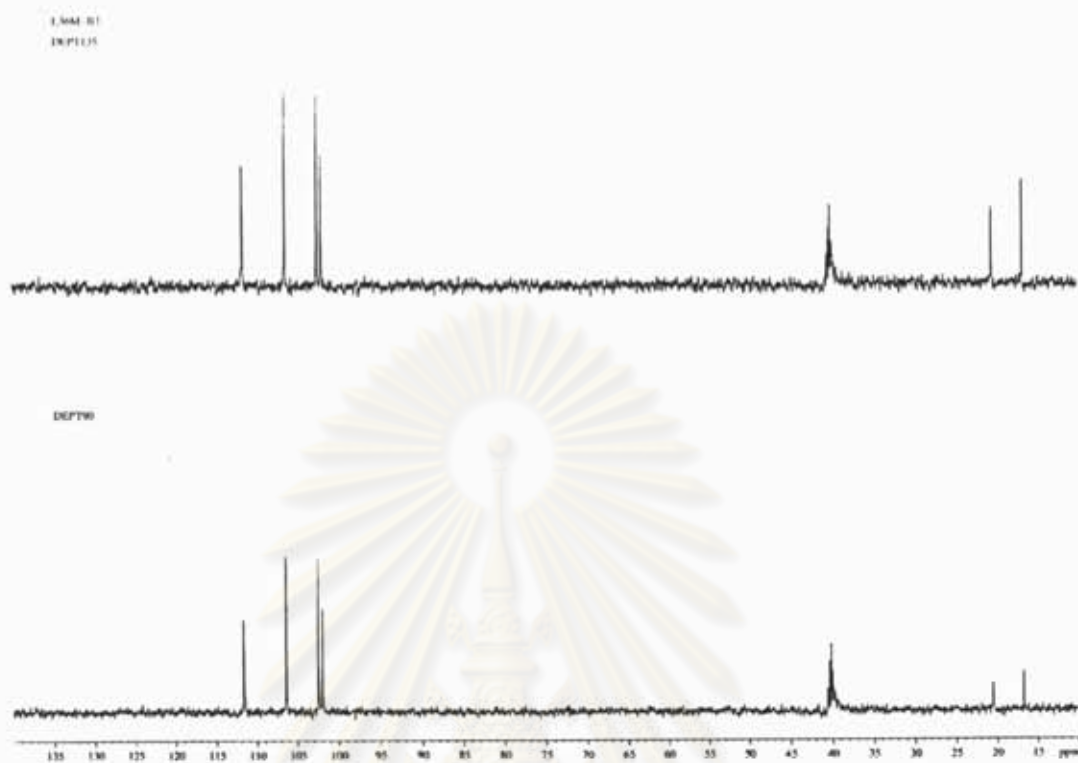
Figure P47    DEPT spectrum of corynether A (20)
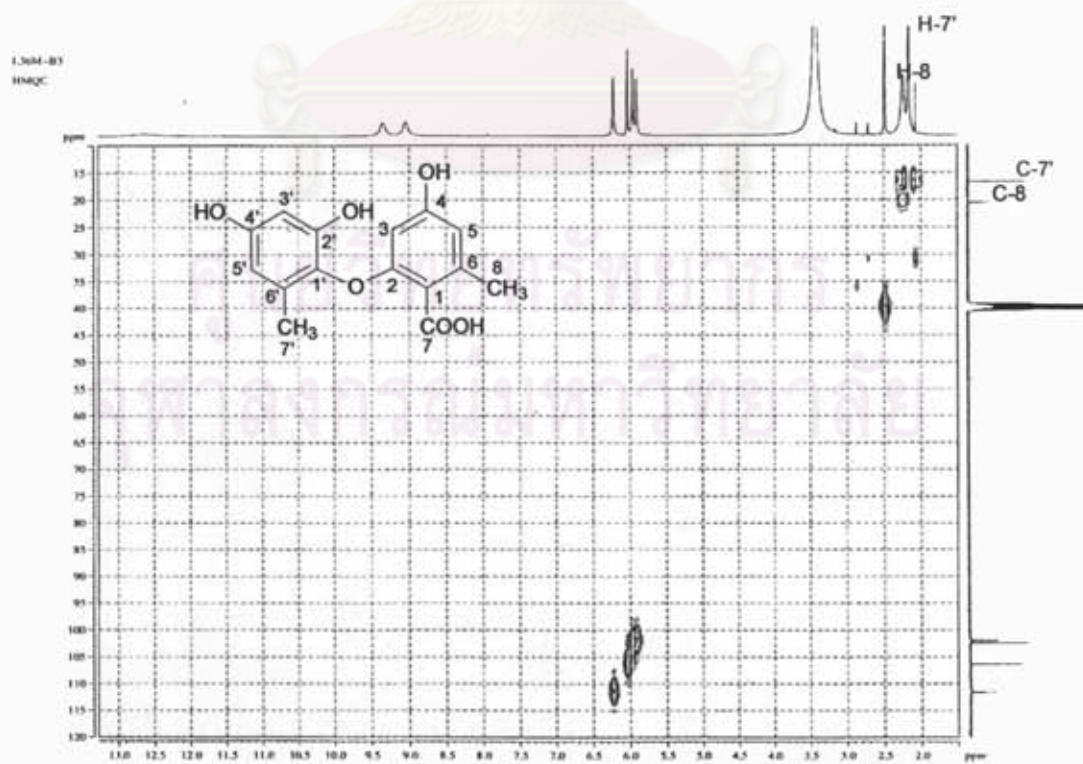


Figure P48    HMQC spectrum of corynether A (20)
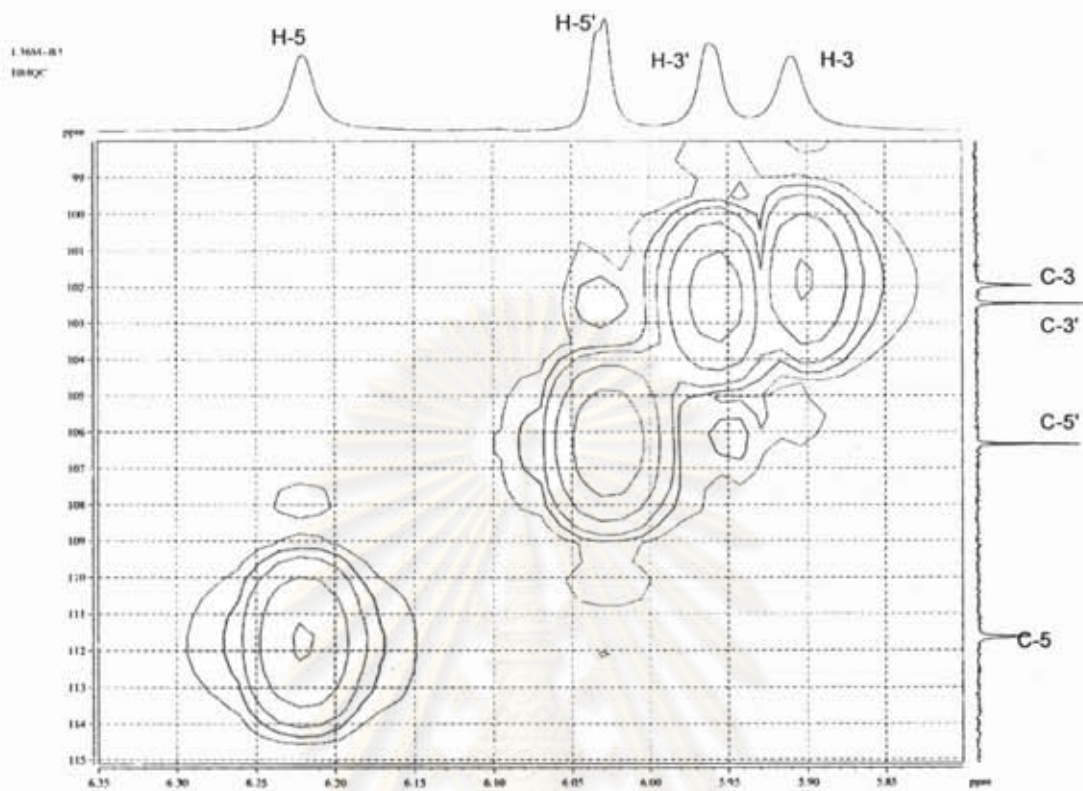
Figure P49  Expansion of Figure P48
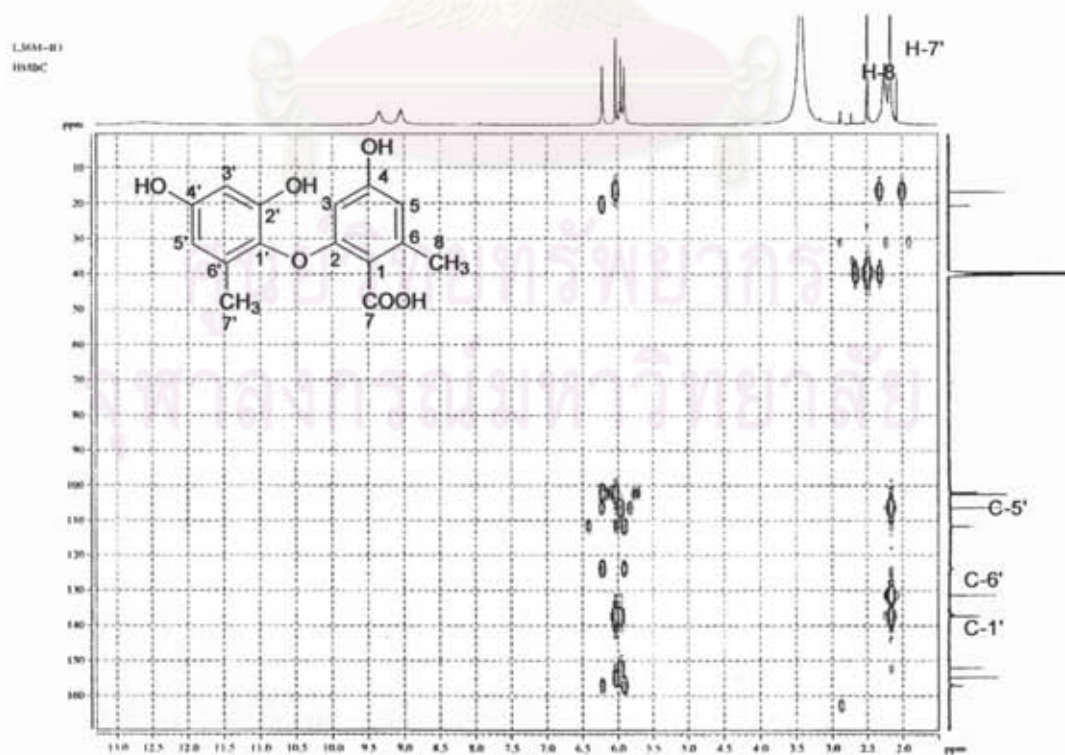


Figure P50  HMBC spectrum of corynether A (20)
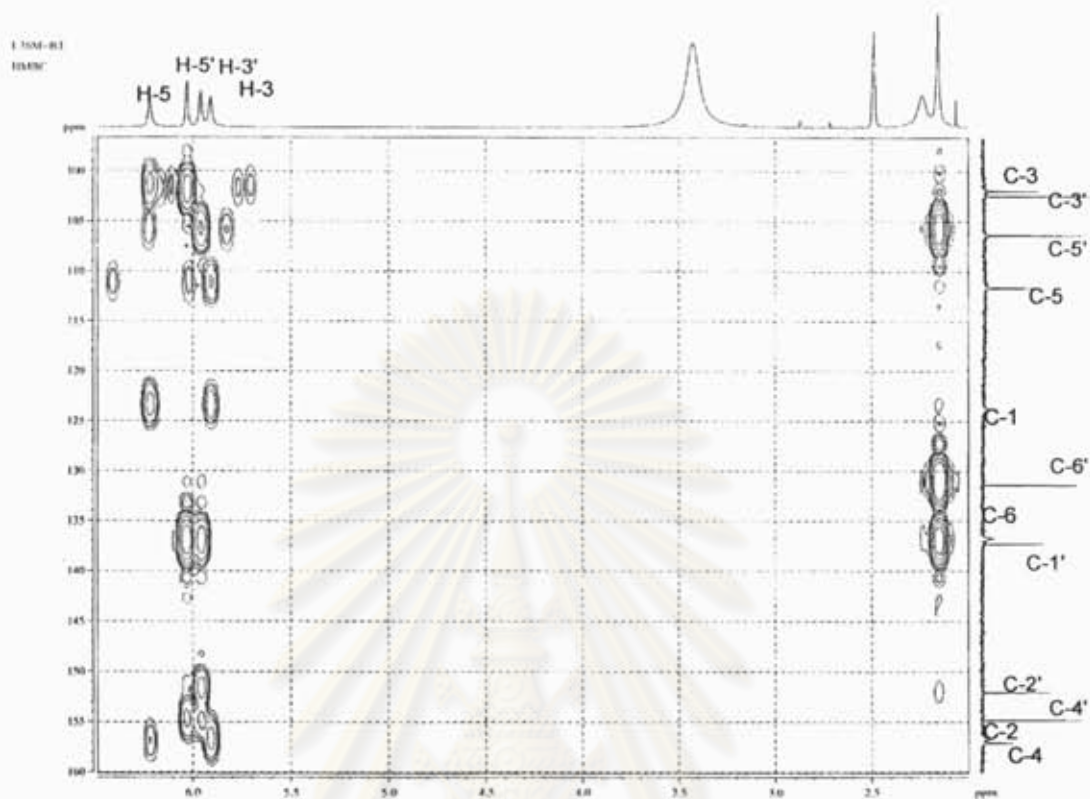
Figure P51    Expansion of Figure P50
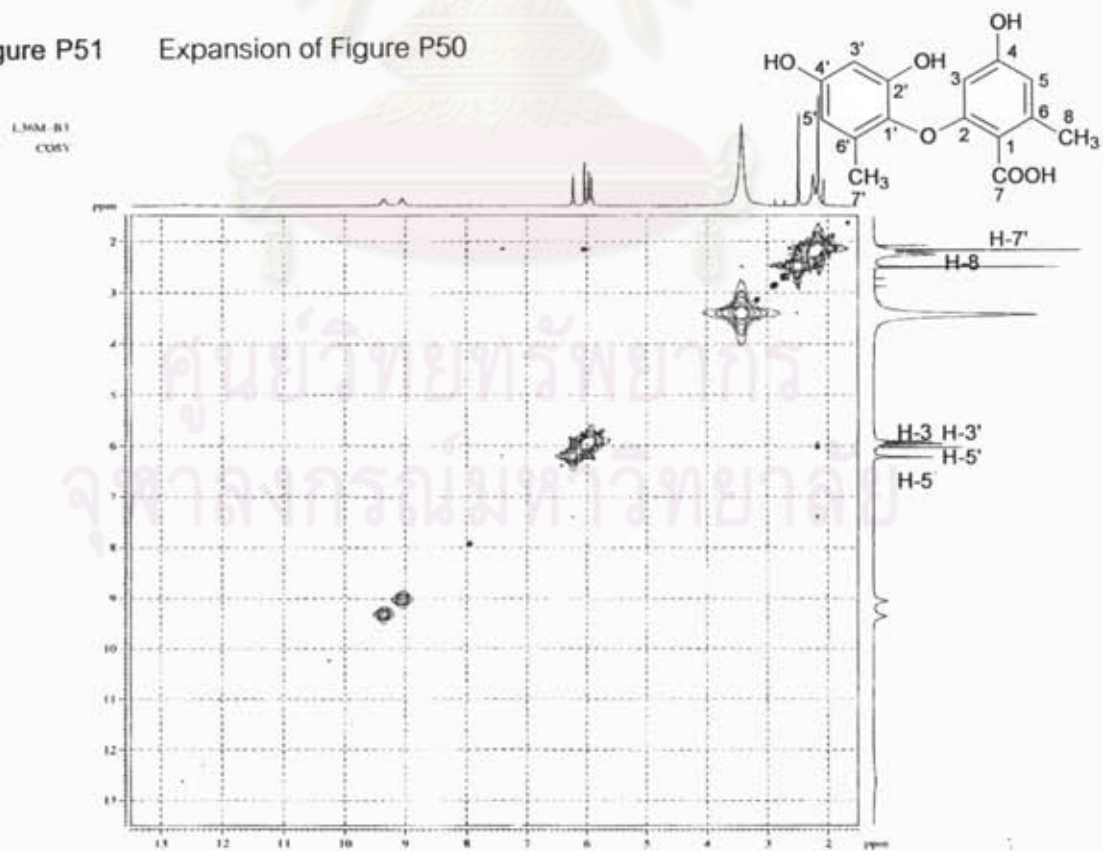


Figure P52    COSY spectrum of corynether A (20)
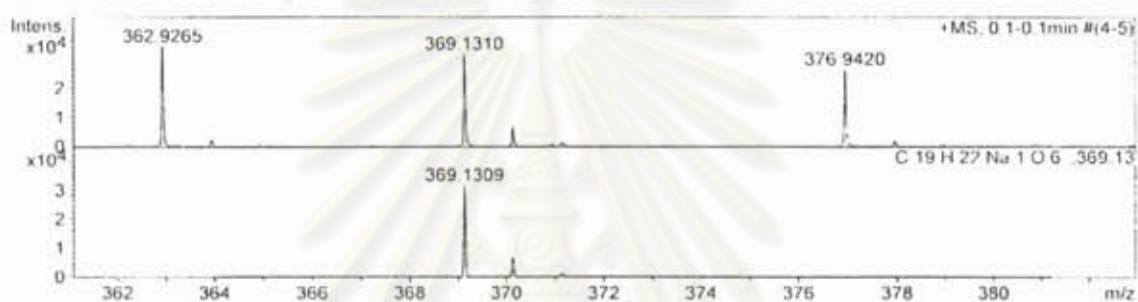
**Figure P53** ESI-TOF spectrum of tetra-*O*-methyl derivative (21)
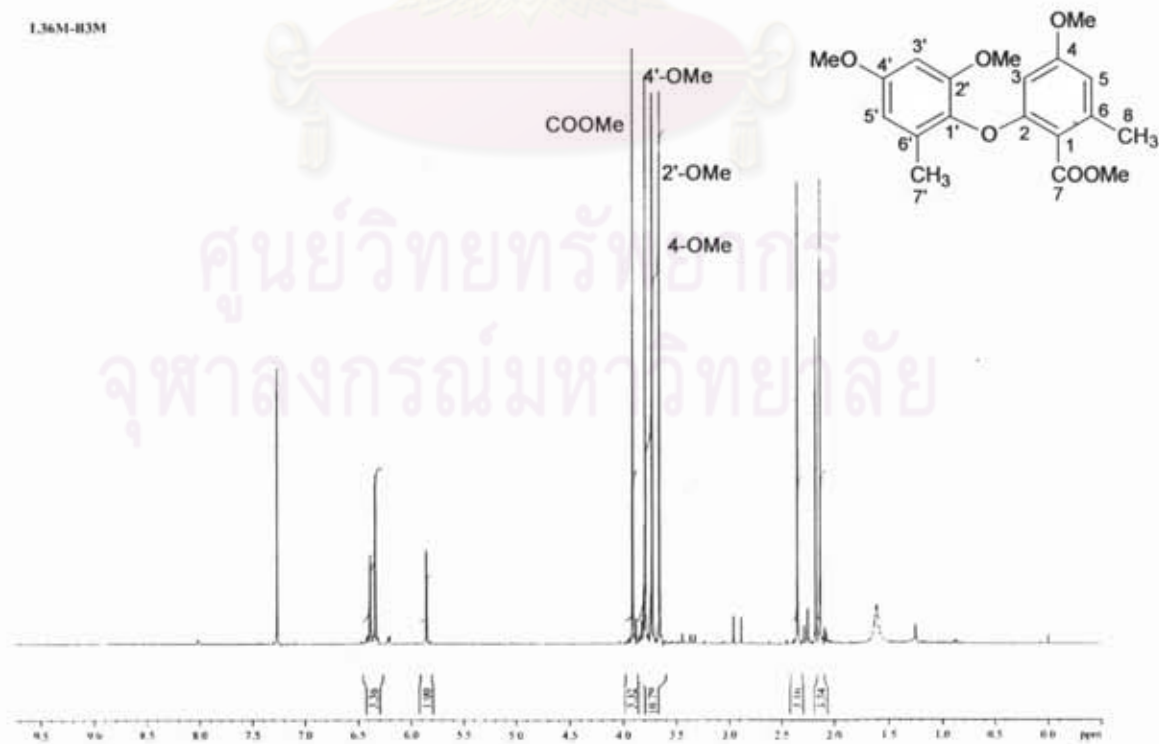


**Figure P54** 600 MHz ¹H NMR (CDCl₃) spectrum of tetra-*O*-methyl derivative (21)

L36M-B3M
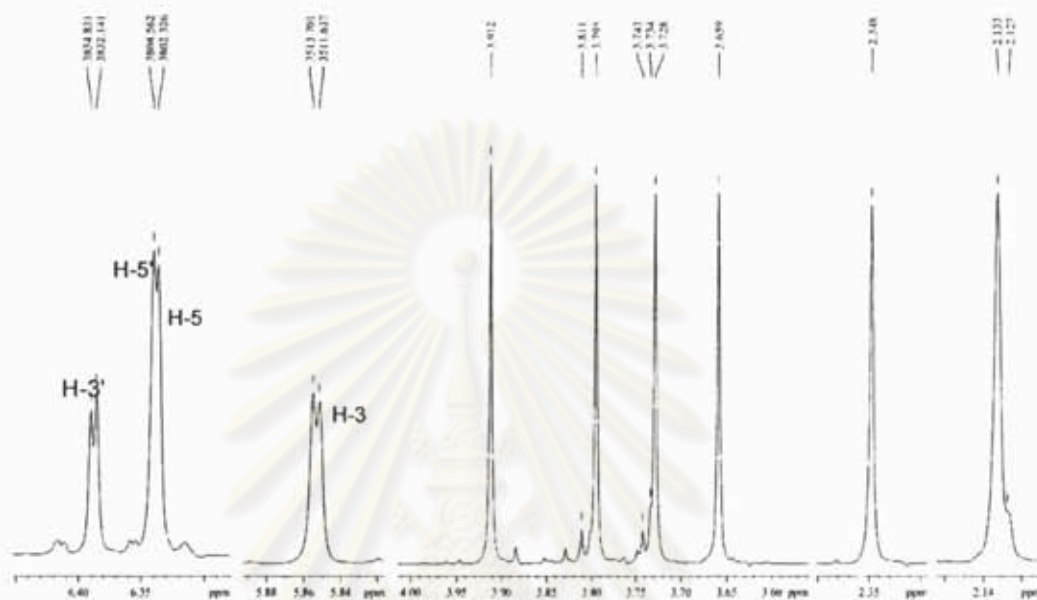


**Figure P55**     Expansion of Figure P54

L36M-B33
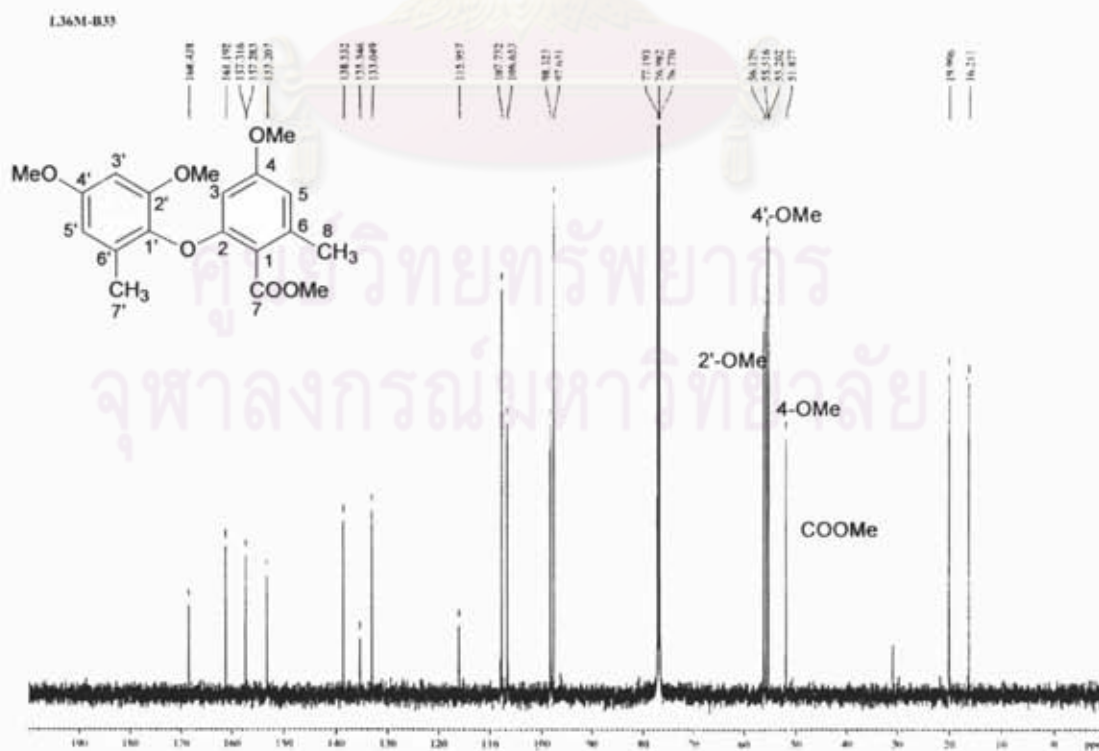


**Figure P56**     ¹³C NMR (CDCl₃) spectrum of tetra-O-methyl derivative (21)
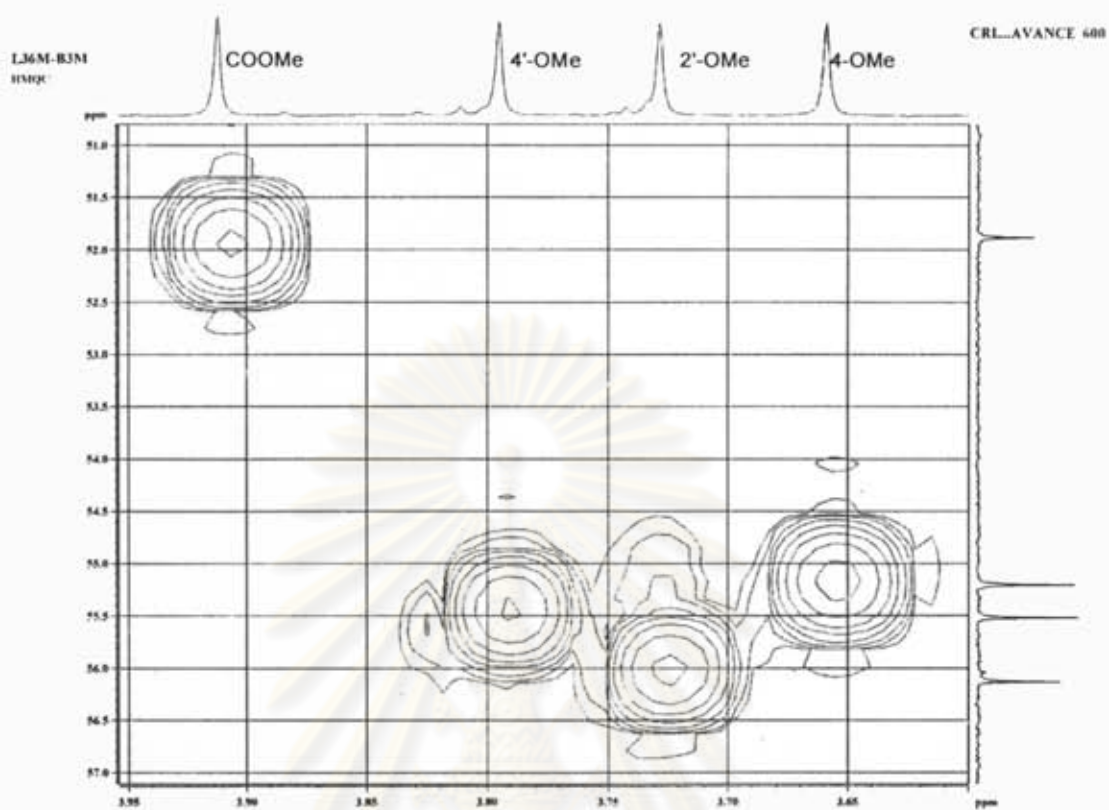
Figure P57    HMQC spectrum of tetra-*O*-methyl derivative (21)
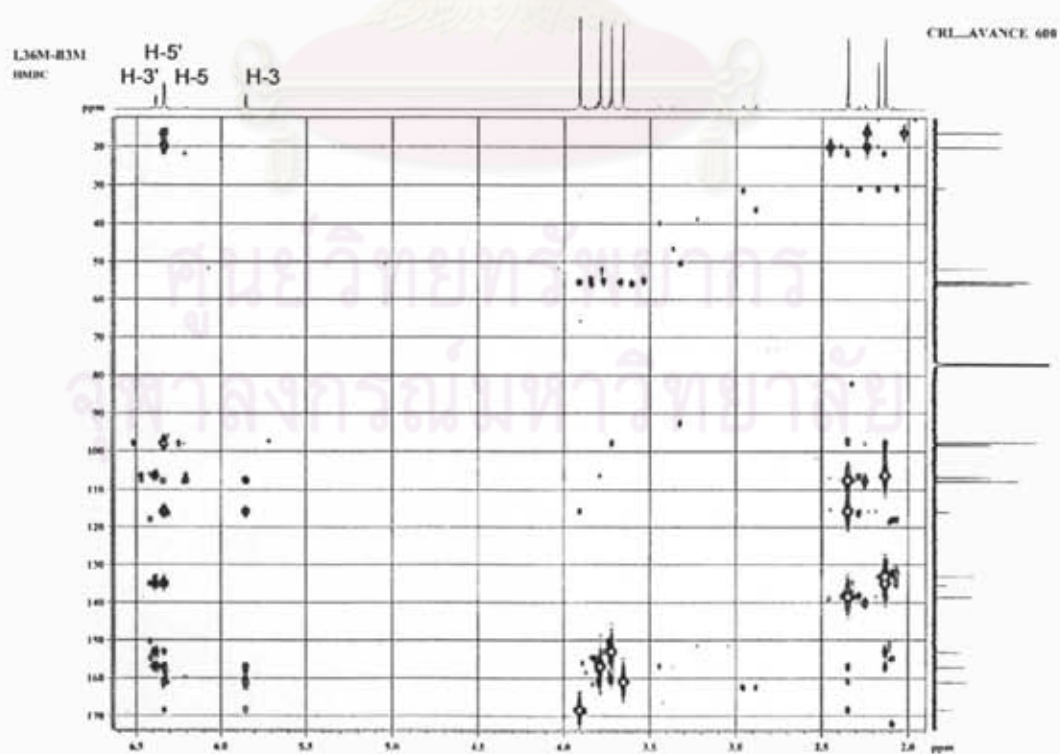


Figure P58    HMBC spectrum of tetra-*O*-methyl derivative (21)
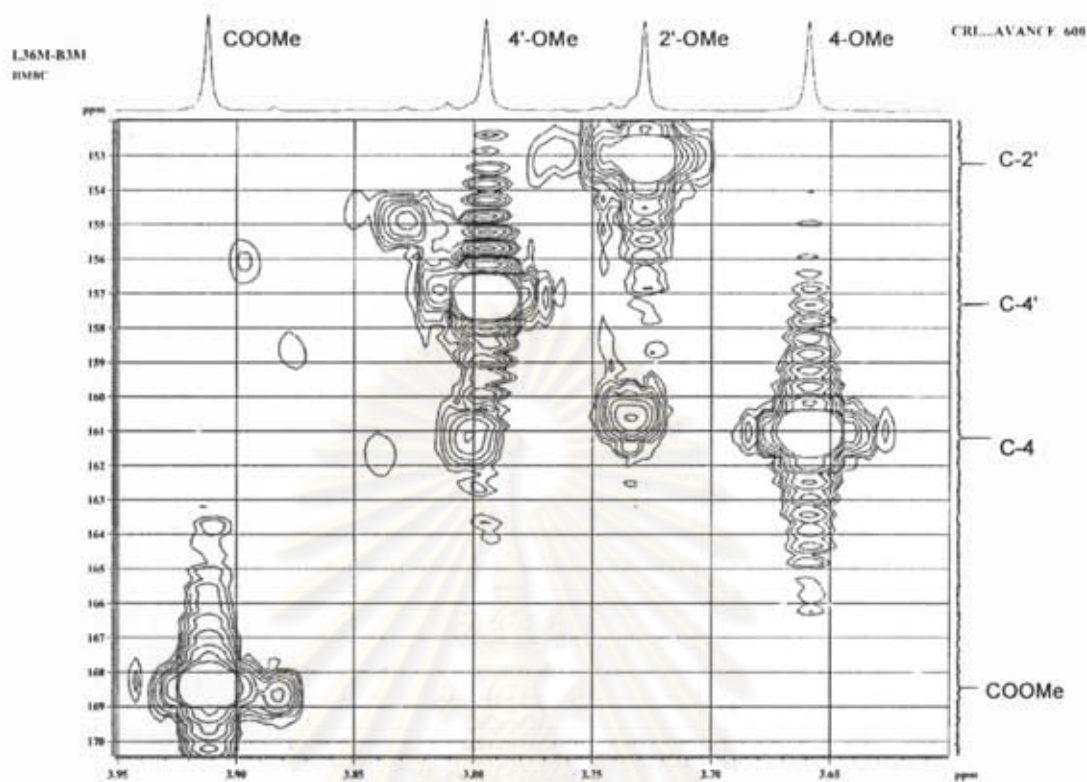
**Figure P59**   Expansion of Figure P58
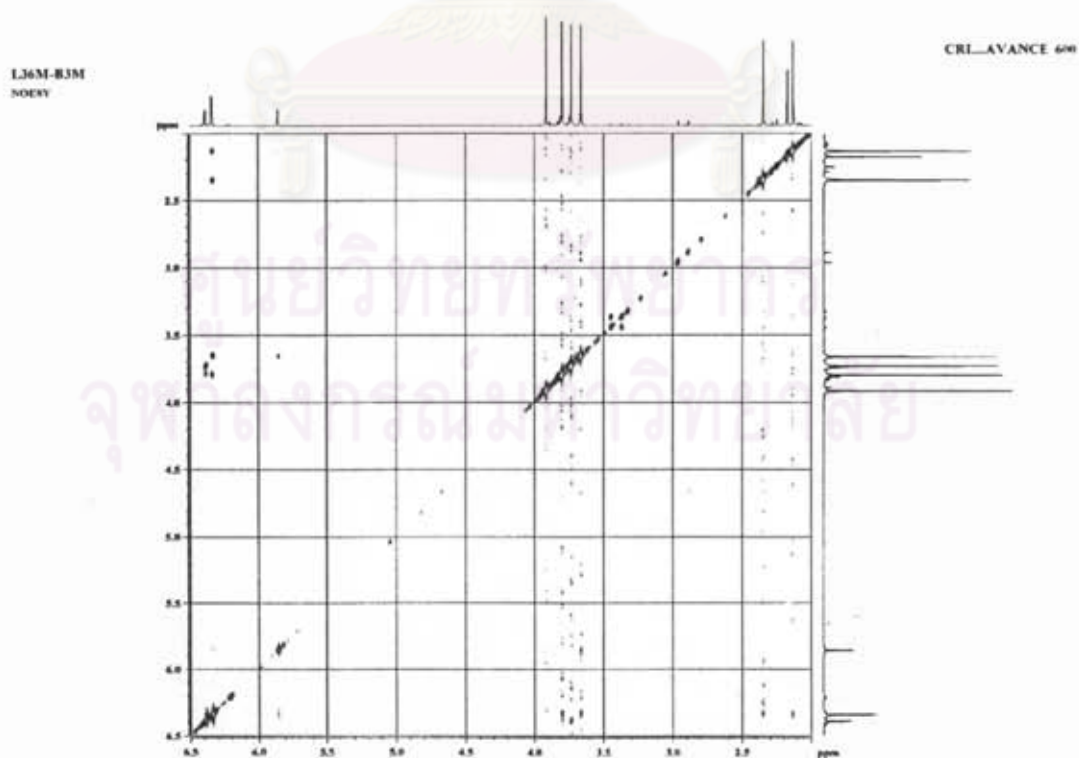


**Figure P60**   NOESY spectrum of tetra-*O*-methyl derivative (21)
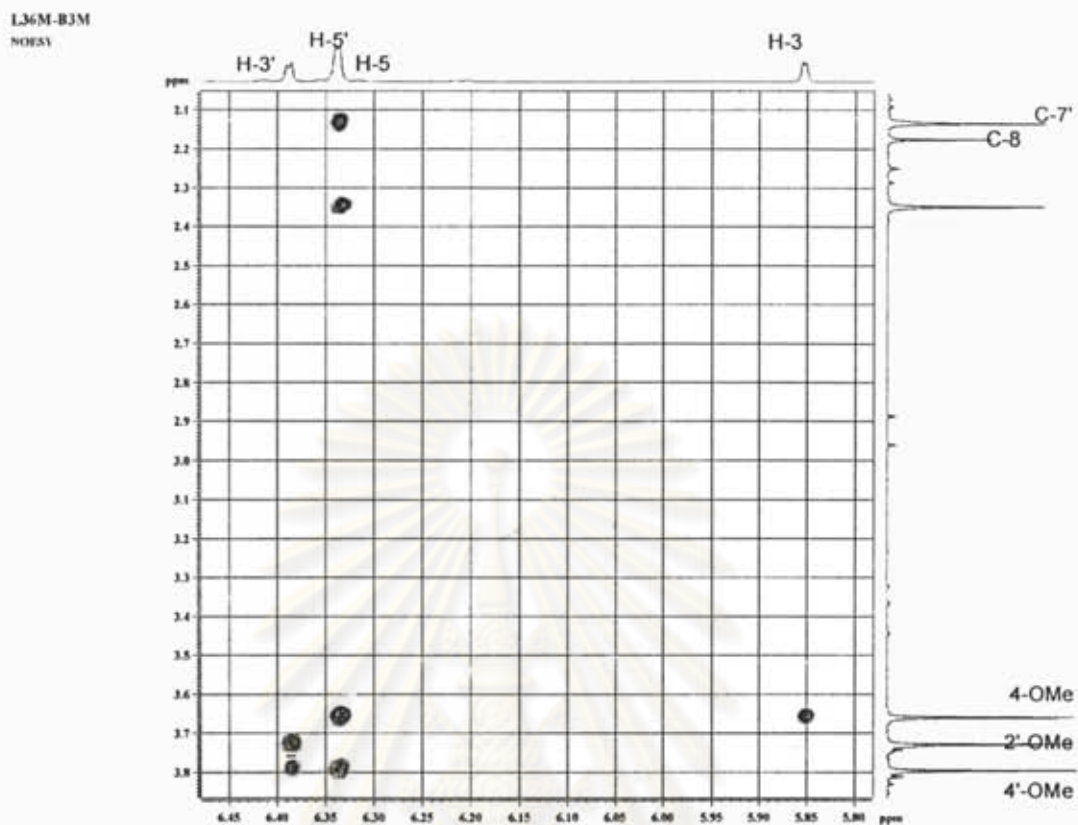
Figure P61    Expansion of Figure P60
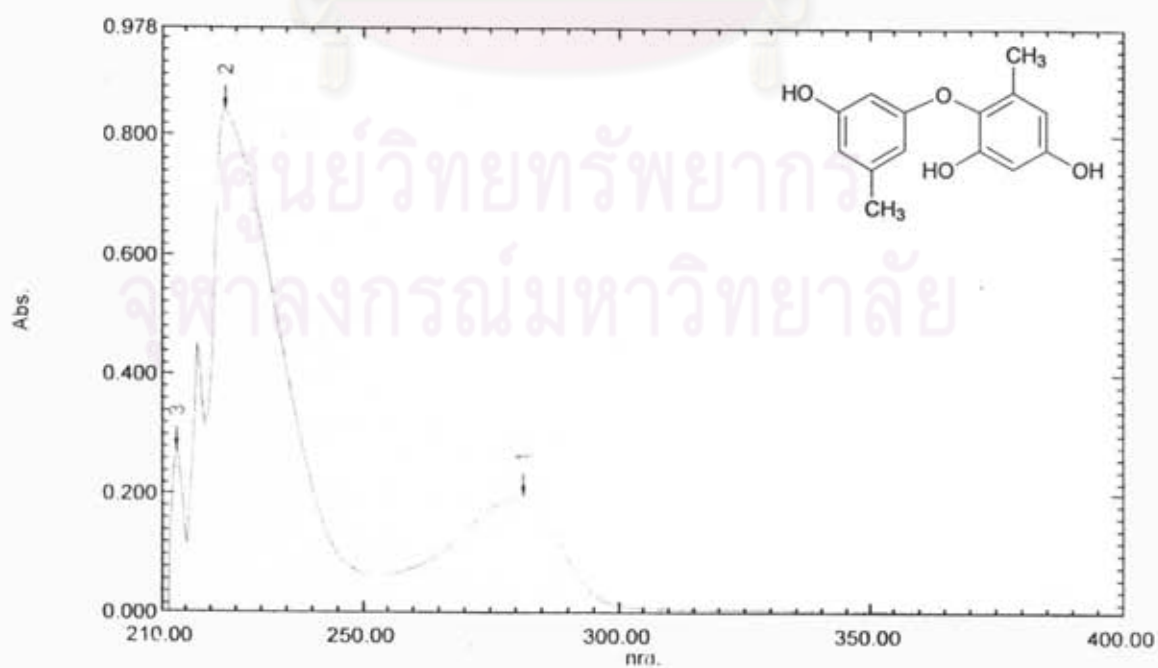


Figure P62    UV spectrum of diaryl ether (22)
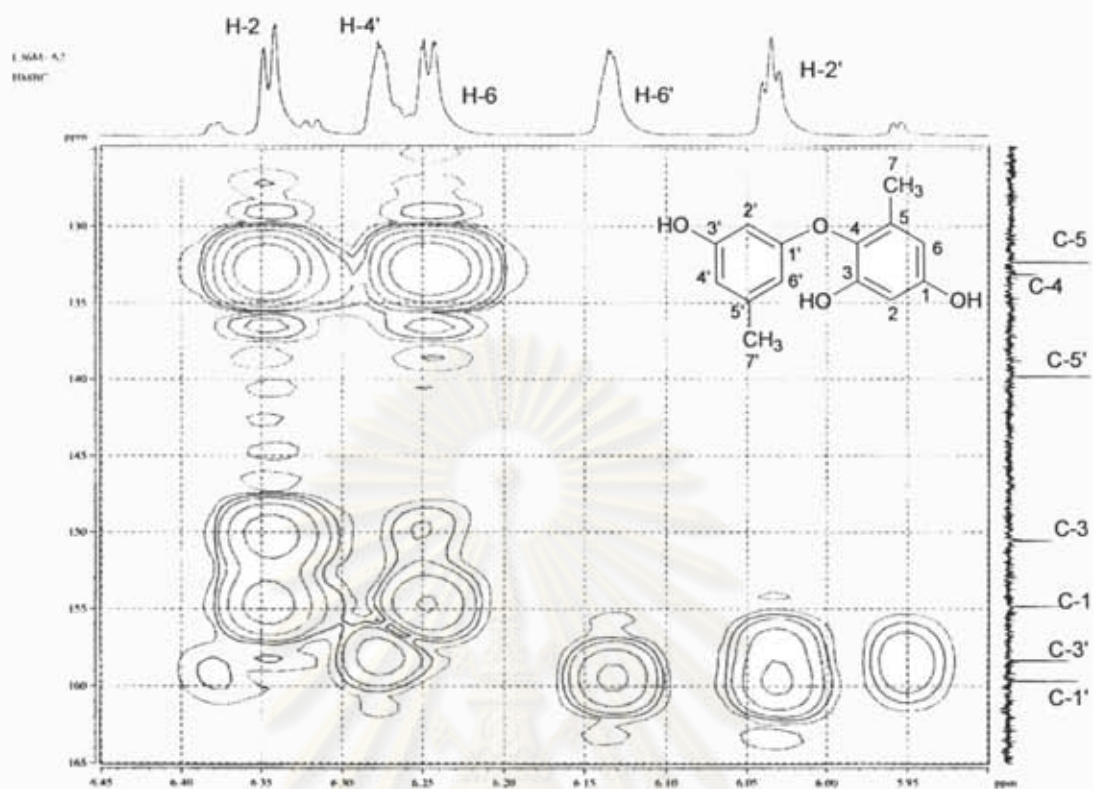
**Figure P63**  IR spectrum of diaryl ether (22)
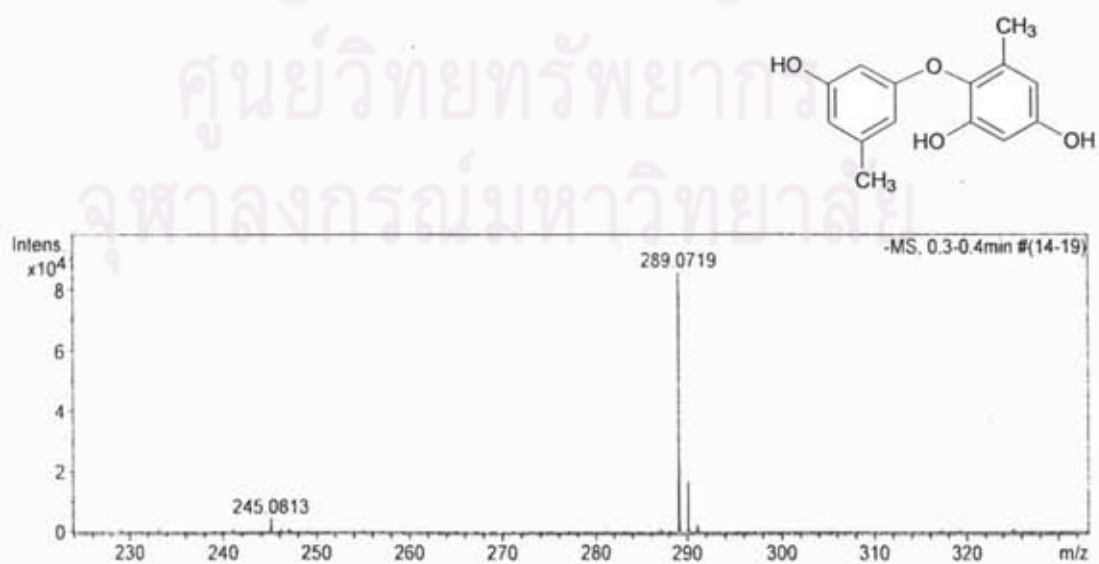


**Figure P64**  ESI-TOF spectrum of diaryl ether (22)
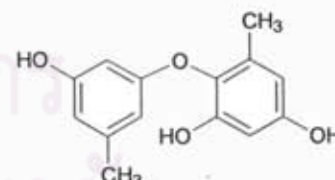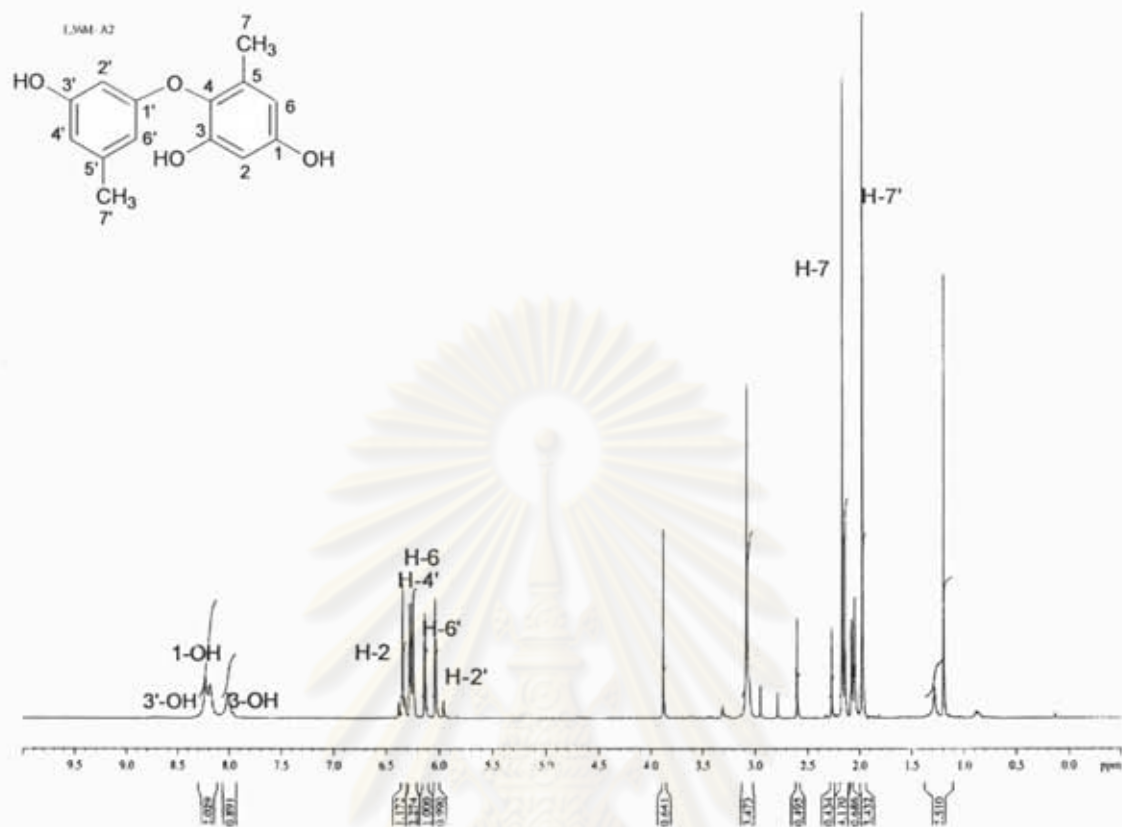
Figure P65     400 MHz $^1$H NMR (Acetone-$d_6$) spectrum of diaryl ether (22)
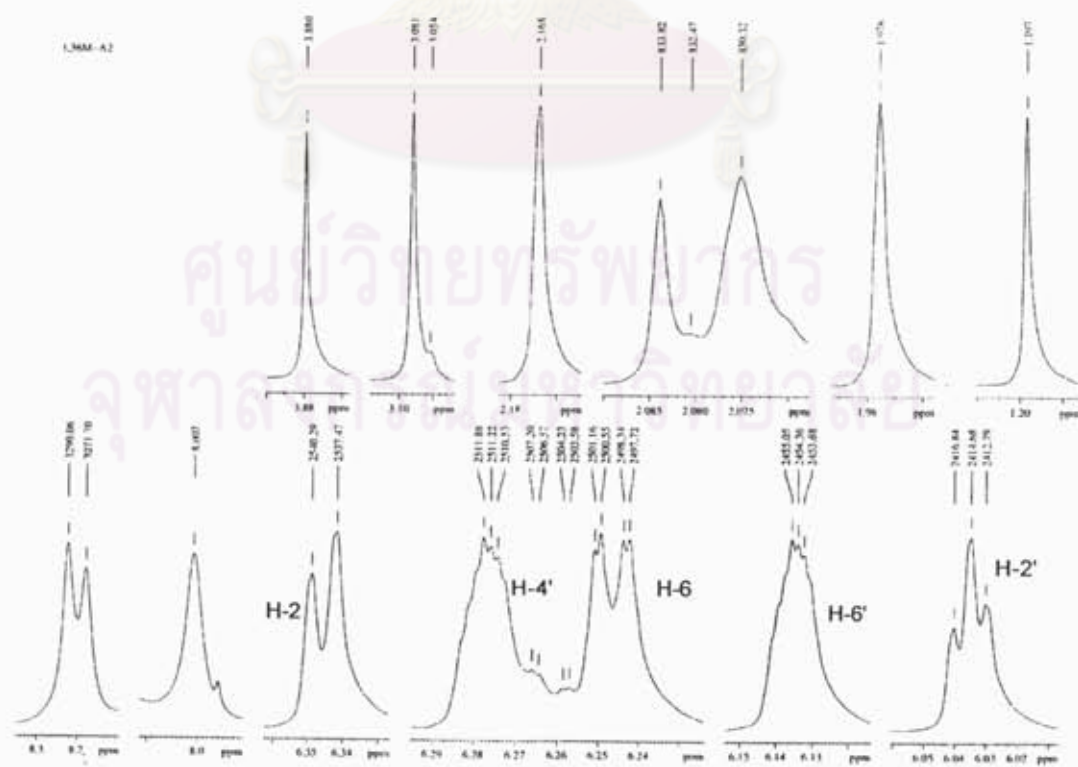


Figure P66     Expansion of Figure P65
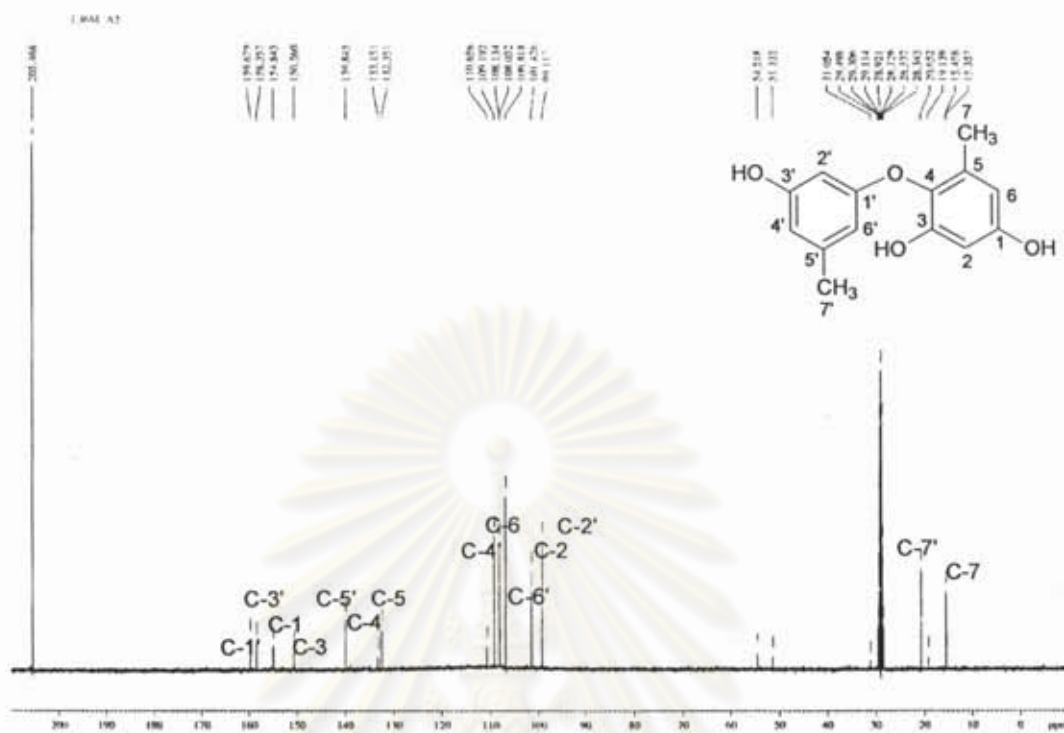
Figure P67    $^{13}$C NMR (Acetone-d$_6$) spectrum of diaryl ether (22)
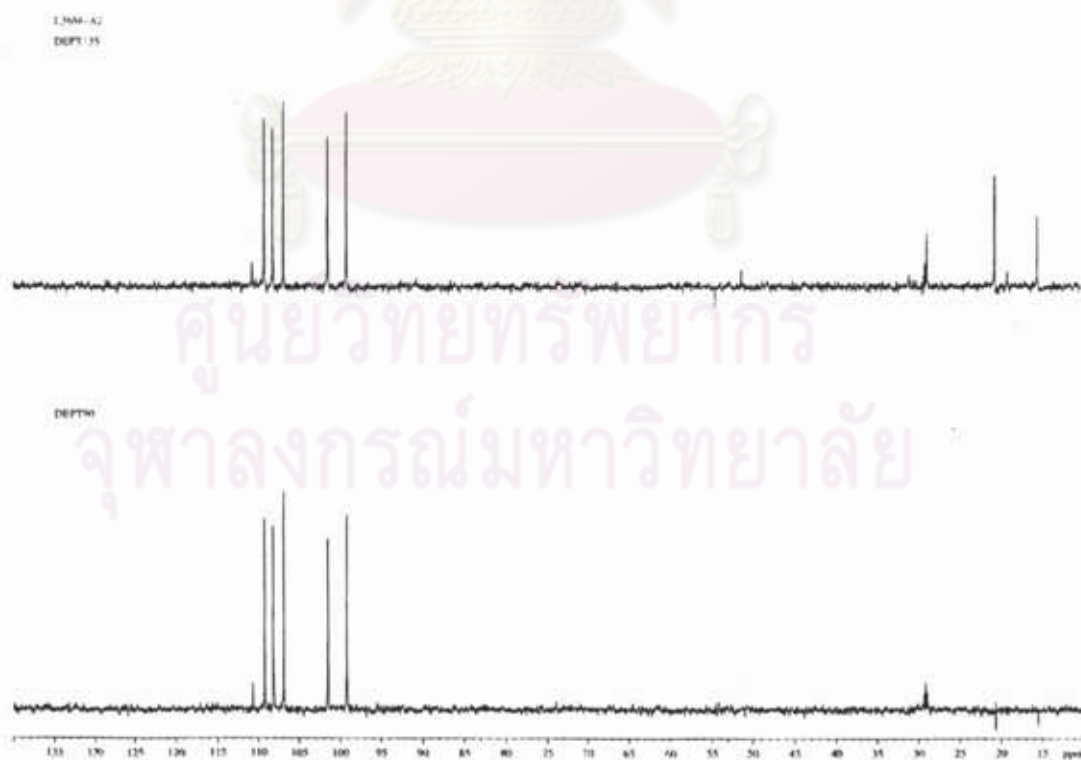


Figure P68    DEPT spectrum of diaryl ether (22)
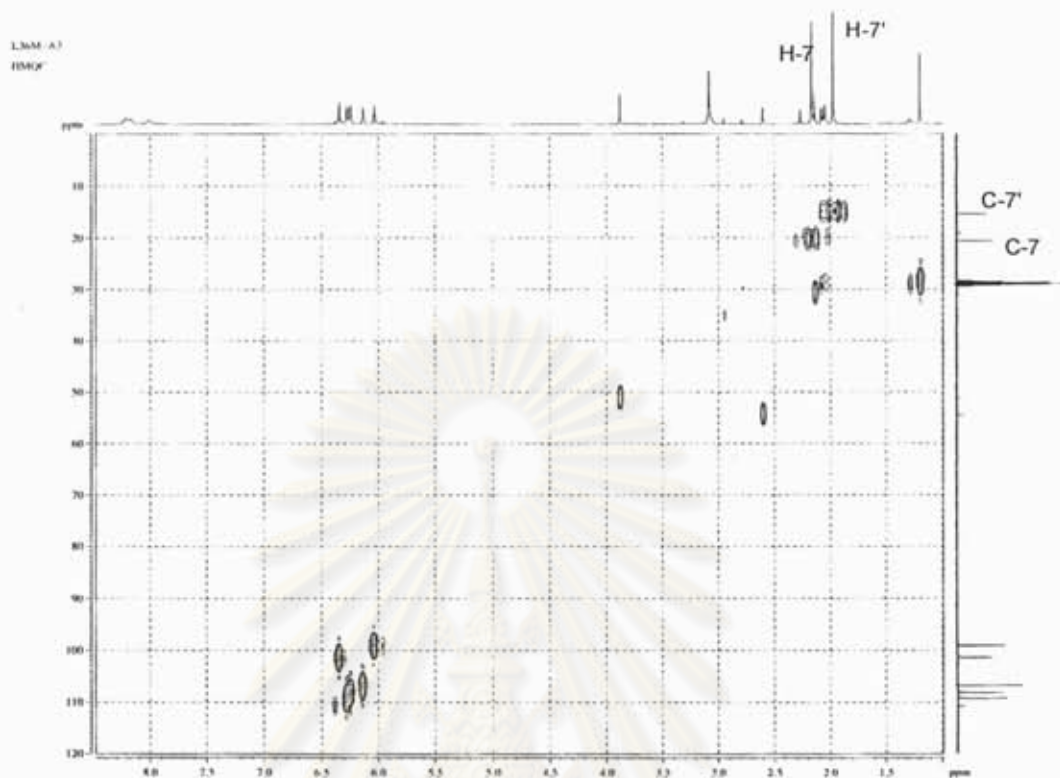
Figure P69    HMQC spectrum of diaryl ether (22)
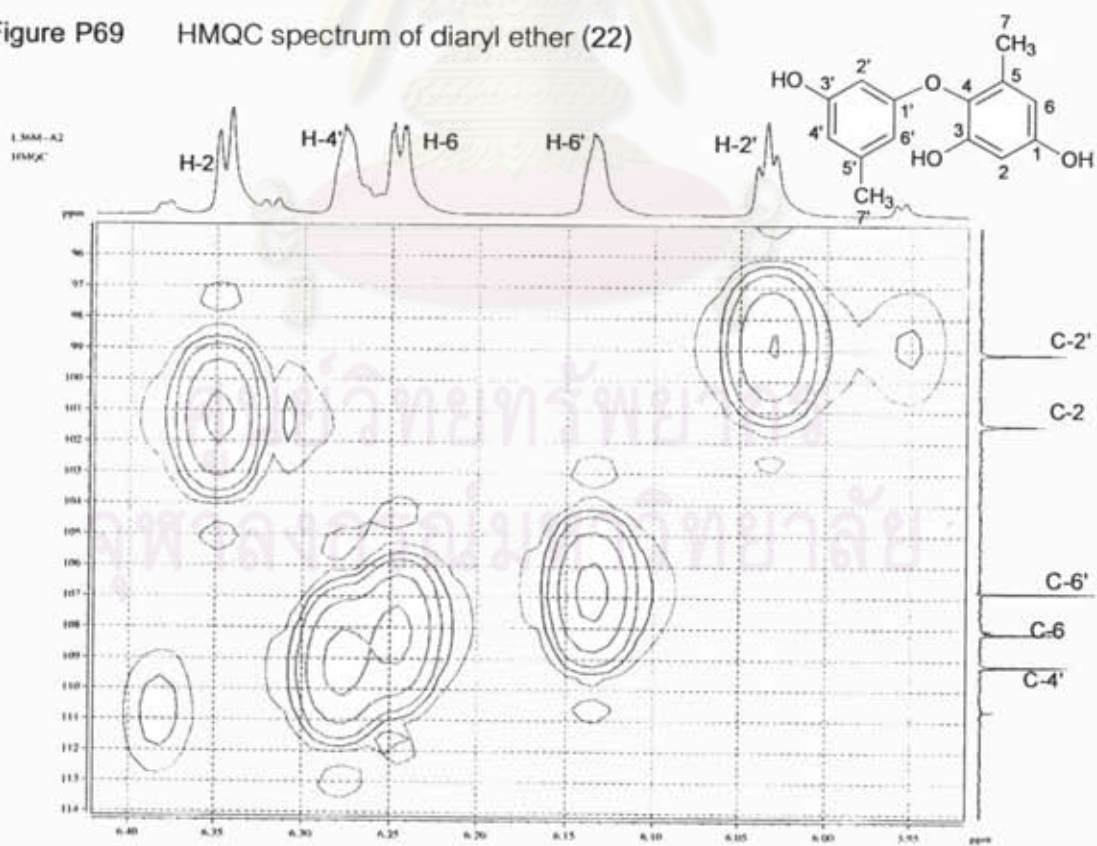


Figure P70    Expansion of Figure P69
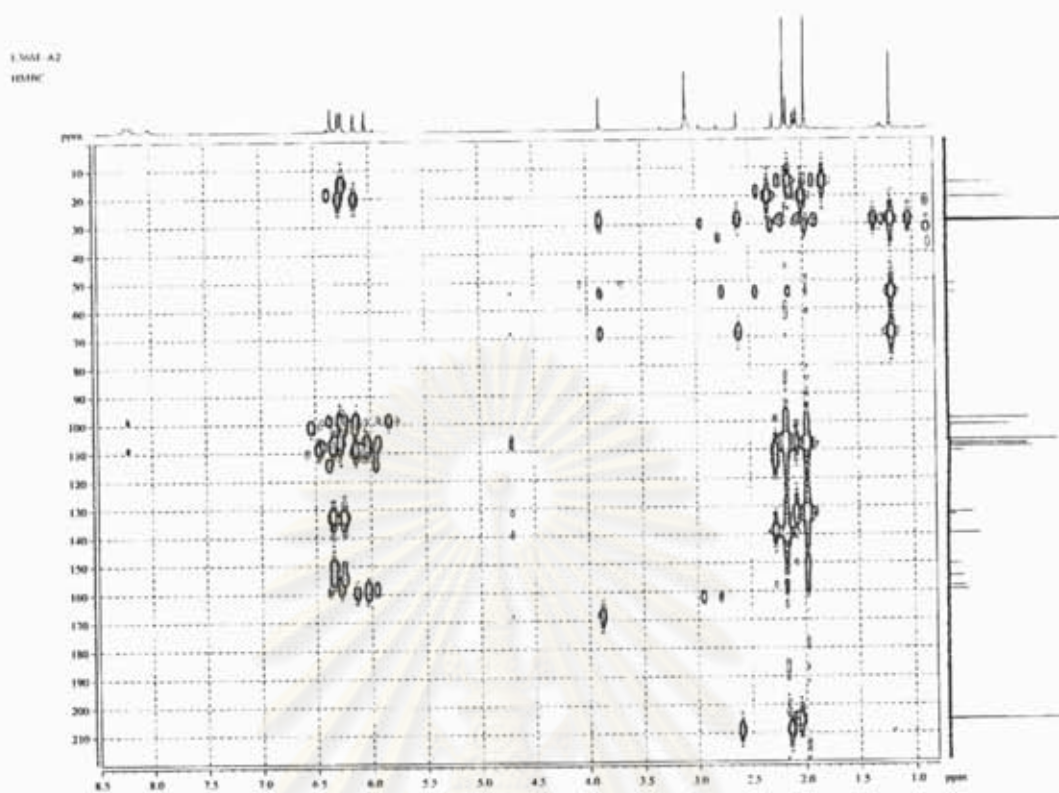
**Figure P71**   HMBC spectrum of diaryl ether (22)
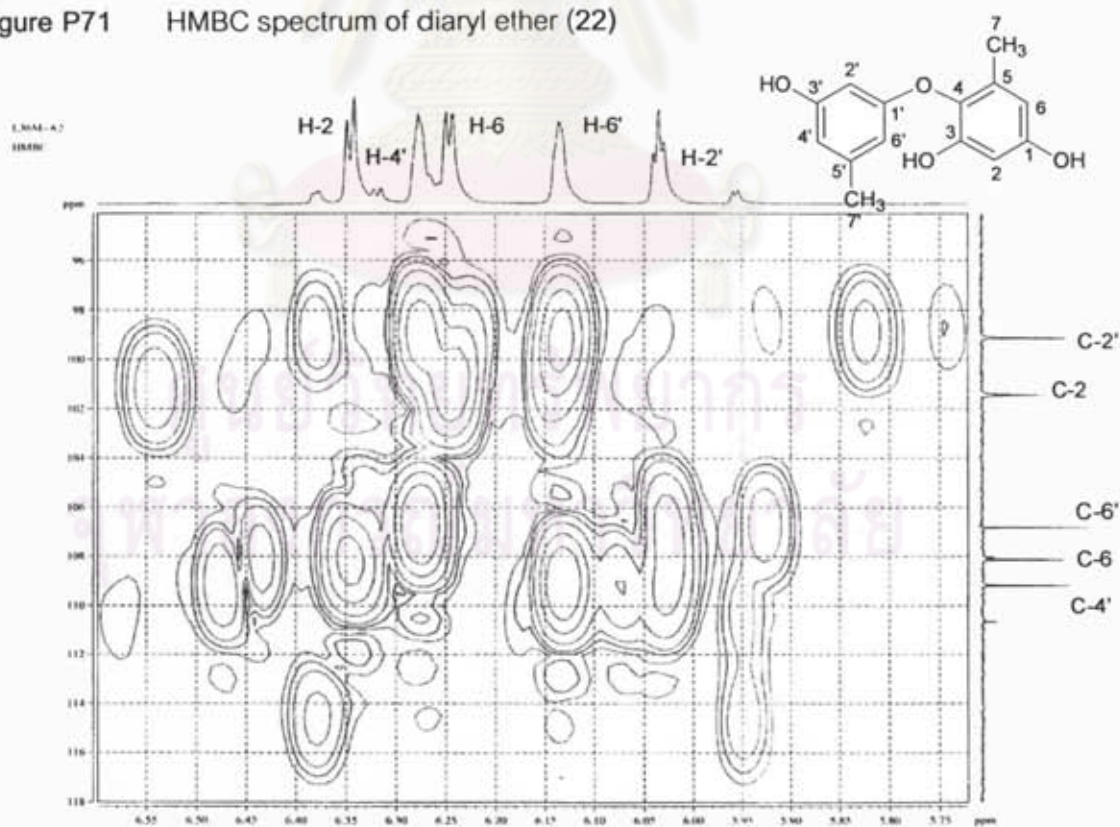


**Figure P72**   Expansion of Figure P71

Figure P73    Expansion of Figure P71



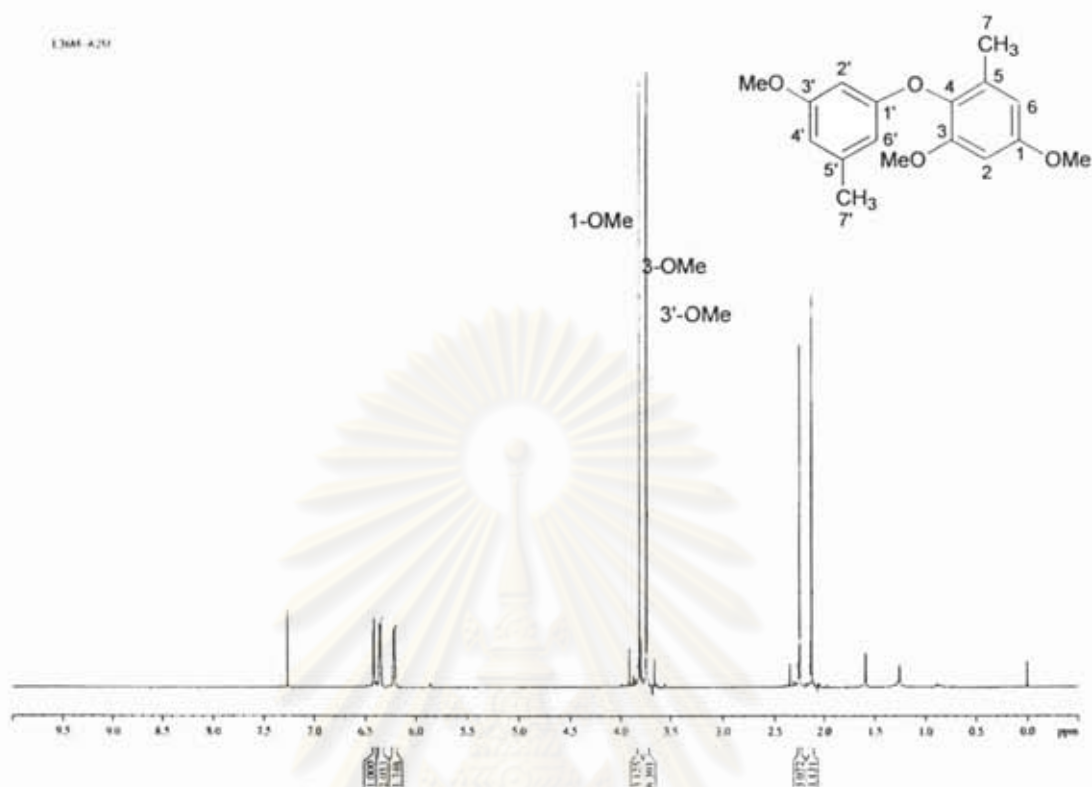Figure P74    COSY spectrum of diaryl ether (22)
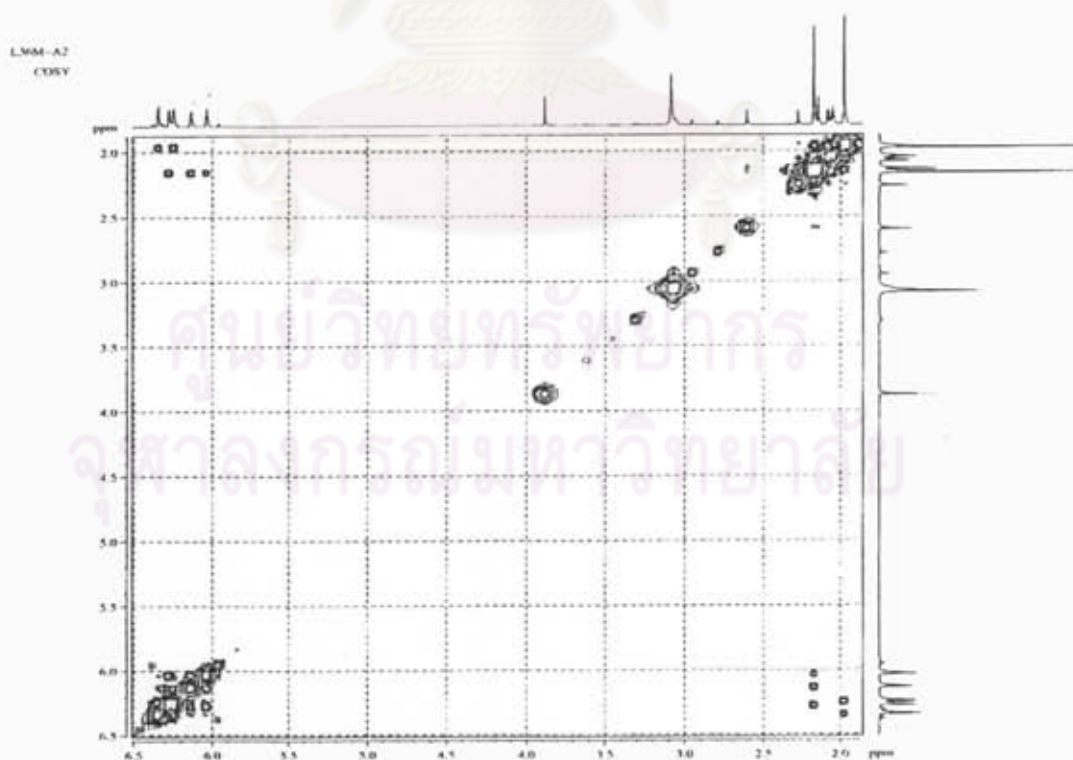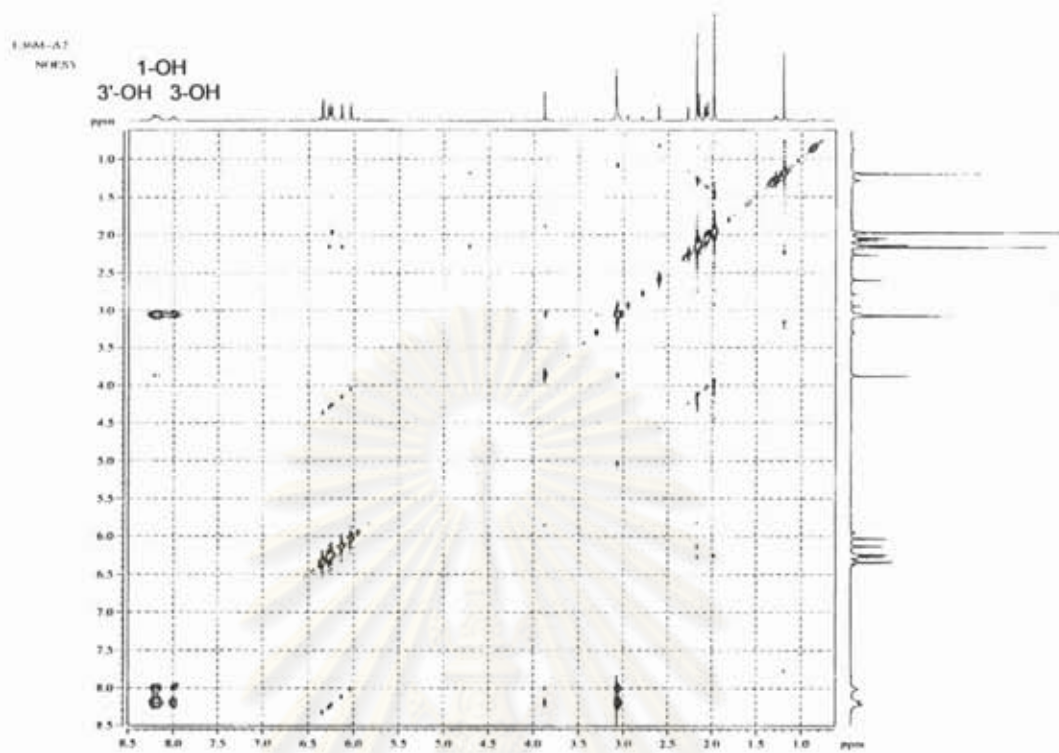
**Figure P75**    NOESY spectrum of diaryl ether (22)
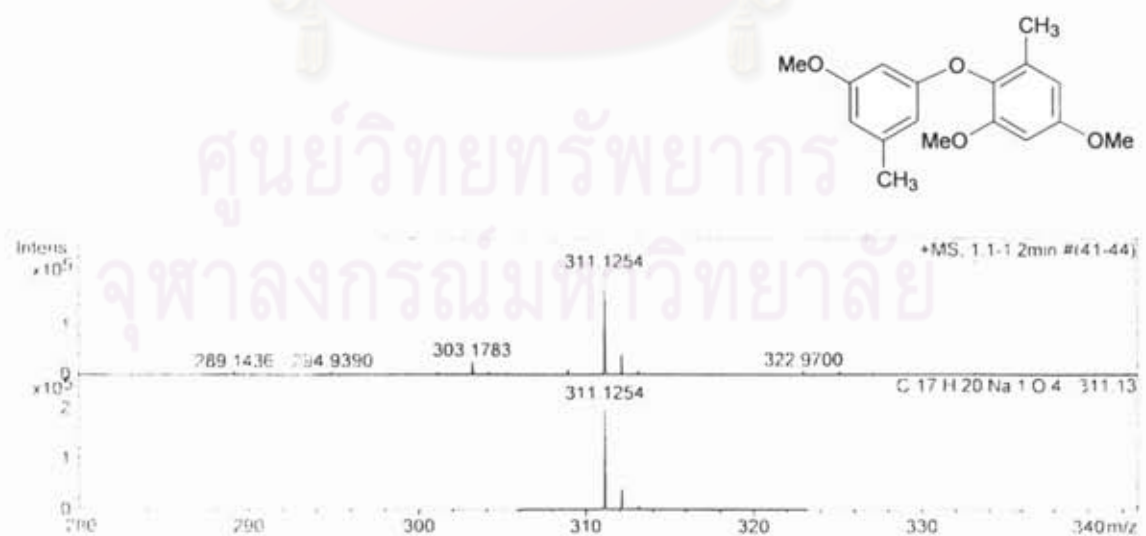


**Figure P76**    ESI-TOF spectrum of methylated derivative (23)

**Figure P77** 400 MHz $^1$H NMR (CDCl$_3$) spectrum of methylated derivative (23)



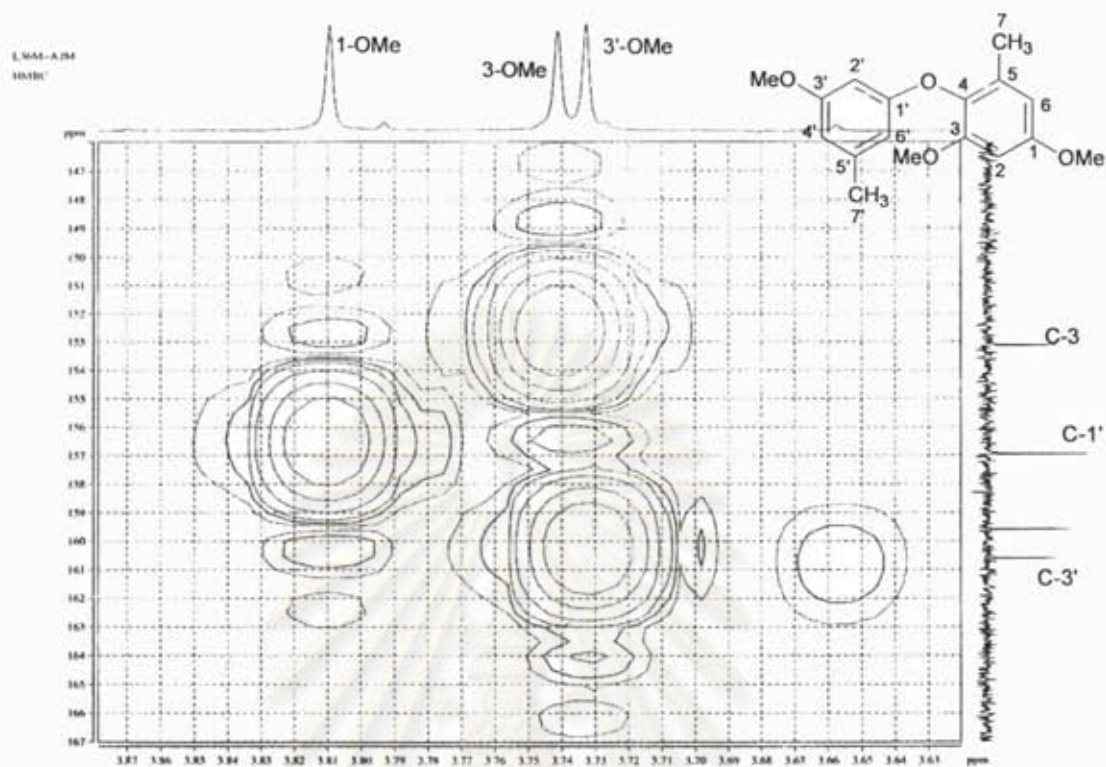**Figure P78** $^{13}$C NMR (CDCl$_3$) spectrum of methylated derivative (23)
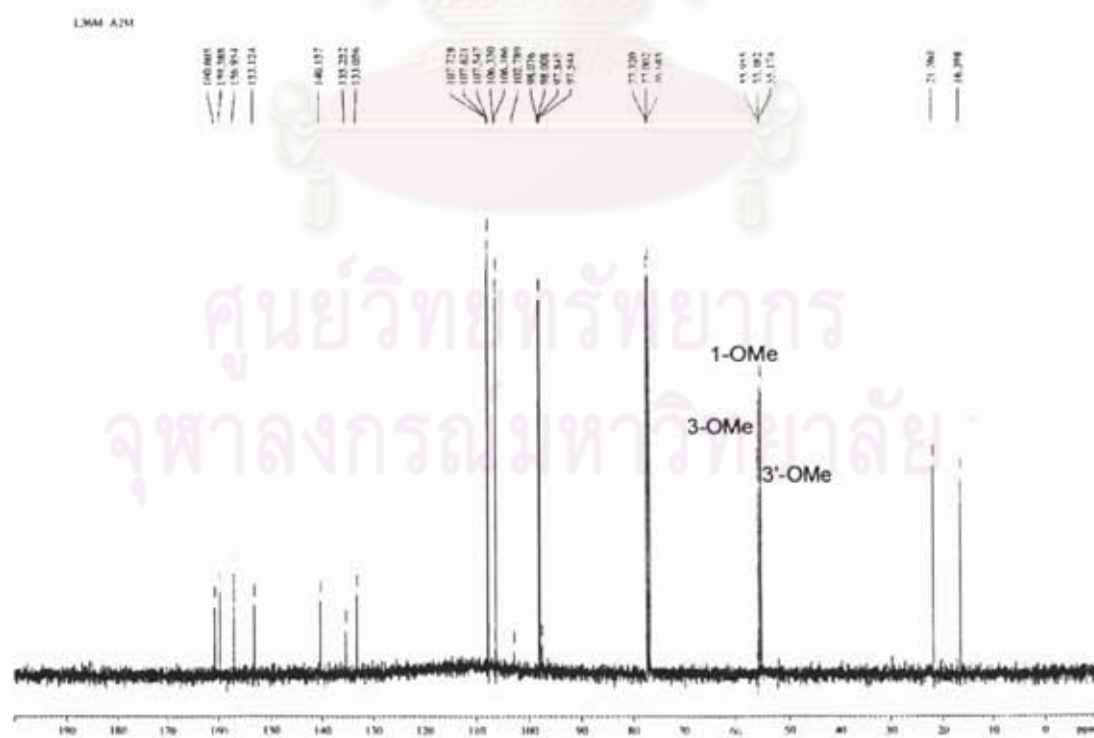
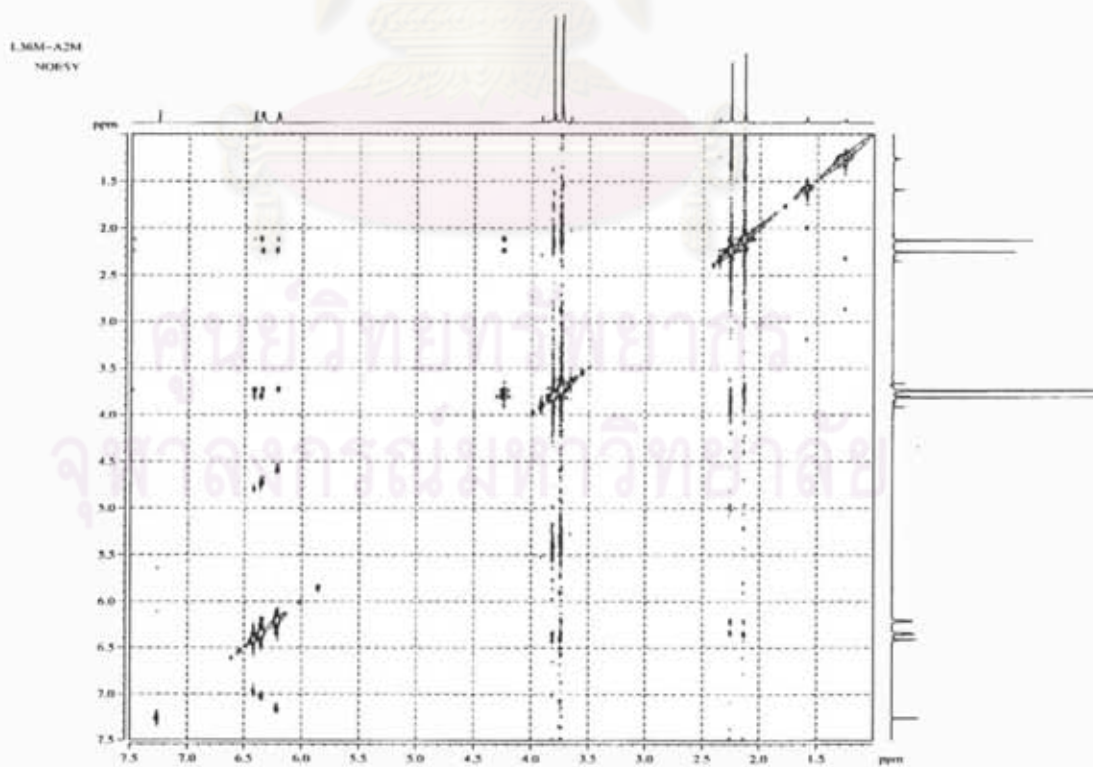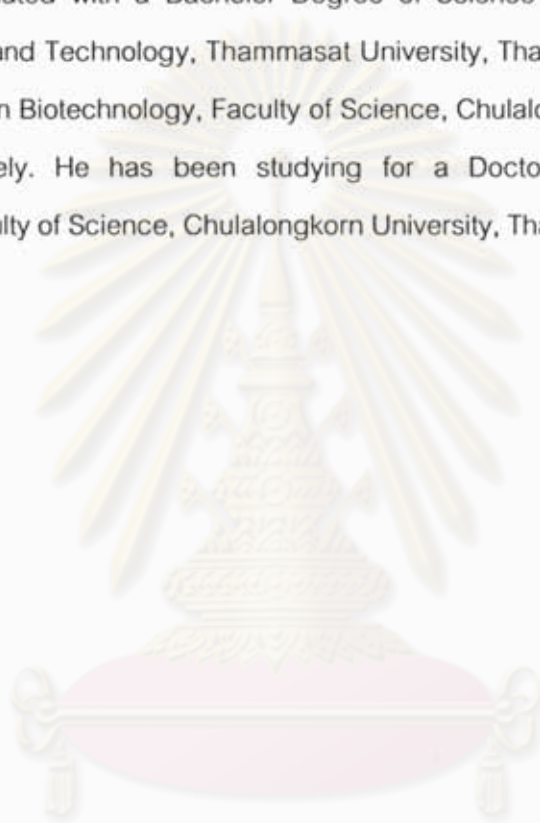Figure P79    HMBC spectrum of methylated derivative (23)



Figure P80    NOESY spectrum of methylated derivative (23)

# BIOGRAPHY

Mr. Porntep Chomcheon was born on December 4, 1977 in Uttaradit province, Thailand. He graduated with a Bachelor Degree of Science in Biotechnology from the Faculty of Science and Technology, Thammasat University, Thailand in 2001, and a Master Degree of Science in Biotechnology, Faculty of Science, Chulalongkorn University, Thailand in 2005, respectively. He has been studying for a Doctoral Degree of Science in Biotechnology, Faculty of Science, Chulalongkorn University, Thailand since 2005.